Facade Greening: Investigating the Potential of Climbing Plants for Air Pollution Mitigation and Water-Stress-Dependent Evapotranspiration

Doctoral thesis

for

the award of the doctoral degree

of the Faculty of Mathematics and Natural Sciences

of the University of Cologne

submitted by

Minka Aduse-Poku

from

Kumasi - Ghana

2025

Reviewers:

First Reviewer: Prof. Dr. Hans. G. Edelmann

Second Reviewer: Prof. Dr. Karl Schneider

Author's Note on Thesis Structure

This dissertation follows a cumulative format, incorporating both published and unpublished work. Due to this structure, readers may encounter some overlap in the presentation of background information, methodologies, or key findings across chapters. While every effort has been made to streamline content, some redundancy is inevitable to ensure that each chapter remains a self-contained unit.

Each chapter has been designed to stand independently, allowing readers to engage with specific sections without requiring extensive cross-referencing. As a result, themes, concepts, and discussions may reappear in multiple chapters where relevant. This approach ensures that all necessary context is provided within each chapter, particularly for those presented as standalone research articles.

Readers are encouraged to approach each chapter as an individual contribution to the broader research theme, while also considering the cumulative insights gained from the thesis as a whole.

Table of Contents

List of Abbreviations

Abbreviation	Full Term
CO_2	Carbon Dioxide
NO_2	Nitrogen Dioxide
O_3	Ozone
PM	Particulate Matter
$PM_{2.5}$	Fine Particulate Matter (diameter ≤ 2.5 μm)
PM_{10}	Coarse Particulate Matter (diameter ≤ 10 μm)
VOCs	Volatile Organic Compounds
EPA	Environmental Protection Agency
EU	European Union
GDP	Gross Domestic Product
NbS	Nature-based Solutions
NBS	Nature-based Solutions (alternative formatting)
IPCC	Intergovernmental Panel on Climate Change
AQP	Aquaporin
WUE	Water Use Efficiency
VPD	Vapor Pressure Deficit
PPFD	Photosynthetic Photon Flux Density
ANOVA	Analysis of Variance
CNSL	Cashew Nut Shell Liquid
CI	Confidence Interval
SO_2	Sulfur Dioxide
HNO_3	Nitric Acid
NH_3	Ammonia
NH_4NO_3	Ammonium Nitrate
CO	Carbon Monoxide
LI-COR	Lincoln Instruments – Correlation (Instrument Brand for Porometers)
FOV	Field of View
SD	Standard Deviation
PCI	Park Cool Islands
DE	Deutschland/Germany (in publisher context)

Abstract

Nature-based solutions such as façade greening offer a sustainable strategy to mitigate urban environmental stressors while improving urban resilience. This dissertation investigates the potential ecological functions of plant species employed for façade greening, focusing on their capacity for air pollutant absorption, water use, and water-stress responses.

This thesis employs multiple experimental approaches to evaluate the performance of various climbing plant species in urban environments. It focuses on three key aspects: air pollutant absorption, evapotranspiration-based cooling potential, and responses to water stress. The study quantifies species-specific capabilities using gravimetric water loss measurements, gas exchange analysis, and stomatal characterization, offering insights into how these plants perform under diverse urban environmental conditions.

Key findings indicate that *Hedera helix* 'Plattensee' and *Hedera hibernica* exhibit high evapotranspiration cooling potential, making them practical for urban heat mitigation but requiring sufficient water availability. In contrast, *Lonicera henryi* and *Clematis montana* demonstrate “water-saving strategies”, making them ideal for drought-prone urban areas. A novel methodology developed for pollutant gas absorption quantification revealed that *H. helix* showed the highest NO_2 uptake, whereas *Wisteria sinensis* excelled in a water-use experiment on a hot day (33°C). The stomatal analysis further demonstrated that stomatal type and density may affect cooling efficiency and water-stress response, indicating the possible need for extensive research to establish a trait-based species selection based on urban microclimatic needs.

Beyond its experimental contributions, this thesis also explores translating scientific findings into educational frameworks, emphasizing the role of teaching environmental awareness in sustainable urban development. Furthermore, the insights derived from this research provide practical recommendations for urban planners, architects, and policymakers, ensuring that façade greening systems may be tailored to site-specific climatic conditions.

By combining air pollution mitigation, water conservation, and microclimate regulation, this study reinforces the potential of façade greening as a multifunctional solution for climate-adaptive cities. The findings contribute to a broader discourse on future sustainable urban infrastructure, emphasizing the necessity of evidence-based species selection to maximize ecosystem services and improve environmental quality in rapidly urbanizing landscapes.

1.0. Introduction

1.1. Urban challenges

Urban environments are increasingly burdened by climate change and anthropogenic pollution's adverse effects, necessitating innovative solutions to enhance resilience and livability. Conventional nature-based solutions, such as tree planting, have long been recognized for their role not only in mitigating urban heat, improving air quality, and enhancing biodiversity. However, the widespread implementation of urban trees faces significant constraints due to the dominance of asphalt, concrete, and underground infrastructure, which limit available planting spaces and root expansion. As a result, alternative greening strategies that capitalize on the existing urban fabric have gained traction.

Among these, vertical greening has emerged as a practical approach to utilizing the vast availability of vertical surfaces on buildings. Covering façades with vegetation not only reduces building energy demands—providing cooling in summer and insulation in winter—but also plays a crucial role in air phytoremediation by absorbing gaseous pollutants such as nitrogen dioxide (NO_2), ozone (O_3), and carbon dioxide (CO_2). This recognition has led to the increasing incorporation of vegetation into modern architecture, primarily through two systems: (1) the wall-bound façade greening system, which is more expensive and maintenance-intensive, and (2) the ground-based façade greening system, which is more cost-effective and adaptable, often implemented in trough-based setups to accommodate preexisting urban infrastructure.

1.2. The Role of Climbing Plants in Façade Greening

Climbing plants are used for ground- and trough-based façade greening due to their ability to adapt to wall surfaces with or without climbing aids. These species are utilized for aesthetic and thermal regulation benefits, but their specific capacity for pollutant gas absorption has not yet been sufficiently researched. While urban trees and green roofs have been studied for their role in improving air quality, the extent to which climbing plants contribute to pollution mitigation—particularly for NO_2, O_3, and CO_2—remains insufficiently quantified (Hellebaut et al., 2022).

This gap in research necessitates further experimental investigation.

Beyond air pollution mitigation, climate-induced stressors such as extreme heatwaves, rapid flooding, and prolonged drought pose additional challenges to urban vegetation. Understanding how climbing plants respond to water scarcity and stress conditions is essential for optimizing species selection in urban greening projects. Differences in transpiration behaviour, water use efficiency, and response to water-limiting conditions among species may influence their long-term viability and ecological contributions. In particular, quantifying water loss under various degrees of water stress can inform decision-making regarding plant selection for sustainable urban environments.

1.3. Research Objectives

Given these knowledge gaps, this study aims to quantify climbing plants' air pollution absorption potential while assessing their water use behaviour under controlled water stress conditions. By combining experimental gas absorption measurements with transpiration and drought tolerance assessments, this research provides critical insights into the ecological functions of climbing plants in façade greening systems. The findings contribute to the broader discourse on sustainable urban infrastructure by informing species selection for urban greening initiatives that effectively mitigate pollution and adapt to climate stressors.

1.4. Structure of the Thesis

This thesis comprises both published and unpublished findings (chapters 3-8) structured as follows:

Chapter 2: Literature Review – A comprehensive overview of research on façade greening, air pollution mitigation, and plant water use .

Chapter 3: Methodology for the quantification of the absorption potential of greenhouse - and pollutant gases by climbing plants used in façade greening; a case study on ivy (*Hedera helix*). Published in “Environmental Advances”.

Chapter 4: Quantifying the potential of façade climbing plants in reducing air pollution: a novel investigation into the absorption capabilities of three climbers for CO_2, NO_2, and O_3 in urban environments. Published in “Urban Ecosystems”.

Chapter 5: Stomata Type and Density in Climbing Plants (unpublished study)

2.0. Current status/ Literature review

2.1. Urban air pollution sources and interdependencies

2.1.1. Sources of air pollution in Cities

Knowledge of the sources of air pollution in urban areas is essential for developing effective strategies to improve air quality and protect public health. Urban environments are characterized by a complex interplay of natural and anthropogenic sources that contribute to the concentration of various pollutants.

2.1.2. Vehicle Emissions

In most cities, vehicular emissions are a significant source of air pollution. The rapid growth of the vehicle industry has led to increased emissions of nitrogen dioxide (NO_2), carbon monoxide (CO), and particulate matter (PM). This situation is exacerbated by the delayed implementation of stringent emission controls, resulting in elevated pollutant levels in urban areas (Tang et al., 2023; Wang et al., 2019).

2.1.3. Industrial Activities

Industrial activities contribute to air pollution through the release of various pollutants, including sulfur dioxide (SO_2), nitrogen oxides (NO_x), volatile organic compounds (VOCs), and particulate matter. These emissions can lead to the formation of secondary pollutants such as ozone (O_3) and particulate matter ($PM_{2.5}$), which have significant health implications (EEA, 2021).

2.1.4. Residential Heating and Cooking

In many urban areas, especially in developing countries, solid fuels like coal and biomass are used for heating and cooking. This practice releases pollutants such as PM, NO_2, and CO into the indoor and outdoor environments, contributing to urban air pollution. Transitioning to cleaner energy sources is crucial for reducing these emissions (Balmes, 2019; Guttikunda et al., 2019).

2.1.5. Construction Activities

Construction sites are dust and particulate matter sources, including $PM_{2.5}$ and PM_{10}. Heavy machinery, demolition activities, and transportation of construction materials can resuspend

dust particles into the air, degrading air quality in surrounding areas (Cui, 2023; Milivojević et al., 2023; Xu et al., 2022).

2.1.6. Natural Sources

While anthropogenic activities are the primary contributors to urban air pollution, natural sources such as wildfires, dust storms, and pollen dispersal can also affect air quality (Holzer et al., 2003; Mues et al., 2012; Sofiev et al., 2008; Zeng & Zhang, 2017). However, their impact is generally less significant than human-induced sources in urban settings.

Addressing urban air pollution requires a comprehensive approach that includes stringent emission controls, promotion of cleaner technologies, urban planning to reduce traffic congestion, and public awareness campaigns. By targeting these key sources, cities can work towards achieving better air quality and enhancing the health and well-being of their residents.

2.2. Interdependencies among pollutant gases (NO_2, O_3, and CO_2).

Understanding the interdependencies among atmospheric pollutants such as nitrogen dioxide (NO_2), ozone (O_3), carbon dioxide (CO_2), and particulate matter (PM) is crucial for comprehending urban air quality dynamics. These pollutants interact through complex chemical and physical processes, influencing each other's concentrations, environmental effects, and human health (Balamurugan et al., 2022; L. T. Molina, 2021; M. J. Molina & Molina, 2004).

2.2.1. Nitrogen Dioxide (NO_2) and Ozone (O_3)

NO_2 is a significant precursor to ozone formation in urban atmospheres (Balamurugan et al., 2022). In the presence of sunlight, NO_2 undergoes photolysis, releasing elemental oxygen (O), which then reacts with molecular oxygen (O_2) to form ozone (O_3):

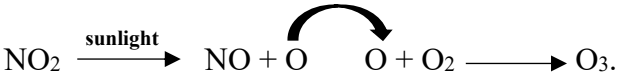

This photochemical reaction is a primary mechanism for ozone formation in urban areas. Elevated NO_2 levels, often from vehicular emissions (Degraeuwe et al., 2016), can lead to increased O_3 concentrations (Gorai et al., 2015), contributing to ground-level ozone, a major component of smog.

2.2.2. NO_2 and Particulate Matter (PM)

NO_2 is a precursor to secondary particulate matter ($PM_{2.5}$) and, under some conditions PM_{10} (Balamurugan et al., 2022). Through atmospheric reactions, NO_2 can contribute to the formation of nitrates. These reactions involve the conversion of NO_2 into nitric acid (HNO_3), which then reacts with ammonia (NH_3) to form ammonium nitrate (NH_4NO_3), a significant constituent of particulate matter (Behera et al., 2015).

2.2.3. Ozone (O_3) and Particulate Matter (PM)

Ozone can influence the chemical composition of particulate matter. For instance, O_3 can react with organic compounds in the atmosphere, forming secondary organic aerosols (SOAs), which may contribute to PM levels. These interactions are complex and depend on various factors, including other pollutants and meteorological conditions (Gu et al., 2023).

2.2.4. Carbon Dioxide (CO_2)

While CO_2 is not directly involved in forming PM or O_3, it is a significant greenhouse gas contributing to climate change, which can, in turn, affect the concentrations and behaviours of other pollutants. For example, climate change can influence atmospheric conditions, such as temperature and humidity, affecting the formation and dispersion of contaminants like O_3 and PM. Understanding these interdependencies is essential for developing effective air quality management strategies. By addressing the sources and interactions of these pollutants, policymakers can implement measures to reduce their concentrations and mitigate their adverse effects on health and the environment (Raviraja. S, 2023).

2.3. Cost of air pollution

Air pollution remains a significant environmental- and health challenge in Europe, with far-reaching economic implications. The European Environment Agency (EEA) has conducted comprehensive analyses to quantify the external costs associated with industrial air emissions, providing crucial insights into the economic burden of pollution on society .

From 2012 to 2021, the estimated external costs of industrial air emissions in Europe ranged from 2.7 to 4.3 trillion €, averaging between 268 and 428 billion € annually. These figures underscore the substantial economic impact of air pollution, with costs equivalent to approximately 2% of the European Union's GDP in 2021. While these numbers are staggering, there is a silver lining: over the decade, these costs have decreased by 33 %,

suggesting that pollution control policies have a positive effect (European Environment Agency (EEA), 2024).

Interestingly, the distribution of pollution sources is highly concentrated, with just 1.3 % of industrial facilities accounting for 50 % of the external costs caused by primary air pollutants in 2021. This concentration of pollution sources presents challenges and opportunities for targeted interventions to reduce further air pollution and its associated costs (European Environment Agency (EEA, 2024).

2.4. Health effects of NO_2

Long-term nitrogen dioxide (NO_2) exposure has been associated with significant health risks, affecting respiratory and cardiovascular systems. A 2024 systematic review reported that long-term NO_2 exposure was linked to a 3-7 % higher risk of all-cause, cardiovascular, and respiratory mortality (Xia et al., 2024). This finding is supported by a meta-analysis of over 15 long-term studies, which revealed a 5 % (95% CI: 3-8%) increase in the risk of death for every 10 µg/m^3 increase in NO_2 (Ritz et al., 2019).

Respiratory health is particularly vulnerable to NO_2 exposure. Studies have shown that long-term exposure is associated with increased incidence and exacerbation of paediatric asthma, as well as worsening asthma symptoms and airway disease (Kashtan et al., 2024). The German Environment Agency (UBA) reported that in 2014, approximately 6,000 premature deaths due to cardiovascular diseases were linked to background NO_2 concentrations in Germany (Umwelt Bundesamt, 2018).

Large-scale studies have demonstrated the cardiovascular effects of NO_2 exposure. Research using UK Biobank data showed a significant relationship between NO_2 exposure and the incidence of cardiovascular diseases (Kashtan et al., 2024). A meta-analysis found that for every 10 ppb increase in annual NO_2 concentrations, there was a 6% (95% CI: 4-8%) increase in all-cause mortality and an 11% (95% CI: 7-16%) increase in cardiovascular mortality (Kasdagli et al., 2024).

Other health outcomes of NO_2 pollution include diabetes mellitus, hypertension, stroke, and chronic obstructive pulmonary disease (COPD) (Kashtan et al., 2024; Umwelt Bundesamt, 2018). Notably, health effects have been observed at NO_2 levels below 40 µg/m^3, with a threshold value of 20 µg/m^3 suggested for confirmed health impacts (Ritz et al., 2019).

These findings underscore the urgent need for stricter air quality standards and intensified efforts to reduce emissions, especially in urban areas with heavy traffic. The health impacts of NO_2 are evident even at levels below current regulatory limits, highlighting the importance of continued research and policy action to protect public health from air pollutants.

2.5. Health effects of Ozone (O_3)

Ozone (O_3) exposure has significant health impacts, affecting respiratory and cardiovascular systems below current regulatory limits. Recent studies have provided compelling evidence of ozone exposure's short-term and long-term health effects (Donzelli & Suarez-Varela, 2024).

2.5.1. Respiratory Effects

Long-term ozone exposure is associated with accelerated lung function decline. A study involving 3,014 European adults from 17 study centers across eight countries found that a 7 $\mu g/m^3$ increase in ozone was associated with a faster decline in FEV1(Forced Expiratory Volume in 1 second) of -2.08 mL/year (95% CI: -2.79, -1.36) and in FVC (Forced Vital Capacity) of -2.86 mL/year (95% CI: -3.73, -1.99) over 20 years (Zhao et al., 2023). This decline pattern suggests a restrictive rather than an obstructive lung function impairment.

Ozone exposure also increases the risk of asthma incidence and exacerbation. A systematic review concluded that chronic exposure to ambient ozone may increase children's asthma development risk (Health Organization & Office for Europe, 2013).

2.5.2. Cardiovascular Effects and Mortality

The American Cancer Society cohort study found significant associations between long-term ozone exposure and cardiopulmonary mortality. A meta-analysis of over 15 long-term studies revealed a 5% (95% CI: 3-8%) increase in the risk of death for every 10 $\mu g/m^3$ increase in ozone (Health Organization & Office for Europe, 2013).

2.5.3. Population Impact

A recent global study estimated that 66.2 % of the worldwide population is exposed to excess ozone for short-term effects (>30 days per year), and 94.2 % suffer from long-term exposure (Y. Wang et al., 2025). This finding highlights the widespread nature of ozone pollution and its potential health impacts.

2.5.4 Sensitive Populations

Certain groups of people are more vulnerable to ozone pollution. A systematic review identified especially children, the elderly, individuals with preexisting respiratory diseases, and those with specific genetic polymorphisms as potentially more sensitive to ozone exposure (Bell et al., 2014).

2.6. Climate Change: The Urban Challenge

Cities worldwide are facing an unprecedented challenge as climate change negatively affects urban landscapes, threatening the lives and livelihoods of billions of people. The Intergovernmental Panel on Climate Change (IPCC) has painted a stark picture of how our urban centres are becoming ground zero for environmental transformation (IPCC, 2023b; IPCC AR6 SYR, 2017).

The urban heat island effect is at the heart of this climate crisis, where cities become significantly warmer than surrounding rural areas. Urban infrastructure absorbs and traps heat, with tall buildings blocking natural ventilation and urban materials acting like massive heat sinks. Studies predict that by 2050, this phenomenon will expose over a billion people in low-lying cities to unprecedented climate risks (IPCC, 2023b; Oke, 1982; Scherer & Endlicher, 2013).

The rise in temperature is not just a matter of discomfort. It is a complex threat that intertwines with air pollution, creating a toxic urban environment. Climate change is expected to increase surface ozone levels, making urban air more dangerous. In polluted cities, meteorological changes create perfect conditions for extreme air pollution episodes, putting millions of urban residents at risk (Heisler & Brazel, 2015; IPCC, 2023; Zhang et al., 2020).

Water presents another critical challenge. Urban areas are predicted to experience dramatic shifts in precipitation patterns, leading to increased flooding risks and water scarcity. Coastal cities face a double threat: rising sea levels and more intense storm surges. By 2050, an additional 350-410 million urban residents will face severe water scarcity, a number that could increase dramatically with continued global warming (Dąbrowska et al., 2023; He et al., 2021; Intergovernmental Panel on Climate Change [IPCC], 2023).

Urban areas are responsible for approximately 70% of global CO_2 emissions, creating a vicious cycle of environmental degradation. In 2020 alone, urban emissions were estimated at

29 gigatons of CO_2 equivalent, highlighting cities' critical role in the problem and potential solution (IPCC, 2023a).

The IPCC reports make one thing abundantly clear: urban adaptation is not optional but rather a most essential need. Cities must transform through innovative urban planning, green infrastructure, and climate-resilient development. This means reimagining urban spaces as living, breathing ecosystems that can adapt, mitigate, and ultimately survive the challenges of climate change.

2.7. Role of Nature-Based Solutions (NbS) in Mitigating Challenges

Nature-based Solutions: A Key Strategy for Urban Climate Resilience

In the face of accelerating climate change and rapid urbanization, cities worldwide are increasingly turning to nature-based solutions (NbS) as a critical strategy for mitigating and adapting to environmental challenges. This paper explores the role of NbS in addressing the adverse effects of climate change and anthropogenic forcings in urban areas.

2.7.1. Defining Nature-based Solutions

Nature-based solutions are defined by the International Union for Conservation of Nature (IUCN) as "actions to protect, sustainably manage and restore natural or modified ecosystems that address societal challenges effectively and adaptively, simultaneously providing human well-being and biodiversity benefits"(United Nations Environment Programme and International Union for Conservation of Nature (2021). Nature-based solutions for climate change mitigation. Nairobi and Gland., 2021). NbS encompasses various interventions in urban contexts, from urban forests and street trees to constructed wetlands, green walls, and green roofs.

2.7.2. Climate Change Mitigation through NbS

Urban trees and vegetation are crucial in mitigating climate change by acting as carbon sinks. According to the Intergovernmental Panel on Climate Change (IPCC), global urban trees collectively store approximately 7.4 billion tonnes of carbon and sequester around 217 million tonnes annually. In addition to carbon sequestration, urban green and blue infrastructure contributes to energy conservation by inducing a cooling effect, which helps lower the demand for air conditioning. This reduction in energy use decreases greenhouse gas

emissions from electricity generation and enhances urban resilience to rising temperatures (IPCC, 2022).

Nature-based solutions offer a robust and multifaceted approach to addressing climate change and anthropogenic pressures in urban areas. By harnessing the power of natural ecosystems, cities can simultaneously mitigate climate change, enhance resilience, and improve the quality of life for urban residents. As urbanization continues to accelerate, integrating NbS into urban planning and development will be crucial for creating sustainable, resilient cities of the future (Maes & Jacobs, 2017; Prigioniero et al., 2021).

2.8. The History of Facade Greening

Façade greening—the integration of vegetation into building exteriors—has deep historical roots dating back to ancient civilizations, with the Hanging Gardens of Babylon (circa 600 BC) as a symbolic early example (Häffner, n.d.; *Romanesque / Gothic : Greening of Buildings in the Middle Ages: Fassadengruen*, n.d.). In the Middle Ages, monasteries cultivated vines along stone walls, harnessing thermal mass for improved crop growth. At the same time, the Renaissance and Baroque periods brought a decorative revival with ivy and fruit-bearing climbers adorning castles and estates (Häffner, n.d.). During the 18th and 19th centuries, classical architecture featured greening as a visual enhancement, exemplified by Karl Friedrich Schinkel's works in Sanssouci Park. The early 20th century saw a surge in functional greening through the garden city movement, notably in Leipzig's Marienbrunn district, where climbing aids supported wild vines. Landscape architect Leberecht Migge championed fruit trellises to blend architecture with nature and promote urban self-sufficiency (Romanesque / Gothic, n.d.). The environmental awareness of the late 20th century shifted focus to façade greening's ecological functions, prompting empirical research on its thermal and moisture-regulating impacts. The practice has advanced in recent decades with green facades rooted in the ground or containers and high-tech living wall systems with modular panels (Häffner, n.d.; Köhler, 2008). Today, façade greening is widely recognized not only for its aesthetic and cultural value but also for its contributions to urban biodiversity, energy efficiency, and climate resilience, including mitigation of the urban heat island effect (Boyano et al., 2013; Gawronski, 2016; Hoelscher et al., 2016; Pérez et al., 2014; Pettit et al., 2018; B. Zhang et al., 2020).

This historical progression demonstrates how facade greening has evolved from ancient decorative and agricultural practices to a multifunctional approach addressing modern urban and environmental challenges.

2.8.6. The Abundance of Vertical Surfaces for Greening in Urban Environments

Urban environments are characterized by a significant amount of vertical surface area on buildings, presenting a vast opportunity for vertical greening. Several researchers have recognized and studied this concept in urban ecology and green infrastructure.

Manfred Köhler, a prominent researcher in green roofs and facades, has highlighted the potential of vertical surfaces for greening. In his work, Köhler defines green or greened façades as typically covered with woody or herbaceous climbers planted into the ground or in planter boxes (Köhler, 2008).This definition underscores the availability of vertical building surfaces as potential greening areas, making climbers a unique category of plant for this type of vertical greening.

2.9. Research on climbers used in façade greening.

climbing plants have emerged as a promising solution to various urban challenges. Their adaptive vertical growth habit on wall surfaces maximizes space utilization in densely populated cities, making them ideal for green infrastructure projects. While extensive research has been conducted on climbers' cooling potential and other ecological benefits, a notable knowledge gap exists regarding their air phytoremediation potential.

Several studies have demonstrated the cooling effects of climbers in urban environments. For instance, research on three evergreen climbing plants *(Hedera nepalensis var. sinensis*, *Ficus pumila, and Euonymus fortunei*) showed significant particulate matter (PM) adsorption capabilities, with *H. nepalensis* exhibiting the highest adsorption capacity. These climbers also demonstrated seasonal variations in PM adsorption, with winter showing the highest rates, followed by autumn, spring, and summer (Lyu et al., 2023a).

The thermal benefits of climber green walls have been attributed to shading, evapotranspiration, and insulation (L. S. H. Lee & Jim, 2019). These mechanisms create Park Cool Islands (PCI), where urban green spaces, including those with climbers, are generally cooler than their surroundings (Reis & Lopes, 2019).

However, the air phytoremediation potential of climbers remains understudied. While all plants perform phytoremediation to some extent, their efficiency varies. The potential for climbers in air phytoremediation could be significant, given their adaptive climbing abilities, vertical growth, and large, enormous potential vertical surface area existing in the urban landscape. Research has shown that vegetation, including climbers, can accumulate pollutants like chromium from the air, indicating their potential for air purification (Gawroński, 2023). Studies have shown that botanical systems have a high potential for formaldehyde removal, with up to 20% removal per pass of air over the plant (Bandehali et al., 2021).

In conclusion, while climbers have shown promise in urban cooling and particulate matter adsorption, there is a significant knowledge gap in understanding their full specific potential for air phytoremediation in urban environments. This gap presents an opportunity for future research to explore the efficiency of different climber species in removing various air pollutants, their performance compared to other plant types, and their potential for large-scale implementation in urban air quality improvement strategies.

3.0 Preface to the paper: **"Methodology for the quantification of the absorption potential of greenhouse - and pollutant gases by climbing plants used in façade greening: a case study on ivy (*Hedera helix*)".**

This study introduces a precise and replicable methodology to quantify the absorption potential of greenhouse and pollutant gases by climbing plants, using *H. helix* "Plattensee" as a case study. The experimental setup involved a custom-built reaction chamber with a regulated light cycle and synthetic air flow, enabling controlled observation of plant–gas interactions under illuminated and dark conditions. Advanced spectroscopic instruments—a mid-infrared laser absorption spectrometer (MIRO) and a cavity-ring-down spectrometer (PICARRO)—were employed to measure the decay of gases injected into the chamber.

To evaluate the plant-specific effects, nitrous oxide (N_2O)—a stable, non-reactive greenhouse gas in the troposphere—was used as a reference. The comparative analysis revealed that nitrogen dioxide (NO_2) exhibited significantly shorter residence times during illuminated periods, indicating active uptake by the plant likely facilitated through open stomata since this effect was only observed during light conditions. In contrast, N_2O and NO showed little to no interaction with the plant, highlighting the selectivity of this absorption behaviour.

The concept of deposition velocity was applied to quantify the gas flux per unit leaf area, offering a standardized metric to compare the plant's air phytoremediation potential. The findings confirmed that *H. helix* can substantially reduce NO_2 concentrations under light, reinforcing its potential role in improving urban air quality.

This methodology enables species-specific analysis of gas absorption and provides a valuable framework for future studies assessing the ecological benefits of façade greening. As cities seek scalable Nature-Based Solutions to mitigate pollution and adapt to climate change, this approach offers critical insights into the functional role of climbing plants in urban environments.

3.0 Methodology for the quantification of the absorption potential of greenhouse - and pollutant gases by climbing plants used in façade greening; a case study on ivy (*Hedera helix*).

Journal article published: Environmental Advances:

Aduse-Poku, M., Rohrer, F., Winter, B., & Edelmann, H. G. (2024). Methodology for the quantification of the absorption potential of greenhouse - and pollutant gases by climbing plants used in façade greening; a case study on ivy (Hedera helix). Environmental Advances, 17, 100568. https://doi.org/10.1016/j.envadv.2024.100568.

Environmental Advances 17 (2024) 100568

Contents lists available at ScienceDirect

Environmental Advances

journal homepage: www.sciencedirect.com/journal/environmental-advances

Methodology for the quantification of the absorption potential of greenhouse - and pollutant gases by climbing plants used in façade greening; a case study on ivy (*Hedera helix)*

Minka Aduse-Poku [a], Franz Rohrer [b], Benjamin Winter [b], Hans G. Edelmann [a,*]

[a] Universität Köln, Institut für Biologiedidaktik, Herbert-Lewin-Str. 2, 50931 Köln
[b] Forschungszentrum Jülich, Institut IEK-8: Troposphäre, 52428 Jülich, Germany

ARTICLE INFO

Keywords:
Hedera helix
Air phytoremediation
Climbing plants
Time scale decay
Residence time
Reactivity
Deposition velocity
Nitrogen dioxide (NO_2)

ABSTRACT

How much do specific climbing plants contribute to the cleansing or absorption of harmful greenhouse and pollutant gases; often regarded as the main environmental threat in cities due to their adverse effects on human health? One of the main hurdles in the quantification of such ecosystem services is associated with the difficulty to obtain and design systems that provide detailed information on the interaction between various gases and the plant in question. To tackle these questions, two highly precise and accurate instruments, namely a mid-infrared laser absorption spectrometer (TDL) and a cavity-ring-down spectrometer (CRDS) were used to monitor the fate of gases when exposed to façade climbing plants like ivy. In a laboratory setting, a relaxation type of experiment was used consisting of a reaction chamber equipped with plant species and continuously flushed by synthetic air. This setup was used to determine the timescales of decay after short injections of the above-mentioned gases. After these injections, all gases followed simple exponential decay curves. N_2O, a non-reactive (inert) tropospheric gas, was used as a reference to which all other gases were compared and thereby quantified. This paper focuses on the detailed description of methods and processes to analyse the gas-absorptive behaviour of plants when exposed to gaseous pollutants. For demonstration purposes, quantified absorption features of nitrogen oxide (NO_2) are presented for ivy of the variety *Hedera helix* "Plattensee". Results of this method of quantification showed that - as compared to N_2O (control), - NO_2 had a reduced residence time (time scale) of 100 s, while N_2O resulted in a 600 s residence time (indicating no interference with the plant). This is equivalent to a 0.3 cm/s deposition velocity/ absorption rate of NO_2 under light conditions.

1. Introduction

Cities increasingly face some of the most challenging issues in contemporary times as a result of climate change. For example, cities have to deal with heat waves, frequent droughts, flooding, and urban heat islands, to name a few. The already stressed city environment faces an additional challenge from its air quality, which has additional detrimental impacts on the health of its inhabitants (Hernandez Carballo, et al., 2022; Juginović, et al., 2021; Mele, et al., 2021; WHO, 2019). The European Union attributes for 2019 40400 premature deaths per year in the 27 EU Member States to chronic nitrogen dioxide ("Health impacts of air pollution in Europe, 2021," 2021). Phytoremediation, the removal of toxic and harmful compounds by plants, can sustainably help to improve air quality. Along with an ever-increasing incidence of soil sealing (Szumacher and Pabjanek, 2017), especially in inner cities, subsurface infrastructure, and the built environment have made the inclusion of trees in many urban sites difficult. Wall-bound climbers are increasingly being valued as a workable Nature-Based-Solution that can provide air phytoremediation.

There is ample evidence showing different absorption potentials of greenhouse- and pollutant gases in some woody plant species (Takahashi et al., 2005). However, information on the air phytoremediation potentials of commonly used climbers in façade greening is limited.

Given the heterogeneous distribution of air pollutants in the built environment (Zhang et al., 2017), a differentiated, scientific approach toward species-based air phytoremediation is required. This paper concentrates and presents the methodology used in the estimation of the

* Corresponding author at: Institut für Biologiedidaktik, Universität zu Köln, 50931 Köln.
E-mail address: h.edelmann@uni-koeln.de (H.G. Edelmann).

https://doi.org/10.1016/j.envadv.2024.100568
Received 8 January 2024; Received in revised form 28 June 2024; Accepted 4 July 2024
Available online 14 July 2024

greenhouse and pollutant gas absorption potential of a common climber species; namely *Hedera helix "Plattensee"*. In a follow-up paper we will compare two additional species (*Clematis montana, Lonicera henryi*).

2. Experiment

2.1. Experimental design

A graphical representation of the instrumental setup is shown below with the ivy subspecies "Plattensee" as an example. The plants were placed in a reaction chamber and subjected to a day-night cycle using an LED lamp. The illuminated phase (day) of the experiments ranged from 9 am to 6 pm, after which the lights were switched off for the dark phase (night). The operating temperature in the chamber has been monitored using a temperature sensor called "ibutton" (Hygrochron data logger) averaging 24°C+- 2°C.

The outflow of a gas mixing unit was directed into the fifty-three litre (53 L) rectangular glass chamber (later on called reaction chamber) in which the plant species were placed for the experiments. The reaction chamber was covered with a plexiglass lid and connected to the mass flow and injection controller box (regulating magnetic three-way-valves and mass flow controllers, see Fig. 1), delivering synthetic air spiked either with the contents of gas bottles or spiked with ambient air at an inflow rate of 5 L/min for the experiments discussed in this paper, respectively 10 L/min for subsequent experiments. Within the reaction chamber, there was a ventilator to ensure fast mixing of gases inside. To exclude any contamination from outside air during the experiment, the lid was sealed tightly. The outflow of the reaction chamber was fed towards the monitoring instruments (MIRO & PICARRO) through connecting tubes. These instruments took a total of 2 L/min from the outflow. The spill over of 3 L/min (at 5 L/min air flow) and the exhaust of the instruments was directed to a common exhaust line out of the laboratory.

2.2. Plant species

The plants used in the experiment were contributed by a plant breeder in the Cologne area (Containerbaumschule + Stauden Michael Kunz, Wusten 2, 42579 Heiligenhaus, Germany). All plants were transplanted into equal size pots with the same type of substrate to ensure uniformity.

Selected plants mentioned above were kept at their field capacity and covered with an expandable plastic film which was stretched to cover the substrate with the plant in the middle, and held around the plant to prevent direct loss of water from the substrate Fig. 2.

2.3. Light source

At the level of the lid of the reaction chamber, a constant illumination of approximately 25 klx (measured with a WinLab luxmeter) or PPFD (Photosynthetically Active Photon Flux Density) of 950 μmol s^{-1} m^{-2} (Photon System Instruments FluorPen FP110-LM/S) was provided by a photosynthetic LED lamp (Niello G 600) during the illuminated phase of the experiment. The transparency of the Plexiglas lid was determined to be about 92 % for the light source. The properties and spectrum of the light source are provided in Fig. 3 below.

2.4. Instrumentation

The main instrumentation consisted of a mid-infrared direct laser absorption spectrometer (MIRO Analytical AG, Wallisellen CH-8304, Switzerland; type MGA10 - GP+) and a cavity-ring-down spectrometer (Picarro Inc. Santa Clara, CA 95054, USA; type G2307). The MIRO instrument is a tunable-diode-laser system with five QCL-lasers observing absorption lines of 10 species. This gas analyser can simultaneously measure 10 greenhouse and pollutant gases, namely: carbon dioxide (CO_2), carbon monoxide (CO), nitrogen monoxide (NO), nitrogen dioxide (NO_2), nitrous oxide (N_2O), nitric acid (HONO), ozone (O_3), carbonyl sulfide (OCS), ammonia (NH_3), and water vapour ($H_2O_{(g)}$). In

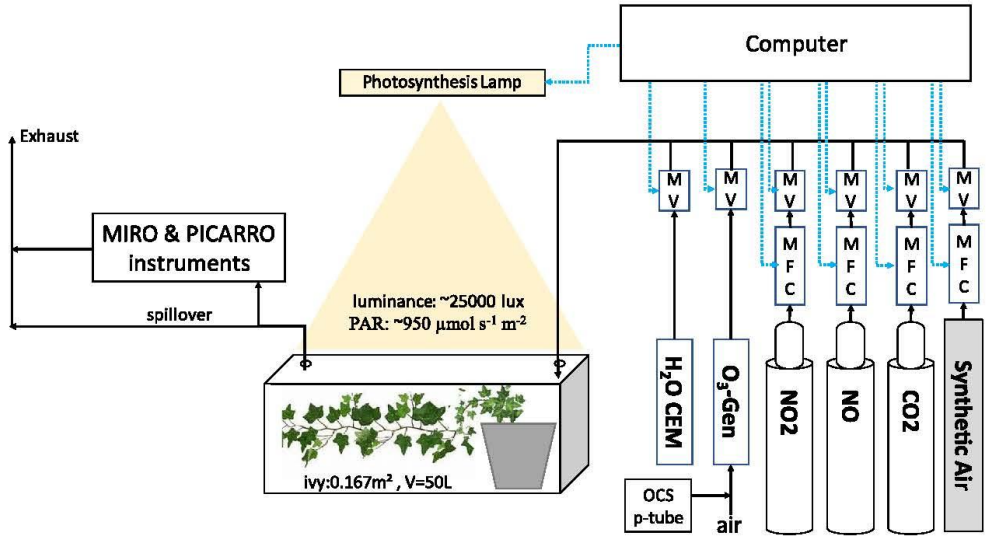

Fig. 1. Experimental setup (with an ivy plant) for the greenhouse and pollutant gas absorption experiment. The reaction chamber (outside dimensions 30 cm*30 cm*60 cm) incorporates a ventilator and a temperature sensor. The volume is 53 L without and 50 L with the deployed plant. The constant volume flow rates of synthetic air through the reaction chamber were 5 L/min in this example, and 10 L/min was used in other subsequent experiments to optimize the experimental outcome. The term "MFC" denotes mass flow controllers and "MV" magnetic three-way-valves. The leaf area of 0.167 m^2 given in this figure relates to a specimen of the ivy variety Hedera helix "Plattensee".

Fig. 2. Plants used in the experiment were watered and after 2 days taken for measurements (at field capacity).

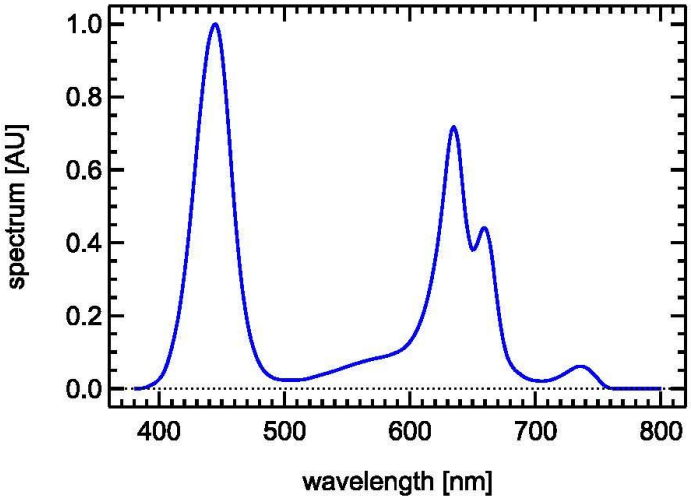

Fig. 3. Properties and spectrum of the photosynthetic 600W LED-lamp used for illumination, 41,1 × 26,7 × 6,5cm type Niello GS-600, Epileds Technologies Inc, No.7 Kanxi Road, Xinshi District, Tainan 744, Taiwan. The spectrum was traced using an illustration supplied by the manufacturer.

some experiments, a Picarro G2307spectrometer was additionally used to determine the concentrations of formaldehyde (HCHO) and methane (CH_4). The principal time resolution of the instruments is 1 s both for the MIRO and for the PICARRO. The detection limits for the different species are given in Table 1.

2.5. The mass flow control unit

This unit controls a constant addition of 5 L/min synthetic air into the reaction chamber and the spiking of intended species following a repeated time schedule. Spiking was done at each full hour XX:00 (XX = any hour of the day) for 3 min with NO, NO_2, CO_2 from gas bottles (containing 10 ppm NO in N_2 from Air Liquid, 500 ppm NO_2 in N_2 from Praxair, 100 % CO_2 from Air Products)

- at each half hour XX:30 for ten minutes with ambient air (containing H_2O, N_2O, CH_4, NO_2, HCHO, CO, CO_2, and OCS) with added O_3 from an ozone generator and extra OCS from a permeation tube.

The synthetic air was produced by mixing evaporated N_2 and O_2 from liquid N_2 and O_2 reservoirs by the gas supply unit of the SAPHIR chamber (Simulation of Atmospheric Photochemistry In a large Reaction

Table 1
Detection limits (2 sigma) at 60s integration time and legally permitted limit values in the European Union.

MIRO (for O_3 and NO_2:1 ppb ≈ 2 μg/m^3)							PICARRO		
CO	CO_2	H_2O	O_3	NO	NO_2	OCS	HCHO	CH_4	H_2O
ppb	Ppm	%abs	ppb	ppb	ppb	ppb	ppb	ppm	%abs
0.03	0.05	0.0005	0.25	0.1	0.03	0.004	0.25	0.005	0.001
global tropospheric concentrations									
100	424	varies	20-60	0-500	0-500	0.5	5-30	1.875	varies
urban concentration limits (European Union - 2010)									
			Maximum daily 8-h mean: 120 μg/m^3		Yearly mean: 40 μg/m^3				

chamber) of the Research Centre Jülich. The synthetic air flow could be enriched with several gases each from gas bottles with the help of flow-controllers (MFC) and magnetic three-way valves (MV, Fluoroware Inc.). Other gases like N_2O were added by using their presence in ambient air which was pushed into the synthetic air flow by an ozone generator with an attached permeation tube for OCS. The used three-way magnetic valves each had two directions, one into a common exhaust line, and the other into the synthetic air flow. The flow controllers were purchased from Bronkhorst Deutschland Nord GmbH, 59174 Kamen, GERMANY, and were of type EL-FLOW. They provided in each case a constant predetermined mass flow of gas in accordance to a temperature of 0°C and a pressure of 1013 mbar. Also, gaseous H_2O could be provided by evaporating purified liquid water by a humidification system from Bronkhorst model "CEM Evaporator W-102A". The Ozone generator labelled "O3-Gen" in Fig. 1 was obtained from 2 B Technologies, Broomfield, CO 80020, USA, model 306 "Ozone Calibration Source". This ozone generator pushed ambient air through a quartz tube adding a selectable amount of ozone by illumination with UV light provided by a Pen-Ray Mercury lamp. The very same air also was enriched with OCS from a permeation tube (Fine Metrology S.r.l.s., 98048 Spadafora, Italy).

2.6. Determination of gas exchange parameters of the plants

2.6.1. Mathematical background

The described experimental setup with a glass chamber, stirred by a ventilator, flushed with a fixed inflow and adequate air outflow represents a so-called "continuously stirred tank reactor". This means that

a) there will be no concentration gradients inside the chamber since the ventilator is mixing all gaseous compounds within seconds, and
b) the concentration of a gas inside the chamber outflow line will be equal to its concentration inside the chamber.

For such an ideal reactor one can set-up the budget for input and output terms of the chamber as follows:

$$\frac{\partial \boldsymbol{X}(\boldsymbol{t})}{\partial \boldsymbol{t}} = \left(\boldsymbol{P\_Inj} + \boldsymbol{P\_plant}\right) - \left(\boldsymbol{D\_plants} + \boldsymbol{D\_surface} + \boldsymbol{D\_DIL}\right) \cdot \boldsymbol{X}(\boldsymbol{t}) \quad (1)$$

X:	*compound of interest*
t:	*time*
P_Inj:	*production rate by dedicated injection of X*
P_plant:	*production rate of X by the plants*
D_plants:	*loss rate coefficient due to removal by the plants*
D_surf:	*loss rate coefficient for removal at the surfaces of the chamber*
D_DIL:	*loss rate coefficient for dilution inside the chamber due to inflow of synthetic air*

$\partial X(t)/\partial t$ denotes the concentration change of a compound X at time t in the reactor which is reflected in the outflow monitored by the instruments. The loss processes inside the chamber are treated here as first order in X. The loss rate coefficients themselves will depend on boundary conditions, namely the internal surface area of the 6 walls of the reaction chamber, the leaf area, the inflow rate of synthetic air, and the volume of the chamber. For a given experiment they can be treated as a constant with unit "s^{-1}". These loss rate coefficients are often called "reactivity". The reciprocal of a loss rate coefficient is called a timescale with the unit "seconds" and denotes the residence time of a substance with respect to a certain process. A timescale is often abbreviated with the letter τ. The above Eq. 1 can be simplified to

$$\frac{\partial \boldsymbol{X}(\boldsymbol{t})}{\partial \boldsymbol{t}} = \boldsymbol{P} - \boldsymbol{D} \cdot \boldsymbol{X}(\boldsymbol{t}) \quad (2)$$

by adding up the individual production and loss terms: *P=P_Inj+P_plant and D= D_plants+D_surface+D_DIL*. The general solution of this first-order partial differential Eq. 2 is

$$\boldsymbol{X}(\boldsymbol{t}) = \left(\boldsymbol{X}(\boldsymbol{t}=0) - \frac{\boldsymbol{P}}{\boldsymbol{D}}\right) \cdot \boldsymbol{e}^{-\boldsymbol{D}\cdot\boldsymbol{t}} + \frac{\boldsymbol{P}}{\boldsymbol{D}} \quad (3)$$

X(t=0) denotes here the starting concentration at time *t=0*. In the special case that *P_Inj* is zero, for example taking the only the time interval just after the injection is finished, Eq. 3 simplifies to

$$\boldsymbol{X}(\boldsymbol{t}) = \left(\boldsymbol{X}(\boldsymbol{t}=0) - \frac{\boldsymbol{P\_plant}}{\boldsymbol{D}}\right) \cdot \boldsymbol{e}^{-\boldsymbol{D}\cdot\boldsymbol{t}} + \frac{\boldsymbol{P\_plant}}{\boldsymbol{D}} \quad (4)$$

In the long term limit $t\to\infty$, $X(t)$ simplifies to a stable value $X(t\to\infty) = P\_plant/D$. This means that after an injection is over, the concentration of X approaches a steady state in the long term if the boundary conditions are kept constant. For the practical issue of fitting the experimental results Eq. 4 can be taken as a three-parameter function of the form

$$\boldsymbol{A}(\boldsymbol{t}) = \boldsymbol{A}0 \cdot \boldsymbol{e}^{-\boldsymbol{t}/\tau} + \boldsymbol{offset} \quad (5)$$

with *A0=(X(t=0) – P_plant/D)*, τ*=1/D*, and *offset=P_plant /D* as defined in Eq. 4. The parameter τ can be understood as the residence time of a molecule inside the reaction chamber. The determination of the parameters *A0*, τ, and *offset* has been done iteratively using a Levenberg-Marquardt algorithm. After each injection of substances, either at the full hour or at the half-hour, the observations of the different species were taken for time intervals of 20 min and were fitted to Eq. 5. The visual inspection of all these observations showed that the decay of the species after injection followed closely the form given in Eq. 5 most of the time except for a few cases when the illumination was switched on or off within the analysed time intervals of 20min. Then, the observed time series of some of the species were more complex since the parameter *D_plant* was not constant in that time frame due to the opening or closure of the stomata of the leaves. These few time points were excluded from analysis since the fitting procedure could not resolve these more complicated decays.

The concept of residence time describes how fast a gas molecule remains in a given setting or system before being eliminated or changed. To show the performance of the described algorithm, one of the species examined (*Hedera helix* "Plattensee") was used for the analysis of NO_2 absorption.

2.6.2. Determination of residence time and time scale

The theoretical residence time of a species inside the empty chamber with a constant inflow rate of 5 L/min is given by dividing the volume of the rectangular chamber with the flow rate. The residence time is thus 53 (L)/5(L/min) =10.6 min or 636 seconds for the empty reaction chamber. However, the air volume within the rectangular glass chamber is subject to change after the introduction of a plant, thus the volume would be the actual air volume (53 L minus the volume of the plant and flowerpot). A smaller volume after the plants are introduced will reduce the residence time of the gases inside the chamber, which in this example with the ivy plant was determined to be about 3 L. This implies a residence time of about 50 (L)/5 (L/min) = 10 min=600 s. To take any change in the exact flow rates, temperature, and plant/flowerpot volume into account, we looked at the observed decay of gases which seems to react neither with the chamber surface nor with the plant/flowerpot. Such a gas can serve as a reference for the residence time. Nitrous Oxide (N_2O) is a fairly stable greenhouse gas with an atmospheric lifetime of 123 years (Prather et al., 2015). In the troposphere, N_2O can be treated as an inert noble gas. Thus, N_2O will not be absorbed by plants and will pass through the reaction chamber unchanged. N_2O can be used to correct the effect of the plant/flowerpot on the effective volume of the reaction chamber and also to account for any effect of a temperature change on the gas density during the experiments.

The experiments involved the injection of NO, NO_2, and CO_2 from gas cylinders, OCS from a permeation tube, and O_3 from an Ozone

generator using a pen-ray UV lamp. N_2O, H_2O, CH_4, and CO were either introduced into the reaction chamber by flushing-in ambient air or, in the case of H_2O, as a result of transpiration of the plants. For this study, the quantitative determination of the absorption of NO_2 by façade climbing plants is the main intent. NO_2 is one of the major pollutants with major emissions from vehicular traffic (Ehlers et al., 2016). Since traffic emissions are often released in close proximity to humans and often lead to hot spots of local pollution in inner city districts (Ehlers et al., 2016), they are contributing to health problems and loss of life on a global scale. Façade greening at least has the potential to improve air quality exactly at these pollution hot spots.

2.7. Leaf area

At the end of the series of experiments, all leaves were removed from a plant. The total weight of all the leaves was then determined and related to the area of five individual leaves by cutting out and weighing equivalent pieces of paper of known grammage. The mean ratio of mass/area of one of the leaves was then used to extrapolate the total area of the leaves of the investigated plant.

3. Results

Fig. 4 and Fig. 5 present the observed concentration time series of N_2O and NO_2 for repeated injections of N_2O at XX:30 and NO_2 at XX:00 hours for a full day. In Fig. 4, N_2O shows very homogeneous injection peaks in width and height for the illuminated and the dark interval since the plant does not interact with N_2O. NO_2 in Fig. 5, on the other hand, behaves differently. During the illuminated interval, the peaks are less high and narrower, which is due to the instantaneous absorption of NO_2 by the plant.

For comparison, Figs. 6 and Fig. 7 show simulated concentration profiles for N_2O and NO_2 using Eq. 4 with a fixed injection rate (P_inj>0) during the time interval of injection and a fixed degradation rate for N_2O. For a realistic simulation, two fixed degradation rates for NO_2 were required, one for the illuminated and the other for the dark phase of the experiment. The peak heights and widths in both observed and simulated results show the effect of the plant on the degradation of both, NO_2 and N_2O. Due to faster degradation during the illuminated time periods, the peak heights and widths for NO_2 are smaller compared to the dark periods. In the N_2O observations, there is a small variability of the peak heights caused by changes in the N_2O content of ambient air over the day which was used for the N_2O injection at each XX:30 h. The similarity between observed and simulated concentration profiles is striking especially if one considers that besides the exact injection times, only two fixed parameters were used for N_2O ($P\_inj(N_2O)$, $D(N_2O)$) and three fixed parameters for NO_2 ($P\_inj(NO_2)$, $D(NO_2, dark)$, and $D(NO_2, illuminated)$).

Fig. 8 shows a closer, high temporal resolution look at one of the ½ h intervals. Within the injection period, the concentration of the species is climbing until the injection is stopped. After this culmination point, the decay is starting. The time between the peak concentration until the beginning of the next injection is used for the analysis fitting the observed data points to Eq. 5.

For every injection period the above explained methods and processes are repeated for each decay curve under both the light and dark phases of the experiment. Results of this fitting procedure for *Hedera helix* "Plattensee" are presented in Fig. 9 and Fig. 10 below. The observed removal of gases after each injection interval followed single exponential decay curves as expressed in Eq. 5. This is expressed in Fig. 10 with logarithmic Y-axis, where the data points appear to lie on a straight line.

The above-described methodology is repeated for each injection over a 24 h period to obtain the sequence of the parameter "timescale" (see Fig. 11). It is important to note that the change in the parameter timescale of NO_2 due to illumination is not directly related to the gas phase reaction $NO_2+O_2 \rightarrow$UV-light$\rightarrow NO+O_3$, the well-known photolysis of NO_2 producing NO and O_3. The amount of UV-light emitted by the LED-

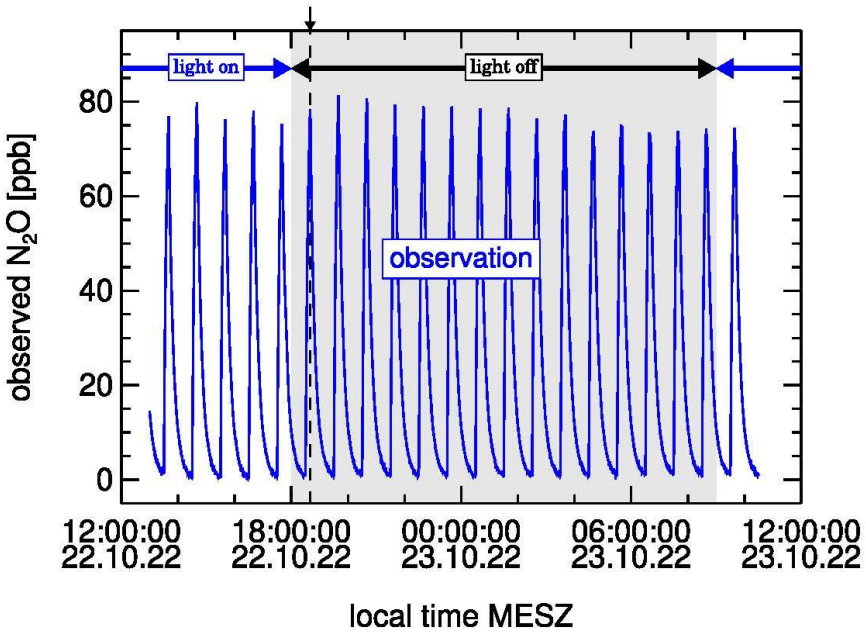

Fig. 4. Observed time series of N_2O showing repeated injections and the almost constant decays with equal peaks heights and widths over 24 h for a Hedera Helix "Plattensee" specimen. The vertical dashed line and the vertical arrow denote the position of the time period shown in Fig. 9 and Fig. 10.

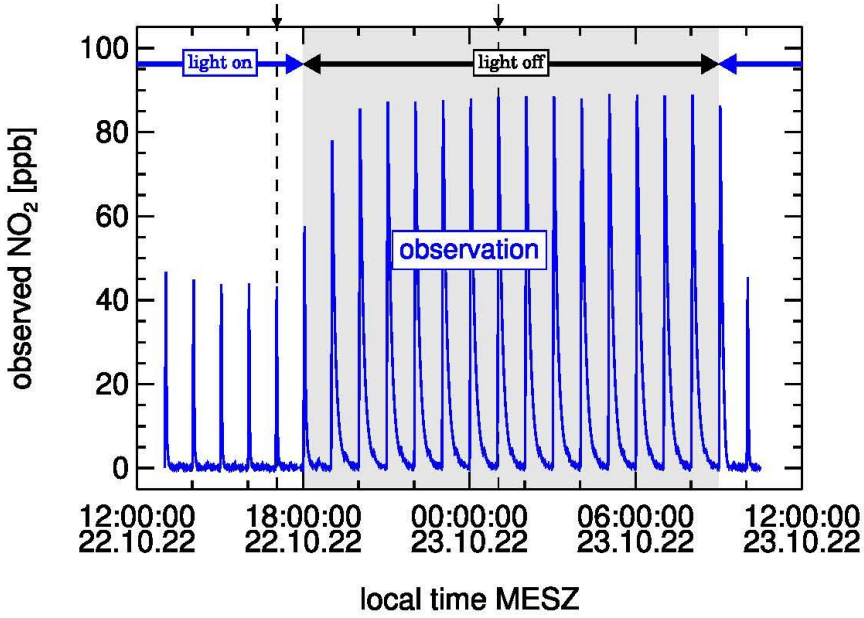

Fig. 5. The decay of NO_2 showing a repeated decay trend with more pronounced absorption with smaller peaks heights and narrower widths at identical injection amounts during the illuminated phase for a Hedera Helix "Plattensee" specimen. The vertical dashed lines and the vertical arrows denote the positions of the time periods shown in Figs. 9 and Fig. 10.

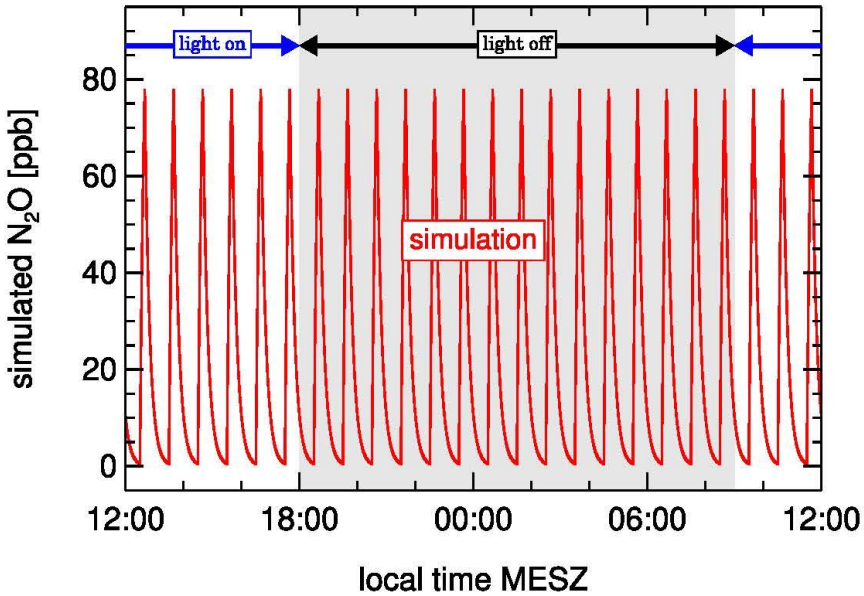

Fig. 6. Simulated (following Eq. 5) time series of N_2O obtained for repeated identical injections and constant decay with τ 600 s. A constant N_2O injection rate P_inj 46.8 ppb/min was selected for all injection intervals to be consistent to the observed average N_2O-value in Fig. 4. P_plant was kept to zero at all times.

lamp is not large enough to activate this photolysis process. Rather, the observed effect depends on an interaction between the plant inside the reaction chamber and the gas phase containing NO_2. This is demonstrated by a separate experiment shown in Figure S1 showing the illumination of a NO_2-containing air mixture in the empty reaction chamber. No effect of light from the LED-lamp could be detected for this

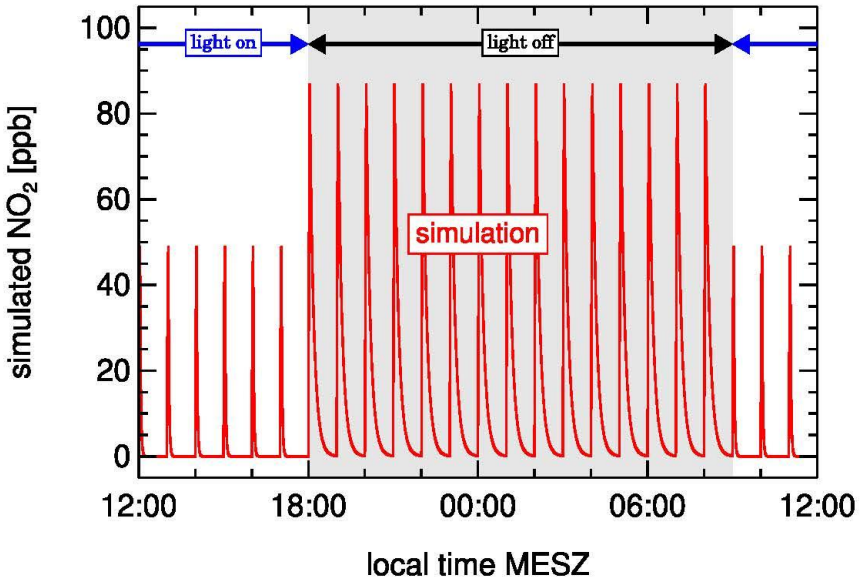

Fig. 7. Simulated (following Eq. 5) time series of NO_2 obtained for repeated identical injections and constant decay with τ 520 s for dark and τ 100s for illuminated periods. A constant NO_2 injection rate P_inj 52.5 ppb/min was selected for all injection intervals to be consistent to the observed NO_2-values in the dark period in Fig. 5. P_plant was kept to zero at all times.

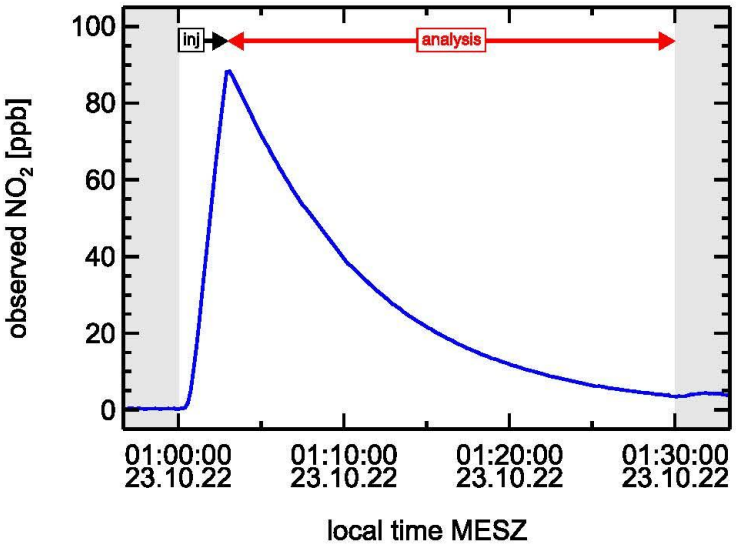

Fig. 8. Zoomed ½ h time interval from Fig. 5 showing the injection period (labeled "inj") and the time frame used for the determination of the exponential decay parameters (labeled "analysis") for the injection of NO_2 starting at 01:00 23.10.2022 MESZ.

condition without the presence of the ivy plant.

3.1. Reactivity and deposition velocity

The reactivity, given here as D=1/τ (where τ = timescale, see Fig. 11–y-axis, and Eqs. 1-5), is a measure of the overall degree to which the plants absorbed or altered a particular greenhouse- or pollutant gas.

From the definition D=D_plant+D_surface+D_DIL follows

$$\frac{1}{\tau_{observed}} = \frac{1}{\tau_{plant}} + \frac{1}{\tau_{surface}} + \frac{1}{\tau_{DIL}} \quad (6)$$

This implies that the reactivity of the plant versus a species like NO_2 can be calculated from the observations of this species and N_2O:

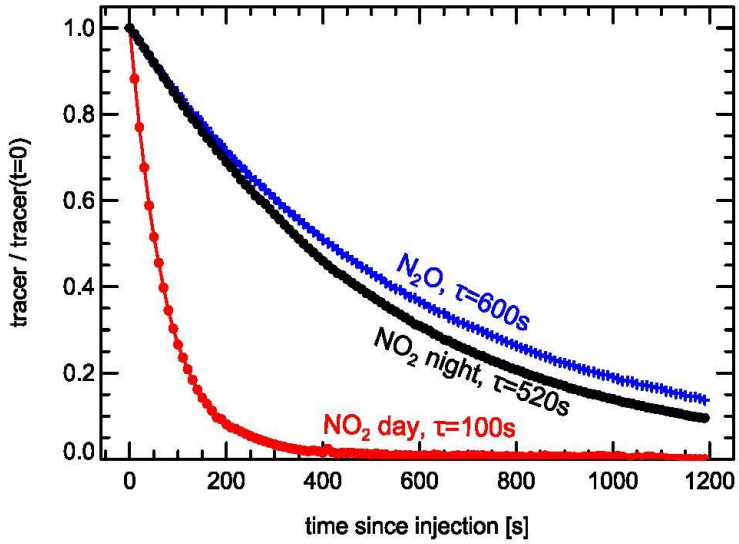

Fig. 9. Time scale decay of observed N_2O (18:40:00 22.10.2022) and NO_2 during illuminated (17:03 22.10.2022) and dark (01:03 23.10.2022) phases of the experiment The tracer concentrations are scaled to the concentrations at the end of the respective injection intervals and are shown here on a linear Y-axis.

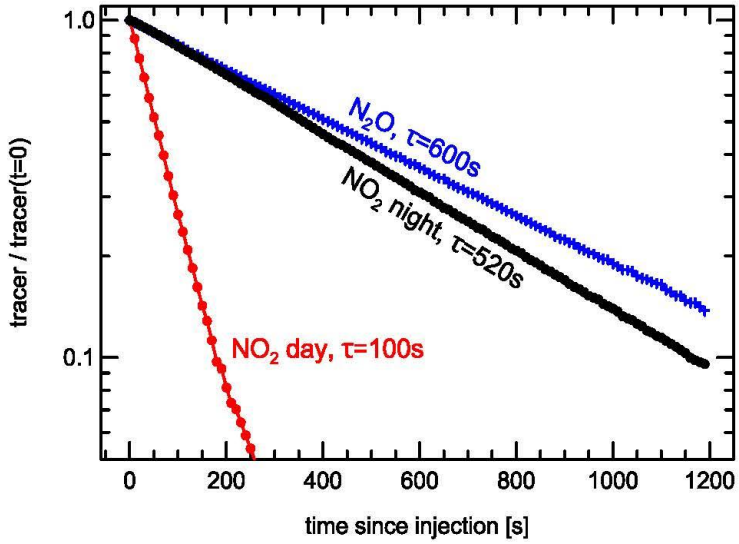

Fig. 10. Logarithmic time scale decay of observed N_2O (18:40:00 22.10.2022) and NO_2 during illuminated (17:03 22.10.2022) and dark (01:03 23.10.2022) phases of the experiment. The tracer concentrations are scaled to the concentrations at the end of the respective injection intervals.

$$D_{plant,NO_2} = \frac{1}{\tau_{observed,NO_2}} - \left(\frac{1}{\tau_{surface,NO_2}} + \frac{1}{\tau_{DIL,NO_2}}\right) = \frac{1}{\tau_{observed,NO_2}} - \frac{1}{\tau_{observed,N_2O}} \quad (7)$$

Eq. 7 uses N_2O as a reference to which the observed timescales of NO_2 and NO are compared to account for the effect of dilution, temperature variations, and the exact volume of the reaction chamber equipped with flowerpot and plant. In a separate experiment without a plant, NO_2 showed the same residence time as N_2O, so $\tau_{surface,NO_2} = 0$ and $\tau_{DIL,NO_2} = \tau_{DIL,N_2O}$. The obtained reactivities of the plant, D_{plant,NO_2} and $D_{plant,NO}$, then can be scaled by the leaf area LA and the effective volume of the reaction chamber VOL_{RC} to produce the deposition velocity (Seinfeld, 1986) v_{dep} of the plant for NO_2 and NO which describes the flux density F at a certain concentration c_{gas} of the gas of interest Fig. 12:

$$F = v_{dep} \cdot c_{gas} = \frac{D_{plant} \cdot VOL_{RC}}{LA} \cdot c_{gas} \quad (8)$$

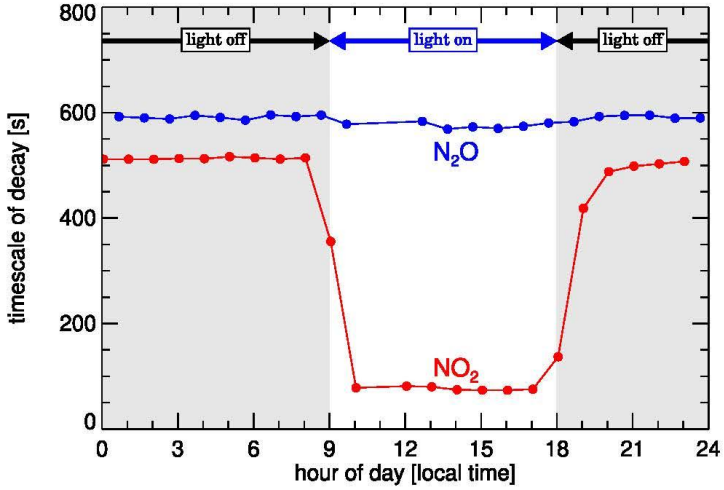

Fig. 11. Diurnal variations of the timescale-of-decay for N_2O and NO_2 using the ivy variety Hedera helix "Plattensee"

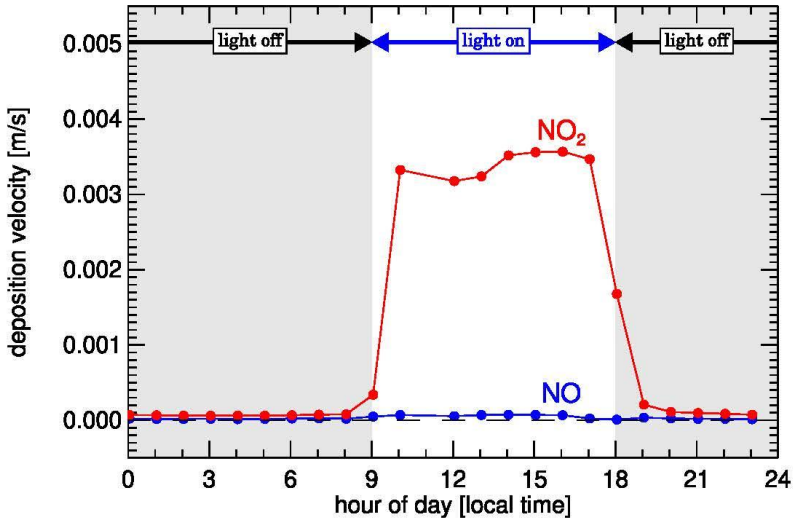

Fig. 12. Deposition velocity (relating reactivity (1/s) to leaf area (m^2) and chamber volume (m^3), see Eq. 8) of NO and NO_2 showing a strong absorption of NO_2 during the illuminated time period but none for NO during an experiment with the ivy variety Hedera helix "Plattensee."

The parameter "deposition velocity" can be used to describe the absorption behaviour of the plants also in different environments like inner-city districts. The derived values of NO and NO_2 on a specimen of the ivy variety *Hedera helix* "Plattensee" are within the range of observed values for other plants (see Table 2). Our results do not show the existence of a compensation point for NO_2. Such a compensation point would work out as a significant concentration of NO_2 applying synthetic air without NO_2. It should be visible at the end of each decay curve as an offset. See for example Fig. 9, where NO_2 is going straight to zero in the illuminated phase. The cited vdep studies use a dynamic branch or leaf enclosure system comparing the NO_2 concentration within two cuvettes, one plant and one empty reference cuvette. In contrast, our study is using a relaxation type of experiment directly observing the flux of a gaseous compound towards a plant.

The observed deposition velocities for NO_2 are directly related to the transpiration of H_2O_{gas} (see Fig. 13). The observations show the humidification of the dry synthetic air entering the reaction chamber by transpiration of the plant. The flowerpot and the surface of the soils within the reaction chamber were covered by a foil so the dominant part of the water can be attributed to evaporation of the leaves and the stem of the plant. It cannot be ruled out that the surface of the soil had some humidification effect but this is expected to be minor.

Table 2
Overview of published data on deposition rates for NO_2 and NO from plants. The values for PAR are given in μmol s^{-1} m^{-2}.

Species	$v_{dep}(NO_2)$ [cm/s]	condition	Reference
Grass	NO_2:0.38 NO:0.02	literature search	(Jonas and Heinemann, 1985)
Corn *Zea mays*	NO_2: 0.14	difference between two cuvettes, PAR 1600	(Hereid and Monson, 2001)
Wheat	NO_2: 0.20	difference between two cuvettes, PAR 1000	(Teklemariam and Sparks, 2006)
Periwinkle	NO_2: 0.12		
Sunflower	NO_2: 0.14		
Corn	NO_2: 0.08		
Norway spruce	NO_2: 0.15 ±1.3	difference between inlet and outlet of a cuvette PAR 500±400	(Rondón, et al., 1993)
Scots pine	NO_2: 0.14 ±1.1		
Norway spruce *Picea abies*	NO_2: 0.09	difference between two cuvettes, PAR 600	(Thoene, et al., 1996)
Fagus sylvatica	NO_2: 0.1	difference between two cuvettes, PAR 170	(Gessler, et al., 2000)
25 tropical tree species	NO_2: 0.17-0.68	difference between two cuvettes, PAR 1000	(Sparks, et al., 2001)
five European tree species	NO_2: 0.2-0.3	difference between two cuvettes, PAR 450, 900	(Chaparro-Suarez, et al., 2011)
Hedera helix "Plattensee"	NO_2:0.3 NO:0.01	PAR 950	this study

4. Discussion

To analyse the potential of plants for cleaning air polluted with greenhouse- and other harmful gases, very accurate and sophisticated measurements of plant gas metabolism are required. For this purpose, high-resolution measurement methods were used in the present study, which can yield very precise absorption parameters resolved in time. These detailed temporary measurements allow to detect instant and direct causal impacts and interactions of the surrounding air with the gas metabolism of the plant, as a function of the changes in the proportions of gas components within the supplied air. An important advantage of the experimental design shown in Fig. 1 is the modulation capability giving the possibility of regulating light quantity and adding constant background concentrations for example for CO_2 and H_2O_{gas}, as envisaged in ongoing further pending investigations. The supply of the measuring chamber with defined N_2O injections, which can be seen in Fig. 4 was carried out at half-hour cycles. This gas, being a strong climate gas (Prather et al., 2015) with a long atmospheric lifetime, can be used as a reference for the undisturbed passage of a gas mixture through a reaction chamber, illustrating a decay (i.e. its decrease in the concentration of the outflow) as to be expected when no interaction with the plant occurs. Thus, its decay remained equal during both illuminated and dark phases of the experiments with and without a plant present in the chamber. This finding can be interpreted as an indication that this gas is not absorbed by the plant, regardless of the state (open or closed) of the stomata. In contrast to this, NO_2 is quickly absorbed at such a rate, that the peak height during the injection interval only develops to approximately half the height observed during the dark phase, as well as a strongly faster decay rate. NO_2 shows– in contrast to N_2O - a pronounced light-dependent absorption capacity, which reveals during the dark phase a similar decay as observed for N_2O. In contrast to NO_2, NO shows no absorption by the plant, neither during the dark nor the illuminated phase. The low absorption of NO_2 in the dark is a hint that it is not interacting with the cuticula or other surfaces of the plant. During the illuminated phase, the stomata open and release water into the gas phase, enabling gas transport to the inner surfaces of the stomata. This allows NO, NO2, and N2O to reach the membranes, facilitating the transport of gas into the liquid phase inside the cells. In principle, this gas-liquid exchange should follow Henry's law which describes the solubility of a gas in liquid water. Astonishingly, the Henry coefficient of N_2O is the largest of the three gases (see Table 3), larger than NO_2, but still in both cases the budget between gas and liquid phase is in favour of the gas phase. Since NO_2 is observed to be removed from the gas phase fast, that means, that NO_2 entering the liquid phase inside the stomata is absorbed and metabolised there quite fast. Since the concentration of

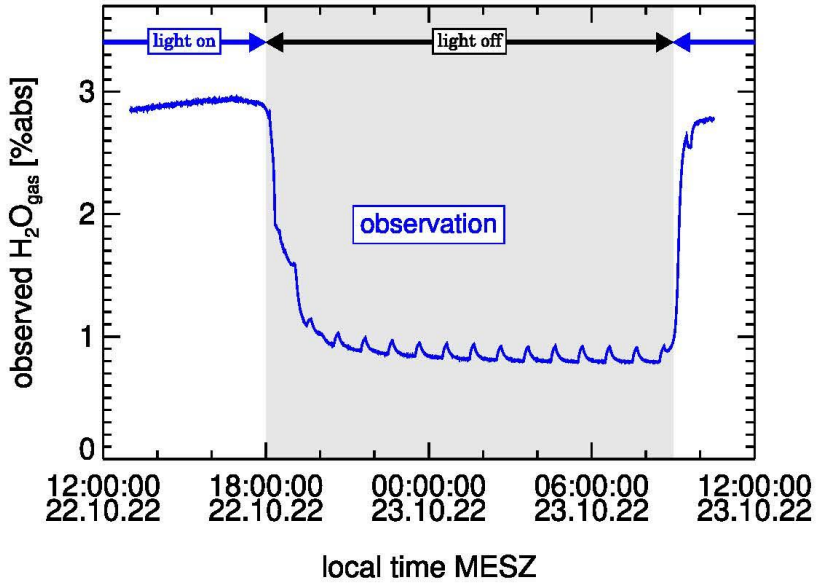

Fig. 13. Observed H_2O_{gas} mixing ratios indicating the opening of stomata during the illuminated phase for the ivy variety Hedera helix "Plattensee".

Table 3
Henry's law constants (Sander, 2015) (k°_{H}) at 298K describing the solubility of a gaseous compound in water. It is specifying the ratio of the concentration in the liquid phase relative to the pressure of the compound in the gas phase. The unit is mol/(m^3*Pa).

NO	NO_2	N_2O	O_3	CO	CO_2	OCS	CH_4	HONO
1.9e-5	1.2e-4	2.4e-4	1.0e-4	9.7e-6	3.3e-4	2.0e-4	1.4e-5	4.7e-1

NO_2 in the liquid phase is going towards zero due to this efficient metabolising process, NO_2 can be transported from the gas phase into the liquid phase constantly over time since the balance described by Henry's law is never reached.

The potential of a range of different climbing plants on the improvement of the air quality with respect to environmentally relevant air compounds will be presented in a following paper. The findings will provide a precise differentiated assessment of the properties and characteristics of the various façade plants, and thus emphasise the relevance of these plants for planting with regard to the challenges expected due to climate change.

5. Conclusion

The results obtained show that the plant specimens tested in this analysis actively reduced the NO_2 concentration under light conditions. This absorption can be attributed to a stomata-controlled activity. Contrary to expectation of Henry's law which describes the solubility of the used gases in water, the observed results strengthen the notion that specific pathways exist in the plant for the removal of NO_2. These removal pathways are clearly lacking for gases like NO and N_2O. Compared to other methods used to determine absorption of greenhouse and pollutant gases, the method described in this study offers a great range of flexibility and repeatability; while given the opportunity to observe quantitatively the changes in plant reaction towards different parameters such as light Intensity, water stress, background gas concentrations (CO_2, NO_2, N_2O, O_3 etc.)

CRediT authorship contribution statement

Minka Aduse-Poku: Investigation, Data curation. **Franz Rohrer:** Methodology, Formal analysis. **Benjamin Winter:** Validation, Resources, Methodology. **Hans G. Edelmann:** Supervision, Conceptualization.

Declaration of competing interest

The authors declare that they have no known competing financial interests or personal relationships that could have appeared to influence the work reported in this paper.

Data availability

Data will be made available on request.

Supplementary materials

Supplementary material associated with this article can be found, in the online version, at doi:10.1016/j.envadv.2024.100568.

References

Chaparro-Suarez, I.G., Meixner, F.X., Kesselmeier, J., 2011. Nitrogen dioxide (NO2) uptake by vegetation controlled by atmospheric concentrations and plant stomatal aperture. Atmos. Environ. 45 (32), 5742–5750. https://doi.org/10.1016/j.atmosenv.2011.07.021.

Ehlers, C., Klemp, D., Rohrer, F., Mihelcic, D., Wegener, R., Kiendler-Scharr, A., Wahner, A, 2016. Twenty years of ambient observations of nitrogen oxides and specified hydrocarbons in air masses dominated by traffic emissions in Germany. Faraday Discuss. 189 (0), 407–437. https://doi.org/10.1016/j.chemosphere.2005.03.03310.1039/C5FD00180C.

Gessler, A., Rienks, M., Rennenberg, H., 2000. NH3 and NO2 fluxes between beech trees and the atmosphere – correlation with climatic and physiological parameters. The New Phytologist 147 (3), 539–560. https://doi.org/10.1016/j.chemosphere.2005.03.03310.1046/j.1469-8137.2000.00712.x.

Health impacts of air pollution in Europe, 2021, 2021. Air quality in Europe 2021. Retrieved from. https://www.eea.europa.eu/publications/air-quality-in-europe-2021/health-impacts-of-air-pollution.

Hereid, D.P., Monson, R.K., 2001. Nitrogen oxide fluxes between corn (Zea mays L.) leaves and the atmosphere. Atmos. Environ. 35 (5), 975–983. https://doi.org/10.1016/S1352-2310(00)00342-3.

Hernandez Carballo, I., Bakola, M., Stuckler, D., 2022. The impact of air pollution on COVID-19 incidence, severity, and mortality: a systematic review of studies in europe and north america. Environ. Res. 215, 114155 https://doi.org/10.1016/j.envres.2022.114155.

Jonas, R., Heinemann, K, 1985. Schädigung von Pflanzen durch abgelagerte Schadstoffe. Staub-Reinhalt. Luft 45, 112–114.

Juginović, A., Vuković, M., Aranza, I., Biloš, V., 2021. Health impacts of air pollution exposure from 1990 to 2019 in 43 European countries. Sci. Rep. 11 (1), 22516. https://doi.org/10.1016/j.chemosphere.2005.03.03310.1038/s41598-021-01802-5.

Mele, M., Magazzino, C., Schneider, N., Strezov, V., 2021. NO2 levels as a contributing factor to COVID-19 deaths: the first empirical estimate of threshold values. Environ. Res. 194, 110663 https://doi.org/10.1016/j.envres.2020.110663.

Prather, M.J., Hsu, J., DeLuca, N.M., Jackman, C.H., Oman, L.D., Douglass, A.R., Funke, B., 2015. Measuring and modeling the lifetime of nitrous oxide including its variability. J. Geophys. Res.: Atmos. 120 (11), 5693–5705. https://doi.org/10.1002/2015JD023267.

Rondón, A., Johansson, C., Granat, L., 1993. Dry deposition of nitrogen dioxide and ozone to coniferous forests. J. Geophys. Res.: Atmos. 98 (D3), 5159–5172. https://doi.org/10.1029/92JD02335.

Sander, R., 2015. Compilation of Henry's law constants (version 4.0) for water as solvent. Atmos. Chem. Phys. 15 (8), 4399–4981. https://doi.org/10.1016/j.chemosphere.2005.03.03310.5194/acp-15-4399-2015.

Seinfeld, J.H, 1986. Atmospheric chemistry and physics of air pollution /John H. Seinfeld. Wiley, New York.

Sparks, J.P., Monson, R.K., Sparks, K.L., Lerdau, M., 2001. Leaf uptake of nitrogen dioxide (NO2) in a tropical wet forest: implications for tropospheric chemistry. Oecologia 127 (2), 214–221. https://doi.org/10.1016/j.chemosphere.2005.03.03310.1007/s004420000594.

Szumacher, I., Pabjanek, P., 2017. Temporal changes in ecosystem services in european cities in the continental biogeographical region in the period from 1990–2012. Sustainability 9 (4). https://doi.org/10.1016/j.chemosphere.2005.03.03310.3390/su9040665.

Takahashi, M., Higaki, A., Nohno, M., Kamada, M., Okamura, Y., Matsui, K., Morikawa, H., 2005. Differential assimilation of nitrogen dioxide by 70 taxa of roadside trees at an urban pollution level. Chemosphere 61 (5), 633–639. https://doi.org/10.1016/j.chemosphere.2005.03.033.

Teklemariam, T.A., Sparks, J.P., 2006. Leaf fluxes of NO and NO2 in four herbaceous plant species: the role of ascorbic acid. Atmos. Environ. 40 (12), 2235–2244. https://doi.org/10.1016/j.atmosenv.2005.12.010.

Thoene, B., Rennenberg, H., Weber, P., 1996. Absorption of atmospheric NO2 by spruce (Picea abies) trees. New Phytol. 134 (2), 257–266. https://doi.org/10.1111/j.1469-8137.1996.tb04630.x.

WHO, 2019. Health consequences of air pollution on populations. WHO Departmental News. Retrieved from. https://www.who.int/news/item/15-11-2019-what-are-health-consequences-of-air-pollution-on-populations.

Zha ng, X.Y., Lu, X.H., Liu, L., Chen, D.M., Zhang, X.M., Liu, X.J., Zhang, Y., 2017. Dry deposition of NO2 over China inferred from OMI columnar NO2 and atmospheric chemistry transport model. Atmos. Environ. 169, 238–249. https://doi.org/10.1016/j.atmosenv.2017.09.017.

4.0 Preface to the publication**: Quantifying the potential of façade-climbing plants in reducing air pollution: a novel investigation into the absorption capabilities of three climbers for CO_2, NO_2, and O_3 in urban environments.**

Building upon the previously established methodology for quantifying gas absorption by climbing plants, this follow-up study applies that framework to assess and compare the pollutant absorption capabilities of three climbers commonly used in façade greening—*H. helix* "Plattensee," *C. montana*, and *L. henryi*. The research focuses on their ability to absorb three major urban air pollutants: carbon dioxide (CO_2), nitrogen dioxide (NO_2), and ozone (O_3).

Using a standardized, light-regulated chamber system and advanced spectroscopic tools, the study quantifies plant-driven reductions in pollutant concentration, correcting for environmental dilution effects with N_2O as a stable reference gas. The results reveal light-dependent absorption patterns consistent with stomatal regulation and highlight apparent differences in species performance. *C. montana* showed the highest average CO_2 uptake, while *H. helix* exhibited superior NO_2 removal. O_3 absorption varied significantly between species, with statistically significant group differences.

The study demonstrates the relevance of climbing plants in mitigating air pollution by translating gas uptake into annualized per-hectare estimates. These findings offer valuable insights for urban planners, environmental designers, and policy-makers interested in integrating vertical greening into sustainable urban air quality strategies. The study confirms that climbing plants can provide quantifiable ecological services beyond aesthetics, including pollutant filtration, climate mitigation, and health co-benefits in dense urban environments.

4.0 Quantifying the potential of façade climbing plants in reducing air pollution: a novel investigation into the absorption capabilities of three climbers for CO2, NO2, and O3 in urban environments.

Journal article published: Urban Ecosystems

Aduse-Poku, M., Edelmann, H.G. Quantifying the potential of façade climbing plants in reducing air pollution: a novel investigation into the absorption capabilities of three climbers for CO_2, NO_2, and O_3 in urban environments. Urban Ecosyst 28, 76 (2025). https://doi.org/10.1007/s11252-025-01689-4

Urban Ecosystems (2025) 28:76
https://doi.org/10.1007/s11252-025-01689-4

Quantifying the potential of façade climbing plants in reducing air pollution: a novel investigation into the absorption capabilities of three climbers for CO_2, NO_2, and O_3 in urban environments

Minka Aduse-Poku[1] · Hans G. Edelmann[1]

Accepted: 2 February 2025

Abstract
Air pollution and climate change will require the advancement of suitable green technologies and mitigation measures in the future, especially in cities. However, the possibilities for this are limited, partly due to the heavily built-up and thus restricted urban open space and sealed surfaces. Incorporating vertical surfaces, abundant in cities, as a valuable space for climbing plants is an ideal opportunity and means of improving air quality. Unfortunately, there are hardly any reliable quantitative facts on the improvement of air quality brought about by these climbing plants. In this study, we analysed and compared typical climbing plants with regard to their absorption potential of gaseous air pollutants. This revealed pronounced differences between *Hedera helix*, (ivy) *Lonicera henryi* (honeysuckle) and *Clematis montana* (anemone clematis) regarding their absorption/filtering capacity of CO_2, NO_2 and O_3, the last two of which are hazardous to health.

Keywords Green facades · Urban climate · Air pollution · Air phytoremediation · NO_2 · Ozone · Carbon dioxide

Introduction

One unique and innovative approach to urban greening is the use of climbing plants in facade greening. Their ability to grow vertically and to cover large surfaces not only presents a distinct solution to the limited horizontal space in densely populated urban areas but also enhances buildings` aesthetic appeal and energy efficiency (Aduse-Poku et al. 2024a, b; Hoelscher et al. 2016). More importantly, these plants reduce urban heat island effects through shading of building surfaces, transpiration and reduction of the overall thermal load of buildings, lowering the overall temperature in urban areas during summer and also improving air quality; one of the ultimate goals of city planners and managers striving to create climate-sensitive urban environments (Baumgardner et al. 2012; Buchin et al. 2016).

Urban air quality is a critical determinant of public health, especially in densely populated neighbourhoods where pollution levels tend to be high (European Environment Agency 2022). Poor air quality in cities is primarily caused by vehicle emissions, industrial activities, and other human activities that release pollutants such as carbon dioxide (CO_2), nitrogen dioxide (NO_2), and ozone (O_3) into the atmosphere (European Environment Agency 2022). These pollutants have been linked to various adverse health effects; improving urban air quality therefore is a vital public health concern. Exposure to high CO_2 -, NO_2 -, and O_3- levels can lead to respiratory and cardiovascular problems (Nowak et al. 2014; Tang et al. 2024). Globally air pollution accounted for a staggering 8.1 million deaths in 2021; an estimation of great concern, as 709,000 were children under 5 years old.

Worldwide, ozone was reported to have contributed to nearly 490,000 deaths, while exposure to NO_2 contributed to the loss of 177,000 healthy years for children and adolescents in the same year (Health Effects Institute 2024).

By understanding and addressing the impacts of air pollutants, cities can create healthier environments for their inhabitants, fostering better public health and well-being.

Various studies have shown that plants have the potential to absorb greenhouse gases and pollutants (Buchin et al. 2016; Jones et al. 2019). Cities increasingly aim to adopt this practical and multi-purpose solution for improving air quality. Yet, the nature and structure of cities (prevalent sealing with concrete, asphalt, underground

✉ Hans G. Edelmann
h.edelmann@uni-koeln.de

[1] Universität Köln, Institut Für Biologiedidaktik, Herbert-Lewin-Str. 2, 50931 Cologne, Germany

Published online: 13 February 2025

infrastructure like communication cables, etc.) make implementing trees very difficult. On the other hand, façade climbing plants have been identified as an excellent option for utilising vertical spaces on city buildings due to their adaptive nature.

Façade greening has recently gained attention due to its numerous benefits, of which air quality improvement is a general main feature. Unfortunately, research into their contribution to reducing gas pollutants is limited, making it necessary for this knowledge gap to be filled for a scientifically based holistic view of their contributions to air quality improvement.

In this study, the absorption potential of three typical façade climbing plants—*Hedera helix* "Plattensee," (Araliaceae) *Clematis montana* (Ranunculaceae) and *Lonicera henryi* (Caprifoliaceae)—with respect to carbon dioxide (CO_2), nitrogen dioxide (NO_2) and ozone (O_3) is analysed to comprehend and assess their phytoremediation potentials. The results presented for the three typical climbing plants provide a scientific basis for evaluating and appraising the phytoremediation potential rarely found for climbing plants.

Materials and methods

Plant preparation and experimental setup

For measurements, pot plants previously grown in the field were transferred and placed in special glass chambers, designed for the flow-through experiments. The plants were maintained at room temperature and well-watered before the experiments. Five (5) individuals of each plant species except for *C. montana* (consisting of 4 individuals) were separately investigated in a 90-L volume glass chamber, as principally illustrated in Fig. 1. The experiments were conducted in a laboratory setting using a photosynthetic lamp with photosynthetic active radiation (PAR) = 950 µm/s/m^2, following the protocols detailed in (Aduse-Poku et al. 2024a, b).

Principal experimental setup

Gas administration and measurement

The experiments involved injecting NO_2, and CO_2 from gas cylinders and O_3 from an ozone generator using a pen-ray UV lamp. Additionally, N_2O was introduced into the reaction chamber through ambient air and in the case of $H_2O_{(g)}$, due to the transpiration of the plants. This created a gas mixture that mimics the external environment with the corresponding pollutant load. High-resolution measuring devices, namely: mid-infrared direct laser absorption spectrometer (MIRO Analytical AG, Wallisellen CH-8304, Switzerland; type MGA10—GP +) and a cavity-ring-down spectrometer (Picarro Inc. Santa Clara, CA 95054, USA; type G2307) recorded peak concentration values after gas injections.

The concentrations of these gases were measured over time as they passed through the chamber's outlet. Since the gases of interest (CO_2, NO_2, and O_3) were known to be absorbed by plants, there was the need to use nitrous oxide (N_2O), a stable greenhouse gas with an atmospheric lifetime of 123 years (Prather et al. 2015); in the troposphere N_2O is regarded as an inert noble gas. Thus, N_2O will not be absorbed by plants and pass through the reaction chamber with unchanged concentrations. Due to its inert nature in the troposphere, it was used as the control in this experiment, providing a base/reference line for comparison.

Leaf surface area measurement

After the gas absorption experiments, the leaves of each plant were detached from the plants to quantify their surface area. A gravimetric method was employed in the estimation directly after detachment. This data was essential in calculating the gas absorption rates/deposition velocity per unit leaf area (Aduse-Poku et al. 2024a, b).

Data analysis

The decrease in the concentration of the injected gases (NO_2, O_3, and CO_2) was analysed and compared to that

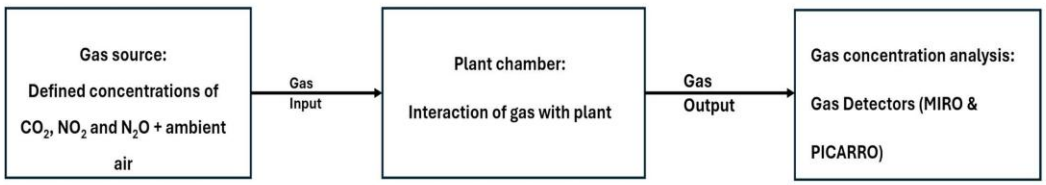

Fig. 1 Diagram depicting the principal experimental setup to analyse the gas absorption potentials of different climbers

of N_2O. This allowed for the calculation of net decreases in concentration over time. The absorption rate for each gas was then determined by considering/referring to each plant's total leaf surface area. Total amounts (mass) absorbed were then calculated according to the prevailing concentration at each point in time. All experiments under each species were analysed using descriptive statistics and ANOVA.

Results

Generally, the plants showed preferences in the type of gases absorbed; NO_2, CO_2, and O_3 were significantly reduced. In contrast, N_2O showed no significant change within the experimental period of about 1 h per each experiment carried out. Also, in additional experiments, i.e. the flow-through tests without plants, no gas absorption was observed (see online resource 4), so that an interaction of the gases with the reaction chamber can be excluded.

One conspicuous finding was the general diurnal absorptive behaviour of the plants. This effect is reflected in the plants' almost insignificant absorptive behaviour during the dark phase and a profound effect under light conditions (representing a clear indication of stomata-controlled absorption). The decrease in gas pollutants in the chamber followed an exponential decay curve, as shown in Fig. 2, highlighting an example of the absorptive trend of concentration reduction in the chamber under light conditions. In Fig. 2, one can observe both gases decreasing exponentially at very different rates. Denoted as 1/e (Euler number e ≈ 2.718) a standard measure to describe the point at which a quantity has reduced to approximately 36.8% of its initial value and mostly used as a measure of decay rates, the absorption of NO_2 depicted in orange was shown to have reached the 1/e = 0.37 on the y-axis within 100 s while the unperturbed N_2O, represented by the blue curve, reached the same 1/e at 600 s. These two values represent the decay time scale for both gases, which is used in the estimation process. Each single value shown in Fig. 3 is based /originates from decay curve analysis as illustrated in Fig. 2.

This decay (rate of reduction) trend resulted in the derivation of the following parameters:

$$\frac{\partial X(t)}{\partial t} = (P\_Inj + P\_plant) - (D\_plants + D\_surface + D\_DIL) \cdot X(t) \quad (1)$$

X	compound of interest
t	time
P_Inj	production rate by dedicated injection of X
P_plant	production rate of X by the plants
D_plants	loss rate coefficient due to removal by the plants
D_surf	loss rate coefficient for removal at the surfaces of the chamber
D_DIL	loss rate coefficient for dilution inside the chamber due to inflow of synthetic air

$$A(t) = A0 \cdot e^{-t/\tau} + offset \quad (2)$$

Where $A0 = (X(t=0) - P\_plant/D)$, $\tau = 1/D$, and $offset = P\_plant/D$. (Aduse-Poku et al. 2024a, b) The parameter τ signifies the time a gas molecule spends in the plant chamber. The parameters A0, τ, and offset were

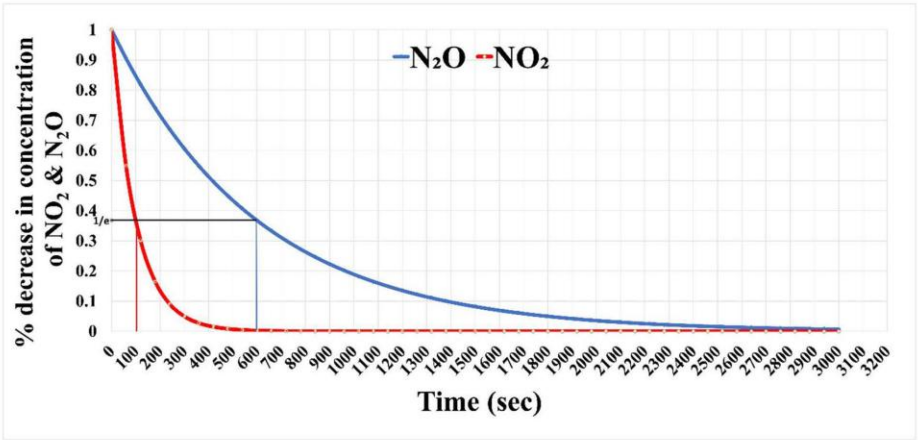

Fig. 2 Decay (time scale) of NO_2 & N_2O as measured in the plant chamber output under light conditions

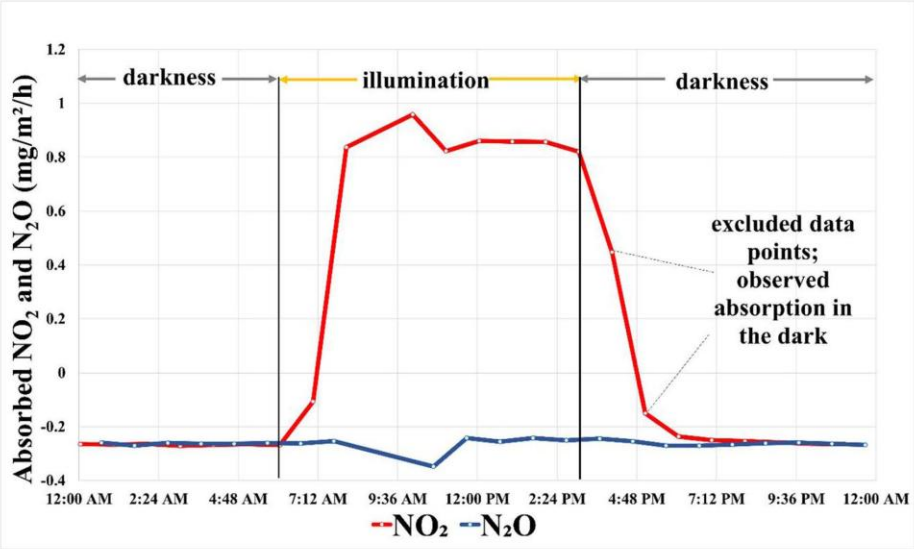

Fig. 3 Diurnal absorption trend of NO_2 (blue line) and N_2O (red line) in *Hedera helix*, derived from the results of decay curves (Fig. 1), as the origin of each point, plotted in this curve as a function of light- and dark conditions

established through iterative processes using a Levenberg–Marquardt algorithm (Gavin 2019) upon visual examination, it was noted that the decrease in gas concentrations (CO_2, NO_2, O_3, and NO_2) following injection closely adhered to the specified pattern given in Eq. 2 most of the time, except for instances where the lighting changed within the timeframe being analysed, leading to pronounced shifts between light and dark. This was because the parameter D_plant was not consistent during that period due to the opening or closing of the stomata in response to light. These specific time points were omitted from the analysis, as the fitting process could not account for these complex decay trends.

Each experiment was analysed following the processes described in detail in (Aduse-Poku et al. 2024a, b) and Fig. 2 above, at concentrations of about 400 ppm for CO_2, 40 ppb for NO_2, and 80 ppb for ozone (in other words, each point in Fig. 3 originates from an independent experiment). These differences were computed for each point during the light and dark phases, as shown in Fig. 3 below. Experimental observations do not start from 0 due to the emission of gases in the dark phase of plant metabolism. Observations of gas absorption in an empty chamber resulted in no absorption of gases (see online resource 4).

Further data analysis will concentrate on the amount of each gas (CO_2, NO_2, and O_3) absorbed in the light phase of the experiment due to the light-dependent absorption trend observed in the example (Fig. 3) above, which can be attributed to stomatal closure during the dark- and opening during the light phase of the experiment.

Absorption of carbon dioxide (CO_2)

H. helix "Plattensee" exhibited an average absorption rate of 0.06 mg/m^2/s, while *C. montana* showed a higher average absorption rate of 0.09 mg/m^2/s. *L. henryi* had an average absorption rate of 0.07 mg/m^2/s, as depicted in Fig. 4. These values indicate that *C. montana* absorbed gases more effectively than the other two species in this study. Given that the *P*-value (0.24) exceeds the alpha level of 0.05 (see online resource 1), we fail to reject the null hypothesis. This indicates that based on the data collected in this study, there are no statistically significant differences in the carbon dioxide absorption rates among *H. helix* "Plattensee," *C. montana*, and *L. henryi*. Therefore, the observed variations in average absorption rates are likely due to random chance rather than actual differences between the species.

Absorption of nitrogen dioxide (NO_2)

A comparative analysis delivered significant differences in absorptive capabilities among the plant species *H. helix* "Plattensee," *C. montana*, and *L. henryi*. The mean measurement values of 0.07 µg/m^2/s, 0.06 µg/m^2/s, and 0.03 µg/m^2/s, along with their respective 95% confidence

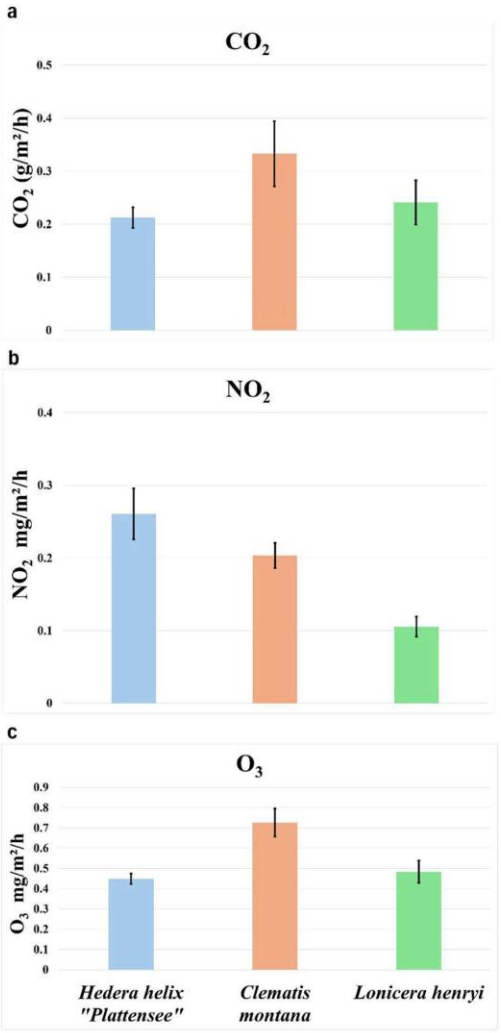

Fig. 4 Absorption potentials of 3 climbers used in façade greening with standard error bars. **a** – carbon dioxide/CO_2 (n=81,34,109). **b** – nitrogen dioxide/NO_2 (n=64,34 and 67), **c** – Ozone/O_3 (n=53, 29 and 63), by *H.helix*, *C.montana*, and *L. henryi*, respectively, under light conditions

intervals, provided valuable insights. ANOVA analysis showed significant group differences (P-value 4.54686E-05), and post hoc comparisons indicated most (2/3) group differences were statistically significant ($P < 0.017$) (see online resource 2).

Absorption of ozone (O_3)

The experiment yielded average absorption rates of 0.12, 0.20, and 0.13 µg/m²/s for *Hedera helix, C. montana,* and *L. henryi*, respectively. All values obtained for each species satisfied the 95% confidence interval, indicating reliable measurements. An ANOVA analysis yielded a P-value of 0.002 (supplementary data), demonstrating significant differences among the groups. Subsequently, a post hoc pairwise comparison using the Bonferroni correction, with an adjusted significance level of 0.017, revealed substantial differences in all pairings except for the comparison between *H. helix* and *L. henryi*. This suggests that while most group differences were statistically significant, the difference between *H. helix* and *L. henryi* was insignificant under the adjusted threshold.

Discussion

In recently growing discussions about the many urgent measures resulting from climate change, more and more voices are being raised in favour of green architecture. However, the specific benefits of the various plants used for this purpose are hardly known. The results of our analysis on three species typically used for façade greening reveal detailed, specific characteristics with regard to their capacity to purify various air pollutants. To facilitate meaningful comparisons with other data and to provide a comprehensive understanding of the plant's capacity for pollutant absorption over a more extended period, the observed absorption rates were converted to annual rates (g or µg/m²/s to kg/ha/a) by multiplying the average annual sun hours in Germany (1764 h in 2023).

Contribution of climbing plants to carbon sequestration

There is a net positive effect concerning carbon absorption and its storage by climbing plants. Climbing plants are characterised by a positive net performance in terms of carbon uptake and storage. This is evident in Fig. 5b, which depicts well-formed woody vines of the plant *Parthenocissus tricuspidata.*

However, the detailed intricacies of the absorbed CO_2 fixed in the form of biomass in the long term cannot be determined within the framework of the study presented here; yet, it can be assumed that a certain proportion is released again through respiration processes (Hartmann et al. 2020; Wang et al. 2016; Zelitch 1969). It would require a longer-term *in-situ* study with many

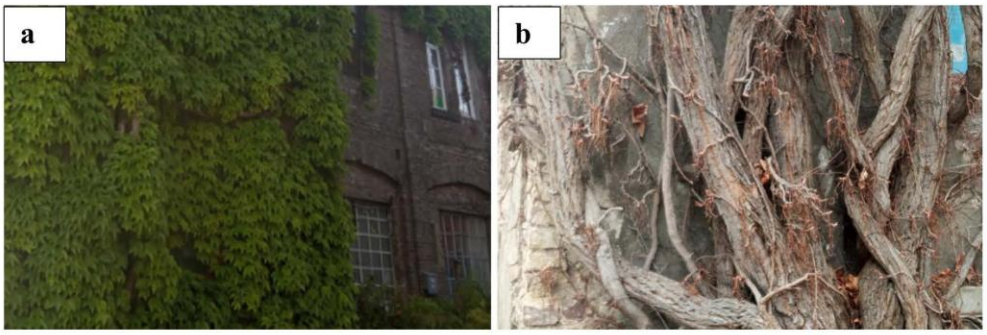

Fig. 5 **a** – Images of foliage-covered vines of *P. tricuspidata*, **b** – Exposed (enlarged) basal vines during deciduousness (illustrating carbon storage)

imponderable aspects, which could only yield operationally defined approximations.

Furthermore, climbers in cities are mainly cultivated for other ecosystem services they provide, such as heat reduction (improving building energy efficiency) (Aduse-Poku et al. 2024a, b; Hunter et al. 2014), aesthetics, biodiversity, besides air quality improvements, which we seek to quantify in this paper.

Climbers generally necessitate a strict management regime that involves regular pruning of their vegetation to control their extent of growth, encourage new shoots, and, as a precautionary measure, regulate the load-bearing capacity of the walls and climbing aides on which they grow. While the reasons mentioned above present challenges, they do not entirely preclude the potential of climbing plants as carbon storage systems in cities. These plants still offer unique advantages that warrant further exploration.

Relevance of CO_2 absorption by urban climbing plants

Urban areas are significantly responsible and contribute to global CO_2 emissions due to transportation, industry, heating, and energy consumption. Addressing these anthropogenic emissions is crucial for mitigating climate change and improving urban air quality. Our results indicate that climbing plants in cities can absorb up to 0.09 mg/m^2/s (0.33 g/m^2/h.) or approximately 6000 kg of CO_2 per hectare per year (see Fig. 4a). The absorption rate per leaf area found in our study is in the range reported for trees (Jo and Mcpherson 1995; Strohbach et al. 2012).

To understand and evaluate the significance of these absorption rates, it is, for example, helpful to compare it with the emissions of CO_2 from private cars, prevalent in urban settings.

Private cars in Europe emit an average of 145 to 153 g of CO_2 per km for petrol and diesel cars, respectively (using the real-world dataset) (Marrero et al. 2020). To put the absorption capacity of urban plants into context, we can estimate the distance that would correspond to the emission of 6000 kg of CO_2 by a private car. This means that one hectare of urban plant leaf surface area absorbing 6000 kg of CO_2 per year offsets the emissions from a car traveling approximately 40,000 km annually. The average annual car distance is estimated at around 18000 km (Marrero et al. 2020). This could account for about 2.2 years of carbon emissions compensation or at least a year, if half of the carbon absorbed is devoted to another loss process in the plant, such as respiration, etc.

Our findings may be useful for urban planners to advocate for the expansion of urban green vertical walls, as their unique climbing abilities fit seamlessly into the efficient use of building vertical spaces.

Contribution of climbing plants to NO_2 reduction

Nitrogen dioxide (NO_2) is a significant air pollutant, primarily emitted from industrial processes, vehicle exhausts, and power generation. It poses severe risks to human health and the environment (Tang et al. 2024). NO_2 is known to cause a range of respiratory problems, including asthma, bronchitis, and other lung diseases. Chronic exposure can lead to diminished lung function and increased susceptibility to respiratory infections (Mele et al. 2021; Tang et al. 2024). By absorbing NO_2, plants help to reduce the concentration of this harmful pollutant in the air, thereby lowering the incidence and severity of these health issues among urban populations.

In the city context, climbing plants' ability to absorb NO_2 is a critical ecological service. Hedera helix's measured maximum absorption rate of 0.07 µg/m^2/s (0.26 mg/m^2/h),

or approximately 5 kg per hectare per year (see Fig. 4 b), substantially benefits urban environments. This significant reduction in NO_2 levels can reassure urban residents about potential health benefits from façade greening.

The obtained results support the deduction that plants inherent affinity for absorption can be considered; this observation can, in turn, be leveraged towards targeted pollution control in cities, where high NO_2-polluted areas can be selected and targeted with *H. helix* and *C. montana*, for example.

NO_2 is crucial in forming ground-level ozone, a harmful pollutant that exacerbates respiratory conditions and damages crops. By absorbing NO_2, plants can help limit ground-level ozone production. This role of climbing plants in reducing ground-level ozone can bring optimism about potential improvements in air quality and healthier ecosystems (Nguyen et al. 2022), contributing to better air quality and healthier ecosystems.

NO_2 also contributes to the formation of acid rain (Menezes and Popowicz 2022), which can harm water bodies, soil, and plant life. By increasing the use of vertical spaces on buildings for façade greening, the potential for plants to absorb NO_2 can increase, helping mitigate the impact of acid rain. With their high absorption rates, climbing plants can significantly reduce the concentration of NO_2 in the air, thereby reducing the formation of acid rain. This protects aquatic and terrestrial environments and helps maintain biodiversity, making climbing plants valuable to urban air quality control strategies.

The investigated plants' absorption of 5 kg of NO_2 per hectare per year is well within the range of other studies involving other tree species. This is a significant ecological service that offers multiple benefits for urban areas (Jones et al. 2019; Nowak et al. 2018). With the ongoing prioritization of air quality and public health in cities, greening existing vertical spaces on buildings should be a key component of urban planning and environmental management efforts.

Significance of ozone absorption by climbing plants in urban air quality control

Ground-level ozone (O_3) is a significant pollutant concern affecting cities today. (Låg and Schwarze 1997). It is formed by the reaction of sunlight with pollutants such as volatile organic compounds (VOCs) and nitrogen oxides (NOx) (Tiwari and Agrawal 2018). High ozone levels can cause respiratory problems, exacerbate asthma, and reduce lung function, posing significant health risks to urban populations (Bell et al. 2007).

In this study, climbing plants absorbed up to 0.2 µg/m^2/s (ca. 0.73 mg/m^2/h) or an approximated 13 kg/ha/a. of ozone (see Fig. 4c). This finding is well in the range of similar studies conducted on trees (Baumgardner et al. 2012; Guidolotti et al. 2016).

Ozone is a major component of smog and is known for its adverse effects on human health and vegetation (Fiscus et al. 2005).

Lowering ozone levels can lead to fewer respiratory problems among urban residents. This may help reduce hospital admissions, improve public health, and lower healthcare costs. Reducing ozone exposure can significantly improve the quality of life for individuals with pre-existing respiratory conditions (Fiscus et al. 2005).

When implemented on a large scale, the cumulative effect of ozone absorption by climbing plants across multiple hectares can be substantial. For instance, greening initiatives that cover hundreds of hectares of leaf area can absorb significant amounts of ozone, leading to measurable improvements in air quality.

Conclusion

This study highlights the significant potential role of climbing plants in urban air quality management. With the capacity to absorb approximately 13 kg of ozone (O_3), 5 kg of nitrogen dioxide (NO_2), and substantial amounts of carbon dioxide (CO_2) per hectare per year, these plants provide crucial ecological services. Depending on the building density and building structure, cities offer a multiple of potential vertical green spaces relative to the built-up area, which in the case of city centres alone extends to many square kilometres. This means that, in addition to the potentially greenable roof areas, the existing vertical façade area offers many-fold potential for greening.

The calculation of pollutant absorption per hectare provides a useful standardized metric; however, it is important to note that the actual absorption capacity largely depends on the vegetation's leaf area index (LAI) and other factors including light availability, which in many cases could be a factor of 3 – 5 and more, depending on species, age, etc. (Hoelscher et al. 2016). This translates to a very significant absorption capacity when viewed from the point that a few climbing plants do not necessarily have to cover a whole acre of land to possess a hectare of leaf area.

Though quantified in an operationally defined environment in order to allow for reproducibility, the presented values may be subject to change depending on prevailing conditions in-situ in nature. These facts, however, apply to almost all ecophysiological studies.

In general, large-scale implementation of green walls and facades covered with climbing plants can significantly improve air quality, contribute to public health, and urban climate resilience at a relatively cheaper cost. By integrating such green façade infrastructure into urban planning,

cities can effectively reduce harmful pollutants. The use of climbing plants can therefore contribute to compliance with the air pollution limits set by the relevant authorities, to the enhancement of biodiversity, to urban aesthetics and to the promotion of long-term health and sustainability.

Supplementary Information The online version contains supplementary material available at https://doi.org/10.1007/s11252-025-01689-4.

Acknowledgements We would like to thank Dr Franz Rohrer, Forschungszentrum Jülich, Institut IEK-8: Troposphäre, Germany, for the constructive and critical discussions and for supporting and providing the laboratory equipment.

Author contributions M. A.-P. an the experiments and prepared the figures and also contributed to the text also written by H.G.E.

Funding Open Access funding enabled and organized by Projekt DEAL. The authors declare that no funds, grants, or other support were received during the preparation of this manuscript and have nonrelevant financial or non-financial conflicts of interests to disclose.

Data availability No datasets were generated or analysed during the current study.

Declarations

Competing interests The authors declare no competing interests.

References

Aduse-Poku M, Niels W, Pacini A, Großschedl J, Edelmann HG, Schlüter K (2024a) Façade greening – from science to school. At-Automatisierungstechnik 72:694–703. https://doi.org/10.1515/auto-2024-0022

Aduse-Poku M, Rohrer F, Winter B, Edelmann HG (2024b) Methodology for the quantification of the absorption potential of greenhouse- and pollutant gases by climbing plants used in façade greening; a case study on ivy (*Hedera helix*). Environ Adv 17:100568. https://doi.org/10.1016/j.envadv.2024.100568

Baumgardner D, Varela S, Escobedo FJ, Chacalo A, Ochoa C (2012) The role of a peri-urban forest on air quality improvement in the Mexico City megalopolis. Environ Pollut 163:174–183. https://doi.org/10.1016/j.envpol.2011.12.016

Bell ML, Goldberg R, Hogrefe C, Kinney PL, Knowlton K, Lynn B, Rosenthal J, Rosenzweig C, Patz JA (2007) Climate change, ambient ozone, and health in 50 US cities. Clim Change 82:61–76. https://doi.org/10.1007/s10584-006-9166-7

Buchin O, Hoelscher MT, Meier F, Nehls T, Ziegler F (2016) Evaluation of the health-risk reduction potential of countermeasures to urban heat islands. Energy Build 114:27–37. https://doi.org/10.1016/j.enbuild.2015.06.038

European Environment Agency (2022) Air quality in Europe 2022 — European environment agency. https://www.eea.europa.eu/publications/air-quality-in-europe-2022. Accessed 06.02.2025

Fiscus EL, Booker FL, Burkey KO (2005) Crop responses to ozone: Uptake, modes of action, carbon assimilation and partitioning. Plant Cell Environ 28:997–1011. https://doi.org/10.1111/j.1365-3040.2005.01349.x

Gavin HP (2019) The levenberg-marquardt algorithm for nonlinear least squares curve-fitting problems. Duke University. https://api.semanticscholar.org/CorpusID:113404737

Guidolotti G, Salviato M, Calfapietra C (2016) Comparing estimates of EMEP MSC-W and UFORE models in air pollutant reduction by urban trees. Environ Sci Pollut Res 23:19541–19550. https://doi.org/10.1007/s11356-016-7135-x

Hartmann H, Bahn M, Carbone M, Richardson AD (2020) Plant carbon allocation in a changing world – challenges and progress: introduction to a Virtual Issue on carbon allocation: Introduction to a virtual issue on carbon allocation. New Phytol 227:981–988. https://doi.org/10.1111/nph.16757

Health Effects Institute (2024) State of global air 2024. Special report. Boston, MA:Health Effects Institute

Hoelscher MT, Nehls T, Jänicke B, Wessolek G (2016) Quantifying cooling effects of facade greening: Shading, transpiration and insulation. Energy Build 114:283–290. https://doi.org/10.1016/j.enbuild.2015.06.047

Hunter AM, Williams NSG, Rayner JP, Aye L, Hes D, Livesley SJ (2014) Quantifying the thermal performance of green façades: a critical review. Ecol Eng 63:102–113. https://doi.org/10.1016/j.ecoleng.2013.12.021

Jo H-K, Mcpherson EG (1995) Carbon storage and flux in urban residential greenspace. J Environ Manage 45(2):109–133. https://doi.org/10.1006/jema.1995.0062

Jones L, Vieno M, Fitch A, Carnell E, Steadman C, Cryle P, Holland M, Nemitz E, Morton D, Hall J, Mills G, Dickie I, Reis S (2019) Urban natural capital accounts: developing a novel approach to quantify air pollution removal by vegetation. J Environ Econ Policy 8:413–428. https://doi.org/10.1080/21606544.2019.1597772

Låg M, Schwarze PE (1997) Helseeffekter av bakkenaert ozon [Health effects of ozone in the environment]. Tidsskr Nor Laegeforen 10;117(1):57–60

Marrero GA, Rodríguez-López J, González RM (2020) Car usage, CO2 emissions and fuel taxes in Europe. Series 11:203–241. https://doi.org/10.1007/s13209-019-00210-3

Mele M, Magazzino C, Schneider N, Strezov V (2021) NO2 levels as a contributing factor to COVID-19 deaths: The first empirical estimate of threshold values. Environ Res 194:110663. https://doi.org/10.1016/J.ENVRES.2020.110663

Menezes F, Popowicz GM (2022) Acid rain and flue gas: quantum chemical hydrolysis of NO2. ChemPhysChem 23:1–6. https://doi.org/10.1002/cphc.202200395

Nguyen DH, Lin C, Vu CT, Cheruiyot NK, Nguyen MK, Le TH, Lukkhasorn W, Vo TDH, Bui XT (2022) Tropospheric ozone and NOx: A review of worldwide variation and meteorological influences. Environ Technol Innov 28:1–13. https://doi.org/10.1016/j.eti.2022.102809

Nowak DJ, Hirabayashi S, Bodine A, Greenfield E (2014) Tree and forest effects on air quality and human health in the United States. Environ Pollut 193:119–129. https://doi.org/10.1016/j.envpol.2014.05.028

Nowak DJ, Hirabayashi S, Doyle M, McGovern M, Pasher J (2018) Air pollution removal by urban forests in Canada and its effect on air

quality and human health. Urban Forestry Urban Green 29:40–48. https://doi.org/10.1016/j.ufug.2017.10.019

Prather MJ, Hsu J, DeLuca NM, Jackman CH, Oman LD, Douglass AR, Fleming EL, Strahan SE, Steenrod SD, Søvde OA, Isaksen ISA, Froidevaux L, Funke B (2015) Measuring and modeling the lifetime of nitrous oxide including its variability. J Geophys Res 120:5693–5705. https://doi.org/10.1002/2015JD023267

Strohbach MW, Arnold E, Haase D (2012) The carbon footprint of urban green space-A life cycle approach. Landsc Urban Plan 104:220–229. https://doi.org/10.1016/j.landurbplan.2011.10.013

Tang Z, Guo J, Zhou J, Yu H, Wang Y, Lian X, Ye J, He X, Han R, Li J, Huang S (2024) The impact of short-term exposures to ambient NO2, O3, and their combined oxidative potential on daily mortality. Environ Res 241. https://doi.org/10.1016/j.envres.2023.117634

Tiwari S, Agrawal M (2018) Tropospheric Ozone Budget: Formation, Depletion and Climate Change. In: Tropospheric Ozone and its Impacts on Crop Plants. Springer International Publishing 31–64. https://doi.org/10.1007/978-3-319-71873-6_2

Wang B, Shugart HH, Shuman JK, Lerdau MT (2016) Forests and ozone: Productivity, carbon storage, and feedbacks. Sci Rep 6. https://doi.org/10.1038/srep22133

Zelitch I (1969) Mechanisms of carbon fixation and associated physiological responses. In: Eastin JD, Haskins HA, Sullivan CY, van Bavel CHM (eds.) Physiological Aspects of Crop Yield 206–226 https://doi.org/10.2135/1969.physiologicalaspects

Preface to ‘Stomata Type and Density in Selected Climbing Plants’

Urban environments pose significant challenges for plant survival, including heat stress, limited water availability, and fluctuating atmospheric conditions. In green façade applications, climbing plants offer an effective solution for mitigating urban heat islands and enhancing thermal comfort. However, their ability to thrive under these conditions is largely determined by their physiological traits, particularly stomatal characteristics.

This chapter explores the diversity of stomatal types and densities among selected climbing plant species, examining their role in transpiration and environmental adaptation. By analyzing stomatal morphology, including anomocytic, anisocytic, and paracytic types, this study will help highlight how different species regulate gas exchange and water loss in subsequent chapters. The research further investigates whether stomatal traits can serve as indicators of a plant’s resilience to heat and drought, providing valuable insights for urban greening strategies.

5.0 Stomata Type and Density in Selected Climbing Plants

5.1 Introduction

Stomata, microscopic pores on leaf surfaces that regulate gas exchange, play a central role in the balance between photosynthesis and transpiration. Generally, each stoma is bordered by guard cells that open or close in response to environmental signals, controlling CO_2 uptake and water vapor release (Drake et al., 2013; Kumar & Sankhla, 2024). This function is vital for plant cooling and water use efficiency, especially under heat- and drought stress in urban environments (Lawson & Blatt, 2014; Santamouris, 2014).

Stomatal traits, particularly density and size, vary widely among species and influence drought resistance and transpiration capacity. Plants in arid environments often develop fewer or smaller stomata to limit water loss, while species with higher stomatal density may enhance cooling but risk more significant water loss (Liu et al., 2021; Van Cotthem, 1970).

Stomata are also classified by the arrangement of surrounding cells: anomocytic (no distinct subsidiary cells), anisocytic (three unequal subsidiary cells), and paracytic (subsidiary cells parallel to guard cells). These variations reflect evolutionary adaptations and may influence species suitability for green infrastructure.

Despite the increasing use of climbers in façade greening, their stomatal characteristics and associated adaptations remain little studied. This study addresses this gap by comparing stomatal density among six common climbing species—*C. montana*, *Hedera hibernica*, *Hedera colchica* ‘Russland’, *L. henryi*, *Wisteria sinensis*, and *H. helix* ‘Plattensee’.

5.2 Research Question

What types of stomata exist in different climbing plant species used in green façades; what is their stomatal density, and what does existing literature suggest about the environmental adaptation strategies associated with different stomatal types?

5.2.1. Hypothesis

Stomatal type and density vary significantly among climbing plant species, affecting their cooling efficiency, transpiration rate, and water stress responses.

5.3. Factors Affecting Stomatal Density

Genetics: The genetic makeup of a plant species establishes a baseline for stomatal density. However, even within a species, there can be genetic variation in stomatal density among different genotypes or cultivars (Doheny-Adams et al., 2012).

Light Quality and Intensity: Higher light intensity generally leads to increased stomatal density. Under high-light conditions, plants need more CO_2 for photosynthesis (Petrova, 2012).

Water Availability*:* Water stress often results in lower stomatal density as a water conservation mechanism (Xu & Zhou, 2008).

CO_2 Concentration*:* Elevated CO_2 concentrations can lead to decreased stomatal density. This is because plants require less stomatal opening to obtain the necessary CO2 for photosynthesis under high CO_2 conditions (Woodward, 1987).

Temperature*:* Temperature can also influence stomatal density, although the relationship is complex and can vary depending on the species (Savvides et al., 2012).

5.4 Materials and Methods

5.4.1 Study Species and Sampling

Stomatal density was investigated in six climbing plant species: *C. montana*, *Wisteria sinensis*, and *H. helix var. Plattensee*, Hedera colchica, *Hedera hibernica*, and *L. henryi*. For each species, 20 leaf samples were randomly collected from healthy plants grown under similar environmental conditions. The random samples were selected to ensure representation of the natural variability within each species.

5.4.2. Microscopy and Image Acquisition

Stomatal density was determined employing a Keyence VHX-7000 digital microscope, operating at magnifications ranging from 100 x to 700 x, depending on the size and clarity of the stomata. High-resolution images were captured using the microscope's 4K CMOS sensor, allowing detailed visualization of the stomatal structures. Multiple images were taken from different fields of view (FOVs) for each leaf sample to account for variability in stomatal distribution across the leaf surface.

5.4.3. Stomatal Density Calculation

Stomatal density was determined manually by counting the number of stomata within a defined area of each image. The area of the FOV was calculated using the microscope's calibration tools, and stomatal density was expressed as the number of stomata per square millimeter (stomata/mm²). At least three FOVs were analyzed per leaf sample, and the average stomatal density was calculated for each species.

5.5. Data Analysis

The stomatal density data for each species were compiled and analysed to determine mean values and standard deviations. Statistical comparisons between species were conducted using one-way analysis of variance (ANOVA) to assess significant differences in stomatal density. Post-hoc tests (e.g., Tukey's HSD) were performed to identify specific pairwise differences between species. The statistical analysis was conducted using a significance level of $p < 0.05$.

5.5.1. Quality Control

All leaf impressions were prepared and analysed following a standardized protocol to ensure consistency. The same operator performed all measurements to minimize observer bias. Additionally, the microscope was calibrated before each session to maintain accuracy in area measurements.

5.6. Results

5.6.1. Microscopic Analyses of Stomatal Features in *C. montana* (Abaxial surface)

The microscopic image of the abaxial (lower) leaf surface of *C. montana* reveals a dense distribution of stomata interspersed among epidermal cells. The stomata appear elliptical, with well-defined guard cells slightly raised above the surrounding epidermal layer, as shown in Figure 1 below. The epidermal cells exhibit a wavy or sinuous pattern, a common trait in plants with hypostomatic or amphistomatic leaves, which helps regulate water loss and optimize gas exchange.

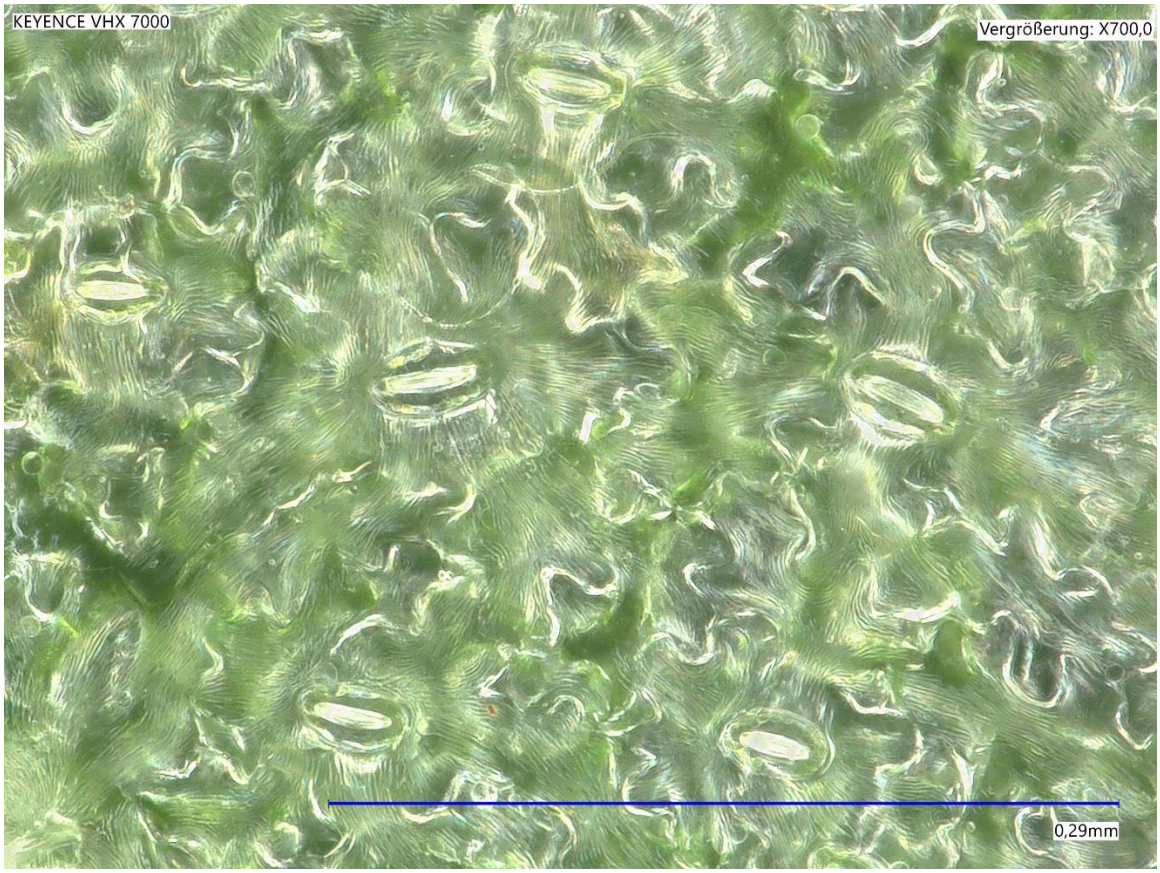

Figure 1. Typical image of stomata of the abaxial surface of *C. montana* leaves at a 700 x magnification; bar represents 0.29 mm.

5.6.1 Stomatal Type and Classification

Based on the visible arrangement, *C. montana* exhibits anisocytic stomata, where each stomatal pore is surrounded by three subsidiary cells of unequal size. This pattern is characteristic of the Ranunculaceae family, which includes Clematis species (IAWA Journal, 2014).

5.6.2. Microscopic Analyses of Stomatal Features in a) *Hedera hibernica*, b) *Hedera colchica* and c) *H. helix* 'Plattensee' (Abaxial Surface)

The microscopic image of the abaxial (lower) leaf surface of *Hedera hibernica* reveals a dense and uniform distribution of stomata, each surrounded by multiple layers of epidermal cells with wavy outlines. The stomata appear as elliptical openings, with well-defined guard cells contrasting against the surrounding epidermal cells, as shown in Figure 2. The guard cells exhibit a slightly raised structure, typical of xeromorphic adaptations in plants that regulate transpiration efficiently.

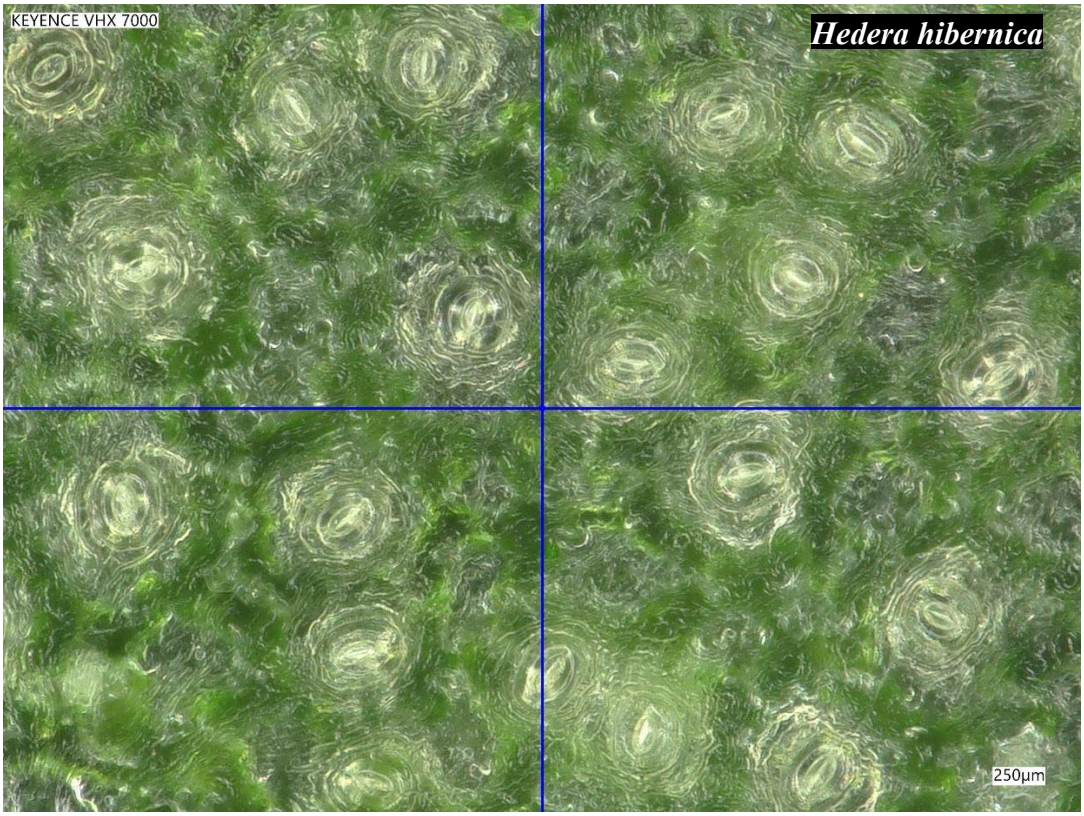

Figure 2. Typical Image of stomata of the abaxial surface of a) *Hedera hibernica*, leaves at a 700 x magnification; bar represents 0.25 mm.

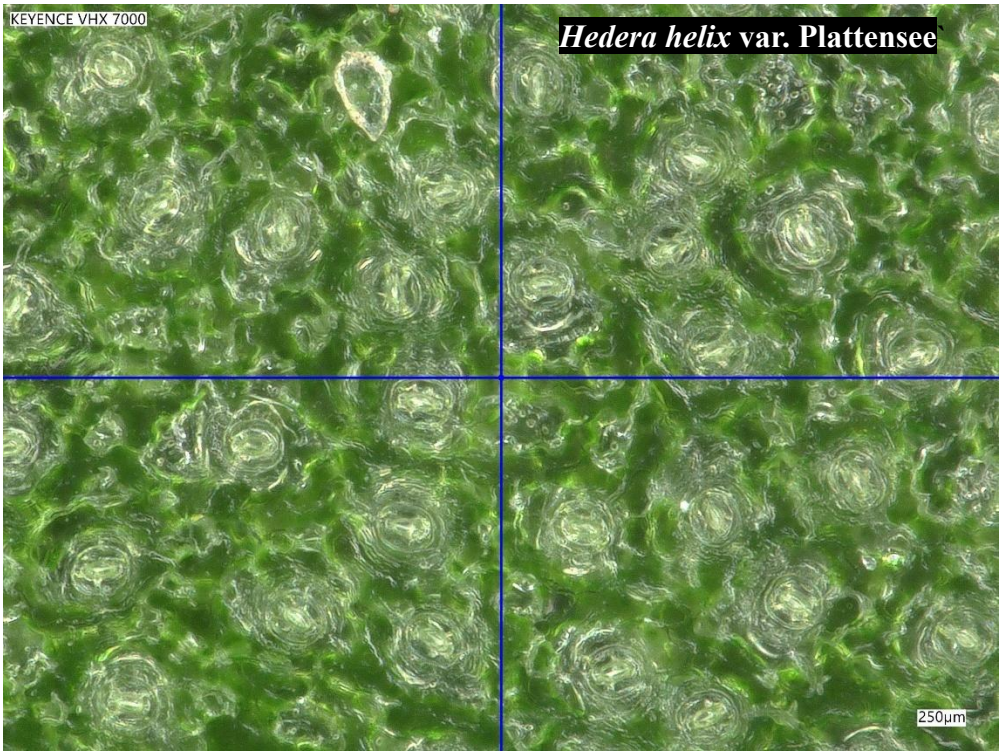

Figure 3. Typical Image of stomata of the abaxial surface of *H. helix var.* Plattensee leaves at a 700 x magnification; bar represents 0.25 mm.

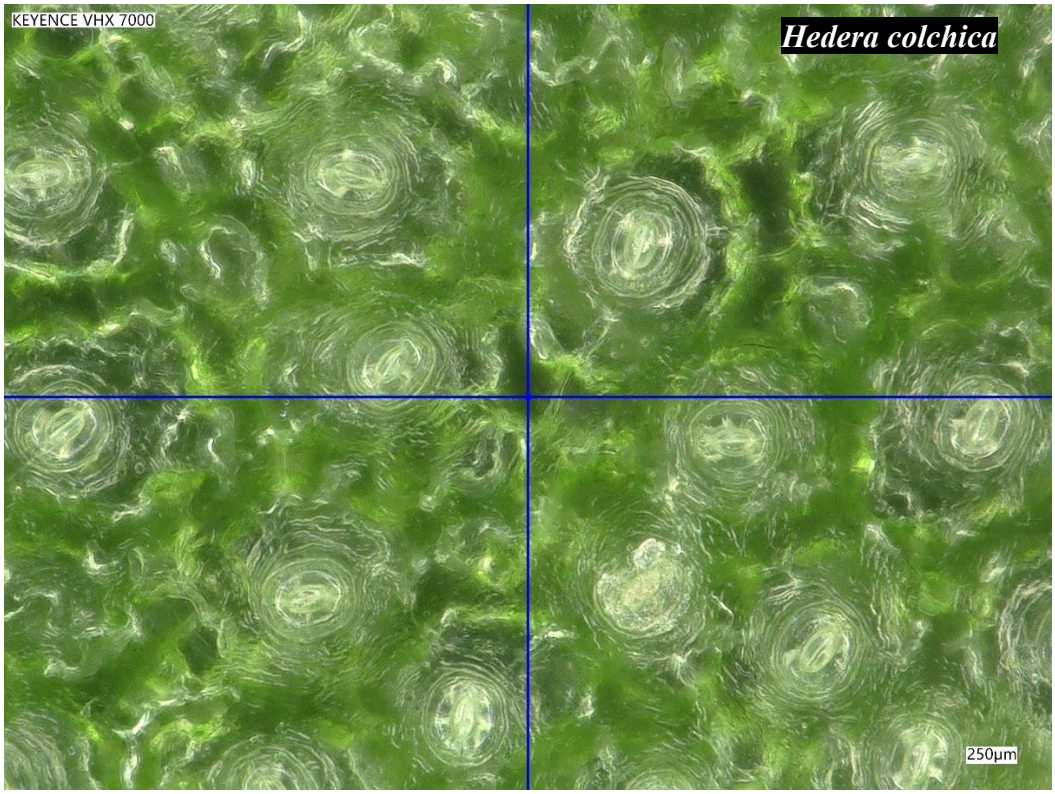

Figure 4. Typical image of stomata of the abaxial surface of *Hedera colchica* leaves at a 700 x magnification; bar represents 0.25 mm.

5.6.3. Stomatal Type and Classification of *Hedera* species

The observed stomatal arrangement in *Hedera* species corresponds to the anomocytic type, characterized by the absence of specialized subsidiary cells surrounding the guard cells. Instead, the stomata are encircled by ordinary epidermal cells, which lack a defined pattern in size or arrangement. This stomatal type is common in many species of the Araliaceae family, to which the *Hedera* species belongs. The uniform distribution of stomata across the surface suggests that this species has evolved a well-regulated transpiration mechanism, potentially aiding in moisture retention and gas exchange under variable environmental conditions.

5.6.4. Microscopic Analyses of Stomatal Features in *L. henryi* (Abaxial Surface)

The microscopic image of the abaxial (lower) leaf surface of *L. henryi* shows a high-resolution view of the epidermal structure, highlighting stomatal distribution, guard cell morphology, and surrounding epidermal cell arrangement, as shown in Figure 3. The stomata

appear as elliptical openings interspersed between irregularly shaped epidermal cells with undulating cell walls, contributing to the leaf surface's structural integrity.

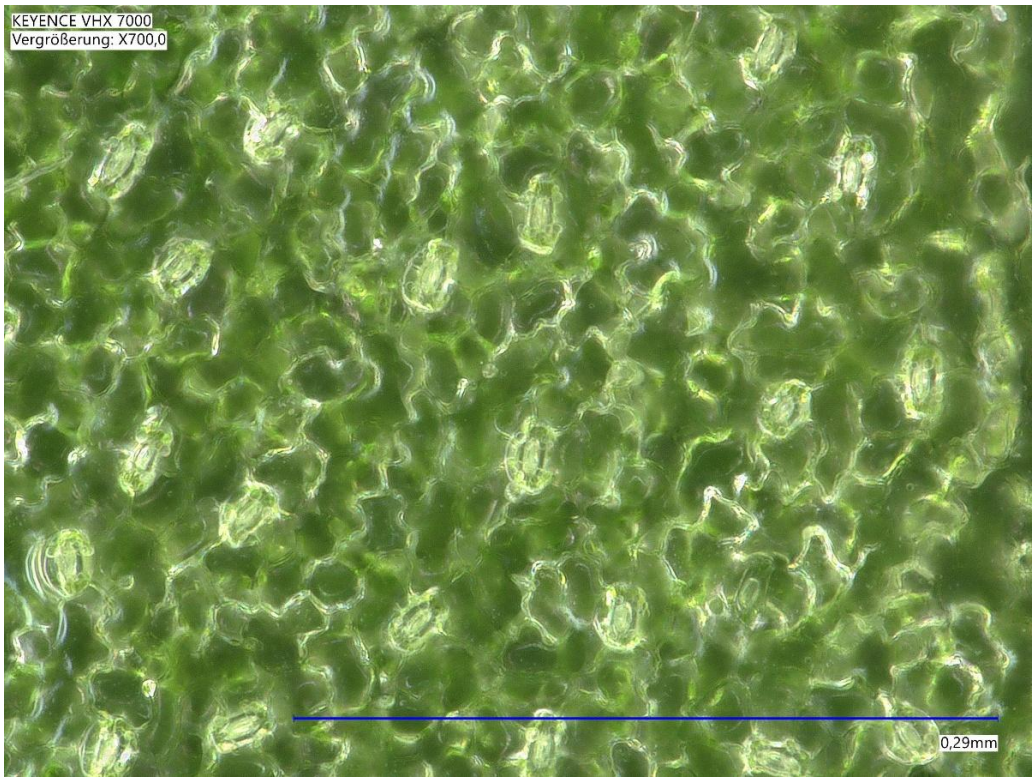

Figure 5. Typical image of stomata of the abaxial surface of *L. henryi* leaves at a 700 x magnification; bar represents 0.29 mm.

5.6.5. Stomatal Type and Classification of *L. henryi*

The stomata in *L. henryi* follow a paracytic (rubiaceous) arrangement, characterized by two lateral subsidiary cells parallel to the guard cells. This stomatal type is commonly found in members of the Caprifoliaceae family and suggests an adaptation for regulated gas exchange. The distribution of stomata appears moderately dense, which may facilitate efficient transpiration while maintaining water conservation under varying environmental conditions.

5.6.6. Microscopic Analyses of Stomatal Features in *Wisteria sinensis* (Abaxial Surface)

The provided image, captured using a Keyence VHX 7000 digital microscope, reveals the microscopic details of the abaxial epidermal surface of a *Wisteria sinensis* leaf. The stomata appear to be anomocytic, meaning they lack specialized subsidiary cells and are surrounded by irregularly shaped epidermal cells. The elliptical guard cells, which form and regulate the stomatal pore responsible for gas exchange and transpiration, are visible. These stomata are distributed non-uniformly across the surface, exhibiting some degree of clustering common

among dicotyledonous plants. The surrounding epidermal cells display undulating anticlinal walls, contributing to the leaf's structural integrity and flexibility. Notably, the image also shows the presence of several trichomes, hair-like structures that may play a role in water conservation and defence against environmental stressors. A scale bar indicates that each stomata measures approximately 20–30 µm, offering a size reference as shown in Figure 6.

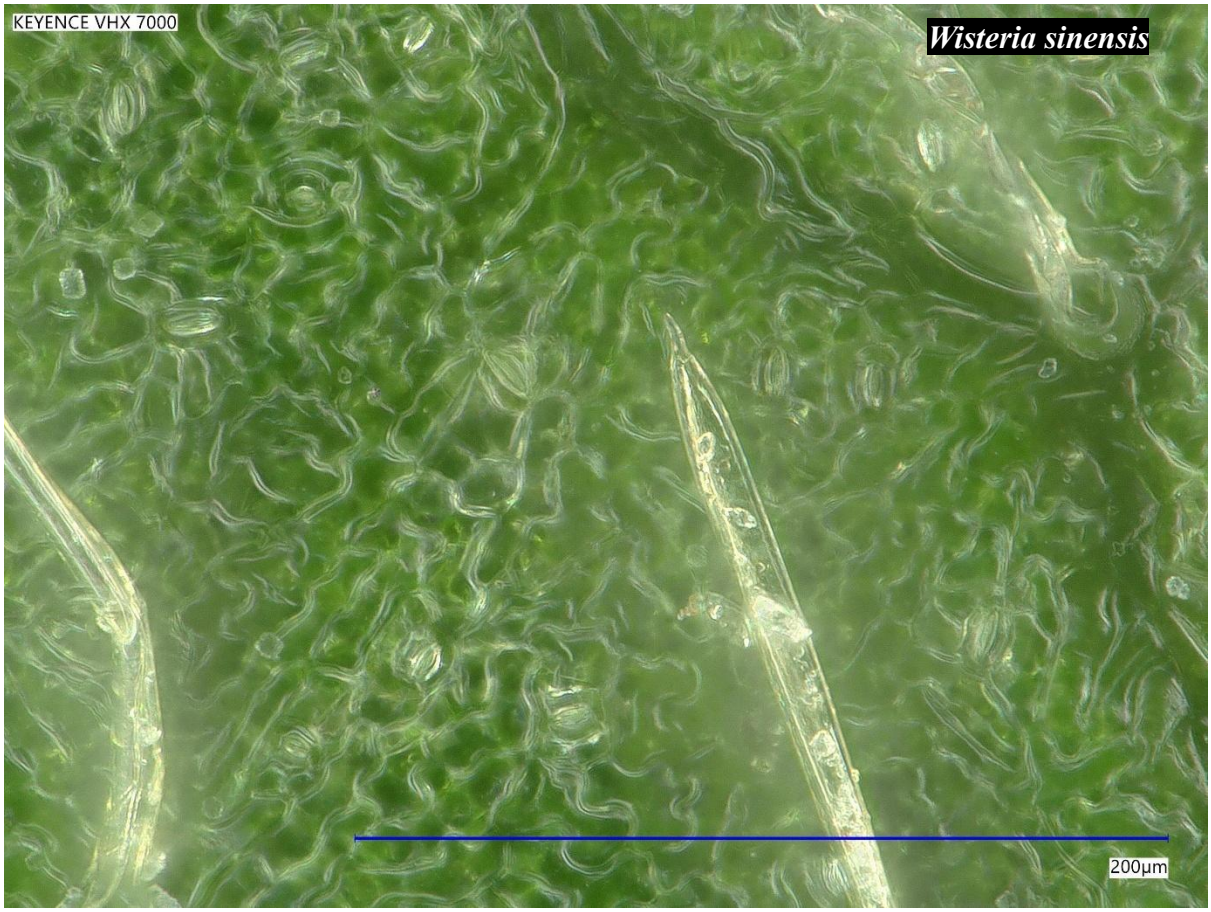

Figure 6. Typical image of stomata of the abaxial surface of *Wisteria sinensis* leaves at a 700 x magnification, trichomes showing as bright sword-like structures; bar represents 0.20 mm.

5.7. Stomatal Density

The experiment examined stomatal density across six plant species: *C. montana*, *H. colchica* var. Russland, *H. helix var. Plattensee*, *H. hibernica*, *L. henryi*, and *W. sinensis*. A one-way ANOVA was conducted to compare the stomatal density differences among species.

5.7.1. Descriptive Statistics

The mean stomatal densities (number/mm²) for each species are presented in figure 7 below:

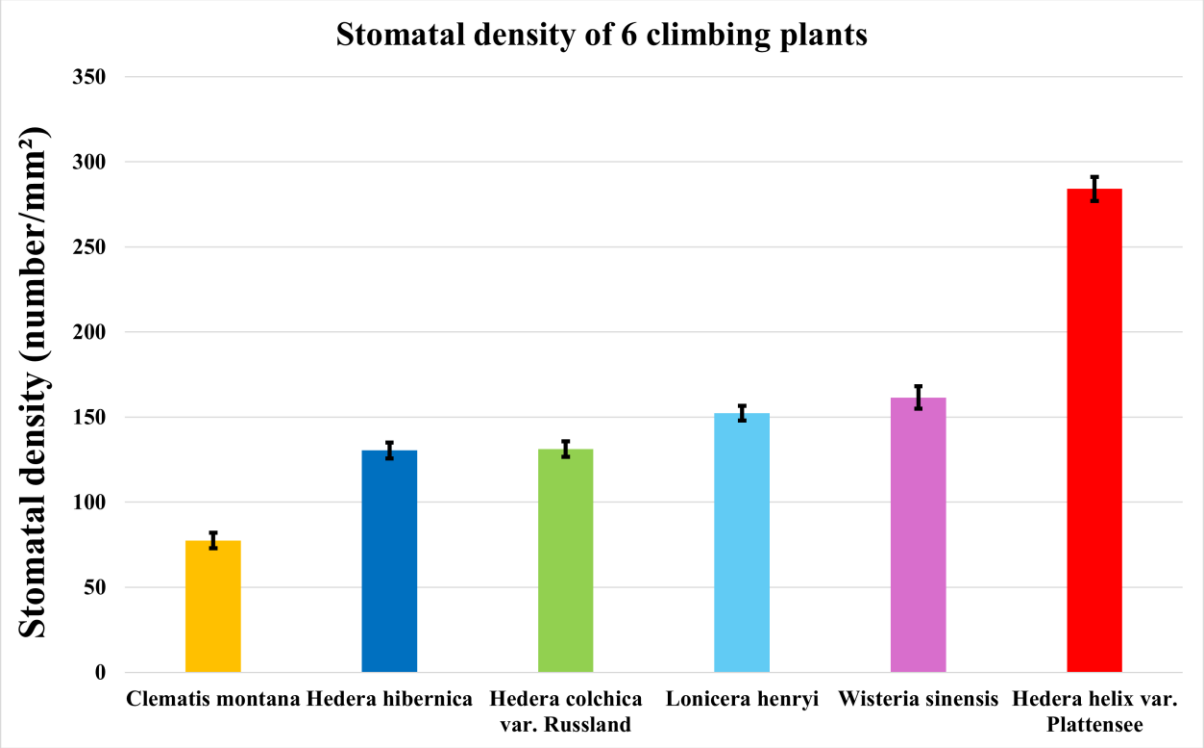

Figure 7. Stomatal density of 6 potted climbing plants growing under similar conditions (n=20), bars representing standard error.

5.7.2. ANOVA Results

The one-way ANOVA revealed a statistically significant difference in stomatal density among the species ($F(5, 114) = 154.135$, $p < 0.001$). The effect size was large, with an eta-squared value of 0.871 (95% CI: 0.865-0.894), indicating that approximately 87.1% of the variance in stomatal density was attributable to species differences.

Summary table of ANOVA

Source of Variation	Sum of Squares	df	Mean Square	F	Sig.
Between Groups	478,006.859	5	95,601.372	154.135	<0.001
Within Groups	70,707.819	114	620.244		
Total	548,714.678	119			

5.7.3. Post-Hoc Analysis

Tukey's HSD test was used for post hoc comparisons. The results showed:

H. helix var. Plattensee had significantly higher stomatal density than all other species ($p < 0.001$ for all comparisons).

C. montana had significantly lower stomatal density than all other species ($p < 0.001$ for all comparisons)

Hedera hibernica and *Hedera colchica* var. Russland did not differ significantly from each other ($p = 1.000$) but had lower stomatal densities than *L. henryi* and *W. sinensis*.

L. henryi and *W. sinensis* did not differ significantly from each other ($p = 0.848$) but had higher stomatal densities than the *Hedera* species, except for *H. helix* var. Plattensee.

5.8. Discussion

The morphological diversity of stomatal types in climbing plants employed for facade greening presents intriguing questions about their potential adaptive roles in urban environments. Despite well-documented variations in stomatal structure—anisocytic in *C. montana*, anomocytic in *Wisteria* and *Hedera* species, and paracytic in *L. henryi* —the functional significance of these differences remains speculative. Current research primarily focuses on descriptive taxonomy or broad ecological benefits (e.g., cooling, pollution mitigation) (Di & Wang, 2010; B. Zhang et al., 2020), with limited empirical investigation into how stomatal morphology may directly influence plant performance in urban settings. The observed variability in stomatal density across sampled species highlights its responsiveness to environmental drivers. While light intensity, atmospheric CO_2 levels, and water availability have been identified as key modulators, the potential thermoregulatory role of stomatal density warrants consideration. Higher densities may enhance transpirational cooling through increased evaporative surface area, particularly under heat stress. However, this cooling capacity appears context-dependent: trade-offs between thermal regulation and hydraulic efficiency in water-limited environments likely constrain stomatal proliferation.

A critical aspect lies in understanding whether specific stomatal types confer advantages under environmental stressors prevalent in cities, such as air pollution, heat islands, or limited water availability.

Future research should prioritize functional validation of stomatal adaptations through controlled stress experiments (e.g. drought, pollutant exposure) and in situ monitoring of facade greening systems. Advanced techniques like chlorophyll fluorescence imaging or eddy covariance measurements could resolve how stomatal morphology influences real-world performance. Until then, species selection for urban greening will remain guided more by tradition and anecdotal success than by evidence-based understanding of stomatal adaptations.

5.9. Conclusion

Stomatal morphology, including anisocytic, anomocytic, and paracytic types, offers potential insights into a plant's adaptation to its habitat. However, its functional significance in urban greening remains speculative and cannot be followed up with the frame of this thesis. Hypotheses about their roles in water-use efficiency, humidity regulation, and gas exchange lack empirical validation, particularly in facade systems. Critical gaps include the absence of studies linking stomatal types to urban stressors like pollution, heat islands, and fluctuating CO_2 levels. Future research must prioritize controlled experiments and field studies to validate these adaptations.

6.0. Preface to the submitted manuscript: **"Evapotranspiration and Water Stress Resistance in Four Façade Greening Climbers: A Comparative Analysis"**

Climbing plants are integral to urban green infrastructure, offering benefits such as thermal regulation, air purification, and aesthetic enhancement. As climate change increases drought frequency and urban heat stress, understanding plant water use and stress responses is vital for selecting resilient species. This section introduces the core findings of a study on four climber species used in façade greening: *H. helix* 'Plattensee', *Hedera hibernica*, *Hedera colchica* 'Russland', and *L. henryi*.

The plants were cultivated in 20-liter pots with uniform substrate and arranged sequentially in fixed positions throughout the experiment to ensure consistent exposure to environmental conditions. Evapotranspiration was measured gravimetrically, using weight loss to estimate plant water loss.

This thesis focuses on the water-limiting phase, following field capacity (pF 2.0) when declining substrate moisture began limiting physiological activity. Although an initial energy-driven phase was recorded, it was excluded due to its short duration and poor statistical robustness (e.g., an R^2 of 1 based on only 5 data points in *L. henryi*).

To reflect the scope of the data, terminology such as "drought resistance" was replaced with "water-use resistance" or "physiological response to water stress", avoiding overstatements about species tolerance in the absence of direct stress markers like wilting or chlorophyll fluorescence.

Statistical analysis was conducted using SPSS. Linear regressions evaluated the relationship between evapotranspiration and environmental drivers (e.g., vapor pressure deficit, temperature, wind speed). Model performance was assessed using R^2 and significance thresholds ($p < 0.05$), with appropriate checks for assumptions such as normality and independence of residuals.

By focusing on water-limited conditions, this study provides insights into the adaptive water-use behaviour of climbers, helping to inform their application in drought-tolerant façade greening for future urban climates.

Submitted Article: **Evapotranspiration and Water Stress Resistance in Four Façade Greening Climbers: A Comparative Analysis**

Evapotranspiration and Water Stress Responses in Four Façade Greening Climbers: A Comparative Analysis

Minka Aduse-Poku[1] *ORCID:* 0009-0003-9923-6135, Alexander H.H. Popov[2], Hans G. Edelmann[1*] *ORCID*: 0000-0001-5397-8895

[1]: Universität Köln, Institut für Biologiedidaktik, Herbert-Lewin-Str. 2, 50931 Cologne, Germany

madusep2@smail.uni-köln.de/a.minka@yahoo.com, h.edelmann@uni-koeln.de

[2]: University of Bonn, Bonn Institute for Organismic Biology (BIOB), 53115, Bonn, Germany.

alexpopovvv@gmail.com

*corresponding author : h.edelmann@uni-koeln.de

Abstract

Abstract

Façade greening is a sustainable urban strategy to mitigate climate change and air pollution, with effectiveness influenced by abiotic factors like soil water potential, temperature, wind, and vapor pressure deficit (VPD). This study examines the evapotranspiration dynamics and water-stress response of four evergreen climbers (*Hedera helix* "Plattensee," *Hedera hibernica*, *Hedera colchica*, and *Lonicera henryi*), assessing their cooling contributions to façade greening systems. Evapotranspiration rates were measured under natural conditions using a weather station to monitor meteorological variables, including air temperature, relative humidity, solar radiation, and wind speed. Key influencing factors—VPD,

photosynthetic photon flux density (PPFD), and soil water potential (pF)—were analyzed to capture plant-atmosphere interactions.

Results show *H. hibernica* has the highest cooling potential but requires consistent water availability, making it more suitable for humid regions. *H. colchica* demonstrates strong water stress resistance, maintaining performance under water-limiting conditions. *H. helix* "Plattensee" balances cooling efficiency and water conservation, ideal for temperate climates. *L. henryi* exhibits low water use and is suitable for water-limited projects.

During the water-limiting phase, pF was the dominant driver of evapotranspiration, while VPD and PPFD affected the energy-driven phase. β-correlation analysis revealed species-specific responses, informing plant selection for urban climates. These findings support optimized species selection for façade greening, enhancing cooling efficiency and water sustainability in urban environments.

1.0. Introduction

Cities are increasingly facing the escalating effects of anthropogenic activities and climate change, such as rising temperatures and frequent heat waves, which pose significant threats to public health and well-being (Kovats & Hajat, 2008; Luber & McGeehin, 2008; Scherer & Endlicher, 2013). Addressing these challenges is urgent, and nature-based solutions, particularly vertical greening systems, are increasingly emerging as viable strategies to mitigate urban heat island effects and improve building energy efficiency (Dütemeyer et al., 2013; Heisler & Brazel, 2015). A key component of these solutions is transpiration cooling, a process through which plants cool their environment by releasing water vapor into the atmosphere while absorbing pollutant gases like CO_2, NO_2, and O_3 (Aduse-Poku & Edelmann, 2025; Nilson & Assmann, 2007; Ziemer, 1979).

Typically, plants respond to water stress by reducing transpiration through stomatal closure, regulated by hydraulic traits and hormonal signals such as abscisic acid (ABA) (Koehler et al., 2023; Nilson & Assmann, 2007). Studies on crops have shown that transpiration is influenced by both soil moisture and atmospheric demand, with stomatal closure occurring when soil-plant hydraulic conductance is limited (Koehler et al., 2023). Water-stressed plants also experience higher leaf temperatures due to reduced transpiration and, thereby, reduced cooling, emphasizing the importance of transpiration in the survival of the leaves and plants as a whole system (Gräf et al., 2021).

Due to the lack of plantable urban areas, climbing plants have become crucial in climate-adapted building designs. However, their evapotranspiration dynamics and responses to water stress have been little studied. While some research has examined their physiological reactions to environmental stressors, such as particulate matter pollution (Lyu et al., 2023), few studies have explored their evapotranspirational behaviour under drought conditions. Lyu et al. focused on species-specific physiological responses to pollution but did not assess how

these plants regulate water loss during periods of limited water availability. This gap in knowledge underscores the need for further research to understand better the water-stress response and ecophysiological role of climbing plants in urban environments.

Besides shading, evapotranspiration is a critical component of plant water relations, playing a central role in the cooling capacity of green façades (Gräf et al., 2021). As these evergreen climbers transpire, they help lower ambient - air and building surface temperatures (Krich et al., 2022; Ziemer, 1979). However, these plants' evapotranspirational cooling potential is inherently dependent on and linked to water availability and prevailing atmospheric conditions at all times.

This study focuses on the evapotranspirational cooling potential and water stress response of four evergreen climbers commonly used in façade greening: *H. helix* "Plattensee," *Hedera colchica* "Russland," *H. hibernica*, and *L. henryi* (honeysuckle). These species were selected for their year-round benefits, providing cooling effects through shading and transpiration in summer and offering natural winter insulation (Aduse-Poku et al., 2024; Köhler, 2008).

Therefore, detailed measurement of evapotranspiration is vital for understanding plant-water relations and responses to environmental stressors. Various methods are available, each with its advantages and limitations. Instantaneous methods, such as porometers, provide a snapshot of stomatal conductance and transpiration rates at specific moments, which helps in the study of rapid changes in plant water status but may not capture long-term trends or daily fluctuations in transpiration (Hasanuzzaman et al., 2023). Conversely, gravimetric methods allow for a more comprehensive water loss assessment over defined periods, offering an integrated estimate of transpiration and evaporation (Cirelli et al., 2012).

Therefore, this study employed the gravimetric method to measure daily water loss, enabling the assessment of the overall water use of climbing plants under natural weather conditions.

1.1. Research Questions

- How do selected climbers respond and adjust evapotranspiration rates during field capacity and water-stress conditions?
- What are the evapotranspiration/cooling potentials under conditions with less water availability?
- How can species-specific water use inform water-efficient urban greening strategies?

1.2. Hypothesis

Climbing plants will show species-specific evapotranspiration patterns under optimal and water-stressed conditions.

2.0. Materials and Methods

2.1. Plant species

Four evergreen climbing species were selected for this study: three from the genus Hedera (Araliaceae) (Metcalfe, 2005a; Valcárcel & Vargas, 2010) and one from the genus Lonicera (Caprifoliaceae) (Gigon & Weber, 2005). The Hedera species included *Hedera helix* 'Plattensee,' *Hedera hibernica*, and *Hedera colchica* 'Russland.' The fourth species was *Lonicera henryi*, commonly known as Henry's honeysuckle.

As depicted in Figure 1 below, *H. helix* 'Plattensee' is distinguished by its dark green leaves with silvery-white veining and compact growth habit.

H. hibernica, or Atlantic ivy, is known for its large, glossy green leaves and vigorous growth, while *H. colchica* 'Russland' features large, heart-shaped leaves and is noted for its cold hardiness (Cobb et al., 2013).

L. henryi is an evergreen honeysuckle native to China (Gigon & Weber, 2005), with lance-shaped, dark green leaves and tubular yellow to ochre flowers tinged with pink or purple.

Fig 1. Images showing the foliage of the four evergreen climbers: a) *H. helix"* Plattensee," b) *H. hibernica*, c) *H. colchica* 'Russland,' and d) *L. henryi* used in the study.

2.2. Experimental Setup

The study was conducted on an open plot exposed to natural sunlight, wind, humidity, and temperature but protected from precipitation. This was achieved using a dome-shaped UV-penetrating tent constructed from transparent plastic sheets. The dome allowed maximum light penetration while shielding the pots from rainfall, ensuring reliable gravimetric measurement of water loss. Adequate air circulation was maintained to replicate natural ambient conditions (Fig 2).

Each of the four species was represented by eight replicate plants (4 species × 8 replicates = 32 individuals) cultivated in 20-liter pots. The pots were filled with a standardized substrate (ED 73) and arranged as shown in figure 2. All individuals were spaced at uniform distances (~50 cm) to prevent mutual shading.

All plants were sourced from a professional horticultural supplier (Container Baumschule & Stauden Michael Kunz, Heiligenhaus, Nordrhein-Westfalen, Germany), ensuring genetic and phenotypic consistency within species. Prior to the beginning of the study, 2 ml of WUXAL NPK liquid fertilizer per 1 liter of water was applied via a fertilizer injector.

2.3. Measurement of Evapotranspiration

The initial soil moisture was adjusted to field capacity, after which plants were allowed to dry naturally to simulate drought stress. A high-precision Kern weighing scale, with a 30 kg capacity and 1 g sensitivity, was used to detect daily changes in mass, representing evapotranspiration.

This approach enabled accurate, non-invasive water use tracking under conditions that mimic real-world exposures, without the confounding influence of precipitation.

2.4. Environmental Monitoring

Microclimatic conditions were continuously recorded using a Davis Vantage Pro2 weather station installed adjacent to the experimental setup. The weather station captured the following parameters at one-hour intervals:

- Air temperature (°C)
- Relative humidity (%)
- Solar radiation (W/m²)
- Wind speed (km/h)

- Barometric pressure (hPa)

This continuous environmental dataset enabled correlation analyses between evapotranspiration rates and dynamic weather conditions.

2.5. Light Variability Considerations

Although the experimental setup allowed for uniform environmental exposure, slight variations in light intensity occurred due to species-specific differences in leaf orientation and sun exposure. Light conditions were not systematically randomized or homogenized across species. This is acknowledged as a potential source of variability in physiological responses and was considered in interpreting results.

Fig 2. Experimental setup showing the arrangement of potted plants used in the study. To prevent the uncontrolled interference of rainwater, a special plastic sheet developed for greenhouses was fitted in an arch shape with wide openings at two sides.

2.6. Determination of Substrate Water Content

The pots were saturated with collected rainwater and allowed to drain for 48 hours, as visualized in Figure 2. After this period, a plastic plate (plant saucer) was used to prevent direct contact between the pot and the soil. Soil samples of about 5 g were taken from each pot, instantaneously weighed in the field, and packed in plastic bags. The soil samples were then transferred to a glass petri dish and weighed again. These samples were dried immediately in an oven at 105° C for 24 hours and weighed repeatedly at two-hour intervals to ensure weight consistency. To determine water content, the mass ratio before and after drying was applied to the subsequent daily measurements, following the rule of proportions method as described in O'Kelly and Sivakumar, (2014).

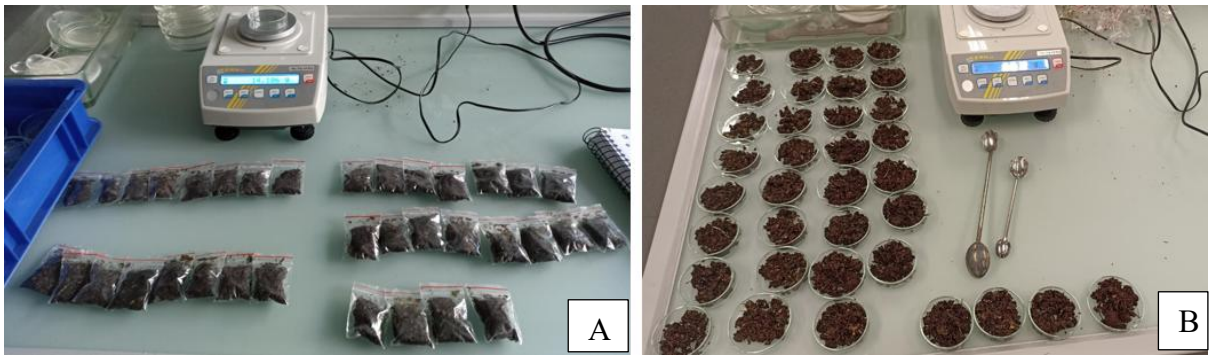

Fig 3. Soil samples removed from pots 48 hours after water saturation (≈ field capacity); A) – before oven drying in small plastic bags (B) – in small Petri dishes after drying.

2.7 Statistical Analysis

Data were analyzed using Multiple Linear Regression (MLR) in IBM SPSS Statistics (version 30.0.0.0 (172)) to evaluate the effects of environmental predictors (vapor pressure deficit [VPD], photosynthetic photon flux density [PPFD], soil water potential [pF], temperature, and wind speed) on evapotranspiration (ET) rates across species.

3.0. Results

Two different observation periods with distinct temporal resolutions were initially analyzed: (1) a seven (7) - month overview of evapotranspiration trends from March to September and (2) daily measurements during September.

For the long-term analysis, monthly evapotranspiration rates were estimated using the total leaf area measured at the end of the experiment in September. However, while this approach ensured a consistent normalization reference to leaf area, it underestimated evapotranspiration in the earlier months, when the actual leaf area was lower. As a result, the calculated water loss during this period (March-August) does not precisely reflect water use or evapotranspiration potential during early growth stages.

For reference purposes, the monthly data from March to September are presented as supplementary material (S1).

The primary focus of the Results section is on the detailed daily evapotranspiration data collected in September when all species had reached full canopy development.

This narrowed focus provides a more accurate and ecologically meaningful comparison of water use dynamics among the climbing species under late-summer conditions, supporting the evaluation of their suitability for façade greening applications.

3.1. Substrate Water Content

At field capacity, the mean water content of the substrate (ED73: Einheitserde) was 58 ± 1% (mean ± standard error, n = 130), consistent with findings by (Menberu et al., 2021) for pristine peat soils. The low standard error indicates uniform water retention across the pots at field capacity, setting consistent water availability across the different plant species. This

field capacity was kept at the start of each experimental cycle, providing a stable baseline for assessing soil water decline throughout the experimental phases (see online resource (S 2) figure on water content).

3.2. Daily Evapotranspiration and Environmental Interactions

Building upon the monthly ET trends, we shifted focus to a daily assessment of evapotranspiration. This analysis examined the relationship between daily ET, soil water retention, and weather parameters. To better understand water availability for plant uptake, we incorporated the pF scale, a logarithmic measure of soil water tension, into the analysis. The pF scale helps determine the onset of water stress, as it indicates how tightly water is held by soil particles in this very substrate and its availability to plants (Markoska et al., 2018; Schwärzel et al., 2002).

By integrating pF as a key variable, this analysis highlights the interplay between daily evapotranspiration rates, soil water retention, and weather conditions.

3.3. Water content and pF scale

The trends of the observed water contents during different weather conditions emphasize the dynamic nature of soil water availability and its direct impact on plant water use. The pF scale, a dimensionless measure representing the negative logarithm (base 10) of soil water potential (typically expressed in centimeters of water [cm H_2O]), was utilized to assess the energy status of water in the soil. This scale is pivotal for understanding how tightly water is bound to soil particles and how accessible it is to plants (Lal, 2020).

This study compared water content from the experiment to pF values of established curves from prior research on similar peat soils, enabling a standardized approach to understand soil water availability and its influence on evapotranspiration. The plants' capacity to maintain

efficient evapotranspiration became critical as the soil transitioned from field capacity conditions (low pF values) to more water-limiting phases (higher pF values). Together with measured water content (see online resource S 2), the onset of water stress was determined to help access the critical water use behaviour of the plants.

The comparison with existing pF curves further validated the methodology and enriched the interpretation of how soil water availability correlates with evapotranspiration rates. These data are vital for understanding how the climber species respond to water-limiting conditions, particularly during drought periods, and their ability to maintain evapotranspirational cooling even under challenging environmental conditions.

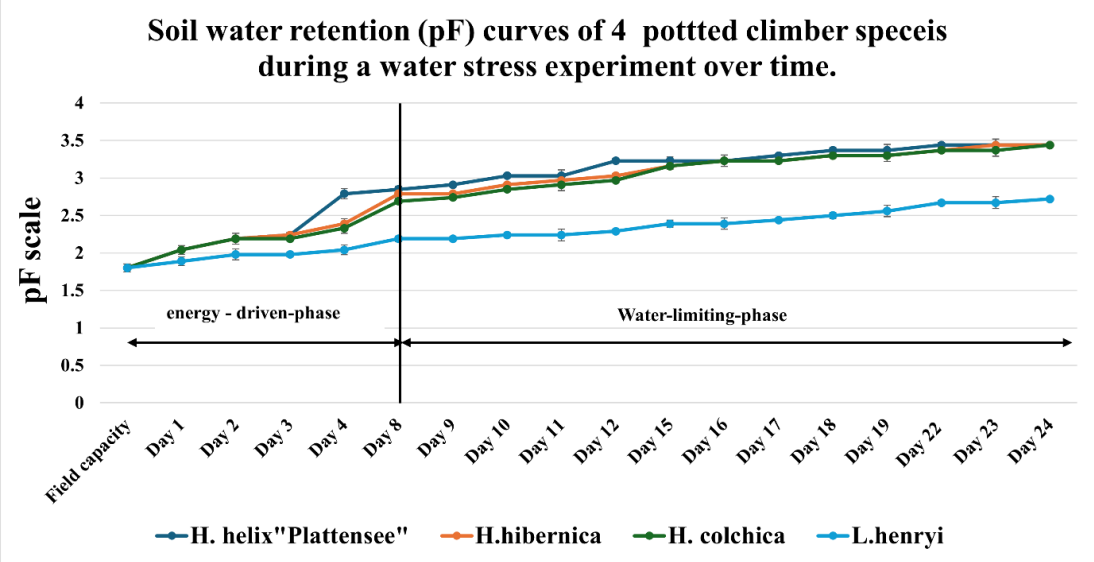

Fig 4. Water retention (pF values) of soils accommodating the different climber plants, indicating the energy-driven and water-limiting phases of evapotranspiration.

3.4 The Energy-Driven Phase of Evapotranspiration and Species-Specific Performance

Analyses of soil water retention (pF) values revealed that the energy-driven phase of evapotranspiration for all *Hedera* species (Figure 4) occurred during the first eight (8) days after the onset of the experiment (field capacity). This phase represents a critical period where environmental conditions, such as vapor pressure deficit (VPD), Photosynthetic Photon Flux

Density (PPFD), and temperature, drive peak evapotranspiration rates, emphasising the species' responsiveness to external environmental factors (Denissen et al., 2022; Ghiat et al., 2021; Katul et al., 2012)

Due to the design of the experiment and prevailing weather conditions, five data points were recorded for the *Hedera* species during the energy-driven phase of the experiment (as indicated in Figure 5 showing an example of a correlation between ET and VPD). This small sample size resulted in an unrealistic perfect linear regression ($R^2 = 1$). Pearson correlation coefficient is then employed to better assess the relationships between evapotranspiration (ET) and key abiotic factors. This statistical measure quantifies the strength and direction of linear associations between continuous variables, where r-values range from -1 to +1 as presented in section **3.5**. A positive correlation indicates that as one variable increases, the other also increases, whereas a negative correlation suggests an inverse relationship (Janse et al., 2021).

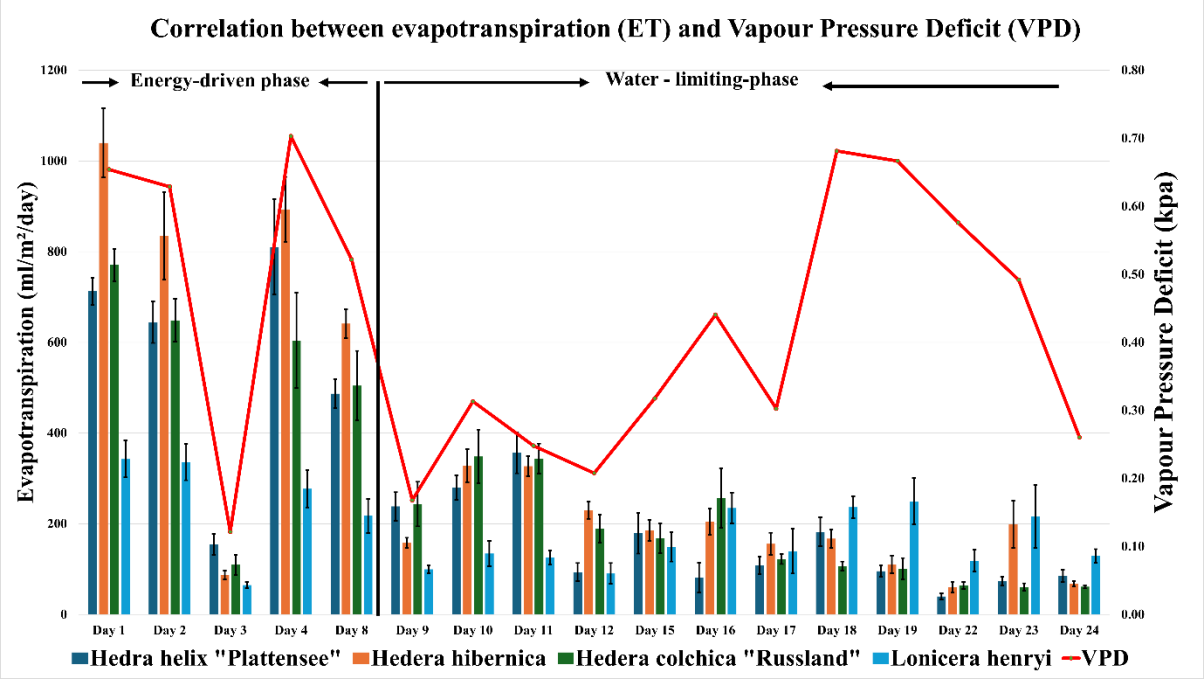

Fig 5. Correlation of the mean evapotranspiration and prevailing vapour Pressure Deficit (VPD). Bars in the bar chart = standard error bars; (columns represent species, and the red line represents VPD).

3.5 Pearson Correlation (r) of ET and Abiotic Factors During the Energy-Driven Phase

The energy-driven phase of evapotranspiration was analyzed for *H. helix* 'Plattensee,' *H. Hibernica,* and *H. colchica* 'Russland.' The mean evapotranspiration (ET) rates varied significantly among species, with *H. hibernica* exhibiting the highest rate at 699 ml/m²/day, followed by *H. helix* 'Plattensee' at 562 ml/m²/day and *H. colchica* 'Russland' at 528 ml/m²/day. The analyses revealed consistent energy-driven evapotranspiration (ET) patterns across *H. helix, H. hibernica*, and *H. colchica*, with minor species-specific variations. All three species showed strong coupling to light (PPFD), temperature, and vapor pressure deficit (VPD), while soil moisture (pF) and wind speed had negligible effects. Below is a synthesis of the findings, supported by a comparative Table 1.

Key Observations:

Significant Energy Drivers

PPFD: The highest correlation was in *H. helix* (r = 0.979), followed by *H. hibernica* (r = 0.978) and *H. colchica* (r = 0.945).

Temperature: Strongest in *H. helix* (r = 0.981), weakest in *H. colchica* (r = 0.921).

VPD: Most critical for *H. colchica* (r = 0.952), though all species exceeded r = 0.95.

Non-Significant Drivers

pF (Soil water potential): No significant correlations (r = −0.183 to 0.149, $p > 0.05$), confirming ET decoupling from soil water in non-limiting conditions.

Wind Speed: presented the weakest effect (r = 0.293 – 0.549, $p > 0.05$).

Colinearity Among Predictors

Temperature and VPD were near-perfectly correlated ($r \approx 0.959$) in all species. PPFD also correlated strongly with temperature/VPD ($r > 0.95$), complicating the isolation of individual effects (see Table 1).

Table 1: Comparative Pearson Correlations (r) for the energy-driven phase of ET Drivers in Hedera Species

Variable	*H. helix*	*H. hibernica*	*H. colchica*	Trend
PPFD (µmol/m²/s)	0.979*	0.978*	0.945*	*H. helix* >*H. hibernica* ≈ *H. colchica*
Temperature (°C)	0.981*	0.950*	0.921*	*H. helix* > *H. hibernica* > *H. colchica*
VPD (kPa)	0.981*	0.972*	0.952*	*H. helix* ≈ *H. hibernica* > *H. colchica*
pF	0.149	-0.183	-0.149	Non-significant (all species)
Wind Speed (km/h)	0.549	0.356	0.293	*H. helix* > *H. hibernica* > *H. colchica*

Notes

- *$p < 0.05$ (significant). N = 5 for all species (small sample size).
- All species shared colinearity between temperature, VPD, and PPFD ($r > 0.95$).

3.6. Observed Evapotranspiration Patterns in *Lonicera henryi*

In contrast to the water loss trends observed in the *Hedera* species during the experimental period, *L. henryi* exhibited low water use (see Figure 4 above).

Vapor Pressure Deficit (VPD) showed a statistically significant positive relationship with evapotranspiration (ET) rates ($p = 0.038$). For every 1 kPa increase in VPD, ET increased by 449.27 ml/m²/day.

Soil Water Potential (pF) values remained below water-limiting thresholds ($pF < 2.8$) throughout the experiment. The observed relationship between pF and ET was not statistically significant ($p = 0.119$). Energy-related predictors, including PPFD ($p = 0.641$), wind speed ($p = 0.527$), and temperature ($p = 0.782$), demonstrated no significant effects on ET rates as shown in Table 2 below.

The regression model for ET (ml/m²/day) = 334.263 - 114.789(pF) - 0.003(PPFD) - 32.730(Wind) - 2.036(Temperature) + 449.269(VPD)

Table 2: Multiple Linear Regression of evapotranspiration in *Lonicera henryi*

Environmental Variable	Unstandardized Coefficient (B)	Standard Error	95% Confidence Interval	p-value (significant at p<= 0.05
Constant	334.263	246.702	(-208.724, 877.250)	0.203
pF	-114.789	67.991	(-264.435, 34.858)	0.119
PPFD (µmol/m²/s)	-0.003	0.006	(-0.016, 0.010)	0.641
Wind Speed (km/h)	-32.73	50.093	(-142.985, 77.525)	0.527
Temperature (°C)	-2.036	7.18	(-17.838, 13.766)	0.782
VPD (kPa)	449.269*	190.642	(29.668, 868.870)	0.038

3.7. Water-Limiting Phase of Evapotranspiration (*Hedera* Species) and species-specific performance

3.7.1. *H. helix* 'Plattensee'

A multiple linear regression model was used to predict evapotranspiration (ml/m²/day) based on soil water potential (pF), photosynthetic photon flux density (PPFD), wind speed, temperature, and vapor pressure deficit (VPD). The model revealed significant effects for two predictors (Table 3):

The intercept term was statistically significant (B = 2097.03, p = 0.023), indicating baseline evapotranspiration under neutral conditions.

Soil water potential (pF): A 1-unit increase in pF (indicating drier soil) significantly reduced evapotranspiration by 541.42 ml/m²/day (B = −541.42, 95% CI: −1001.26 to − 81.59, p =0.028). This predictor exhibited the most substantial standardized effect (β = − 0.997), highlighting its dominant role in explaining variability in evapotranspiration.

Other predictors, including PPFD (B = − 0.009, p = 0.498), wind speed (B = 37.24, p = 0.682), temperature (B = − 15.98, p = 0.279), and VPD (B=384.61, p = 0.322), did not reach statistical significance. Despite its large unstandardized coefficient (B = 384.61), VPD showed no significant association with evapotranspiration (β = 0.702, p = 0.322).

The final regression equation was:

Evapotranspiration = 2097.03 − 541.42(pF) − 0.009(PPFD) + 37.24(Wind) − 15.98(Temperature) + 384.61(VPD).

Table 3: Regression coefficients for predictors of evapotranspiration (ml/m²/day) – *Hedera helix* 'Plattensee'

Predictor	Unstandardized Coefficient (B)	95% CI for B	Standardized Coefficient (ß)	p-value
Constant (Intercept)	2097.03*	(408.19, 3785.87)		0.023
pF	-541.42*	(-1001.26, -81.59)	-0.997	0.028
PPFD (µmol/m²/s)	-0.009	(-0.039, 0.021)	-0.243	0.498
Wind (km/h)	37.24	(-174.31, 248.79)	0.105	0.682
Temperature (°C)	-15.98	(-48.82, 16.85)	-0.473	0.279
VPD (kPa)	384.61	(-488.21, 1257.44)	0.702	0.322

- *Significant at $p < 0.05$

3.7.2 *H. hibernica*

The analysis revealed several key relationships (see Table 4):

The intercept was statistically significant (B = 1858.28, p = 0.016), representing baseline evapotranspiration under neutral conditions.

Soil water potential (pF): A 1-unit increase in pF significantly decreased evapotranspiration by 395.22 ml/m²/day (B = -395.22, 95% CI: -773.62 to -16.82, p = 0.043). This predictor showed the strongest standardized effect (β = -0.985).

Vapor pressure deficit (VPD): While not statistically significant ($p = 0.084$), VPD demonstrated a substantial positive relationship ($B = 685.52$, $\beta = 1.428$), suggesting its potential influence on evapotranspiration under certain conditions.

Temperature: Approached significance ($B = -29.65$, $p = 0.054$), with a negative relationship indicating potential thermal regulation effects.

Other predictors, including PPFD ($B = -0.020$, $p = 0.143$) and wind speed ($B = -41.08$, $p = 0.646$), did not show statistically significant effects.

The final regression equation was:

Evapotranspiration = 1858.28 - 395.22(pF) - 0.020(PPFD) - 41.08(Wind) - 29.65(Temperature) + 685.52(VPD)

Table 4: Regression coefficients for (*H. hibernica*) predictors of evapotranspiration ($ml/m^2/day$).

Predictor	Unstandardized Coefficient (B)	95% CI for B	Standardized Coefficient (β)	p-value
Constant	1858.28*	(497.03, 3219.54)	-	0.016
pF	-395.22*	(-773.62, -16.82)	-0.985	0.043
PPFD ($\mu mol/m^2/s$)	-0.02	(-0.048, 0.009)	-0.619	0.143
Wind (km/h)	-41.08	(-249.22, 167.07)	-0.133	0.646
Temperature (°C)	-29.65†	(-60.01, 0.71)	-1.002	0.054
VPD (kPa)	685.52 †	(-123.83, 1494.87)	1.428	0.084

- $p < 0.05$; † $p < 0.10$ (marginally significant)

3.7.3 *H. colchica* 'Russland'

The average ET in *H. colchica* was 171.96 ml/m²/day (SD: ±105.13 ml/m²/day). The regression model explained 72.4% of the variance ($R^2 = 0.724$). The analysis revealed that soil water potential (pF) was the only statistically significant predictor ($p < 0.05$), while other measured variables showed no significant effects. The resulting regression equation is as follows:

ET (ml/m²/day) = 1457.98 - 388.36(pF) + 0.001(PPFD) - 0.70(Wind) - 6.78(Temperature) + 105.86(VPD)

The model demonstrated several key relationships:

Soil Water Potential (pF) emerged as the dominant predictor of ET rates, with each unit increase in pF (indicating drier soil conditions) resulting in a decrease of 388.36 ml/m²/day (95% CI: -769.95 to -6.78; $p = 0.047$). This strong negative relationship (standardized $\beta = -0.853$) confirms that soil moisture availability is the primary limiting factor for evapotranspiration in this system.

Constant or intercept term was statistically significant ($B = 1457.98$; $p = 0.038$), representing the baseline ET rate when all predictor variables are at zero. The wide confidence interval (115.87 to 2800.08) suggests some variability in this baseline estimate.

Non-significant predictors included:

Photosynthetic photon flux density (PPFD: $B = 0.001$, $p = 0.966$)

Wind speed ($B = -0.70$, $p = 0.995$)

Temperature ($B = -6.78$, $p = 0.656$)

Vapor pressure deficit (VPD: $B = 105.86$, $p = 0.779$)

Notably, the extremely small coefficients for PPFD and wind speed, combined with their high p-values, indicate these factors had virtually no measurable influence on ET rates under the study conditions. While not statistically significant, the negative coefficient for temperature ($p = 0.656$) suggests a potential trend toward reduced ET at higher temperatures that may warrant further investigation.

These results strongly suggest that soil moisture availability is the primary determinant of evapotranspiration rates in the water-limiting phase, with other measured environmental variables playing minimal roles under the observed conditions. The model highlights the critical importance of water availability during this phase as a limiting factor for evapotranspiration processes.

Table 5: Multiple linear regression coefficients predicting evapotranspiration (ml/m²/day)

Predictor	Unstandardized Coefficient (B)	Standard Error	Standardized coefficient (β)	t-value	p-value	95% Confidence Interval for B
Constant	1457.98*	548.49	-	2.658	0.038	(115.87, 2800.08)
pF	-388.36*	155.95	-0.853	-2.49	0.047	(-769.95, -6.78)
PPFD (µmol/m²/s)	0.001	0.013	0.014	0.044	0.966	(-0.03, 0.03)
Wind (km/h)	-0.7	97.14	-0.002	-0.007	0.995	(-249.22, 167.07)
Temperature (°C)	-6.78	14.46	-0.186	-0.469	0.656	(-60.01, 0.71)
VPD (kPa)	105.86	359.93	0.179	0.294	0.779	(-123.83, 1494.87)

Note: $p < 0.05$ indicates statistical significance (*significant).

3.8 Water-stress Response and Cooling Potential

A detailed summary of the findings is presented in Table 6 below, including urban suitability ratings based on plant responses:

Water-stress resistance rating: This rating evaluates each species' ability to sustain evapotranspiration under water-limiting conditions. *H. helix* 'Plattensee' demonstrates the highest drought resistance, characterized by its strong negative correlation with pF and lower ET, indicating efficient water conservation strategies.

Cooling Potential Rating: Assesses the species' capacity to mitigate urban heat through evapotranspiration. *H. hibernica* exhibits a high cooling potential, driven by its higher mean ET and high response to VPD, suggesting greater effectiveness in temperature regulation.

Best Urban Application: Identifies the most suitable urban settings for each species based on their evapotranspiration dynamics and resistance to water stress.

This comparative analysis highlights the key differences in evapotranspiration performance among the three *Hedera* species under water-limiting conditions, providing valuable insights into their suitability for façade greening applications.

Detailed results of all climber species' correlation and regression analyses are presented in supplementary data.

Table 6: Regression analysis data of the water-limiting phase of evapotranspiration

Parameter	*H. helix* 'Plattensee'	*H. hibernica*	*H. colchica* 'Russland'
Mean ET (ml/m²/day)	151 (±97)	183 (±85)	172 (±105)
pF Coefficient (B)	-541.42* (p = 0.028)	-395.22* (p = 0.043)	-388.36* (p = 0.047)
VPD Coefficient (B)	384.61 (p = 0.322)	685.52† (p = 0.084)	105.86 (p = 0.779)
PPFD Coefficient (B)	-0.009 (p = 0.498)	-0.020 (p = 0.143)	0.001 (p = 0.966)
Wind Speed (B)	37.24 (p = 0.682)	-41.08 (p = 0.646)	-0.70 (p = 0.995)
Temperature (B)	-15.98 (p = 0.279)	-29.65† (p = 0.054)	-6.78 (p = 0.656)
R^2 (Model Fit)	0.751 (75.1%)	0.703 (70.3%)	0.724 (72.4%)
Dominant ET Driver	pF (β = -0.997)	pF (β = -0.985) + VPD†	pF (β = -0.853)
Water-Use Strategy	Strict drought avoidance	Dual soil/atmospheric reliance	Intermediate drought response
Cooling Potential	Moderate (VPD-insensitive)	High (VPD-sensitive)	Moderate (VPD-insensitive)
Urban Application	Dry climates, water conservation	Humid cities, high cooling	Mixed environments

- *significant at $p < 0.05$; † $p < 0.10$ (marginally significant)

4.0. Discussion

4.1. Energy-Driven Phase of Evapotranspiration.

During the energy-driven phase of the experiment (i.e., characterized by an in-trend steep slope of water loss during the first 8 days), evapotranspiration (ET) rates varied significantly among the climber species, reflecting their differing responses to environmental factors. *H. hibernica* exhibited the highest ET rate (699 ml/m²/day), followed by *H. helix* 'Plattensee' (562 ml/m²/day) and *H. colchica* 'Russland' (528 ml/m²/day). In contrast, *L. henryi* had the lowest ET rate (186 ml/m²/day), suggesting a more conservative water-use strategy.

The strong positive correlations between ET and vapor pressure deficit (VPD) and photosynthetic photon flux density (PPFD) highlight the crucial role of these factors in driving evapotranspiration during this phase. VPD, in particular, emerged as a dominant driver across all species, with correlation coefficients ranging from 0.952 for *H. colchica* 'Russland' to 0.981 for *H. helix* 'Plattensee.' These findings align with previous research, where VPD is identified as a key factor influencing ET in green roof systems (Broughton & Conaty, 2022; Grossiord et al., 2020; Medina et al., 2019).

While research on *L. henryi* is limited, studies on other *Lonicera* species have documented dormancy mechanisms affecting germination and growth (Lee et al., 2024; Santiago et al., 2013). The comparatively lower ET rate observed in *L. henryi* may be attributed to a potential dormancy period in September (Gillespie & Volaire, 2017), characterized by reduced physiological activity and lower water demand.

These findings underscore the importance of carefully considering species selection in urban greening projects. With higher ET rates, Hedera species are well-suited for environments where cooling through evapotranspiration can be maximized. In contrast, *L. henryi* 's low ET rate makes it more appropriate for water-conserving applications, even in sufficient water conditions.

4.2. Water-Limiting Phase of Evapotranspiration

These findings reveal distinct hydraulic strategies among the three *Hedera* cultivars that reflect their adaptation to urban moisture constraints. The strong negative response to soil water potential (pF coefficients: -5541.42 to -3.88.36, all $p < 0.05$) confirms soil moisture as the primary ET regulator, consistent with observations of Blinkova et al. (2024) and Meineke and Frank (2018) water-limited urban plant growth. However, the cultivars partition water use differently:

H. helix 'Plattensee'

Exhibited the steepest ET decline per pF unit (-541.42 ml/m²/day, $p = 0.028$), confirming its drought-avoidance response. This matches observations of its xeromorphic traits (thick cuticles, sunken stomata) by Slot et al. (2021). Its negligible VPD response ($p = 0.322$) suggests strict stomatal regulation, making it ideal for water-scarce installations—consistent with its low water-use efficiency (6.3 mmol) in shaded conditions (Metcalfe, 2005).

H. hibernica

This cultivar showed dual sensitivity to pF (-395.22 ml/m²/day, $p = 0.043$) and VPD (685.52, $p = 0.084$ (marginal significance)), indicating reliance on both soil and atmospheric moisture. This aligns with earlier findings of cuticular water loss in some *Hedera* species (Kerstiens,

1996), which may contribute to its superior cooling potential but necessitates irrigation in dry settings for sustainable plant vitality and maximum evapotranspirational cooling.

H. colchica 'Russland' demonstrated intermediate water-use traits, with a smaller but significant pF effect (-388.36, $p = 0.047$) and negligible VPD response ($p = 0.779$). This balanced strategy corroborates field data (Blinkova et al., 2023), suggesting adaptability to mixed environments.

4.3 Limitations

This study has some constraints to be considered when interpreting the findings. It is based on 20-liter potted plants; therefore, the findings may not fully replicate water use dynamics in façade greening systems planted directly in the ground. Yet, in situ conditions prevent the precise values that gravimetric measurements can deliver.

In addition, control pots, intended to estimate sole evaporation for the eventual calculation of transpiration, proved unsuitable. Evaporation in control pots often exceeded total evapotranspiration in potted plants, particularly during the water-limiting phase. Consequently, these control values were excluded from the final analyses.

5.0 Conclusion

This study provides comprehensive, detailed insights into the evapotranspiration characteristics of climber species commonly used for façade greening, namely *Hedera* and *Lonicera* species, under energy-driven and water-limiting conditions. The findings summarised in Table 6 (see above) have implications for optimizing façade greening

strategies, particularly in urban environments susceptible to short-term environmental stressors like dry spells and heat islands.

6.0 References

Aduse-Poku M, Edelmann HG. Quantifying the potential of façade climbing plants in reducing air pollution: a novel investigation into the absorption capabilities of three climbers for CO2, NO2, and O3 in urban environments. Urban Ecosyst. 2025;28(2):76. https://doi.org/10.1007/s11252-025-01689-4

Aduse-Poku M, Niels W, Pacini A, Großschedl J, Edelmann HG, Schlüter K. Façade greening – from science to school. At-Automatisierungstechnik. 2024;72(7):694–703. https://doi.org/10.1515/auto-2024-0022

Blinkova O, Rawlik K, Jagodziński AM. The impact of environmental factors on traits of Hedera helix L. vegetative shoots. Preprint. 2023. https://doi.org/10.21203/rs.3.rs-2742184/v1

Blinkova O, Rawlik K, Jagodziński AM. Effects of limiting environmental conditions on functional traits of Hedera helix L. vegetative shoots. Front Plant Sci. 2024;15:1464006. https://doi.org/10.3389/fpls.2024.1464006

Broughton KJ, Conaty WC. Understanding and exploiting transpiration response to vapor pressure deficit for water-limited environments. Front Plant Sci. 2022;13:893994. https://doi.org/10.3389/fpls.2022.893994

Cirelli D, Lieffers VJ, Tyree MT. Measuring whole-plant transpiration gravimetrically: A scalable automated system built from components. Trees Struct Funct. 2012;26(5):1669–76. https://doi.org/10.1007/s00468-012-0731-6

Cobb R, Cummings S, Furlong B, Rouse D, Pfaff D, Wong P, et al. The American Ivy Society. Ivy J. 2013;39. Available from: www.ivy.org

Denissen JMC, Teuling AJ, Pitman AJ, Koirala S, Migliavacca M, Li W, et al. Widespread shift from ecosystem energy to water limitation with climate change. Nat Clim Change. 2022;12(7):677–84. https://doi.org/10.1038/s41558-022-01403-8

Di HF, Wang DN. Cooling effect of ivy on a wall. J Wind Eng Ind Aerodyn. 2010. https://doi.org/10.1080/089161599269708

Dütemeyer D, Barlag AB, Kuttler W, Axt-Kittner U. Measures against heat stress in the city of Gelsenkirchen, Germany. Erde. 2013;144(3–4):181–201. https://doi.org/10.12854/erde-144-14

Ghiat I, Mackey HR, Al-Ansari T. A review of evapotranspiration measurement models, techniques, and methods for open and closed agricultural field applications. Water (Basel). 2021;13(18):2523. https://doi.org/10.3390/w13182523

Gigon A, Weber E. Invasive Neophyten in der Schweiz – Lagebericht und Handlungsbedarf. Geobotanisches Institut, ETH. 2005.

Gillespie LM, Volaire FA (2017) Are winter and summer dormancy symmetrical seasonal adaptive strategies? The case of temperate herbaceous perennials. Ann Bot 119:311–323. https://doi.org/10.1093/aob/mcw264

Gräf M, Immitzer M, Hietz P, Stangl R (2021) Water-stressed plants do not cool: Leaf surface temperature of living wall plants under drought stress. Sustainability (Switzerland) 13:73910. https://doi.org/10.3390/su13073910

Grossiord C, Buckley TN, Cernusak LA, Novick KA, Poulter B, Siegwolf RTW, Sperry JS, McDowell NG (2020) Plant responses to rising vapor pressure deficit. New Phytol 226:1550–1566. https://doi.org/10.1111/nph.16485

Hasanuzzaman M, Chakraborty K, Zhou M, Shabala S (2023) Measuring residual transpiration in plants: a comparative analysis of different methods. Funct Plant Biol 50:983–992. https://doi.org/10.1071/FP23157

Heisler GM, Brazel AJ (2015) The Urban Physical Environment: Temperature and Urban Heat Islands. pp 29–56. https://doi.org/10.2134/agronmonogr55.c2

Janse RJ, Hoekstra T, Jager KJ, Zoccali C, Tripepi G, Dekker FW, Van Diepen M (2021) Conducting correlation analysis: Important limitations and pitfalls. Clin Kidney J 14:2332–2337. https://doi.org/10.1093/ckj/sfab085

Katul GG, Oren R, Manzoni S, Higgins C, Parlange MB (2012) Evapotranspiration: A process driving mass transport and energy exchange in the soil-plant-atmosphere-climate system. Rev Geophys 50:RG3002. https://doi.org/10.1029/2011RG000366

Kerstiens G (1996) Cuticular water permeability and its physiological significance. J Exp Bot 47:1813–1832. https://doi.org/10.1093/jxb/47.12.1813

Koehler T, Wankmüller FJP, Sadok W, Carminati A (2023) Transpiration response to soil drying versus increasing vapor pressure deficit in crops: physical and physiological mechanisms and key plant traits. J Exp Bot 74:4789–4807. https://doi.org/10.1093/jxb/erad221

Köhler M (2008) Green facades—a view back and some visions. Urban Ecosyst 11:423–436. https://doi.org/10.1007/s11252-008-0063-x

Kovats RS, Hajat S (2008) Heat stress and public health: A critical review. Annu Rev Public Health 29:41–55. https://doi.org/10.1146/annurev.publhealth.29.020907.090843

Krich C, Mahecha MD, Migliavacca M, De Kauwe MG, Griebel A, Runge J, Miralles DG (2022) Decoupling between ecosystem photosynthesis and transpiration: A last resort against overheating. Environ Res Lett 17:045005. https://doi.org/10.1088/1748-9326/ac583e

Lal R (2020) Soil organic matter and water retention. Agron J 112:3265-3277. https://doi.org/10.1002/agj2.20282

Lee J, Park K, Lee H, Jang BK, Cho JS (2024) Improving seed germination: effect of stratification and dormancy-release priming in *Lonicera insularis* Nakai. Front Plant Sci 15. https://doi.org/10.3389/fpls.2024.1484114

Luber G, McGeehin M (2008) Climate change and extreme heat events. Am J Prev Med 35:429-435. https://doi.org/10.1016/j.amepre.2008.08.021

Lyu X, Chang L, Lu Z, Li J (2023) The ability of three climbing plant species to capture particulate matter and their physiological responses at different environmental sampling sites. Front Environ Sci 10. https://doi.org/10.3389/fenvs.2022.1084902

Markoska V, Spalevic V, Lisichkov K, Atkovska K, Gulaboski R (2018) Determination of water retention characteristics of perlite and peat. J Agric For 64:3. https://doi.org/10.17707/agricultforest.64.3.10

Medina S, Vicente R, Nieto-Taladriz MT, Aparicio N, Chairi F, Vergara-Diaz O, Araus JL (2019) The plant-transpiration response to vapor pressure deficit (VPD) in durum wheat is associated with differential yield performance and specific expression of genes involved in primary metabolism and water transport. Front Plant Sci 9. https://doi.org/10.3389/fpls.2018.01994

Meineke EK, Frank SD (2018) Water availability drives urban tree growth responses to herbivory and warming. J Appl Ecol 55:1701-1713. https://doi.org/10.1111/1365-2664.13130

Menberu MW, Marttila H, Ronkanen AK, Haghighi AT, Kløve B (2021) Hydraulic and physical properties of managed and intact peatlands: Application of the Van Genuchten-Mualem models to peat soils. Water Resour Res 57:7. https://doi.org/10.1029/2020WR028624

Metcalfe DJ (2005) *Hedera helix* L. J Ecol 93:632-648. https://doi.org/10.1111/j.1365-2745.2005.01021.x

Nilson SE, Assmann SM (2007) The control of transpiration. Insights from *Arabidopsis*. Plant Physiol 143:19-27. https://doi.org/10.1104/pp.106.093161

O'Kelly BC, Sivakumar V (2014) Water content determinations for peat and other organic soils using the oven-drying method. Dry Technol 32:6. https://doi.org/10.1080/07373937.2013.849728

Rahman MA, Dervishi V, Moser-Reischl A, Ludwig F, Pretzsch H, Rötzer T, Pauleit S (2021) Comparative analysis of shade and underlying surfaces on cooling effect. Urban For Urban Green 63. https://doi.org/10.1016/j.ufug.2021.127223

Santiago A, Herranz JM, Copete E, Ferrandis P (2013) Species-specific environmental requirements to break seed dormancy: Implications for selection of regeneration niches in three *Lonicera* (Caprifoliaceae) species. Botany 91:225-233. https://doi.org/10.1139/cjb-2012-0169

Scherer D, Endlicher W (2013) Editorial: Urban climate and heat stress - Part 1. Erde 144:175-180. https://doi.org/10.12854/erde-144-13

Schwärzel K, Renger M, Sauerbrey R, Wessolek G (2002) Soil physical characteristics of peat soils. J Plant Nutr Soil Sci 165:479-486. https://doi.org/10.1002/1522-2624(200208)165:4<479::AID-JPLN479>3.0.CO;2-8

Slot M, Nardwattanawong T, Hernández GG, Bueno A, Riederer M, Winter K (2021) Large differences in leaf cuticle conductance and its temperature response among 24 tropical tree species from across a rainfall gradient. New Phytol 232:1618-1631. https://doi.org/10.1111/nph.17626

Valcárcel V, Vargas P (2010) Quantitative morphology and species delimitation under the general lineage concept: optimization for *Hedera* (Araliaceae). Am J Bot 97:1555-1573. https://doi.org/10.3732/ajb.l000115

Ziemer RR (1979) Evaporation and transpiration. Rev Geophys 17:1175-1186. https://doi.org/10.1029/RG017i006p01175

Supplementary/Online resources:

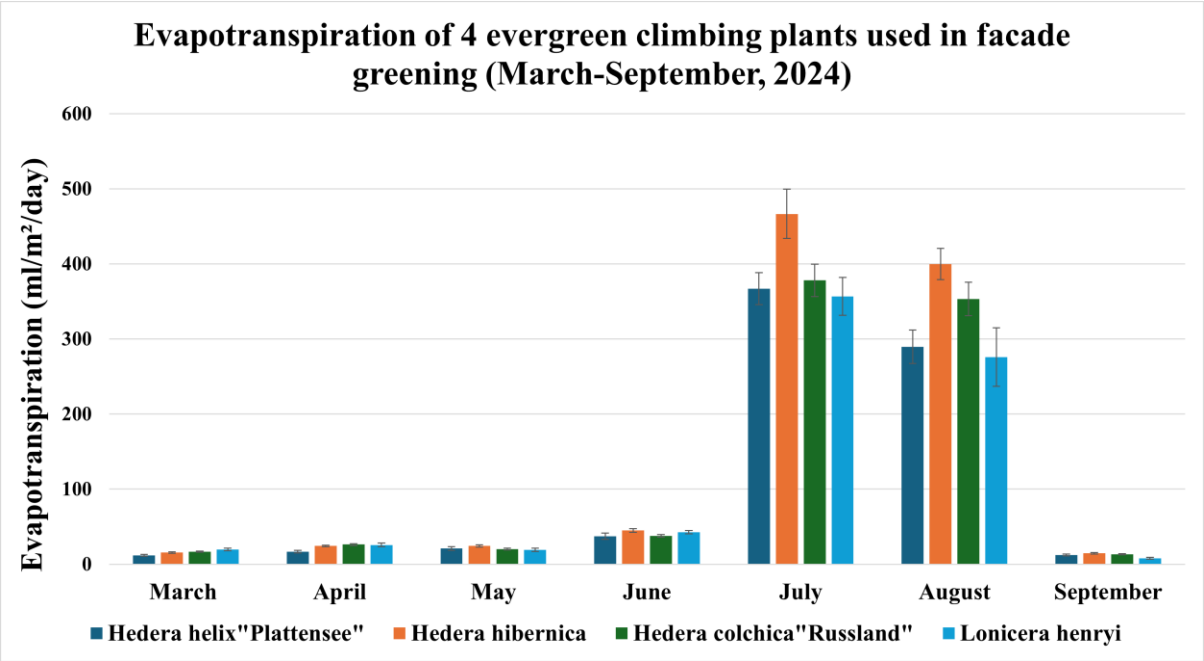

Fig S 1 Illustrates the monthly variations in evapotranspiration rates for the four evergreen climbing species: *H. helix* 'Plattensee,' *H. hibernica, H. colchica* 'Russland,' and *L. henryi*,' from March to September.

Online resource figure S 2

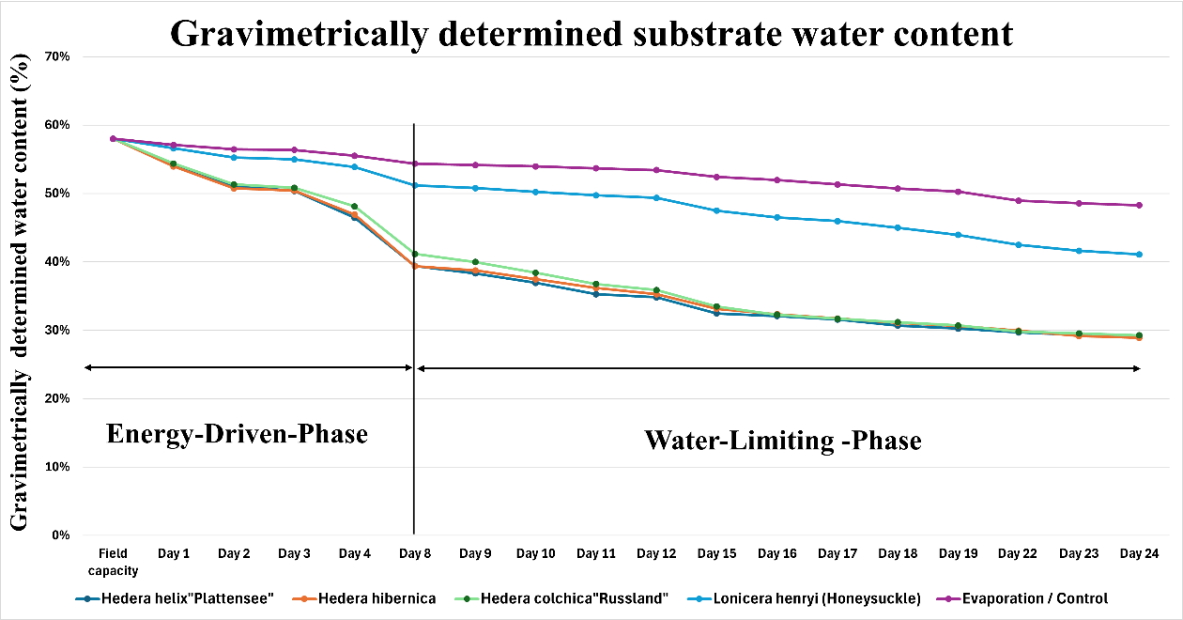

Fig S 2 Species progression of water content (%) from field capacity to the end of the experiment.

7.0 Preface to the study on the physiological response of 7 climbers under high temperatures (33° C ± 0.5 °C)

As cities worldwide grapple with the intensifying impacts of climate change—particularly rising temperatures and more frequent heat waves—the role of nature-based solutions in urban resilience has become increasingly critical. Among these, façade greening with climbing plants offers a promising approach for cooling buildings, improving microclimates, and enhancing urban biodiversity. However, a deeper understanding of how different climbers physiologically respond to heat stress is essential to harness their potential fully. This study builds on this need by examining seven commonly used climbing plant species under controlled high-temperature conditions (33°C), ensuring water was not a limiting factor. By isolating temperature effects, it provides valuable insights into species-specific transpiration rates, stomatal behavior, water use efficiency, and photosynthetic performance—all of which influence a plant's ability to contribute to urban cooling.

The results reveal distinct physiological strategies across species. For instance, *H. helix* 'Plattensee' displayed the highest transpiration and cooling capacity, while *Wisteria sinensis* demonstrated superior water use efficiency. These findings underscore the importance of matching plant traits to specific urban climate challenges, such as cooling demand versus water scarcity, and offer guidance for selecting climbers suited to various façade orientations, urban densities, and climate zones.

By linking physiological plant responses to practical greening applications, this research provides a scientific foundation for improving species selection in façade greening systems. In turn, it supports the development of more climate-adaptive and sustainable urban environments.

7.1 Physiological response of 7 climbers under high temperatures (ca. 33° C ± 0.5° C)

7.1.1 Abstract.

Understanding the physiological responses of climbing plants to heat stress is crucial for optimizing their use in green infrastructure solutions, particularly facade greening systems. This study investigates seven climbing plant species' water use dynamics and heat stress responses when water is not a limiting factor. It provides valuable insights into their potential for urban cooling and water use efficiency during high temperatures with sufficient water availability. Results show *H. helix var.* Plattensee has the best transpiration, and *Wisteria sinensis* shows the best water use efficiency.

7.2 Introduction

According to Di & Wang, 2010; Hoelscher et al., 2016; Rahman et al., 2021 façade greening systems can reduce facade surface temperatures by 5–30°C and decrease ambient air temperatures in their vicinity by 2–6°C, depending on the system design and plant species used (Aduse-Poku et al., 2024; Santamouris, 2014).

In the context of climbing plants used for facade greening, ET is vital for providing cooling effects and plant water consumption. The cooling capacity of climbing plants is directly related to their transpiration rates, which vary significantly among species and under different environmental conditions (Hoelscher et al., 2016).

Previous research has established that climbing plants demonstrate varying physiological responses to environmental stressors. In a study by Cameron et al., 2014) different climber species exhibited distinct transpiration rates and water use efficiencies when subjected to varying light intensities and vapor pressure deficit (VPD) conditions. Similarly, Hoelscher et al. (2016) reported that facade greening systems can reduce the ambient air temperature by up to 2.6°C through evapotranspiration cooling, with the cooling effect correlating with the transpiration rates of the constituent plants.

While these studies have investigated the cooling potential of climbing plants in urban environments, there remains a significant knowledge gap regarding species-specific

physiological responses to heat stress during sufficient water supply. Most previous research has focused on water-limited conditions or examined a limited number of species. Specifically, comprehensive physiological data comparing multiple climbing species under controlled water conditions is lacking for climber species commonly used in central European facade greening systems.

7.2.1. Research questions and objectives

The primary objective of this research is to provide a comprehensive physiological characterization of seven climbing plant species commonly used in facade greening systems, focusing on their responses to heat stress under optimal water availability conditions.

This study addresses the following research questions:

How do different climbing plant species respond physiologically to heat stress during field capacity?

Are there significant species-specific differences in water use efficiency, transpiration rates, and photosynthetic efficiency under high-temperature conditions?

How do environmental factors such as leaf temperature and vapor pressure deficit influence the physiological responses of different climbing species?

Which climbing plant species demonstrate the most favourable physiological response for facade greening systems in hot urban environments?

7.2.2. Hypothesis

Climbing plants will exhibit species-specific responses to heat stress, influenced by stomatal regulation, leaf cooling capacity, and transpiration efficiency.

7.3. Materials and Methods

7.3.1. Plant Material and Growth Conditions

The study examined seven climbing plant species commonly used in facade greening systems: *C. montana* , *Parthenocissus tricuspidata*, *Hedera hibernica*, *Hedera helix*

'Plattensee,' *Hedera colchica* ' Russland', *Wisteria sinensis*, and *Lonicera henryi*. Each species was represented by four potted plants (except for *C. montana*, which had three potted plants), each grown in a 20-liter pot containing a standard growing medium (ED-73). Plants were maintained at field capacity (48 hours after saturation) before measurements to ensure that water was not a limiting factor during the experiment. This allowed for the effects of temperature on plant physiological responses without the confounding influence of water stress.

7.3.2. Measurement Protocol

Physiological measurements were conducted on the midday of August 11, 2023; a critical time window was chosen to minimize variations in ambient environmental conditions while ensuring that plants were exposed to peak daily temperatures. This timing allowed for the comparison of plants under similar ecological stress conditions.

Ten fully expanded leaves were selected from each potted plant for measurement, resulting in 30-40 measurements per species. The measurements were performed using a Li-Cor LI-600 Porometer/Fluorometer, an advanced instrument measuring gas exchange parameters and chlorophyll fluorescence (Li-cor Environmental).

With this device, the following parameters were synchronously recorded for each leaf:

Stomatal conductance (gsw, mol/m²/s): a measure of the rate of passage of water vapor or carbon dioxide through the stomata

Transpiration rate (E_apparent, mmol/m²/s): the rate of water loss from the leaf surface

Leaf-to-air vapor pressure deficit (VPDleaf, kPa): the difference between the vapor pressure inside the leaf and the surrounding air

Leaf temperature (Tleaf, °C): the temperature of the leaf surface

Quantum yield of photosystem II (PhiPS2): a measure of photosynthetic efficiency

Electron transport rate (ETR, µmol/m²/s): the rate of electron flow through photosystem II

Ambient light intensity (Qamb, μmol/m²/s): the photosynthetically active radiation at the leaf surface

By conducting measurements consistently and under field capacity conditions, the study design allowed for direct comparisons of how different climbing species respond physiologically to heat stress when water is not limiting.

This comprehensive dataset provides insights into climbing plants' water use dynamics and heat stress responses. It has significant implications for selecting and managing species for facade greening systems in urban environments facing increasing thermal stress due to climate change.

7.4. Results

7.4.1. Statistical Analysis

A Generalized Linear Model (GLM) was employed to evaluate species-specific differences in physiological responses. The model included Plant Species as a fixed factor and Light Intensity (Qamb) as a covariate, with an interaction term (Species × Qamb) to assess whether species responded differently to light conditions. This approach allowed for a robust comparison of transpiration rate (E_apparent), stomatal conductance (gsw), calculated poxy (ETR/E_apparent) to water use efficiency (WUE), photosynthetic efficiency (PhiPS2, ETR), and environmental responses (Tleaf, VPDleaf) while accounting for variability in light conditions.

A primary objective of this study was to identify species-specific differences in physiological traits under varying light conditions. To achieve this, the General Linear Model (GLM) was employed to analyze the effects of plant species and ambient light intensity (Qamb) on parameters such as transpiration rate, stomatal conductance, and leaf temperature. Table 1 summarizes the results of these analyses, highlighting the statistical significance of species, light, and their interactive effects.

Table 1: Statistical summary of Type III Tests of Model Effects for Physiological Parameters

Parameter	Species effect (p)	Qamb Effect (p)	Interaction (species x Qamb)(p)
E_apparent	< 0.001*	< 0.001*	0.924
gsw	< 0.001*	0.022*	0.986
VPDLeaf	0.027*	< 0.001*	0.396
PhiPS2	0.070 (marginal)	< 0.001*	0.026*
ETR	0.969	< 0.001*	0.041*
Tleaf	0.073 (marginal)	< 0.001*	0.657
Water use efficiency	0.987 (not significant)	0.183	0.166

*significant at $p < 0.05$)

7.4.1.1. Transpiration Rate (E_apparent)

Significant species differences were detected ($p < 0.001$), indicating that transpiration rates vary.

H. helix 'Plattensee' had the highest transpiration rate, followed by *Hedera hibernica*.

Wisteria sinensis showed the lowest transpiration, suggesting it may be more water-efficient.

Effect of light intensity (Qamb): Light has a significant impact ($p < 0.001$), but the interaction term (Species × Qamb) was not significant ($p = 0.924$), meaning all species responded similarly to increasing light.

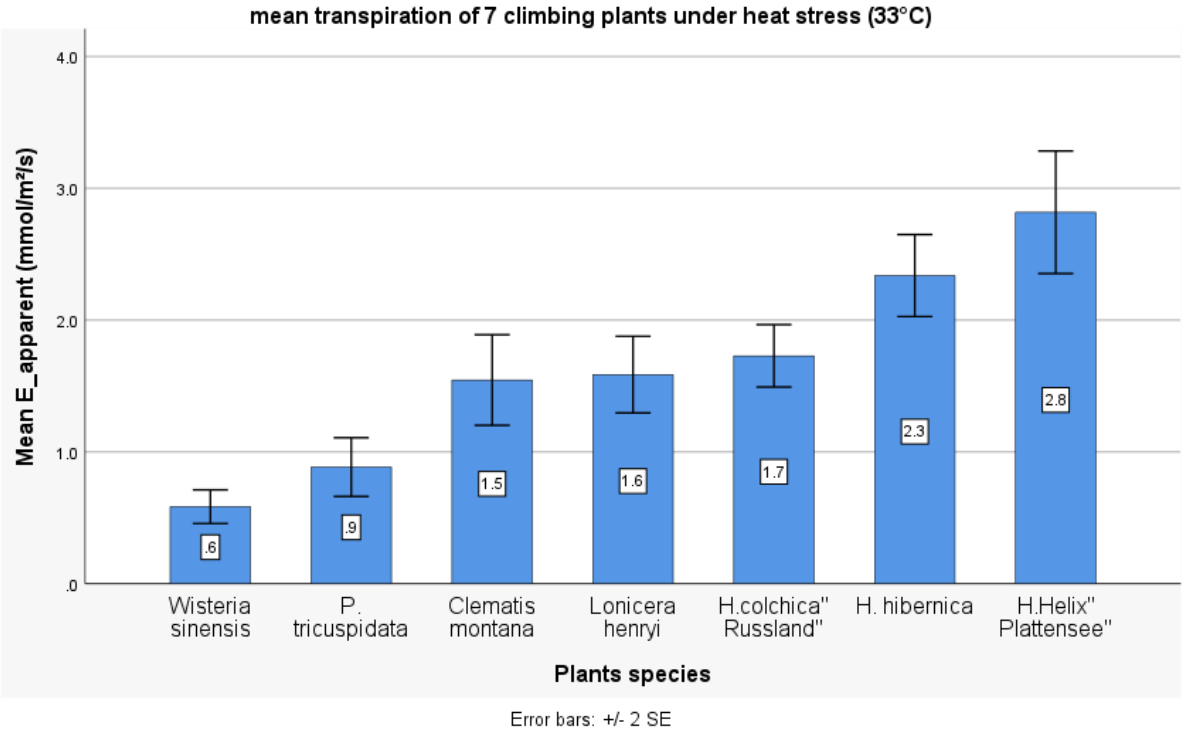

Figure 1. Mean transpiration rates of 7 climbers at field capacity and heat stress conditions (33 ± 0.5° C)

7.4.1.2. Stomatal Conductance (gsw)

Species differences were highly significant ($p < 0.001$).

H. helix 'Plattensee' exhibited the highest stomatal conductance, while *W. sinensis* and *P. tricuspidata* had the lowest.

Higher gsw indicates more significant water loss, while lower values suggest water conservation strategies.

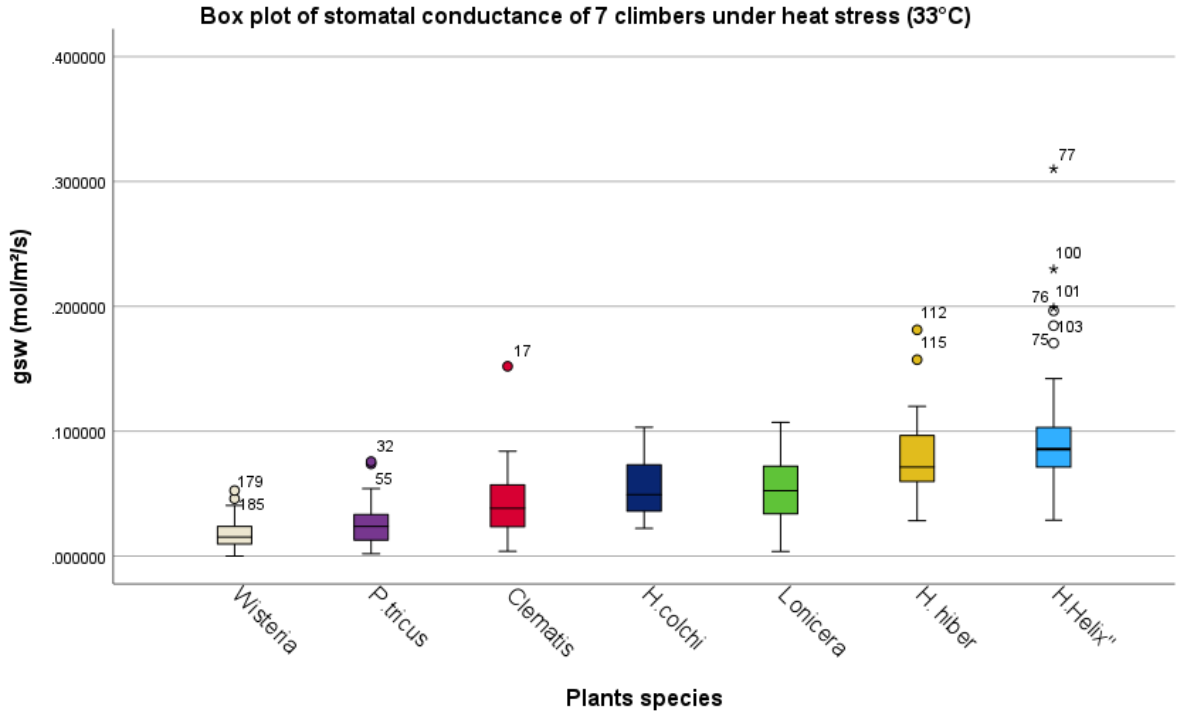

Figure 2. Stomatal conductance of 7 climbers at field capacity (pF= 2) during heat stress (average 33 ± 0.5° C).

7.4.1.3. Water Use Efficiency (Proxy to WUE = ETR / E_apparent)

Water Use Efficiency was calculated as the ratio of ETR to E_apparent. While this approach provides a useful proxy for relative comparisons across species, it does not reflect direct CO_2 assimilation rates. Hence, interpretation should be made with caution, particularly under conditions where photosynthesis and stomatal behaviour may become decoupled.

No significant species differences were found among the species ($p = 0.987$), but some trends emerged:

W. sinensis and *P. tricuspidata* had relatively high WUE, making them better suited for water conservation. *Hedera* species showed lower WUE, indicating higher water consumption.

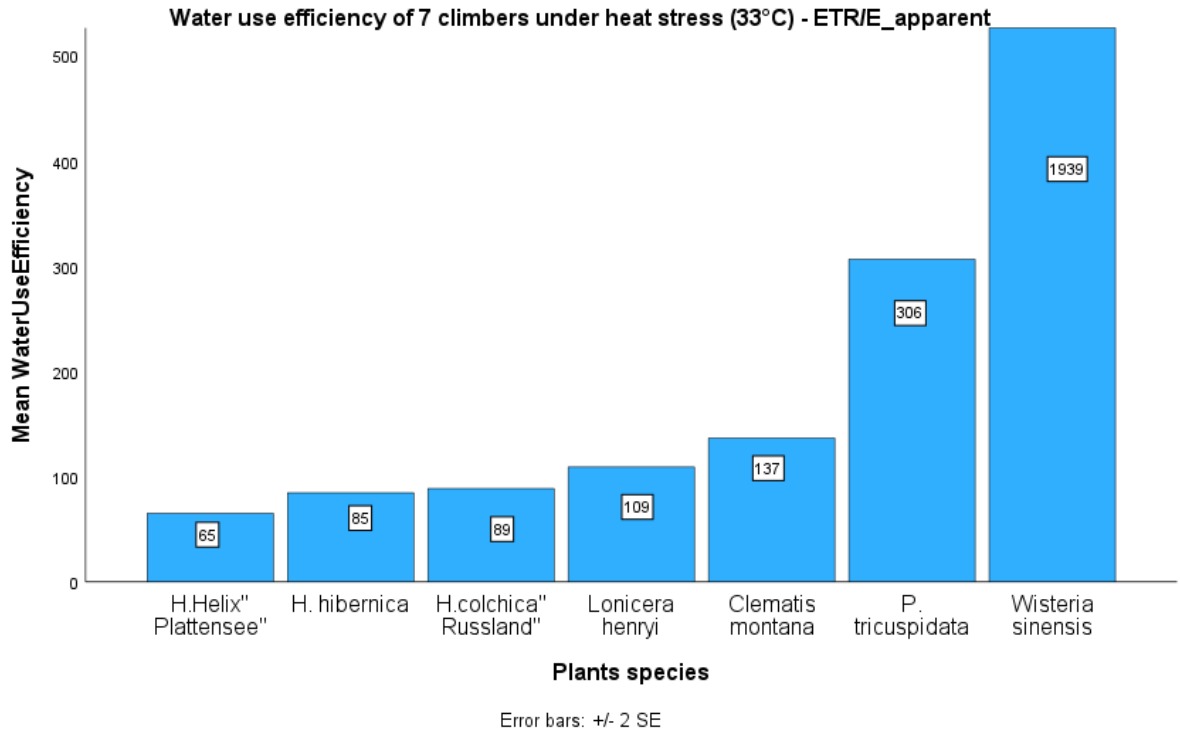

Figure 3. Mean water use efficiency of 7 climbers at field capacity (pF = 2) and an average temperature of 33° C.

7.4.1.4. Photosynthetic Efficiency (PhiPS2) & Electron Transport Rate (ETR)

Significant species differences in PhiPS2 ($p = 0.070$) and ETR ($p = 0.041$).

H. helix 'Plattensee' and *L. henryi* exhibited the highest ETR, meaning they are more effective at capturing light for photosynthesis.

C. montana and *P. tricuspidata* exhibited lower photosynthetic efficiency.

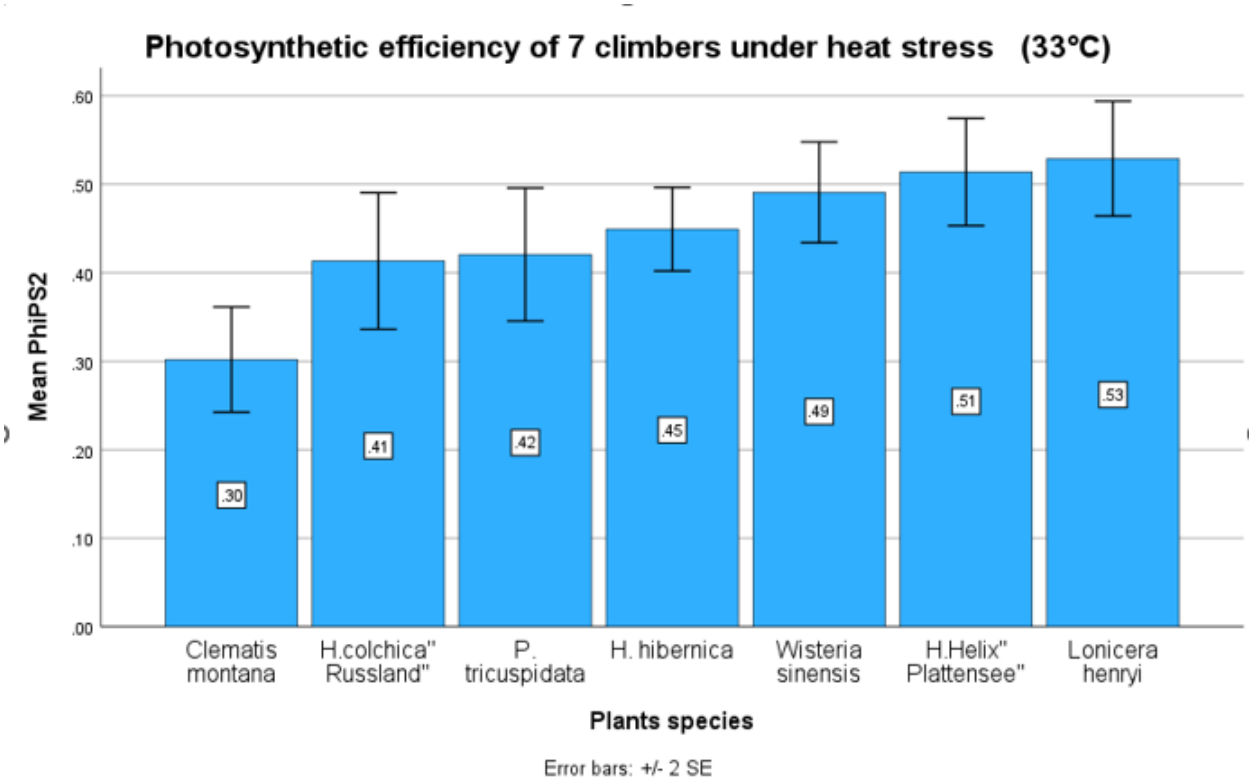

Figure 4. Photosynthetic efficiency of 7 climbers at field capacity (pF=2) at a temperature 33° C.

7.4.1.5. Leaf Temperature (Tleaf) & Vapor Pressure Deficit (VPDleaf)

There were significant differences in leaf temperature ($p = 0.073$), with *P. tricuspidata* and *C. montana* showing higher leaf temperatures, suggesting lower cooling efficiency.

H. helix 'Plattensee' had a relatively lower leaf temperature, indicating better-cooling potential.

VPDleaf showed moderate differences (p = 0.027), with *H. hibernica* and *H. colchica* showing slightly better coping strategies towards vapor pressure deficit.

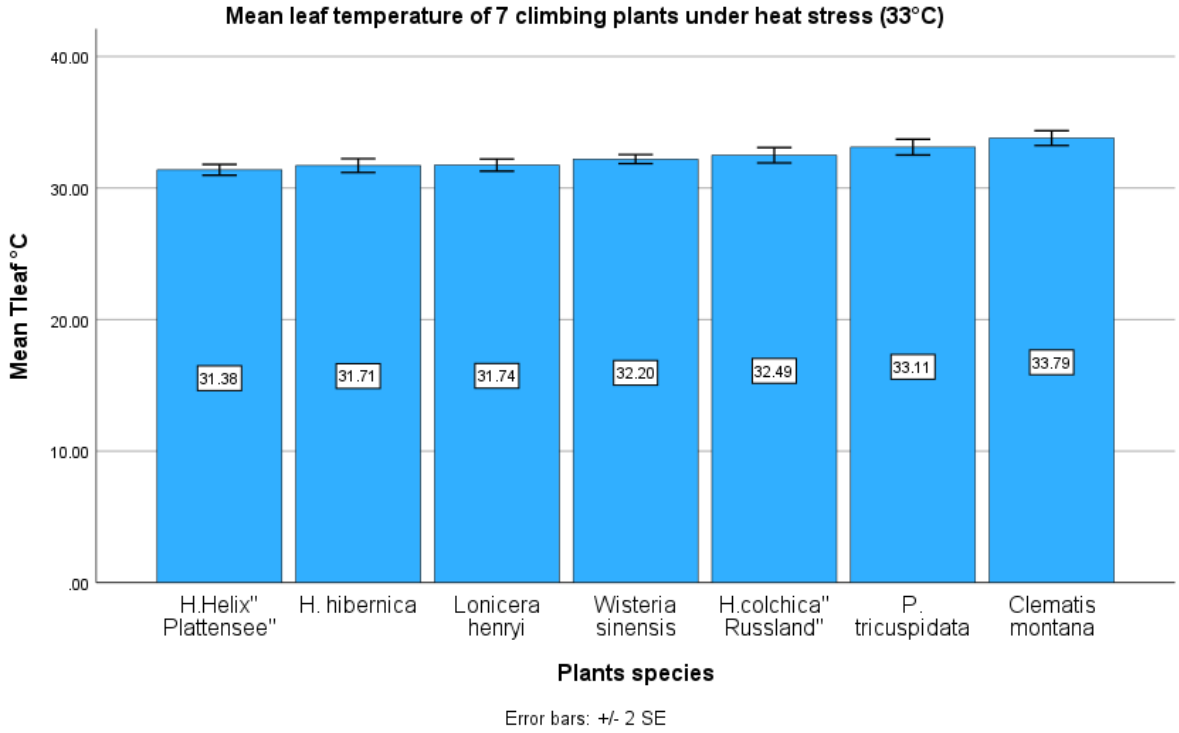

Figure 5. Mean leaf temperature of 7 climbing plants at field capacity (pF=2) at a temperature of 33° C.

The estimated marginal means derived from Generalized Linear Models (GLMs) revealed significant differences in physiological parameters among the plant species evaluated. Table 2 presents the estimated marginal means for transpiration rate (E_apparent), stomatal conductance (gsw), photosynthetic efficiency (PhiPS2), electron transport rate (ETR), leaf temperature (Tleaf), and leaf-level vapor pressure deficit (VPDleaf) for each species at a standardized ambient light level (Qamb) of 897.48 µmol/m²/s.

Hedera helix 'Plattensee' exhibited the highest estimated marginal mean for transpiration rate (2.81 mmol/m²/s) and stomatal conductance (0.10 mol/m²/s), suggesting a strong capacity for evaporative cooling. In contrast, Wisteria sinensis showed the lowest transpiration rate (0.66 mmol/m²/s) and stomatal conductance (0.02 mol/m²/s) among the species tested.

The estimated marginal means for photosynthetic efficiency (PhiPS2) ranged from 0.34 for *C.montana* to 0.52 for *H. helix* 'Plattensee'. *L. henryi* displayed a relatively high PhiPS2 of 0.50, indicating efficient light energy conversion even under ambient conditions.

Electron transport rates (ETR) varied among species, with *H. helix* 'Plattensee' showing the highest value (160.77 µmol/m²/s) and *P. tricuspidata* the lowest (106.64 µmol/m²/s). Leaf temperatures ranged from 31.36°C for H. helix 'Plattensee' to 33.35°C for *P. tricuspidata*.

Leaf-level vapor pressure deficits (VPDleaf) ranged from 2.84 kPa for *H. helix* 'Plattensee' to 3.50 kPa for *P. tricuspidata*. Higher VPDleaf values suggest a greater evaporative demand at the leaf surface.

Table 2: Estimated Marginal Means (EMMs) and Standard Errors (SE) of Physiological Parameters by Species at Qamb = 897.48 µmol/m²/s

Species	E_apparent (mmol/m²/s)	gsw (mol/m²/s)	VPDleaf (kPa)	PhiPS2	ETR (µmol/m²/s)	Tleaf (°C)
C. montana	1.39 (0.21)	0.04 (0.01)	3.40 (0.13)	0.34 (0.03)	117.62 (14.46)	33.06 (0.34)
Hedera hibernica	2.28 (0.21)	0.08 (0.01)	3.03 (0.13)	0.46 (0.03)	156.72 (14.46)	31.55 (0.34)
H. colchica 'Russland'	1.70 (0.21)	0.05 (0.01)	3.28 (0.13)	0.43 (0.03)	124.48 (14.46)	32.38 (0.34)
H. helix 'Plattensee'	2.81 (0.21)	0.10 (0.01)	2.84 (0.13)	0.52 (0.03)	160.77 (14.46)	31.36 (0.34)
L. henryi	1.71 (0.21)	0.06 (0.01)	3.15 (0.13)	0.50 (0.03)	159.42 (14.46)	32.07 (0.34)
P. tricuspidata	0.94 (0.21)	0.03 (0.01)	3.50 (0.13)	0.38 (0.03)	106.64 (14.46)	33.35 (0.34)
W. sinensis	0.66 (0.21)	0.02 (0.01)	3.27 (0.13)	0.45 (0.03)	153.27 (14.46)	32.53 (0.34)

To further investigate the significant effects of plant species observed in the Generalized Linear Models (GLMs) on various physiological parameters, Tukey's Honestly Significant Difference (HSD) post-hoc tests were conducted. These tests allowed for pairwise comparisons among the plant species to determine which specific groups differed significantly from one another. The results revealed distinct patterns of significant differences

among the species for each physiological parameter (E_apparent, gsw, VPDleaf, PhiPS2, ETR and Tleaf).

Specifically, homogeneous subsets derived from the Tukey's HSD tests indicated groupings of plant species that did not significantly differ from each other (Table 3).

E_apparent (mmol/m²/s): The post-hoc analysis for E_apparent revealed three distinct homogeneous subsets: Subset 1 included *C. montana, L. henryi, H. colchica*, and *P. tricuspidata*; Subset 2 comprised *H. hibernica* and *H. helix* 'Plattensee'; and Subset 3 consisted solely of *W. sinensis*.

gsw (mol/m²/s): For gsw, two homogeneous subsets were identified: Subset 1 included *C. montana*, *L.henryi*, and *H.colchica*, while Subset 2 comprised *P. tricuspidata*, *H.hibernica*, *H. helix* 'Plattensee', and *W. sinensis*.

VPDleaf (kPa): The analysis of VPDleaf showed two homogeneous subsets: Subset 1 included *L. henryi, H. colchica, H. hibernica*, and H. helix 'Plattensee', and Subset 2 comprised *C. montana, P. tricuspidata*, and *W. sinensis*.

PhiPS2: The post-hoc test for PhiPS2 revealed three subsets: Subset 1 included *P. tricuspidata, H. hibernica,* and *W. sinensis*; Subset 2 comprised *C. montana* and *H. helix* 'Plattensee'; and Subset 3 consisted of *L. henryi* and *H. colchica*.

ETR (µmol/m²/s): For ETR, two subsets were identified: Subset 1 included *C. montana, L. henryi,* and *H. colchica*, while Subset 2 comprised *P. tricuspidata, H. hibernica, H. helix* 'Plattensee'*, and W. sinensis.*

Tleaf (°C): The post-hoc analysis of Tleaf identified two homogeneous subsets: Subset 1 included *P. tricuspidata, H. hibernica, H. helix* 'Plattensee', and W. sinensis, and Subset 2 comprised *C. montana, L. henryi*, and *H. colchica*.

Table 3: Post-hoc groupings of plant species based on physiological response (Tukey's HSD Tests)

Plant ID	E_apparent	gsw	VPDleaf	PhiPS2	ETR	Tleaf
C. montana	1	1	2	2	1	2
L. henryi	1	1	1	3	1	2
H. colchica	1	1	1	3	1	2
P. tricuspidata	1	2	2	1	2	1
H. hibernica	2	2	1	1	2	1
H. helix ' Plattensee'	2	2	1	2	2	1
W. sinensis	3	2	2	1	2	1

7. 5. Discussion

7.5.1. Physiological Responses of Climbing Plants to Heat and Light Intensity

The findings of this study reveal distinct species-specific physiological responses to high temperatures and varying light intensities at field capacity conditions. Transpiration rate (E_apparent), stomatal conductance (gsw), and water use efficiency (WUE) exhibited significant variation among species, highlighting their differing adaptive strategies for urban façade greening. The results align with previous research, indicating that species with higher transpiration rates tend to provide better cooling benefits in urban environments (Cameron et al., 2014; Perini & Rosasco, 2013).

7.5.2. Transpiration and Cooling Potential

Transpiration rates varied significantly among species, with *H. helix* 'Plattensee' showing the highest values, while *W. sinensis* and *P. tricuspidata* exhibited the lowest transpiration rates. To facilitate practical comparisons, transpiration rates were converted from mmol/m²/s to L/m²/day using the formula:

To convert mmol/m²/s to L/m²/day, use the conversion formula:

$L/m^2/day = mmol/m^2/s \times (18/1000) \times 86{,}400$ – results in figure 6 below

(Where:*18 g/mol is the molecular weight of water; 86,400 s/day converts per-second values to per-day; 1 mmol = 0.001 moles*)

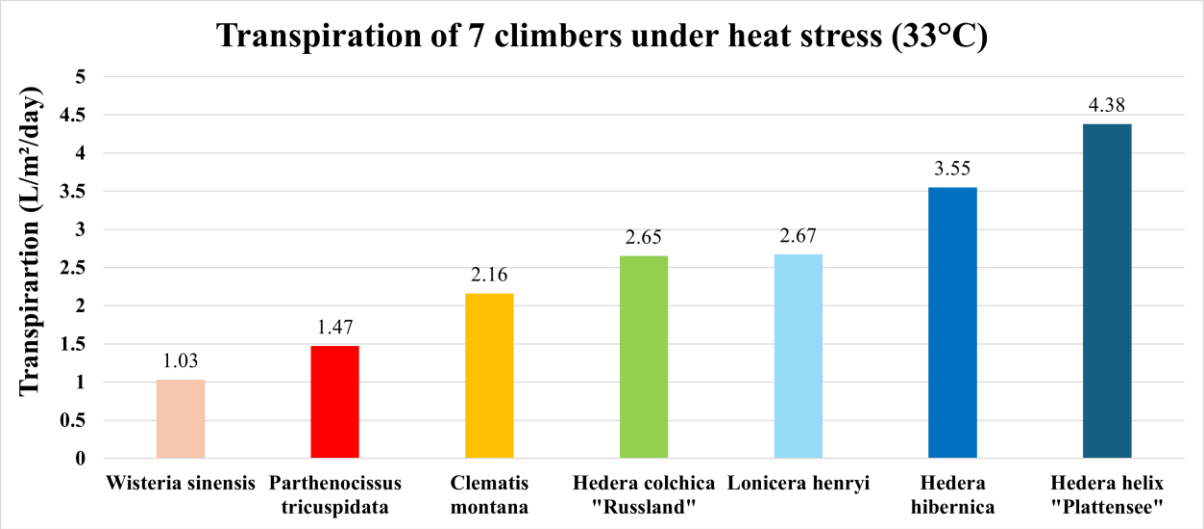

Figure 6. Average transpiration rates of climbers under light conditions at field capacity and 33 ± 0.5° C.

H. helix 'Plattensee' had an approximate daily transpiration rate of 4.38 L/m²/day, compared to *Wisteria sinensis*, which transpired only 1.03 L/m²/day. The high transpiration rates observed in *H. helix* species suggest superior cooling potential, making them ideal candidates for green façades in high-heat urban areas where evapotranspiration cooling is a priority (Bakhshoodeh et al., 2022).

7.5.3. Water Use Efficiency and Drought Adaptation

While *H. helix* 'Plattensee' demonstrated high transpiration rates, its water use efficiency (WUE) was lower, implying a trade-off between cooling efficiency and water conservation. Conversely, *Wisteria sinensis* and *Parthenocissus tricuspidata* exhibited the highest approximated WUE, indicating superior adaptation to water-limited environments. This aligns with findings from (Gillner et al., 2017), which suggests that species with low WUE are less suited for regions with prolonged drought conditions.

7.5.4 Leaf Temperature and Heat Adaptability (Resistance)

Species also varied in their leaf temperature regulation. *P. tricuspidata* and *C. montana* exhibited the highest leaf temperatures, suggesting poor heat dissipation, whereas *H. helix* 'Plattensee' maintained lower leaf temperatures. Lower leaf temperatures are crucial for plant

survival in extreme heat, as they reduce the risk of thermal stress (Manso et al., 2021). This suggests that *H. helix* species offer cooling benefits and demonstrate resilience under heat stress.

7.5.5. Implications for Urban Façade Greening under Heat Stress

The results indicate that different species have strengths in different urban conditions:

High-transpiring species (e.g. *H. helix* 'Plattensee') are ideal for hot and humid cities where cooling potential is more important than water conservation.

High-WUE species (e.g. *W. sinensis*, *P. tricuspidata*) are better suited for drought-prone urban areas where water efficiency is a priority.

Moderate performers (e.g. *L. henryi*) balance cooling potential and water efficiency, making them versatile for different façade orientations.

7.6. Conclusion

With increasing urban heat islands (UHI) and prolonged drought spells due to climate change, selecting the right species for façade greening is crucial (Heisler & Brazel, 2015; Santamouris, 2014). If sufficient water is available, *H. helix*'s high transpiration and cooling potential can mitigate urban overheating, while species like *W. sinensis* ensure sustainability in cities facing water scarcity and have a reduced transpirational cooling effect. The findings highlight the relevance of species-specific water use under high temperatures. This presents a sound scientific basis for optimizing plant-based cooling strategies in cities.

8.0. Preface: From Science to School (Published in De Gruyter Oldenbourg)

While the technical benefits of façade greening – including cooling effects, insulation properties, and air pollutant absorption – are increasingly well-documented (Di & Wang, 2010; Hoelscher et al., 2016; Rahman et al., 2021)The transition from scientific findings to widespread urban implementation requires public understanding and support. Recognizing this, researchers at the Institut für Biologiedidaktik at the University of Cologne have initiated efforts to bring this knowledge into schools through project days and hands-on experiments. As detailed in Aduse-Poku et al. (2024) below, this approach aims to foster long-term changes in students' environmental knowledge and potentially influence their attitudes toward climate-adaptation strategies. The paper builds upon the foundational efforts, examining the impact of introducing climate-related concepts such as facade greening, bioengineering, and adaptation strategies into the classroom. By investigating the intersection of scientific research and educational outreach, this work seeks to contribute to developing more resilient, sustainable, and climate-adaptive cities for the future.

Façade greening – from science to school.

Journal article published: DE GRUYTER OLDENBOURG

Aduse-Poku, M., Niels, W., Pacini, A., Großschedl, J., Edelmann, H.G., & Schlüter, K. (2024). Façade greening – from science to school. at - Automatisierungstechnik, 72, 694 - 703. https://doi.org/10.1515/auto-2024-0022

Survey

Minka Aduse-Poku, Wibke Niels, Annalisa Pacini, Jörg Großschedl, Hans Georg Edelmann and Kirsten Schlüter*

Façade greening – from science to school

Fassadenbegrünung – Forschung gestaltet Unterricht

https://doi.org/10.1515/auto-2024-0022
Received January 30, 2024; accepted April 22, 2024

Abstract: The growing need for cities to adapt to anthropogenic climate change has ushered into a new paradigm where architecture synergistically meets nature. Façade greening may help to take over multifunctional ecosystem services that impact on city residents' well-being as well as on building energy budget. In recent studies on façade greenings, we demonstrated a cooling effect in summer, an insulation effect in winter and a Nitrogen dioxide absorption potential. Introducing this knowledge into school by offering project days led to longer-term changes in students' knowledge, but not in their environmental attitudes. The latter will probably require constant reminders such as a series of project days focusing on environmental issues, bioengineering solutions and personal adaptation strategies.

Keywords: façade greening; climate change; energy saving; air quality; teaching; school experiments

Zusammenfassung: Die Anpassung an den anthropogenen Klimawandel wird für Städte immer notwendiger. Dies hat zu einem neuen Paradigma geführt, bei dem Architektur und Natur synergetisch zusammenwirken. Ein Beispiel dafür sind Fassadenbegrünungen. Sie können multifunktionale Ökosystemleistungen übernehmen, die sich auf das Wohlbefinden der Stadtbewohner und den Energiehaushalt der Gebäude auswirken. In aktuellen Studien zu Fassadenbegrünungen konnten wir einen Kühleffekt im Sommer, einen Dämmeffekt im Winter und ein relevantes Stickstoffdioxid-Absorptionspotenzial nachweisen. Der Transfer dieser Erkenntnisse in die Schule erfolgte durch das Angebot eines Projekttags im universitären Schülerlabor. Dieser führte bei den Jugendlichen zu längerfristigen Veränderungen bzgl. ihres Wissens, aber nicht ihrer Umwelteinstellungen. Um Letzteres zu erreichen, wäre ein umfangreicheres Angebot wünschenswert, wie z. B. eine Reihe von Projekttagen, die sich mit verschiedenen Umweltfragen, Lösungen aus den Bioingenieurswissenschaften und persönlichen Anpassungsstrategien befassen.

Schlagwörter: Fassadenbegrünung; Klimawandel; Energieeinsparung; Luftqualität; Unterricht; Schulexperimente

1 What science tells us

1.1 Introduction

Cities contribute to climate change and are themselves severely affected by its consequences. Prolonged high temperatures with increasingly tropical nights turn densely built and heavily sealed urban neighborhoods into heat islands with negative effects on the health of city dwellers, biodiversity and urban greenery. Climate protection and adaptation to climate change are therefore necessary strategies that cities need to adopt.

Harnessing plants' refined and multifunctional ability to guarantee ecosystem services such as urban heat reduction and air phytoremediation is one example of how "nature's engineering" might help cities to adapt to the various detrimental effects of anthropogenic climate change. Incorporating plants into densely built environments presents a sustainable solution, helping to decrease urban heat [1] and gas pollutants such as Nitrogen Dioxide (NO_2) and Ozone (O_3) [2], to reduce noise and to preserve and strengthen biodiversity.

The potential for reducing the heat budget of buildings through façade greenings has been a subject of discussion for quite some time. The reason for the lack of consensus on specific values is primarily due to the dynamic nature of the topic under investigation. Different experiments conducted under varying climatic conditions have

Hans Georg Edelmann and Kirsten Schlüter share senior authorship.

***Corresponding author: Kirsten Schlüter**, University of Cologne, Institute of Biology Education, Herbert-Lewin-Str. 10, 50931 Köln, Germany, E-mail: kirsten.schlueter@uni-koeln.de
Minka Aduse-Poku, **Wibke Niels**, **Annalisa Pacini**, **Jörg Großschedl and Hans Georg Edelmann**, University of Cologne, Institute of Biology Education, Herbert-Lewin-Str. 10, 50931 Köln, Germany, E-mail: minka.aduse-poku@uni-koeln.de (M. Aduse-Poku), Wibke.Niels@uni-koeln.de (W. Niels), apacini1@uni-koeln.de (A. Pacini), h.edelmann@uni-koeln.de (H. G. Edelmann)

resulted in various degrees of cooling achieved by different façade greening systems [3]–[6]. In addition, there is limited information available regarding the air phytoremediation potential of climbing plants, as the relevance of façade greening for urban climate adaptation has only recently been recognized.

The aim of the various projects of our research group is to carry out measurements on thermal impacts of façade greening systems under real conditions. Also, data were collected from gas-flow measurements under experimentally standardized laboratory conditions, to compare the influence of green ("green architecture") and non-green ("grey architecture") façades on parameters such as temperature, Nitrogen Dioxide (NO_2) and Ozone (O_3) – both considered as harmful anthropogenic gases in cities [7].

The results of the data collection will be incorporated into an overall assessment of the thermal benefit potential of façade greening systems (to improve the urban climate) and air quality as an ultimate urban adaptation strategy to climate change.

1.2 Cooling and insulation potential of green façades

To quantify the cooling and insulation effects of ground-based ivy façade and wall-bound façade greening, wall-surface temperature profiles were collected using data loggers on south exposed façades in two different locations.

1.2.1 Ground-based ivy façade

1.2.1.1 Methods

Data loggers (iButtons) were programmed for an hourly reading and placed on the wall surfaces of two buildings adjacent to each other in the city of Bonn (Figure 1). The house under investigation has had a *Hedera helix* (ivy) façade greening for the past 25–30 years. While the adjacent house was a white-painted façade without greening. Both had concrete surfaces. Results obtained from predominantly hot and cold days were compared to each other as shown below.

1.2.1.2 Results

Wall surface temperatures (shown in Figure 2) varied up to about 25 °C on a typical summer day with peak periods between 12 and 2 pm where the temperature difference was at the highest.

During cold periods the green façade acted as an additional insulating layer, providing a warmer temperature on the surface of the wall as compared to the adjacent wall as shown in Figure 3.

1.2.2 Wall-bound façade greening

1.2.2.1 Methods

Similar to the previously described method, data loggers were fixed to the surfaces of both a greened and a white wall without greening (Figure 4).

1.2.2.2 Results

The data collected for the temperature parameter shows that the wall-mounted façade greening has a consistent cooling effect on warmer days, compared to the non-greened façade sections (see Figure 5).

The temperature profiles for colder periods also showed that the wall-bound façade greening has a continuous insulating effect compared to non-greened façade sections.

1.2.3 Discussion

Improvements in the building's energy budget can be observed in both extreme weather conditions (hot and cold days).

Figure 1: An image of the ground-based façade greening under investigation; with arrows showing locations of data loggers.

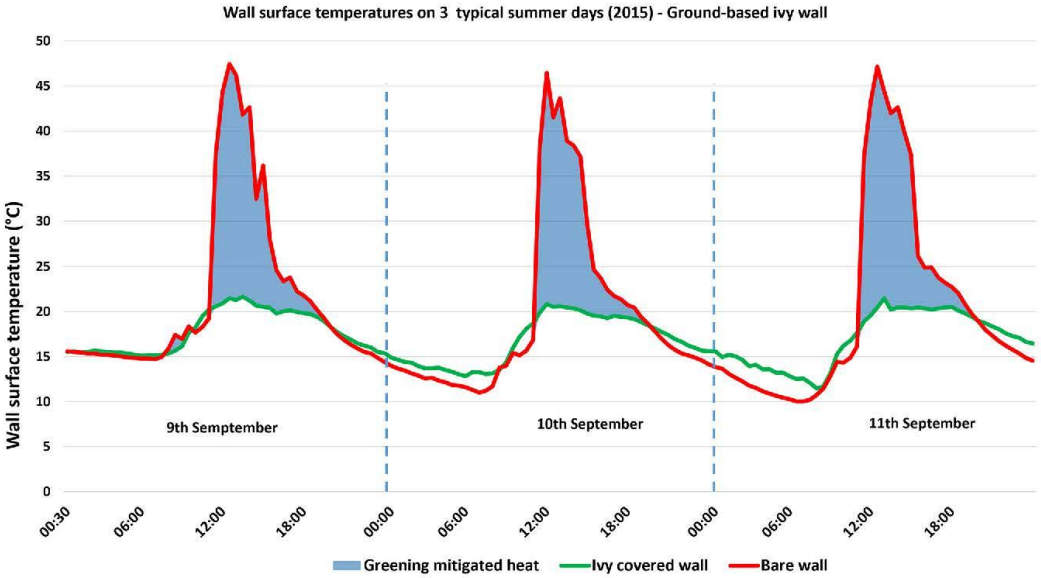

Figure 2: Temperature profiles of a greened and a white painted wall; showing surface temperature differences on summer days, and a relatively stable surface temperature of the greened wall while the white wall undergoes temperature rise and fall.

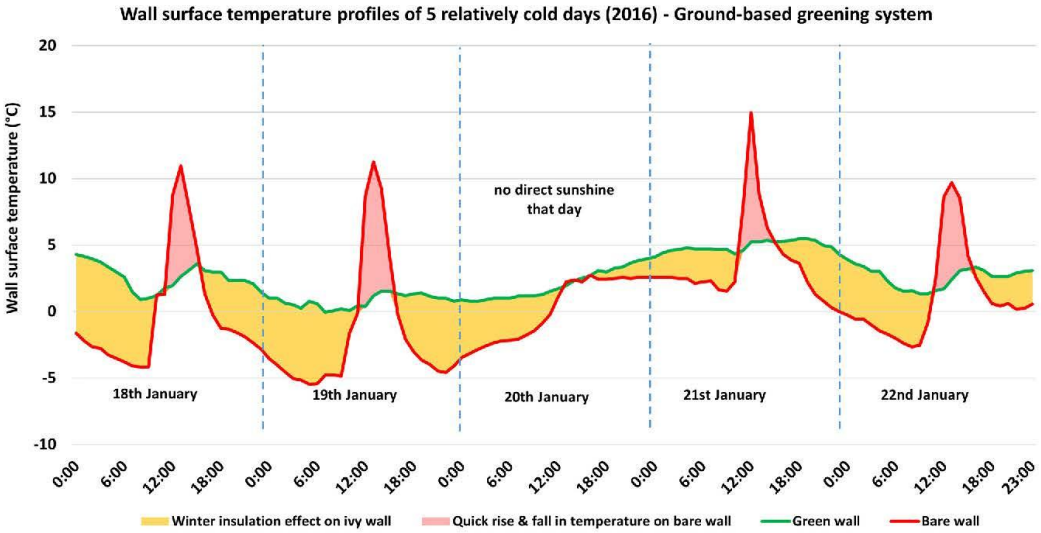

Figure 3: Surface temperature profiles of an ivy wall and white painted wall; showing insulation effect of the greened wall and its relatively stable temperature while the white wall undergoes temperature rise and fall.

During warm periods, the climbing plants offer a protective layer which prevents direct sunlight from reaching the surface of the wall it is covering, hence reducing the amount of energy incident onto the surface of the wall. This is due to the proximity of the plants to the wall with the leaves absorbing light energy and casting their

Figure 4: Image of the wall-bound façade under investigation.

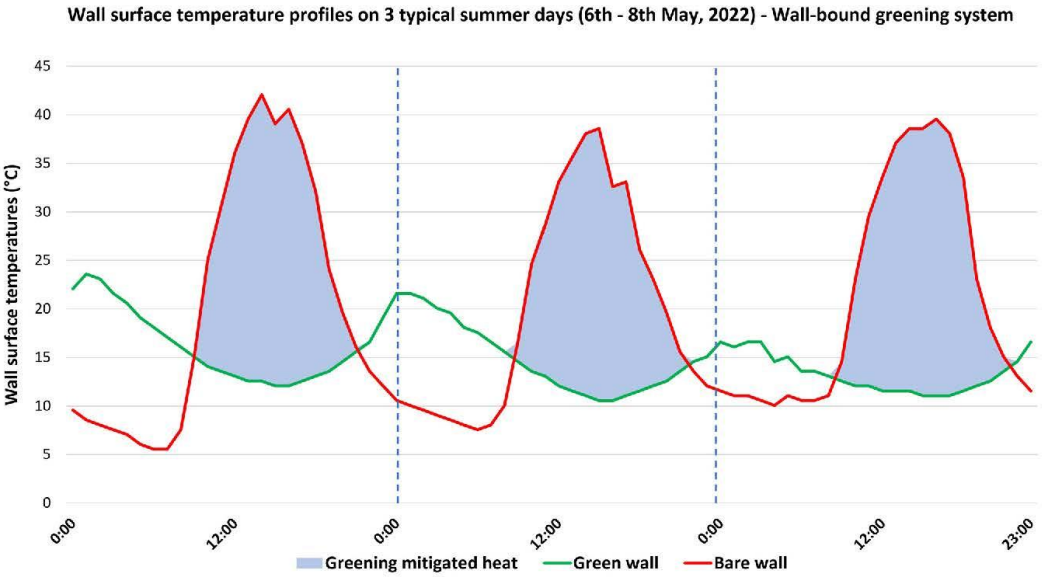

Figure 5: Temperature profiles on a south oriented façade: showing the difference in temperature on the surfaces of both greened and bare-white wall simultaneously (6th–8th May 2022).

shadows onto the surface which contributes to temperature reduction.

In addition, the process of evapotranspiration or transpirational cooling which involves the use of energy from the leaves and its environment as temperature regulating mechanism contributes to the overall cooling effect observed on the surface of the green wall as compared to that of the white wall.

On the other hand, cold temperatures tend to produce a rather more interesting effect as an evergreen vegetation layer (like an ivy façade) assumes the role of an extra insulation layer. During cold temperatures the flow of heat

energy from buildings is usually from within the apartment to the outside environment. This is because temperatures inside are mostly between 18 and 20 °C making energy loss from inside to the outside environment the main driver of energy consumption. With the extra vegetation acting as an insulation layer, the rate of heat loss from the greened house is significantly reduced.

There are great similarities between the cooling effect of both ground-based and wall-bound systems; however, there is also a noticeable difference: the wall-bound system presents a peculiar rise in wall-surface temperatures at night. This is cooled through out the day and rises again at night. This could be explained by the possible blocking of the radiative heat energy emitted by the building at night, as it serves as an insulation layer preventing or reducing the dissipation of heat energy from the building at night.

Finally, there is an important aspect of façade greening often overlooked which is the protection of the building from extreme thermal stress which has a direct link to the longevity of the building.

1.3 Absorption of pollutant gases (NO_2 & O_3)

There is ample evidence showing different absorption potentials of greenhouse and pollutant gases in some woody plant species [8]. However, information on the air phytoremediation potentials of commonly used climbers in façade greening is limited. Given the heterogeneous distribution of air pollutants in the built environment, plants happen to be the best options for their control in our sparsely greened cities.

To methodically examine this effect, we subjected common climbing plants in a flow-through device to specified amounts of air constituents and examined how these compounds were affected by the plants by examining the compositions of the effluent air with two gas analyzers namely, a mid-infrared laser absorption spectrometer (TDL) and a cavity-ring-down spectrometer (CRDS).

The fundamental idea behind the experimental strategy was to apply brief, pulse-like feeds of gases and analyze the concentration changes that occurred right after the pulses. The quick impacts of the plants on the filtration of the applied gas components were analyzed by plotting the time-dependent lowering of the pulse-induced peaks in both illuminated and dark-phases. In this section the absorption potential of NO_2 will be presented because of its status as a pollutant gas of great concern in cities. N_2O, which is a stable tropospheric gas was used as a control, with its source being ambient air.

1.3.1 Experimental design

A graphical representation of the instrumental setup is shown below (Figure 6) with the ivy subspecies "Plattensee"

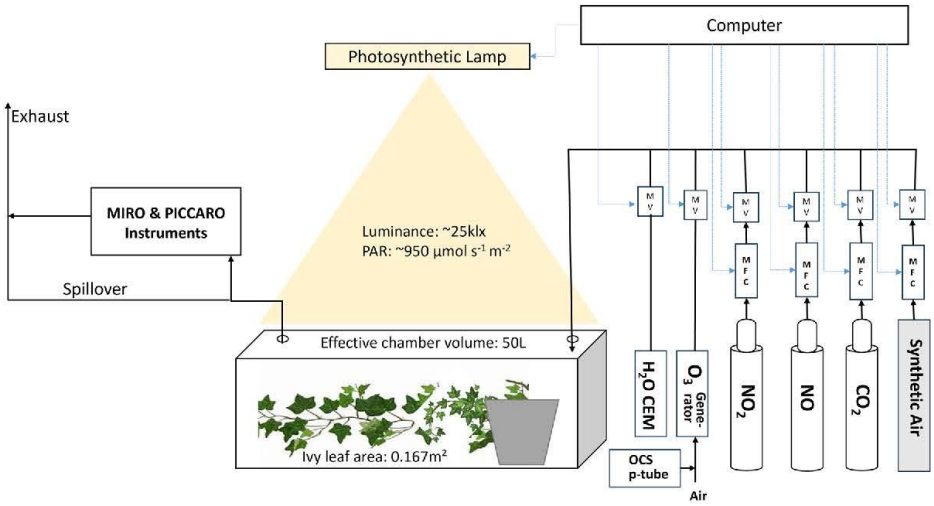

Figure 6: Experimental setup (with an ivy plant) for the greenhouse and pollutant gas absorption experiment. The reaction chamber incorporates a ventilator and a temperature sensor. The constant volume flow rate of synthetic air through the reaction chamber is 10 L/min. The term "MFC" denotes mass flow controllers and "MV" magnetic three-way-valves. The leaf area of 0.167 m^2 given in this figure relates to a specimen of the ivy variety *Hedera helix* "Plattensee" used in this experiment.

as an example. The plants were placed in a small reaction chamber and subjected to a day-night cycle using an LED lamp. The illuminated phase (day) of the experiments ranged from 9 am to 6 pm, after which the lights were switched off for the dark phase (night). The operating temperature in the chamber has been monitored using a temperature sensor called "ibutton" (Hygrochron data logger) averaging 24 °C+/−2 °C.

1.3.2 Results

It was observed that the absorption of NO_2 presented diurnal variations, with most of the absorption occurring in the illuminated phase of the experiment. The results for *H. helix* "Plattensee" are summarized and presented in Figures 7 and 8. Similar results were also obtained for other plant species used for façade greenery.

The time scale in Figure 7, collated over a 24-h period under both illuminated and dark phases of the experiment translates into an absorption rate of about 95 µg/h NO_2 for a leaf area of 0.16 m^2 at a concentration of 40 µg/m^3 NO_2 during the illuminated phase of the experiment as shown in Figure 8 below.

A more detailed explanation of how the absorption rates were calculated can be accessed through Aduse-Poku et al. [9].

1.3.3 Discussion

The permissible limits of Nitrogen Dioxide (NO_2) in the European Union have been revised to align more with the Air Quality Guidelines of the World Health Organization by 2030 because of the EU- Green Deal [10]. For NO_2 this results in a reduction of 50 % from an annual average of 40 µg/m^3 to 20 µg/m^3. What this means is that cities will have to find innovative ways to reduce these pollutants to conform with the revised limits by 2030.

This will be a constraint on the cities already exceeding the current limits. According to the results obtained, *H. helix* at a concentration of 20 ppb NO_2 (about 40 µg/m^3) has the potential to reduce 5493 µg NO_2/m^2 leaf area/day. Projecting these results onto a typical street canyon with the conditions of the laboratory experiments presents about a 17 % reduction in NO_2 pollution levels if the street is covered by an ivy plant.

2 What students should know

2.1 Introduction

It is important that the knowledge gained about the environmental effectiveness of green façades is passed on to

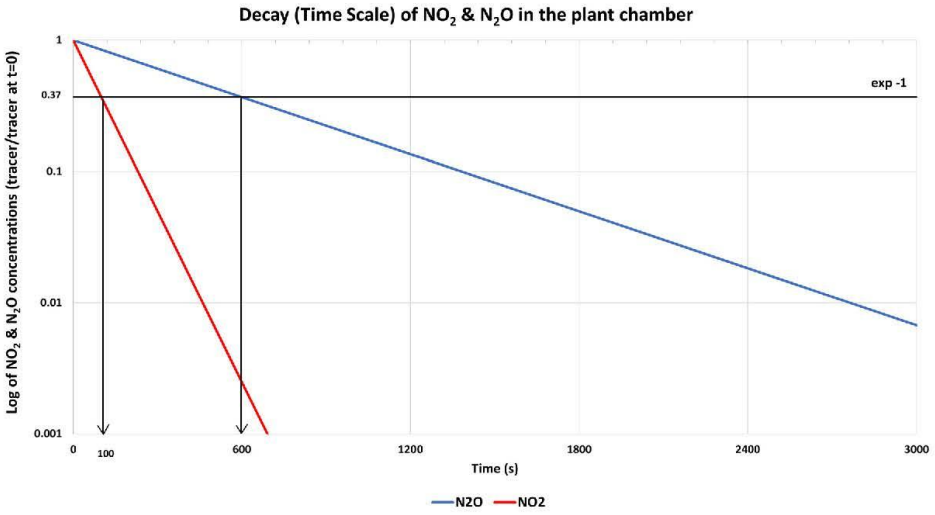

Figure 7: Timescale of decay – the time taken for N_2O (control) and NO_2 to be absorbed or eliminated from the plant chamber using the ivy variety *Hedera helix* "Plattensee". Every hourly collated point (see Figure 8) is a summary of the above-described decay trends of both NO_2 and N_2O.

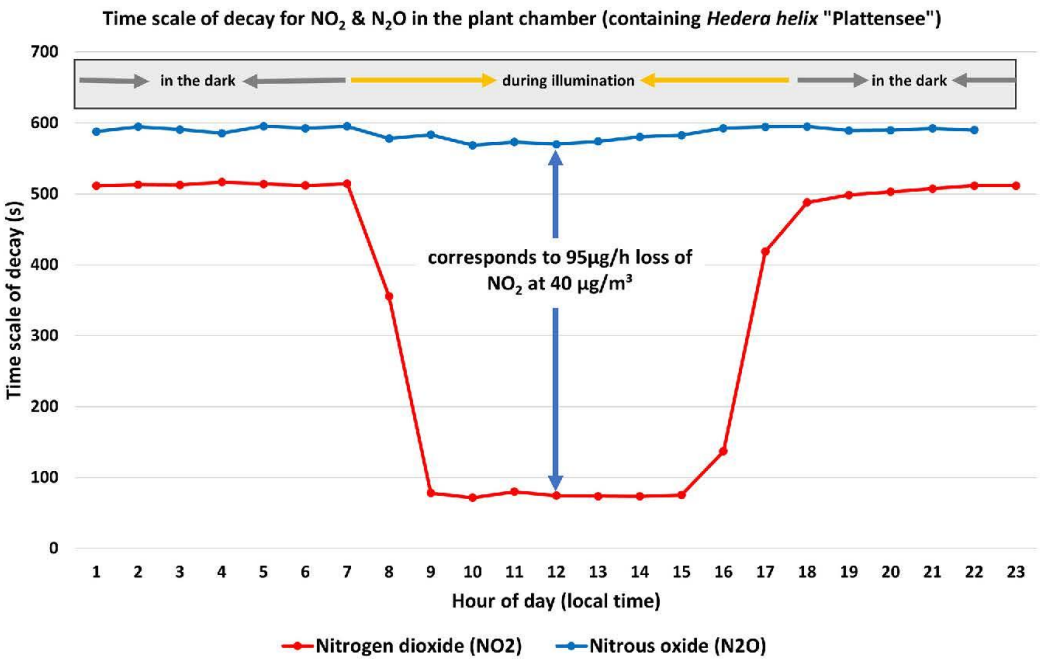

Figure 8: NO_2 uptake by *Hedera helix* "Plattensee" with a leaf surface area of 0.16 m^2.

the next generation [11]. By this, the acceptance of climate-friendly measures (in this case green façades) should be strengthened and the implementation of these measures, particularly in urban centers, should be accelerated. Schools offer themselves as a place of mediation, so that young people can transfer the newly acquired knowledge to their families and support climate-friendly initiatives.

However, the question remains as to how these current topics can be integrated into school lessons, even if the curricula do not (yet) specify them. Three strategies are briefly outlined here. (i) Linkages could be established between the new topic to be taught (in this case green façades) and existing curriculum content. The basic scientific knowledge (on photosynthesis, shading, evaporative cooling and knowledge of species) is then applied in a new context, namely that of façade greening. (ii) New topics, such as façade greening, can be integrated into pre-service-teacher training so that student teachers can bring their experience directly into their lessons when they enter the profession and act as multipliers. (iii) In order to reach in-service-teachers with their classes, teacher training programs can be developed on the one hand and school project days can be offered on the other. Such project days can be organized as extracurricular learning opportunities provided by scientific institutions, e.g. in their school laboratories.

2.2 Intervention

At the University of Cologne, we developed a project day on the topic of façade greening for students in grades seven to nine and tested it with a total of more than 130 pupils. It allows pupils to acquire new knowledge using (a) models, (b) simple experiments (taken from the literature but being newly compiled) and (c) current data from scientific research. The project day is divided into three phases, which are briefly described below. This description refers to a more comprehensive version of the project day than the one tested for effectiveness (see below).

The project day starts with a short introductory phase in which different environmental problems in urban centers are identified by asking students for their prior knowledge in a plenary discussion. The following overarching question is whether façade greening can contribute to mitigating at least some of the problems identified by the pupils.

The work phase is a station-based learning program. The aim of this phase is to familiarize students with the

different types (station 1) and effects of green façades (station 2–6). The stations address topics of biology and physics lessons, like photosynthesis (station 2), absorption and thermodynamics (station 3 and 4) or biodiversity (station 6). Three stations (2–4) refer to experiments in which individual plants (such as ivy) are used as models for an entire façade. Other stations focus on scientific activities like species identification (station 6) or interpreting scientific data (station 5).

- The aim of Station 1 is to introduce students to different types of façade greening using models (or alternatively real façades or photos). The focus here is not only on the technical construction, but also on familiarizing students with different plant species that are suitable for different types of façades. In this way, students' knowledge of species is also increased.
- At station 2, students investigate the extent to which plants reduce the level of the greenhouse gas CO_2 in the air. For this purpose, the change in the CO_2 content is measured in closed containers (e.g. aquariums), with and without plants, using a sensor over a defined period of time. If required, the effect of CO_2 as a greenhouse gas can also be demonstrated in a separate experiment by irradiating closed containers containing air with different CO_2 concentrations with a light source and measuring the temperature increase.
- Station 3 demonstrates the shading effect of a green façade, which leads to a lower temperature rise inside a building. This is also a model experiment in which a temperature sensor is located in a wooden box that is exposed to a radiation source either directly (naked) or covered with ivy.
- Station 4 demonstrates that plants transpire and that this process leads to a cooling of the environment. In total, there should be two separate model experiments. In the first experiment, a sensor is used to demonstrate an increase in humidity in a closed container when a plant is present. In a second experiment, students should experience the cooling effect caused by the evaporation of water molecules from a moistened cloth.
- Station 5 deals with the topic of particulate matter concentration in the air and the extent to which this can be reduced by green façades. As student experiments on this topic are difficult to carry out, experimental data from research is presented, which should then be interpreted by the students. Ideally, the young people would be shown a short video of the experiment at the beginning so that they have a better idea of how the results were obtained.
- At Station 6, the influence of façade greening on biodiversity is to be recorded. For this purpose, living organisms can be searched for on a bare as well as a green façade and assigned to different animal groups in order to record the diversity of species and number of individuals. Alternatively, students can work digitally with photos of different magnification levels.

In the final phase of the lesson, the collected data is summarized and it is examined to what extent the problems which students have associated with conurbations, can be reduced by green façades. Based on the modelling experiments and the recorded data, qualitative statements can be made. If the measured effects could additionally be extrapolated to an entire building façade or a whole street canyon, then the effects would be even more impressive. This could further enhance the project day and may be a task for the future.

2.3 Analysis

Ongoing research on the effectiveness of our project day has so far led to the following findings: It resulted in an increase in students' knowledge, which was still present four weeks later. This knowledge includes both general environmental knowledge relating to green façades and specialized experimental knowledge acquired by the students as a result of carrying out the experiments. However, the project day did not bring about a change in general environmental attitudes. Only the attitude towards green façades changed to a more positive one immediately after the project day, but had decreased again four weeks later. Longer-term and/or repeated interventions are necessary if major changes in environmental attitudes are to be achieved [12], [13]. This could involve a series of several project days on various environmental topics, through which the relevance of environmental measures is repeatedly reminded to the pupils. It would therefore make sense for school laboratories to expand their programs by developing several project days relating to biological engineering and its potential for environmental protection.

2.4 Conclusions

In conclusion, it can be said that the topic of façade greening is very well suited to transferring scientific findings into school education because of its concreteness, good comprehensibility and comparatively easy implementation. Wherever possible, such a relationship between science and school should be established to demonstrate the benefits of biological engineering in moving our society towards greater sustainability. School laboratories can play a major

role here when it comes to imparting solution-based knowledge relating to environmental problems.

Acknowledgments: Our thanks go to Simon Meul, who developed the first version of the project day on façade greening as part of his Master's thesis, to Marie Brüggemann, who analyzed the student data, and to Maren Flottmann for her constant support and feedback. In addition, we want to thank Dr. Franz Rohrer of the FZJ – Forschungszentrum Jülich, who made the quantification of the gas pollutants possible, and the company KREBS & CONRADS whom through their innovative window greening project BILLY-GREEN gave room for experiments for the scientific part of this paper. Finally, we are grateful for the financial support provided by the ZIM programme of the Federal Ministry for Economic Affairs and Climate Action and by the funding line GRÜN hoch 3 of the City of Cologne.

Research ethics: The present survey did not require the approval of an ethics committee, because the research did not pose any threats or risks to the respondents, and it was not associated with high physical or emotional stress.

Author contributions: The authors have accepted responsibility for the entire content of this manuscript and approved its submission.

Competing interests: The authors state no conflict of interest.

Research funding: Project: Innovative façade greening system to increase the energy efficiency of buildings: "BILLY-GREEN". Funding line: Central Innovation Programme for small and medium-sized enterprises (SMEs). Funding organization: Federal Ministry for Economic Affairs and Climate Action Application number: KK5136801AJ0. Project term: 01.02.2021 bis 31.07.2023. Project title: GrüneFassadeKöln: Optimization of building energy efficiency by means of façade greening. Funding line: GRÜN hoch 3/GREEN to the power of 3. Funding organization: City of Cologne. Project term: 01.10.2021 bis 31.05.2023.

Data availability: The data presented in this paper are available on request from: Bio-data: HE, Educational data: KS.

References

[1] G. M. Heisler and A. J. Brazel, "The urban physical environment: temperature and urban heat islands," *Agron. Monogr.*, vol. 55, pp. 29–56, 2015.

[2] S. W. Gawronski, H. Gawronska, S. Lomnicki, A. Sæbo, and J. Vangronsveld, "Plants in air phytoremediation," *Adv. Bot. Res.*, vol. 83, pp. 319–346, 2017.

[3] O. Buchin, M. T. Hoelscher, F. Meier, T. Nehls, and F. Ziegler, "Evaluation of the health-risk reduction potential of countermeasures to urban heat islands," *Energy Build.*, vol. 114, pp. 27–37, 2016.

[4] C. Y. Jim and H. He, "Estimating heat flux transmission of vertical greenery ecosystem," *Ecol. Eng.*, vol. 37, no. 8, pp. 1112–1122, 2011.

[5] S. Schubert and S. Grossman-Clarke, "The influence of green areas and roof albedos on air temperatures during extreme heat events in Berlin, Germany," *Meteorol. Z.*, vol. 22, no. 2, pp. 131–143, 2013.

[6] T. Sternberg, H. Viles, and A. Cathersides, "Evaluating the role of ivy (Hedera helix) in moderating wall surface microclimates and contributing to the bioprotection of historic buildings," *Build. Environ.*, vol. 46, no. 2, pp. 293–297, 2011.

[7] European Environment Agency, "Air quality in Europe - 2016 report," EEA Report, no. 28, 2016.

[8] M. Takahashi, *et al.*, "Differential assimilation of nitrogen dioxide by 70 taxa of roadside trees at an urban pollution level," *Chemosphere*, vol. 61, no. 5, pp. 633–639, 2005.

[9] M. Aduse-Poku, F. Rohrer, B. Winter, and H. G. Edelmann, "Methods and applications in the quantification of the absorption potential for greenhouse- and pollutant gases by climbing plants commonly used in façade greening," n.d. Available at: https://ssrn.com/abstract=4608448.

[10] V. Halleux, "Revision of EU air quality legislation," 2023. Available at: https://www.europarl.europa.eu/RegData/etudes/BRIE/2023/747087/EPRS_BRI(2023)747087_EN.pdf.

[11] A. Pacini, H. G. Edelmann, J. Großschedl, and K. Schlüter, "A literature review on facade greening: how research findings may Be used to promote sustainability and climate literacy in school," *Sustainability*, vol. 14, no. 8, p. 4596, 2022.

[12] T.-M. Baierl, F. G. Kaiser, and F. X. Bogner, "The supportive role of environmental attitude for learning about environmental issues," *J. Environ. Psychol.*, vol. 81, 2022, Art. no. 101799.

[13] F. X. Bogner, "The influence of short-term outdoor ecology education on long-term variables of environmental perspective," *J. Environ. Educ.*, vol. 29, no. 4, pp. 17–29, 1998.

Bionotes

Minka Aduse-Poku
University of Cologne, Institute of Biology Education, Herbert-Lewin-Str. 10, 50931 Köln, Germany
minka.aduse-poku@uni-koeln.de

Minka Aduse-Poku is currently a PhD student at the University of Cologne. He earned his Master's Degree in Environmental Sciences (MSc.) at the University of Cologne (IMES/International Master of Environmental Sciences; https://imes.uni-koeln.de) and his BSc.degree in Natural Resource Management at KNUST – Ghana. His research interests are: transpiration, plant drought stress, climate adaptation in cities, façade greening and climbing plants.

Wibke Niels
University of Cologne, Institute of Biology Education, Herbert-Lewin-Str. 10, 50931 Köln, Germany
Wibke.Niels@uni-koeln.de

Wibke Niels holds a degree in geography and studied at the Universities of Cologne and Bonn. Ms Niels has been working at the University's Institute of Biology Education since 2019, including in the working group on "Climate change and green facades" (https://lmy.de/DTzV). Ms Niels is a PhD student at the Institute of Biology Education and the Institute of Geography Education since 2023. Her research interests are education for sustainable development, façade greening and the transfer from science to school.

Annalisa Pacini
University of Cologne, Institute of Biology Education, Herbert-Lewin-Str. 10, 50931 Köln, Germany
apacini1@uni-koeln.de

Annalisa Pacini is a PhD student at the Institute of Biology Education of the University of Cologne. She is also a teacher of Mathematics and Sciences in a public school in Italy. She has a degree in Environmental Sciences earned at the University of "La Tuscia", Italy. Her main research interests are environmental education, green façades and sustainability, and education for sustainable development.

Jörg Großschedl
University of Cologne, Institute of Biology Education, Herbert-Lewin-Str. 10, 50931 Köln, Germany

Jörg Großschedl has been a professor at the Institute of Biology Education of the University of Cologne since 2016. Before this, he worked as a research assistant at the Leibniz Institute for Science and Mathematics Education at Kiel University. He received his Ph.D. (Dr. rer. nat.) from Kiel University in 2010. His main research interests lie in teaching and learning strategies, teacher professional development, and the learning of evolution.

Hans Georg Edelmann
University of Cologne, Institute of Biology Education, Herbert-Lewin-Str. 10, 50931 Köln, Germany
h.edelmann@uni-koeln.de

Hans Georg Edelmann is professor at the Institute of Biology Education of the University of Cologne. His teaches a wide range of biological sciences disciplines. He also teaches within the IMES (International Master of Environmental Sciences) programme of the University of Cologe. After years of research into the hormonal and gravi-dependent regulation of plant development, he has been devoting his research since 2015 to the eco-physiological relevance of façade greening, its potential on temperature reduction as well as air purification.

Kirsten Schlüter
University of Cologne, Institute of Biology Education, Herbert-Lewin-Str. 10, 50931 Köln, Germany
kirsten.schlueter@uni-koeln.de

Kirsten Schlüter is professor and head of the Institute of Biology Education at the University of Cologne. She is a biologist with a PhD in genetic engineering/technology assessment and an additional qualification as a secondary school teacher (ETH Zurich). As a postdoc, she turned to didactic research and additionally started teaching in school. Since 2004 she has held a professorship in biology education. Her research interests include inquiry-based learning, health and environmental education.

9.0. Synthesis of Findings from Chapters 3-8

9.1. Introduction

This synthesis integrates key findings from Chapters 3-8, focusing on façade greening performance in urban microclimates and its application in educational programs for climate action. Using the "From Science to School" framework, the analysis connects empirical research on cooling effects, pollutant absorption, and species-specific traits to practical applications for sustainable urban design and environmental education.

9.2. Methodological Integration

Quantifying pollution absorption required the use of TDL/CRDS spectrometry in controlled chamber experiments, as discussed in Chapters 3 and 4. These experiments provided a baseline for pollutant uptake by using N_2O control experiments, ensuring that measurements accurately reflected species performance. Among the species studied, *Hedera helix* 'Plattensee' demonstrated the highest NO_2 absorption due to its high stomatal density, highlighting the critical role of species-specific physiological traits in urban air quality management.

Microclimate dynamics, explored in Chapter 6, were monitored through high-frequency logging by the Davis Vantage Pro2 weather station. The study employed gravimetric evapotranspiration (ET) analysis to assess water use efficiency. Furthermore, the development of a pF-VPD-ET framework provided insights into how urban greening species regulate water use under varying climatic conditions, offering predictive tools for sustainable vegetation planning in cities.

Field physiology studies in Chapter 7 validated laboratory findings by analyzing plant responses under real-world summer heatwave conditions, with temperatures reaching 33°C. Using the LI-600 Portable Photosynthesis System, seven species were evaluated, including *Hedera helix* 'Plattensee', *H. colchica*, *L. henryi, P. tricuspidata, W. sinensis, C. montana*, and *H. hibernica*. The results established strong correlations between stomatal conductance (from Chapter 5) and both pollutant absorption (Chapter 3) and cooling efficiency (Chapter 6).

High-ET species were effective in microclimate modification but exhibited higher water demands, reinforcing the importance of species selection in urban greening strategies.

9.3. Key Findings and Cross-Chapter Linkages

Species with high ET rates, such as *Hedera helix* 'Plattensee', provided substantial cooling benefits (Chapter 7). However, this cooling efficiency came with a trade-off, as these species required approximately 128% more water than low-ET species such as *L. henryi* (Chapters 5 and 6). This finding highlights a key consideration in urban greening: while some species provide superior temperature regulation, their water consumption may pose challenges in water-scarce environments.

Pollution absorption was closely linked to stomatal density, a characteristic explored in Chapter 5. Species with higher stomatal densities demonstrated enhanced NO_2 uptake efficiency (Chapter 3). However, this increased pollutant absorption came at the cost of greater sensitivity to heat and water availability (Chapter 6), illustrating a clear trade-off between air quality improvement and water conservation in urban landscapes.

The ability of certain species to sustain evapotranspiration under extreme temperatures is critical for heat resilience. *L. henryi*, for example, maintained stable ET levels even under hot (33°C) weather conditions, making it a water-stress-resilient alternative (Chapters 5 and 7). Unlike species that close their stomata under high heat to reduce water loss, *L. henryi*'s paracytic stomata enabled continued transpiration without excessive water expenditure. This characteristic suggests that *L. henryi* can be used in areas with prolonged heat stress where high-ET species like *H. helix* may struggle due to excessive water requirements.

Validation across chapters strengthened the reliability of findings. Microclimate data collected through Davis weather stations confirmed the accuracy of gravimetric ET calculations, with deviations of less than 5% (Chapter 6). Additionally, species with high stomatal conductance (Chapter 5) were shown to have high cooling potential (Chapter 7) and effective pollutant uptake (Chapter 3). These cross-verifications ensured that experimental results translated well into real-world applications.

9.4. From Science to School: Educational Applications

The findings from this research provide educational strategies for integrating urban greening into school curricula. Middle school students can conduct evapotranspiration experiments to understand plant-water interactions, while pollution absorption studies provide valuable case studies for urban ecology lessons. The implementation of school-based façade greening projects offers students hands-on experience with sustainable landscaping practices. Additionally, citizen science programs that involve students in urban microclimate monitoring foster environmental awareness and contribute to community-based climate action initiatives.

9.5. Limitations and Future Directions

While the study provides significant insights, long-term field validation is necessary to assess the multi-year performance of selected species under varying environmental conditions.

9.6. Conclusion

This synthesis establishes Hedera helix 'Plattensee' as an optimal species for cooling and pollutant mitigation, while recognizing *L. henryi* as a water-stress-resistant alternative suited for heat-stressed urban environments. By leveraging species-specific functional traits, urban planners can design targeted greening systems that optimize air quality improvement and climate adaptation. The methodologies refined in this study—particularly the novel approach to quantifying climbers contribution to air phytoremediation—provide a good foundation for future research in sustainable urban greening strategies.

10.0 Summary

10.1 Key Findings

This dissertation has systematically investigated the role of climbing plants in façade greening, focusing on their ability to mitigate air pollution, regulate water use, and adapt to urban climate stressors. Through a combination of field experiments, laboratory analyses, and literature synthesis, several key insights have emerged:

10.1.1 Absorption of Air Pollutants:

Climbing plants exhibit significant potential for the absorption of NO_2, O_3, and CO_2, with species-specific variations.

H. helix 'Plattensee' demonstrated high NO_2 uptake, making it particularly suitable for urban areas with high vehicular emissions.

L. henryi and *C. montana* showed moderate absorption rates but excelled in sustaining gas exchange under varying urban conditions.

10.1.2 Evapotranspiration and Water Stress Response:

Species showed distinct transpirational cooling potentials, with *H. hibernica* demonstrating high cooling efficiency but requiring higher water availability.

L. henryi exhibited a low water-use strategy, making it an ideal candidate for water-scarce environments.

Soil water availability (pF levels) and vapor pressure deficit (VPD) were dominant drivers of transpiration, influencing species' suitability for different climates.

10.1.3 Stomatal Adaptations and Urban Resilience:

Hedera species with anomocytic stomata showed high adaptability to fluctuating humidity, while *Lonicera*'s paracytic stomata provided controlled transpiration efficiency.

The diversity in stomatal density and type among species suggests that strategic plant selection can enhance the effectiveness of façade greening.

10.1.4 Practical Application in Urban Green Infrastructure:

Different cities require tailored approaches to façade greening based on temperature, humidity, and pollution levels.

In humid, heat-stressed environments, species with high transpiration rates (e.g., *Hedera helix*) should be prioritized.

Water stress-resistant climbers (e.g. *L. henryi*, *C. montana*) are better suited for cities with water scarcity and prolonged dry spells. The summary table below provides a comparative overview of species performance and suitability for different façade greening applications, based on the key findings of this research.

Summary Table of Climbing Plant Traits, Air Pollution Mitigation, and Water Use Efficiency for Façade Greening Applications

Species	NO_2 Absorption & Mitigation	O_3 & CO_2 Uptake & Mitigation	Stomatal Characteristics & Gas Exchange	Water-Use Efficiency & Drought Resistance	Recommended Façade Greening Application	Additional Insights
H. helix 'Plattensee'	Highest NO_2 uptake, significant PM mitigation	High O_3 uptake, CO_2 reduction	High stomatal density, anomocytic; high transpiration	Moderate water needs, regular irrigation	High pollution urban areas, regular watering, cooling priority	Ideal for street canyons; provides thermal insulation but requires reliable water access
Hedera hibernica	Moderate NO_2 absorption & mitigation	Moderate O_3 uptake, CO_2 reduction	High stomatal density, anomocytic; balanced transpiration	Moderate water needs, some drought tolerance	Temperate climates, general air purification, and shading	Suitable for diverse conditions; benefits from trough-based systems
Hedera colchica 'Russland'	Lower NO_2 absorption	Lower O_3 uptake, CO_2 reduction	Medium stomatal density, anomocytic; moderate transpiration	High drought tolerance, very low water needs	Semi-arid climates, low maintenance, water conservation priority	Resilient to drought but less effective in highly polluted zones
L. henryi	Moderate NO_2 absorption & mitigation	Moderate O_3 uptake, high gas exchange	Medium stomatal density, paracytic; efficient water use	High drought resistance, very low water needs	Drought-prone cities, minimal irrigation, adaptable	Adapts well to diverse surfaces; good for promoting biodiversity
C. montana	Low NO_2 absorption	Hight CO_2 and O_3 uptake	Medium stomatal density, anomocytic; stable under heat stress	Moderate water needs, some drought tolerance	Aesthetic greening, limited cooling, CO_2 reduction focus	Better suited for aesthetic appeal rather than primary pollution control
Wisteria sinensis	Moderate NO_2 absorption	Moderate O_3 uptake, high CO_2 uptake	Low stomatal density, paracytic; efficient water use	High water-use efficiency, moderate transpiration	Water-limited environments, efficient CO_2 reduction, drought adaptable	Effective for carbon sequestration, suitable for buildings needing water conservation

10.2 Contribution to Science and Urban Sustainability

This thesis contributes to efforts towards the scientific understanding of:
The functional role of stomatal traits in climate adaptation.
The linkage between transpiration, evapotranspiration, and air pollutant absorption.
The suitability of climbing plants for targeted urban microclimate improvements.
Quantitative data on drought resilience and heat tolerance of climbing plants.

From an applied perspective, these findings can guide urban planners, policymakers, and architects in designing efficient façade greening systems tailored to specific environmental conditions.

10.3 Limitations and Future Research Directions

While this research has provided new insights, several open questions remain:

- Long-term performance: How do these plants respond to multi-year drought cycles and climate change impacts?
- Building Integration: How do different façade greening systems (e.g., soil-based vs. hydroponic) influence plant performance?
- Biodiversity and Ecology: How do climbing plants contribute to urban biodiversity beyond air purification and cooling?

Future studies should integrate remote sensing techniques, long-term field observations, and advanced modelling to predict plant performance under future climate scenarios.

10.4 Final Thoughts: Towards Greener Cities

In a rapidly urbanizing world, nature-based solutions like façade greening offer scalable, cost-effective, and sustainable strategies to combat urban heat islands, poor air quality, and water stress. This thesis demonstrates that climbing plants are aesthetic and functional in mitigating urban environmental challenges.

The findings reinforce the need for evidence-based urban planning, where scientific data guides plant selection to maximize ecosystem services. By leveraging the unique properties of climbing plants, cities can move towards a climate-resilient and healthier future.

The future of sustainable urban architecture lies in integrating plant-based solutions—green façades are no longer an option but a necessity.

11.0 References

Aduse-Poku, M., & Edelmann, H. G. (2025). Quantifying the potential of façade climbing plants in reducing air pollution: a novel investigation into the absorption capabilities of three climbers for CO2, NO2, and O3 in urban environments. *Urban Ecosystems*, *28*(2), 76. https://doi.org/10.1007/s11252-025-01689-4

Aduse-Poku, M., Niels, W., Pacini, A., Großschedl, J., Edelmann, H. G., & Schlüter, K. (2024). Façade greening – from science to school. *At-Automatisierungstechnik*, *72*(7), 694–703. https://doi.org/10.1515/auto-2024-0022

Bakhshoodeh, R., Ocampo, C., & Oldham, C. (2022). Evapotranspiration rates and evapotranspirative cooling of green façades under different irrigation scenarios. *Energy and Buildings*, *270*. https://doi.org/10.1016/j.enbuild.2022.112223

Balamurugan, V., Chen, J., Qu, Z., Bi, X., & Keutsch, F. N. (2022). Secondary PM2.5decreases significantly less than NO2emission reductions during COVID lockdown in Germany. *Atmospheric Chemistry and Physics*, *22*(11), 7105–7129. https://doi.org/10.5194/acp-22-7105-2022

Balmes, J. R. (2019). Household air pollution from domestic combustion of solid fuels and health. In *Journal of Allergy and Clinical Immunology* (Vol. 143, Issue 6). https://doi.org/10.1016/j.jaci.2019.04.016

Bandehali, S., Miri, T., Onyeaka, H., & Kumar, P. (2021). Current state of indoor air phytoremediation using potted plants and green walls. In *Atmosphere* (Vol. 12, Issue 4). MDPI AG. https://doi.org/10.3390/atmos12040473

Behera, S. N., Sharma, M., Mishra, P. K., Nayak, P., Damez-Fontaine, B., & Tahon, R. (2015). Passive measurement of NO2 and application of GIS to generate spatially-distributed air monitoring network in urban environment. *Urban Climate*, *14*. https://doi.org/10.1016/j.uclim.2014.12.003

Bell, M. L., Zanobetti, A., & Dominici, F. (2014). Who is more affected by ozone pollution? A systematic review and meta-analysis. In *American Journal of Epidemiology* (Vol. 180, Issue 1, pp. 15–28). Oxford University Press. https://doi.org/10.1093/aje/kwu115

Blinkova, O., Rawlik, K., & Jagodziński, A. M. (2023). *The Impact of Environmental Factors on Traits of Hedera Helix L. Vegetative Shoots*. https://doi.org/10.21203/rs.3.rs-2742184/v1

Blinkova, O., Rawlik, K., & Jagodziński, A. M. (2024). Effects of limiting environmental conditions on functional traits of Hedera helix L. vegetative shoots. *Frontiers in Plant Science*, *15*. https://doi.org/10.3389/fpls.2024.1464006

Boyano, A., Hernandez, P., & Wolf, O. (2013). Energy demands and potential savings in European office buildings: Case studies based on EnergyPlus simulations. *Energy and Buildings*, *65*, 19–28. https://doi.org/10.1016/j.enbuild.2013.05.039

Broughton, K. J., & Conaty, W. C. (2022). Understanding and Exploiting Transpiration Response to Vapor Pressure Deficit for Water Limited Environments. *Frontiers in Plant Science*, *13*. https://doi.org/10.3389/fpls.2022.893994

Cameron, R. W. F., Taylor, J. E., & Emmett, M. R. (2014). What's "cool" in the world of green façades? How plant choice influences the cooling properties of green walls. *Building and Environment*, *73*, 198–207. https://doi.org/10.1016/j.buildenv.2013.12.005

Cirelli, D., Lieffers, V. J., & Tyree, M. T. (2012). Measuring whole-plant transpiration gravimetrically: A scalable automated system built from components. *Trees - Structure and Function*, *26*(5), 1669–1676. https://doi.org/10.1007/s00468-012-0731-6

Cobb, R., Cummings, S., Furlong, B., Rouse, D., Pfaff, D., Wong, P., Pfaff, D., Hammer, P. R., Nier, H., Pierot, S., Sulgrove, S., & Windle, R. (2013). The American Ivy Society. *Ivy Journal*, *39*. www.ivy.orgwww.ivy.org

Cui, T. (2023). Development of Dust Monitoring in Urban Construction Sites and Suggestions on Dust Control. *Journal of Innovation and Development*, *2*(2). https://doi.org/10.54097/jid.v2i2.5904

Dąbrowska, J., Menéndez Orellana, A. E., Kilian, W., Moryl, A., Cielecka, N., Michałowska, K., Policht-Latawiec, A., Michalski, A., Bednarek, A., & Włóka, A. (2023). Between flood and drought: How cities are facing water surplus and scarcity. In *Journal of Environmental Management* (Vol. 345). https://doi.org/10.1016/j.jenvman.2023.118557

Degraeuwe, B., Thunis, P., Clappier, A., Weiss, M., Lefebvre, W., Janssen, S., & Vranckx, S. (2016). Impact of passenger car NOx emissions and NO2 fractions on urban NO2 pollution - Scenario analysis for the city of Antwerp, Belgium. *Atmospheric Environment*, *126*, 218–224. https://doi.org/10.1016/j.atmosenv.2015.11.042

Denissen, J. M. C., Teuling, A. J., Pitman, A. J., Koirala, S., Migliavacca, M., Li, W., Reichstein, M., Winkler, A. J., Zhan, C., & Orth, R. (2022). Widespread shift from ecosystem energy to water limitation with climate change. *Nature Climate Change*, *12*(7), 677–684. https://doi.org/10.1038/s41558-022-01403-8

Di, H. F., & Wang, D. N. (2010). *COOLING EFFECT OF IVY ON A WALL*. https://doi.org/10.1080/089161599269708

Doheny-Adams, T., Hunt, L., Franks, P. J., Beerling, D. J., & Gray, J. E. (2012). Genetic manipulation of stomatal density influences stomatal size, plant growth and tolerance to restricted water supply across a growth carbon dioxide gradient. *Philosophical Transactions of the Royal Society B: Biological Sciences*, *367*(1588), 547–555. https://doi.org/10.1098/rstb.2011.0272

Donzelli, G., & Suarez-Varela, M. M. (2024). Tropospheric Ozone: A Critical Review of the Literature on Emissions, Exposure, and Health Effects. In *Atmosphere* (Vol. 15, Issue 7). Multidisciplinary Digital Publishing Institute (MDPI). https://doi.org/10.3390/atmos15070779

Drake, P. L., Froend, R. H., & Franks, P. J. (2013). Smaller, faster stomata: Scaling of stomatal size, rate of response, and stomatal conductance. *Journal of Experimental Botany*, *64*(2), 495–505. https://doi.org/10.1093/jxb/ers347

Dütemeyer, D., Barlag, A. B., Kuttler, W., & Axt-Kittner, U. (2013). Measures against heat stress in the city of gelsenkirchen, germany. *Erde*, *144*(3–4), 181–201. https://doi.org/10.12854/erde-144-14

EEA. (2021). Costs of air pollution from European industrial facilities 2008–2017. *EEA Technical Report. Eionet Report - ETC/ATNI 2020/4*, *July*.

European Environment Agency (EEA). (2024, January 25). *The costs to health and the environment from industrial air pollution in Europe – 2024 update — European Environment Agency*. https://www.eea.europa.eu/publications/the-cost-to-health-and-the

Gawronski, S. (2016). Air phytoremediation: An environmental biotechnology for ambient air improvement. *New Biotechnology*, *33*. https://doi.org/10.1016/j.nbt.2016.06.1255

Gawroński, S. W. (2023). Plants for saving the environment - Phytoremediation. In *Acta Societatis Botanicorum Poloniae* (Vol. 92, Issue 1). Polish Botanical Society. https://doi.org/10.5586/asbp/171278

Ghiat, I., Mackey, H. R., & Al-Ansari, T. (2021). A review of evapotranspiration measurement models, techniques and methods for open and closed agricultural field applications. In *Water (Switzerland)* (Vol. 13, Issue 18). MDPI. https://doi.org/10.3390/w13182523

Gigon, A., & Weber, E. (2005). Invasive Neophyten in der Schweiz - Lagebericht und Handlungsbedarf. *Geobotanisches Institut, ETH*.

Gillespie, L. M., & Volaire, F. A. (2017). Are winter and summer dormancy symmetrical seasonal adaptive strategies? The case of temperate herbaceous perennials. In *Annals of Botany* (Vol. 119, Issue 3, pp. 311–323). Oxford University Press. https://doi.org/10.1093/aob/mcw264

Gillner, S., Korn, S., Hofmann, M., & Roloff, A. (2017). Contrasting strategies for tree species to cope with heat and dry conditions at urban sites. *Urban Ecosystems*, *20*(4), 853–865. https://doi.org/10.1007/s11252-016-0636-z

Gorai, A. K., Tuluri, F., Tchounwou, P. B., & Ambinakudige, S. (2015). Influence of local meteorology and NO2 conditions on ground-level ozone concentrations in the eastern part of Texas, USA. *Air Quality, Atmosphere and Health*, *8*(1). https://doi.org/10.1007/s11869-014-0276-5

Gräf, M., Immitzer, M., Hietz, P., & Stangl, R. (2021). Water-stressed plants do not cool: Leaf surface temperature of living wall plants under drought stress. *Sustainability (Switzerland)*, *13*(7). https://doi.org/10.3390/su13073910

Grossiord, C., Buckley, T. N., Cernusak, L. A., Novick, K. A., Poulter, B., Siegwolf, R. T. W., Sperry, J. S., & McDowell, N. G. (2020). Plant responses to rising vapor pressure deficit. In *New Phytologist* (Vol. 226, Issue 6, pp. 1550–1566). Blackwell Publishing Ltd. https://doi.org/10.1111/nph.16485

Gu, Y., Huang, R. J., Duan, J., Xu, W., Lin, C., Zhong, H., Wang, Y., Ni, H., Liu, Q., Xu, R., Wang, L., & Li, Y. J. (2023). Multiple pathways for the formation of secondary organic aerosol in the North China Plain in summer. *Atmospheric Chemistry and Physics*, *23*(9). https://doi.org/10.5194/acp-23-5419-2023

Guttikunda, S. K., Nishadh, K. A., & Jawahar, P. (2019). Air pollution knowledge assessments (APnA) for 20 Indian cities. *Urban Climate*, *27*. https://doi.org/10.1016/j.uclim.2018.11.005

Häffner, K. (n.d.). *Greening Facades - A Historical Introduction - Biotope City Journal*. Retrieved February 7, 2025, from https://biotope-city.net/en/greening-facades-a-historical-introduction/

Hasanuzzaman, M., Chakraborty, K., Zhou, M., & Shabala, S. (2023). Measuring residual transpiration in plants: a comparative analysis of different methods. *Functional Plant Biology*, *50*(12), 983–992. https://doi.org/10.1071/FP23157

He, C., Liu, Z., Wu, J., Pan, X., Fang, Z., Li, J., & Bryan, B. A. (2021). Future global urban water scarcity and potential solutions. *Nature Communications*, *12*(1). https://doi.org/10.1038/s41467-021-25026-3

Health Organization, W., & Office for Europe, R. (2013). *Review of evidence on health aspects of air pollution-REVIHAAP Project Technical Report*. http://www.euro.who.int/pubrequest

Heisler, G. M., & Brazel, A. J. (2015). *The Urban Physical Environment: Temperature and Urban Heat Islands* (pp. 29–56). https://doi.org/10.2134/agronmonogr55.c2

Hellebaut, A., Boisson, S., & Mahy, G. (2022). Do plant traits help to design green walls for urban air pollution control? A short review of scientific evidences and knowledge gaps. In *Environmental Science and Pollution Research* (Vol. 29, Issue 54, pp. 81210–81221). Springer Science and Business Media Deutschland GmbH. https://doi.org/10.1007/s11356-022-23439-1

Hoelscher, M. T., Nehls, T., Jänicke, B., & Wessolek, G. (2016). Quantifying cooling effects of facade greening: Shading, transpiration and insulation. *Energy and Buildings*, *114*, 283–290. https://doi.org/10.1016/j.enbuild.2015.06.047

Holzer, M., McKendry, I. G., & Jaffe, D. A. (2003). Springtime trans-Pacific atmospheric transport from east Asia: A transit-time probability density function approach. *Journal of Geophysical Research: Atmospheres*, *108*(22). https://doi.org/10.1029/2003jd003558

IAWA Journal, E. (2014). Anatomy of the Dicotyledons Volume I, Second Edition. C.R. Metcalfe ' L. Chalk, 276 pp., text figs. + 18 photoplates, 1988 (1979). Clarendon Press, Oxford. Price:UK£ 25.00 (paperback). *IAWA Journal*, *9*(4). https://doi.org/10.1163/22941932-90001102

Intergovernmental Panel on Climate Change [IPCC], 1992. (2023). SYNTHESIS REPORT OF THE IPCC SIXTH ASSESSMENT REPORT (AR6) IPCC. *Climate Change 2021 – The Physical Science Basis*.

IPCC. (2022). IPCC, 2022: Summary for Policy Makers. In *Climate Change 2022: Impacts, Adaptation and Vulnerability*.

IPCC. (2023a). Intergovernmental Panel on Climate Change - AR6 Synthesis Report: Climate Change 2023. In *Climate Change 2022 – Impacts, Adaptation and Vulnerability*.

IPCC. (2023b). SYNTHESIS REPORT OF THE IPCC SIXTH ASSESSMENT REPORT (AR6): Summary for Policymakers. In *European University Institute* (Issue 2).

IPCC AR6 SYR. (2017). IPCC AR6 Synthesis Report: Climate Change 2023. *European University Institute*, *2*.

Janse, R. J., Hoekstra, T., Jager, K. J., Zoccali, C., Tripepi, G., Dekker, F. W., & Van Diepen, M. (2021). Conducting correlation analysis: Important limitations and pitfalls. In *Clinical Kidney Journal* (Vol. 14, Issue 11, pp. 2332–2337). Oxford University Press. https://doi.org/10.1093/ckj/sfab085

Kasdagli, M.-I., Orellano, P., Pérez Velasco, R., & Samoli, E. (2024). Long-Term Exposure to Nitrogen Dioxide and Ozone and Mortality: Update of the WHO Air Quality Guidelines Systematic Review and Meta-Analysis. *International Journal of Public Health*, *69*. https://doi.org/10.3389/ijph.2024.1607676

Kashtan, Y., Nicholson, M., Finnegan, C. J., Ouyang, Z., Garg, A., Lebel, E. D., Rowland, S. T., Michanowicz, D. R., Herrera, J., Nadeau, K. C., & Jackson, R. B. (2024). Nitrogen dioxide exposure, health outcomes, and associated demographic disparities due to gas and propane combustion by U.S. stoves. In *Sci. Adv* (Vol. 10). https://www.science.org

Katul, G. G., Oren, R., Manzoni, S., Higgins, C., & Parlange, M. B. (2012). Evapotranspiration: A process driving mass transport and energy exchange in the soil-plant-atmosphere-climate system. In *Reviews of Geophysics* (Vol. 50, Issue 3). Blackwell Publishing Ltd. https://doi.org/10.1029/2011RG000366

Kerstiens, G. (1996). Cuticular water permeability and its physiological significance. In *Journal of Experimental Botany* (Vol. 47, Issue 305, pp. 1813–1832). Oxford University Press. https://doi.org/10.1093/jxb/47.12.1813

Koehler, T., Wankmüller, F. J. P., Sadok, W., & Carminati, A. (2023). Transpiration response to soil drying versus increasing vapor pressure deficit in crops: physical and physiological mechanisms and key plant traits. In *Journal of Experimental Botany* (Vol. 74, Issue 16, pp. 4789–4807). Oxford University Press. https://doi.org/10.1093/jxb/erad221

Köhler, M. (2008). Green facades-a view back and some visions. *Urban Ecosystems*, *11*(4), 423–436. https://doi.org/10.1007/s11252-008-0063-x

Kovats, R. S., & Hajat, S. (2008). Heat stress and public health: A critical review. *Annual Review of Public Health*, *29*, 41–55. https://doi.org/10.1146/annurev.publhealth.29.020907.090843

Krich, C., Mahecha, M. D., Migliavacca, M., De Kauwe, M. G., Griebel, A., Runge, J., & Miralles, D. G. (2022). Decoupling between ecosystem photosynthesis and transpiration: A last resort against overheating. *Environmental Research Letters*, *17*(4). https://doi.org/10.1088/1748-9326/ac583e

Kumar, N., & Sankhla, N. (2024). Stomata Responses to Heat Stress. *Kumar & Sankhla Biological Forum-An International Journal*, *16*(4), 133.

Lal, R. (2020). Soil organic matter and water retention. *Agronomy Journal*, *112*(5), 3265–3277. https://doi.org/10.1002/agj2.20282

Lawson, T., & Blatt, M. R. (2014). Stomatal size, speed, and responsiveness impact on photosynthesis and water use efficiency. *Plant Physiology*, *164*(4), 1556–1570. https://doi.org/10.1104/pp.114.237107

Lee, J., Park, K., Lee, H., Jang, B. K., & Cho, J. S. (2024). Improving seed germination: effect of stratification and dormancy-release priming in Lonicera insularis Nakai. *Frontiers in Plant Science*, *15*. https://doi.org/10.3389/fpls.2024.1484114

Lee, L. S. H., & Jim, C. Y. (2019). Transforming thermal-radiative study of a climber green wall to innovative engineering design to enhance building-energy efficiency. *Journal of Cleaner Production*, *224*, 892–904. https://doi.org/10.1016/j.jclepro.2019.03.278

Liu, C., Li, Y., Xu, L., Li, M., Wang, J., Yan, P., & He, N. (2021). Stomatal Arrangement Pattern: A New Direction to Explore Plant Adaptation and Evolution. *Frontiers in Plant Science*, *12*. https://doi.org/10.3389/fpls.2021.655255

Luber, G., & McGeehin, M. (2008). Climate Change and Extreme Heat Events. In *American Journal of Preventive Medicine* (Vol. 35, Issue 5, pp. 429–435). https://doi.org/10.1016/j.amepre.2008.08.021

Lyu, X., Chang, L., Lu, Z., & Li, J. (2023a). The ability of three climbing plant species to capture particulate matter and their physiological responses at different environmental sampling sites. *Frontiers in Environmental Science*, *10*. https://doi.org/10.3389/fenvs.2022.1084902

Lyu, X., Chang, L., Lu, Z., & Li, J. (2023b). The ability of three climbing plant species to capture particulate matter and their physiological responses at different environmental sampling sites. *Frontiers in Environmental Science*, *10*. https://doi.org/10.3389/fenvs.2022.1084902

Maes, J., & Jacobs, S. (2017). Nature-Based Solutions for Europe's Sustainable Development. *Conservation Letters*, *10*(1), 121–124. https://doi.org/10.1111/conl.12216

Manso, M., Teotónio, I., Silva, C. M., & Cruz, C. O. (2021). Green roof and green wall benefits and costs: A review of the quantitative evidence. In *Renewable and Sustainable Energy Reviews* (Vol. 135). Elsevier Ltd. https://doi.org/10.1016/j.rser.2020.110111

MARKOSKA, V., SPALEVIC, V., LISICHKOV, K., ATKOVSKA, K., & GULABOSKI, R. (2018). DETERMINATION OF WATER RETENTION CHARACTERISTICS OF PERLITE AND PEAT. *The Journal "Agriculture and Forestry," 64*(3). https://doi.org/10.17707/agricultforest.64.3.10

Medina, S., Vicente, R., Nieto-Taladriz, M. T., Aparicio, N., Chairi, F., Vergara-Diaz, O., & Araus, J. L. (2019). The plant-transpiration response to vapor pressure deficit (VPD) in durum wheat is associated with differential yield performance and specific expression of genes involved in primary metabolism and water transport. *Frontiers in Plant Science*, *9*. https://doi.org/10.3389/fpls.2018.01994

Meineke, E. K., & Frank, S. D. (2018). Water availability drives urban tree growth responses to herbivory and warming. *Journal of Applied Ecology*, *55*(4), 1701–1713. https://doi.org/10.1111/1365-2664.13130

Menberu, M. W., Marttila, H., Ronkanen, A. K., Haghighi, A. T., & Kløve, B. (2021). Hydraulic and Physical Properties of Managed and Intact Peatlands: Application of the Van Genuchten-Mualem Models to Peat Soils. *Water Resources Research*, *57*(7). https://doi.org/10.1029/2020WR028624

Metcalfe, D. J. (2005b). Hedera helix L. In *Journal of Ecology* (Vol. 93, Issue 3, pp. 632–648). https://doi.org/10.1111/j.1365-2745.2005.01021.x

Milivojević, L., Mrazovac Kurilić, S., Božilović, Z., Koprivica, S., & Krčadinac, O. (2023). Study of Particular Air Quality and Meteorological Parameters at a Construction Site. *Atmosphere*, *14*(8). https://doi.org/10.3390/atmos14081267

Molina, L. T. (2021). Introductory lecture: Air quality in megacities. *Faraday Discussions*, *226*, 9–52. https://doi.org/10.1039/d0fd00123f

Molina, M. J., & Molina, L. T. (2004). Megacities and atmospheric pollution. *Journal of the Air and Waste Management Association*, *54*(6), 644–680. https://doi.org/10.1080/10473289.2004.10470936

Mues, A., Manders, A., Schaap, M., Kerschbaumer, A., Stern, R., & Builtjes, P. (2012). Impact of the extreme meteorological conditions during the summer 2003 in Europe on

particulate matter concentrations. *Atmospheric Environment*, *55*. https://doi.org/10.1016/j.atmosenv.2012.03.002

Nilson, S. E., & Assmann, S. M. (2007). The control of transpiration. Insights from arabidopsis. In *Plant Physiology* (Vol. 143, Issue 1, pp. 19–27). American Society of Plant Biologists. https://doi.org/10.1104/pp.106.093161

Oke, T. R. (1982). The energetic basis of the urban heat island. In *Quart. J. R. Met. Soc* (Vol. 108, Issue 455).

O'Kelly, B. C., & Sivakumar, V. (2014). Water Content Determinations for Peat and Other Organic Soils Using the Oven-Drying Method. *Drying Technology*, *32*(6). https://doi.org/10.1080/07373937.2013.849728

Pérez, G., Coma, J., Martorell, I., & Cabeza, L. F. (2014). Vertical Greenery Systems (VGS) for energy saving in buildings: A review. In *Renewable and Sustainable Energy Reviews* (Vol. 39, pp. 139–165). Elsevier Ltd. https://doi.org/10.1016/j.rser.2014.07.055

Perini, K., & Rosasco, P. (2013). Cost-benefit analysis for green façades and living wall systems. *Building and Environment*, *70*, 110–121. https://doi.org/10.1016/j.buildenv.2013.08.012

Petrova, Y. (2012). The effect of light intensity on the stomatal density of lavender, Lavandula angustifolia. *Young Scientists Journal*, *5*(12). https://doi.org/10.4103/0974-6102.105078

Pettit, T., Irga, P. J., & Torpy, F. R. (2018). Towards practical indoor air phytoremediation: A review. In *Chemosphere* (Vol. 208). https://doi.org/10.1016/j.chemosphere.2018.06.048

Prigioniero, A., Zuzolo, D., Niinemets, Ü., & Guarino, C. (2021). Nature-based solutions as tools for air phytoremediation: A review of the current knowledge and gaps. In *Environmental Pollution* (Vol. 277). https://doi.org/10.1016/j.envpol.2021.116817

Rahman, M. A., Dervishi, V., Moser-Reischl, A., Ludwig, F., Pretzsch, H., Rötzer, T., & Pauleit, S. (2021). Comparative analysis of shade and underlying surfaces on cooling effect. *Urban Forestry and Urban Greening*, *63*. https://doi.org/10.1016/j.ufug.2021.127223

Raviraja. S. (2023). Future climate change. *GSC Advanced Research and Reviews*, *14*(1), 050–054. https://doi.org/10.30574/gscarr.2023.14.1.0373

Reis, C., & Lopes, A. (2019). Evaluating the cooling potential of urban green spaces to tackle urban climate change in Lisbon. *Sustainability (Switzerland)*, *11*(9). https://doi.org/10.3390/su11092480

Ritz, B., Hoffmann, B., & Peters, A. (2019). The effects of fine dust, ozone, and nitrogen dioxide on health. In *Deutsches Arzteblatt International* (Vol. 116, Issues 51–52, pp. 881–886). Deutscher Arzte-Verlag GmbH. https://doi.org/10.3238/arztebl.2019.0881

Romanesque / Gothic : Greening of Buildings in the Middle Ages: Fassadengruen. (n.d.). Retrieved February 7, 2025, from https://www.fassadengruen.de/en/building-greening-in-the-middle-ages.html

Santamouris, M. (2014). Cooling the cities - A review of reflective and green roof mitigation technologies to fight heat island and improve comfort in urban environments. *Solar Energy*, *103*, 682–703. https://doi.org/10.1016/j.solener.2012.07.003

Santiago, A., Herranz, J. M., Copete, E., & Ferrandis, P. (2013). Species-specific environmental requirements to break seed dormancy: Implications for selection of regeneration niches in three Lonicera (Caprifoliaceae) species. *Botany*, *91*(4), 225–233. https://doi.org/10.1139/cjb-2012-0169

Savvides, A., Fanourakis, D., & Van Ieperen, W. (2012). Co-ordination of hydraulic and stomatal conductances across light qualities in cucumber leaves. *Journal of Experimental Botany*, *63*(3), 1135–1143. https://doi.org/10.1093/jxb/err348

Scherer, D., & Endlicher, W. (2013). Editorial: Urban climate and heat stress - Part 1. In *Erde* (Vol. 144, Issues 3–4, pp. 175–180). Gesellschaft fur Erdkunde zu Berlin. https://doi.org/10.12854/erde-144-13

Schwärzel, K., Renger, M., Sauerbrey, R., & Wessolek, G. (2002). Soil physical characteristics of peat soils. *Journal of Plant Nutrition and Soil Science*, *165*(4), 479–486. https://doi.org/10.1002/1522-2624(200208)165:4<479::AID-JPLN479>3.0.CO;2-8

Slot, M., Nardwattanawong, T., Hernández, G. G., Bueno, A., Riederer, M., & Winter, K. (2021). Large differences in leaf cuticle conductance and its temperature response among 24 tropical tree species from across a rainfall gradient. *New Phytologist*, *232*(4), 1618–1631. https://doi.org/10.1111/nph.17626

Sofiev, M., Siljamo, P., Karppinen, A., & Kukkonen, J. (2008). Air quality forecasting during summer 2006: Forest fires as one of major pollution sources in Europe. In *NATO Science for Peace and Security Series C: Environmental Security*. https://doi.org/10.1007/978-1-4020-8453-9_33

Tang, S., Xue, X., Li, F., Gu, Z., Jia, H., & Cao, X. (2023). Identification of Pollution Sources in Urban Wind Environments Using the Regularized Residual Method. *Atmosphere*, *14*(12). https://doi.org/10.3390/atmos14121786

Umwelt Bundesamt. (2018, March 9). *Nitrogen dioxide has serious impact on health | Umweltbundesamt*. https://www.umweltbundesamt.de/en/press/pressinformation/nitrogen-dioxide-has-serious-impact-on-health

United Nations Environment Programme and International Union for Conservation of Nature (2021). Nature-based solutions for climate change mitigation. Nairobi and

Gland. (2021). *Nature-based solutions for climate change mitigation*. http://www.un.org/Depts/Cartographic/

Valcárcel, V., & Vargas, P. (2010). Quantitative morphology and species delimitation under the general lineage concept: Optimization for Hedera (Araliaceae). *Source: American Journal of Botany*, *97*(9), 1555–1573. https://doi.org/10.3732/ajb.l000115

Van Cotthem, W. R. J. (1970). A classification of stornatal types. In *Bot. J. Linn. Soc* (Vol. 63).

Wang, J., Wu, Q., Liu, J., Yang, H., Yin, M., Chen, S., Guo, P., Ren, J., Luo, X., Linghu, W., & Huang, Q. (2019). Vehicle emission and atmospheric pollution in China: Problems, progress, and prospects. *PeerJ*, *7*. https://doi.org/10.7717/peerj.6932

Wang, Y., Yang, Y., Yuan, Q., Li, T., Zhou, Y., Zong, L., Wang, M., Xie, Z., Ho, H. C., Gao, M., Tong, S., Lolli, S., & Zhang, L. (2025). Substantially underestimated global health risks of current ozone pollution. *Nature Communications* , *16*(1). https://doi.org/10.1038/s41467-024-55450-0

Woodward, F. I. (1987). *Stomatal numbers are sensitive to increases in CO 2 from pre-industrial levels*.

Xia, X., Meng, X., Liu, C., Guo, Y., Li, X., Niu, Y., Lam, K. B. H., Wright, N., Kartsonaki, C., Chen, Y., Yang, L., Du, H., Yu, C., Sun, D., Lv, J., Chen, J., Yang, X., Gao, R., Wu, S., … Qu, C. (2024). Associations of long-term nitrogen dioxide exposure with a wide spectrum of diseases: a prospective cohort study of 0·5 million Chinese adults. *The Lancet Public Health*, *9*(12), e1047–e1058. https://doi.org/10.1016/S2468-2667(24)00264-0

Xu, Z., Ran, Y., & Rao, Z. (2022). Design and integration of air pollutants monitoring system for emergency management in construction site based on BIM and edge computing. *Building and Environment*, *211*. https://doi.org/10.1016/j.buildenv.2021.108725

Xu, Z., & Zhou, G. (2008). Responses of leaf stomatal density to water status and its relationship with photosynthesis in a grass. *Journal of Experimental Botany*, *59*(12), 3317–3325. https://doi.org/10.1093/jxb/ern185

Zeng, S., & Zhang, Y. (2017). The effect of meteorological elements on continuing heavy air pollution: A case study in the chengdu area during the 2014 spring festival. *Atmosphere*, *8*(4). https://doi.org/10.3390/atmos8040071

Zhang, B., Cao, D., & Zhu, S. (2020). Use of plants to clean polluted air: A potentially effective and low-cost phytoremediation technology. In *BioResources* (Vol. 15, Issue 3). https://doi.org/10.15376/biores.15.3.4650-4654

Zhang, R., Sun, C., Zhu, J., Zhang, R., & Li, W. (2020). Increased European heat waves in recent decades in response to shrinking Arctic sea ice and Eurasian snow cover. *Npj Climate and Atmospheric Science*, *3*(1). https://doi.org/10.1038/s41612-020-0110-8

Zhao, T., Markevych, I., Fuertes, E., de Hoogh, K., Accordini, S., Boudier, A., Casas, L., Forsberg, B., Garcia Aymerich, J., Gnesi, M., Holm, M., Janson, C., Jarvis, D., Johannessen, A., Jörres, R. A., Karrasch, S., Leynaert, B., Maldonado Perez, J. A., Malinovschi, A., … Heinrich, J. (2023). Impact of long-term exposure to ambient ozone on lung function over a course of 20 years (The ECRHS study): a prospective cohort study in adults. *The Lancet Regional Health - Europe*, *34*. https://doi.org/10.1016/j.lanepe.2023.100729

Ziemer, R. R. (1979). Evaporation and transpiration. In *Reviews of Geophysics* (Vol. 17, Issue 6, pp. 1175–1186). https://doi.org/10.1029/RG017i006p01175

12.0 Acknowledgments

Completing this doctoral thesis has been a journey I could not have undertaken alone. I am deeply grateful to the many individuals and institutions whose support, guidance, and encouragement made this achievement possible.

First and foremost, I would like to express my profound gratitude to my supervisor, Prof. Dr. Hans G. Edelmann, whose unwavering commitment, insightful feedback, and steadfast belief in my potential guided me through every stage of this research. Your mentorship has been a cornerstone of my academic growth, and I am forever indebted to you for your patience and wisdom.

I am equally thankful to Prof. Dr. Karl Schneider and Prof. Dr. Michael Bonkowski, whose pivotal roles in shaping my academic journey cannot be overstated. Your expertise, encouragement, and constructive critiques have been invaluable in refining my work and broadening my intellectual horizons.

A special thanks goes to Dr. Franz Rohrer and Benjamin Winter at the Institute of Tropospheric Chemistry at the Forschungszentrum Jülich. Your immense support during the gas absorption experiments was instrumental in overcoming technical challenges and achieving meaningful results.

To the entire team at the Institut für Biodidaktik, particularly Prof. Dr. Kirsten Schlüter, Wibke Niels, Andrea Germund, Jürgen Hintzsche, and everyone who contributed in many ways—thank you for your unwavering support through thick and thin. Your encouragement and camaraderie helped me navigate the highs and lows of this journey.

Finally, to my family—Josephine Lawson, Samuel Hans Aduse-Poku, and Horlali Aduse-Poku—this achievement is as much yours as it is mine. Your love, sacrifices, and unwavering belief in me have been my anchor during the most challenging times. I could not have done this without you.

This thesis is a testament to the collective effort of everyone who stood by me, and I am profoundly grateful for your contributions. Thank yo

13.0 Appendix

Regression of the energy driven phase of evapotranspiration for *H.helix* "Plattensee"

Notes

Output Created		20-JAN-2025 11:19:02
Comments		
Input	Active Dataset	DataSet7
	Filter	<none>
	Weight	<none>
	Split File	<none>
	N of Rows in Working Data File	12
Missing Value Handling	Definition of Missing	User-defined missing values are treated as missing.
	Cases Used	Statistics are based on cases with no missing values for any variable used.
Syntax		REGRESSION /DESCRIPTIVES MEAN STDDEV CORR SIG N /MISSING LISTWISE /STATISTICS COEFF OUTS CI(95) R ANOVA CHANGE /CRITERIA=PIN(.05) POUT(.10) TOLERANCE(.0001) /NOORIGIN /DEPENDENT Evapotranspirationmlm²day /METHOD=ENTER pF PPFDµmolm²s WindKmh Temperature°C VPDkPa

		/SCATTERPLOT=(*ZRESID ,*ZPRED) /RESIDUALS NORMPROB(ZRESID).
Resources	Processor Time	00:00:00.00
	Elapsed Time	00:00:00.02
	Memory Required	7808 bytes
	Additional Memory Required for Residual Plots	488 bytes

Warnings

For the final model with dependent variable Evapotranspiration (ml/m²/day), influence statistics cannot be computed because the fit is perfect.

The chart: *zresid by *zpred Scatterplot is not produced because it is empty.

Descriptive Statistics

	Mean	Std. Deviation	N
Evapotranspiration (ml/m²/day)	561.75	256.57	5
pF	2.422	.371	5
PPFD (µmol/m²/s)	12489.3	5987.49	5
Wind (Km/h)	.205	.141	5
Temperature °C	21.583	2.471	5
VPD (kPa)	.526	.235	5

Correlations

		Evapotranspiration (ml/m²/day)	pF	PPFD (µmol/m²/s)
Pearson Correlation	Evapotranspiration (ml/m²/day)	1.000	.149	.979
	pF	.149	1.000	.040
	PPFD (µmol/m²/s)	.979	.040	1.000
	Wind (Km/h)	.549	.773	.383
	Temperature °C	.981	-.005	.957
	VPD (kPa)	.981	.183	.956

Sig. (1-tailed)	Evapotranspiration (ml/m²/day)	.	.405	.002
	pF	.405	.	.474
	PPFD (µmol/m²/s)	.002	.474	.
	Wind (Km/h)	.169	.063	.262
	Temperature °C	.002	.497	.005
	VPD (kPa)	.002	.384	.005
N	Evapotranspiration (ml/m²/day)	5	5	5
	pF	5	5	5
	PPFD (µmol/m²/s)	5	5	5
	Wind (Km/h)	5	5	5
	Temperature °C	5	5	5
	VPD (kPa)	5	5	5

Correlations

		Wind (Km/h)	Temperature °C	VPD (kPa)
Pearson Correlation	Evapotranspiration (ml/m²/day)	.549	.981	.981
	pF	.773	-.005	.183
	PPFD (µmol/m²/s)	.383	.957	.956
	Wind (Km/h)	1.000	.484	.563
	Temperature °C	.484	1.000	.959
	VPD (kPa)	.563	.959	1.000
Sig. (1-tailed)	Evapotranspiration (ml/m²/day)	.169	.002	.002
	pF	.063	.497	.384
	PPFD (µmol/m²/s)	.262	.005	.005
	Wind (Km/h)	.	.204	.161
	Temperature °C	.204	.	.005
	VPD (kPa)	.161	.005	.
N	Evapotranspiration (ml/m²/day)	5	5	5
	pF	5	5	5
	PPFD (µmol/m²/s)	5	5	5
	Wind (Km/h)	5	5	5
	Temperature °C	5	5	5
	VPD (kPa)	5	5	5

Variables Entered/Removed[a]

Model	Variables Entered	Variables Removed	Method
1	VPD (kPa), pF, Wind (Km/h), PPFD (µmol/m²/s)[b]	.	Enter

a. Dependent Variable: Evapotranspiration (ml/m²/day)

b. Tolerance = .000 limit reached.

Model Summary[b]

Model	R	R Square	Adjusted R Square	Std. Error of the Estimate	Change Statistics	
					R Square Change	F Change
1	1.000[a]	1.000	.	.	1.000	.

Model Summary[b]

Model	Change Statistics		
	df1	df2	Sig. F Change
1	4	0	.

a. Predictors: (Constant), VPD (kPa), pF, Wind (Km/h), PPFD (µmol/m²/s)

b. Dependent Variable: Evapotranspiration (ml/m²/day)

ANOVA[a]

Model		Sum of Squares	df	Mean Square	F	Sig.
1	Regression	263317.938	4	65829.485	.	.[b]
	Residual	.000	0	.		
	Total	263317.938	4			

a. Dependent Variable: Evapotranspiration (ml/m²/day)

b. Predictors: (Constant), VPD (kPa), pF, Wind (Km/h), PPFD (µmol/m²/s)

Coefficients[a]

Model		Unstandardized Coefficients B	Unstandardized Coefficients Std. Error	Standardized Coefficients Beta	t	Sig.
1	(Constant)	206.762	.000		.	.
	pF	-93.604	.000	-.135	.	.
	PPFD (µmol/m²/s)	.036	.000	.848	.	.
	Wind (Km/h)	583.621	.000	.321	.	.
	VPD (kPa)	15.614	.000	.014	.	.

Coefficients[a]

Model		95.0% Confidence Interval for B Lower Bound	95.0% Confidence Interval for B Upper Bound
1	(Constant)	206.762	206.762
	pF	-93.604	-93.604
	PPFD (µmol/m²/s)	.036	.036
	Wind (Km/h)	583.621	583.621
	VPD (kPa)	15.614	15.614

a. Dependent Variable: Evapotranspiration (ml/m²/day)

Excluded Variables[a]

Model		Beta In	t	Sig.	Partial Correlation	Collinearity Statistics Tolerance
1	Temperature °C	.[b]	.	.	.	.000

a. Dependent Variable: Evapotranspiration (ml/m²/day)

b. Predictors in the Model: (Constant), VPD (kPa), pF, Wind (Km/h), PPFD (µmol/m²/s)

Residuals Statistics[a]

	Minimum	Maximum	Mean	Std. Deviation	N
Predicted Value	154.12	810.56	561.75	256.57	5
Residual	.00	.00	.00	.00	5
Std. Predicted Value	-1.589	.970	.000	1.000	5
Std. Residual	.	.	.	.	0

a. Dependent Variable: Evapotranspiration (ml/m²/day)

Regression of the energy driven phase of evapotranspiration for *Hedera hibernica*

Notes

Output Created		20-JAN-2025 11:25:25
Comments		
Input	Active Dataset	DataSet8
	Filter	<none>
	Weight	<none>
	Split File	<none>
	N of Rows in Working Data File	12
Missing Value Handling	Definition of Missing	User-defined missing values are treated as missing.
	Cases Used	Statistics are based on cases with no missing values for any variable used.
Syntax		REGRESSION /DESCRIPTIVES MEAN STDDEV CORR SIG N /MISSING LISTWISE /STATISTICS COEFF OUTS CI(95) R ANOVA CHANGE /CRITERIA=PIN(.05) POUT(.10) TOLERANCE(.0001) /NOORIGIN

		/DEPENDENT Hederahibernica /METHOD=ENTER pF PPFDµmolm²s WindKmh Temperature°C VPD /SCATTERPLOT=(*ZRESID ,*ZPRED) /RESIDUALS NORMPROB(ZRESID).
Resources	Processor Time	00:00:00.00
	Elapsed Time	00:00:00.02
	Memory Required	7680 bytes
	Additional Memory Required for Residual Plots	488 bytes

Warnings

For the final model with dependent variable Hedera hibernica, influence statistics cannot be computed because the fit is perfect.

The chart: *zresid by *zpred Scatterplot is not produced because it is empty.

Descriptive Statistics

	Mean	Std. Deviation	N
Hedera hibernica	699.015	370.990	5
pF	2.330	.286	5
PPFD µmol/m²/s	12489.28	5987.494	5
Wind (Km/h)	.205	.141	5
Temperature °C	21.583	2.471	5
VPD	.526	.235	5

Correlations

		Hedera hibernica	pF	PPFD µmol/m²/s	Wind (Km/h)
Pearson Correlation	Hedera hibernica	1.000	-.183	.978	.356
	pF	-.183	1.000	-.215	.539
	PPFD µmol/m²/s	.978	-.215	1.000	.383

	Wind (Km/h)	.356	.539	.383	1.000
	Temperature °C	.950	-.274	.957	.484
	VPD	.972	-.024	.956	.563
Sig. (1-tailed)	Hedera hibernica	.	.384	.002	.278
	pF	.384	.	.364	.174
	PPFD µmol/m²/s	.002	.364	.	.262
	Wind (Km/h)	.278	.174	.262	.
	Temperature °C	.007	.328	.005	.204
	VPD	.003	.485	.005	.161
N	Hedera hibernica	5	5	5	5
	pF	5	5	5	5
	PPFD µmol/m²/s	5	5	5	5
	Wind (Km/h)	5	5	5	5
	Temperature °C	5	5	5	5
	VPD	5	5	5	5

Correlations

		Temperature °C	VPD
Pearson Correlation	Hedera hibernica	.950	.972
	pF	-.274	-.024
	PPFD µmol/m²/s	.957	.956
	Wind (Km/h)	.484	.563
	Temperature °C	1.000	.959
	VPD	.959	1.000
Sig. (1-tailed)	Hedera hibernica	.007	.003
	pF	.328	.485
	PPFD µmol/m²/s	.005	.005
	Wind (Km/h)	.204	.161
	Temperature °C	.	.005
	VPD	.005	.
N	Hedera hibernica	5	5
	pF	5	5
	PPFD µmol/m²/s	5	5
	Wind (Km/h)	5	5
	Temperature °C	5	5
	VPD	5	5

Variables Entered/Removed[a]

Model	Variables Entered	Variables Removed	Method
1	VPD, pF, Wind (Km/h), PPFD µmol/m²/s[b]	.	Enter

a. Dependent Variable: Hedera hibernica

b. Tolerance = .000 limit reached.

Model Summary[b]

Model	R	R Square	Adjusted R Square	Std. Error of the Estimate	Change Statistics	
					R Square Change	F Change
1	1.000[a]	1.000	.	.	1.000	.

Model Summary[b]

Model	Change Statistics		
	df1	df2	Sig. F Change
1	4	0	.

a. Predictors: (Constant), VPD, pF, Wind (Km/h), PPFD µmol/m²/s

b. Dependent Variable: Hedera hibernica

ANOVA[a]

Model		Sum of Squares	df	Mean Square	F	Sig.
1	Regression	550533.257	4	137633.314	.	.[b]
	Residual	.000	0	.		
	Total	550533.257	4			

a. Dependent Variable: Hedera hibernica

b. Predictors: (Constant), VPD, pF, Wind (Km/h), PPFD µmol/m²/s

Coefficients[a]

Model		Unstandardized Coefficients B	Unstandardized Coefficients Std. Error	Standardized Coefficients Beta	t	Sig.
1	(Constant)	-101.891	.000		.	.
	pF	6.995	.000	.005	.	.
	PPFD µmol/m²/s	.007	.000	.108	.	.
	Wind (Km/h)	-685.578	.000	-.260	.	.
	VPD	1600.813	.000	1.016	.	.

Coefficients[a]

Model		95.0% Confidence Interval for B Lower Bound	95.0% Confidence Interval for B Upper Bound
1	(Constant)	-101.891	-101.891
	pF	6.995	6.995
	PPFD µmol/m²/s	.007	.007
	Wind (Km/h)	-685.578	-685.578
	VPD	1600.813	1600.813

a. Dependent Variable: Hedera hibernica

Excluded Variables[a]

Model		Beta In	t	Sig.	Partial Correlation	Collinearity Statistics Tolerance
1	Temperature °C	.[b]	.	.	.	.000

a. Dependent Variable: Hedera hibernica

b. Predictors in the Model: (Constant), VPD, pF, Wind (Km/h), PPFD µmol/m²/s

Residuals Statistics[a]

	Minimum	Maximum	Mean	Std. Deviation	N
Predicted Value	86.58	1039.60	699.01	370.99	5
Residual	.00	.00	.00	.00	5

Std. Predicted Value	-1.651	.918	.000	1.000	5
Std. Residual	.	.	.	.	0

a. Dependent Variable: Hedera hibernica

Regression of the energy driven phase of evapotranspiration for *H.colchica* "Russland"

Notes

Output Created		20-JAN-2025 11:36:45
Comments		
Input	Active Dataset	DataSet9
	Filter	<none>
	Weight	<none>
	Split File	<none>
	N of Rows in Working Data File	12
Missing Value Handling	Definition of Missing	User-defined missing values are treated as missing.
	Cases Used	Statistics are based on cases with no missing values for any variable used.
Syntax		REGRESSION /DESCRIPTIVES MEAN STDDEV CORR SIG N /MISSING LISTWISE /STATISTICS COEFF OUTS CI(95) R ANOVA CHANGE /CRITERIA=PIN(.05) POUT(.10) TOLERANCE(.0001) /NOORIGIN /DEPENDENT Evapotranspiration /METHOD=ENTER pF PPFDµmolm²s WindKmh Temperature°C VPD

		/SCATTERPLOT=(*ZRESID ,*ZPRED) /RESIDUALS NORMPROB(ZRESID).
Resources	Processor Time	00:00:00.00
	Elapsed Time	00:00:00.02
	Memory Required	7808 bytes
	Additional Memory Required for Residual Plots	488 bytes

Warnings

For the final model with dependent variable Evapotranspiration, influence statistics cannot be computed because the fit is perfect.

The chart: *zresid by *zpred Scatterplot is not produced because it is empty.

Descriptive Statistics

	Mean	Std. Deviation	N
Evapotranspiration	527.52	252.41	5
pF	2.2880	.24702	5
PPFD µmol/m²/s	12489.28	5987.494	5
Wind (Km/h)	.205	.141	5
Temperature °C	21.583	2.471	5
VPD	.526	.235	5

Correlations

		Evapotranspiration	pF	PPFD µmol/m²/s	Wind (Km/h)
Pearson Correlation	Evapotranspiration	1.000	-.149	.945	.293
	pF	-.149	1.000	-.187	.555
	PPFD µmol/m²/s	.945	-.187	1.000	.383
	Wind (Km/h)	.293	.555	.383	1.000
	Temperature °C	.921	-.238	.957	.484
	VPD	.952	.015	.956	.563
Sig. (1-tailed)	Evapotranspiration	.	.405	.008	.316
	pF	.405	.	.382	.166

	PPFD µmol/m²/s	.008	.382	.	.262
	Wind (Km/h)	.316	.166	.262	.
	Temperature °C	.013	.350	.005	.204
	VPD	.006	.491	.005	.161
N	Evapotranspiration	5	5	5	5
	pF	5	5	5	5
	PPFD µmol/m²/s	5	5	5	5
	Wind (Km/h)	5	5	5	5
	Temperature °C	5	5	5	5
	VPD	5	5	5	5

Correlations

		Temperature °C	VPD
Pearson Correlation	Evapotranspiration	.921	.952
	pF	-.238	.015
	PPFD µmol/m²/s	.957	.956
	Wind (Km/h)	.484	.563
	Temperature °C	1.000	.959
	VPD	.959	1.000
Sig. (1-tailed)	Evapotranspiration	.013	.006
	pF	.350	.491
	PPFD µmol/m²/s	.005	.005
	Wind (Km/h)	.204	.161
	Temperature °C	.	.005
	VPD	.005	.
N	Evapotranspiration	5	5
	pF	5	5
	PPFD µmol/m²/s	5	5
	Wind (Km/h)	5	5
	Temperature °C	5	5
	VPD	5	5

Variables Entered/Removed[a]

Model	Variables Entered	Variables Removed	Method
1	VPD, pF, Wind (Km/h), PPFD µmol/m²/s[b]	.	Enter

a. Dependent Variable: Evapotranspiration

b. Tolerance = .000 limit reached.

Model Summary[b]

Model	R	R Square	Adjusted R Square	Std. Error of the Estimate	Change Statistics	
					R Square Change	F Change
1	1.000[a]	1.000	.	.	1.000	.

Model Summary[b]

Model	Change Statistics		
	df1	df2	Sig. F Change
1	4	0	.

a. Predictors: (Constant), VPD, pF, Wind (Km/h), PPFD µmol/m²/s

b. Dependent Variable: Evapotranspiration

ANOVA[a]

Model		Sum of Squares	df	Mean Square	F	Sig.
1	Regression	254834.620	4	63708.655	.	.[b]
	Residual	.000	0	.		
	Total	254834.620	4			

a. Dependent Variable: Evapotranspiration

b. Predictors: (Constant), VPD, pF, Wind (Km/h), PPFD µmol/m²/s

Coefficients[a]

Model	Unstandardized Coefficients		Standardized Coefficients	t	Sig.
	B	Std. Error	Beta		

1	(Constant)	8.242	.000		.	.
	pF	.104	.000	.000	.	.
	PPFD µmol/m²/s	-.017	.000	-.400	.	.
	Wind (Km/h)	-799.090	.000	-.446	.	.
	VPD	1699.164	.000	1.585	.	.

Coefficients[a]

Model		95.0% Confidence Interval for B	
		Lower Bound	Upper Bound
1	(Constant)	8.242	8.242
	pF	.104	.104
	PPFD µmol/m²/s	-.017	-.017
	Wind (Km/h)	-799.090	-799.090
	VPD	1699.164	1699.164

a. Dependent Variable: Evapotranspiration

Excluded Variables[a]

Model		Beta In	t	Sig.	Partial Correlation	Collinearity Statistics Tolerance
1	Temperature °C	.[b]	.	.	.	.000

a. Dependent Variable: Evapotranspiration

b. Predictors in the Model: (Constant), VPD, pF, Wind (Km/h), PPFD µmol/m²/s

Residuals Statistics[a]

	Minimum	Maximum	Mean	Std. Deviation	N
Predicted Value	109.57	770.53	527.52	252.41	5
Residual	.00	.00	.00	.00	5
Std. Predicted Value	-1.656	.963	.000	1.000	5
Std. Residual	.	.	.	.	0

a. Dependent Variable: Evapotranspiration

Multiple Linear Regression Results of *L. henryi*

Notes

Output Created		20-JAN-2025 13:12:16
Comments		
Input	Active Dataset	DataSet11
	Filter	<none>
	Weight	<none>
	Split File	<none>
	N of Rows in Working Data File	17
Missing Value Handling	Definition of Missing	User-defined missing values are treated as missing.
	Cases Used	Statistics are based on cases with no missing values for any variable used.
Syntax		REGRESSION /DESCRIPTIVES MEAN STDDEV CORR SIG N /MISSING LISTWISE /STATISTICS COEFF OUTS CI(95) R ANOVA CHANGE /CRITERIA=PIN(.05) POUT(.10) TOLERANCE(.0001) /NOORIGIN /DEPENDENT Evapotranspiration /METHOD=ENTER pF PPFDμmolm²s WindKmh Temperature°C VPD /SCATTERPLOT=(*ZRESID ,*ZPRED) /RESIDUALS

		NORMPROB(ZRESID).
Resources	Processor Time	00:00:00.14
	Elapsed Time	00:00:00.27
	Memory Required	7728 bytes
	Additional Memory Required for Residual Plots	488 bytes

Descriptive Statistics

	Mean	Std. Deviation	N
Evapotranspiration	185.927	84.839	17
pF	2.316	.258	17
PPFD µmol/m²/s	11085.78	3853.758	17
Wind (Km/h)	.243	.240	17
Temperature °C	17.530	3.809	17
VPD	.430	.199	17

Correlations

		Evapotranspiration	pF	PPFD µmol/m²/s	Wind (Km/h)
Pearson Correlation	Evapotranspiration	1.000	-.287	.692	.186
	pF	-.287	1.000	-.247	.050
	PPFD µmol/m²/s	.692	-.247	1.000	.207
	Wind (Km/h)	.186	.050	.207	1.000
	Temperature °C	.776	-.351	.488	.110
	VPD	.855	.002	.759	.316
Sig. (1-tailed)	Evapotranspiration	.	.132	.001	.237
	pF	.132	.	.170	.424
	PPFD µmol/m²/s	.001	.170	.	.213
	Wind (Km/h)	.237	.424	.213	.
	Temperature °C	.000	.083	.023	.336
	VPD	.000	.497	.000	.108
N	Evapotranspiration	17	17	17	17
	pF	17	17	17	17
	PPFD µmol/m²/s	17	17	17	17
	Wind (Km/h)	17	17	17	17
	Temperature °C	17	17	17	17
	VPD	17	17	17	17

Correlations

		Temperature °C	VPD
Pearson Correlation	Evapotranspiration	.776	.855
	pF	-.351	.002
	PPFD µmol/m²/s	.488	.759
	Wind (Km/h)	.110	.316
	Temperature °C	1.000	.777
	VPD	.777	1.000
Sig. (1-tailed)	Evapotranspiration	<.001	<.001
	pF	.083	.497
	PPFD µmol/m²/s	.023	.000
	Wind (Km/h)	.336	.108
	Temperature °C	.	.000
	VPD	.000	.
N	Evapotranspiration	17	17
	pF	17	17
	PPFD µmol/m²/s	17	17
	Wind (Km/h)	17	17
	Temperature °C	17	17
	VPD	17	17

Variables Entered/Removed[a]

Model	Variables Entered	Variables Removed	Method
1	VPD, pF, Wind (Km/h), PPFD µmol/m²/s, Temperature °C[b]	.	Enter

a. Dependent Variable: Evapotranspiration

b. All requested variables entered.

Model Summary[b]

Model	R	R Square	Adjusted R Square	Std. Error of the Estimate	Change Statistics	
					R Square Change	F Change

1	.907[a]	.823	.742	43.087518621489110	.823	10.206

Model Summary[b]

Model	Change Statistics		
	df1	df2	Sig. F Change
1	5	11	<.001

a. Predictors: (Constant), VPD, pF, Wind (Km/h), PPFD µmol/m²/s, Temperature °C

b. Dependent Variable: Evapotranspiration

ANOVA[a]

Model		Sum of Squares	df	Mean Square	F	Sig.
1	Regression	94740.310	5	18948.062	10.206	<.001[b]
	Residual	20421.877	11	1856.534		
	Total	115162.187	16			

a. Dependent Variable: Evapotranspiration

b. Predictors: (Constant), VPD, pF, Wind (Km/h), PPFD µmol/m²/s, Temperature °C

Coefficients[a]

Model		Unstandardized Coefficients		Standardized Coefficients	t	Sig.
		B	Std. Error	Beta		
1	(Constant)	334.263	246.702		1.355	.203
	pF	-114.789	67.991	-.348	-1.688	.119
	PPFD µmol/m²/s	-.003	.006	-.130	-.480	.641
	Wind (Km/h)	-32.730	50.093	-.093	-.653	.527
	Temperature °C	-2.036	7.180	-.091	-.284	.782
	VPD	449.269	190.642	1.055	2.357	.038

Coefficients[a]

Model		95.0% Confidence Interval for B	
		Lower Bound	Upper Bound
1	(Constant)	-208.724	877.250
	pF	-264.435	34.858
	PPFD µmol/m²/s	-.016	.010
	Wind (Km/h)	-142.985	77.525
	Temperature °C	-17.838	13.766
	VPD	29.668	868.870

a. Dependent Variable: Evapotranspiration

Residuals Statistics[a]

	Minimum	Maximum	Mean	Std. Deviation	N
Predicted Value	91.123527526855470	310.759765625000000	185.927440406621600	76.949784854398440	17
Residual	-86.793395996093750	45.900993347167970	.000000000000061	35.726283103732690	17
Std. Predicted Value	-1.232	1.622	.000	1.000	17
Std. Residual	-2.014	1.065	.000	.829	17

a. Dependent Variable: Evapotranspiration

Charts

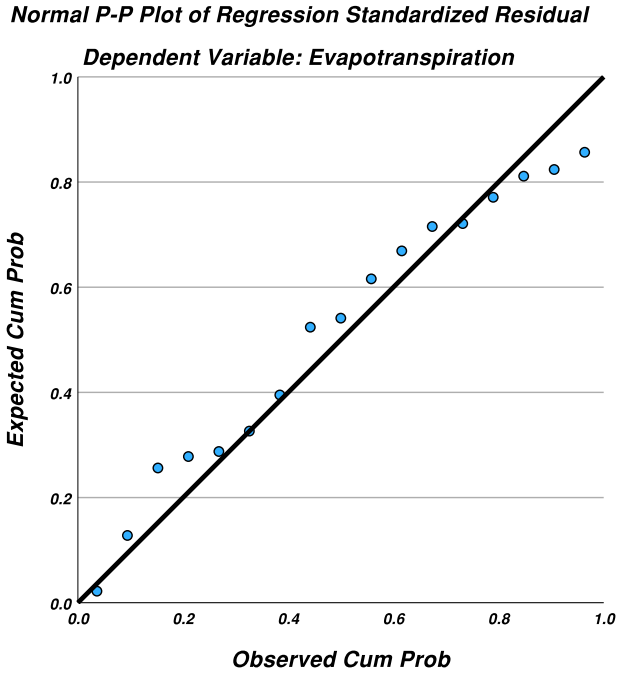
Normal P-P Plot of Regression Standardized Residual
Dependent Variable: Evapotranspiration
Expected Cum Prob
Observed Cum Prob
0.0
0.2
0.4
0.6
0.8
1.0

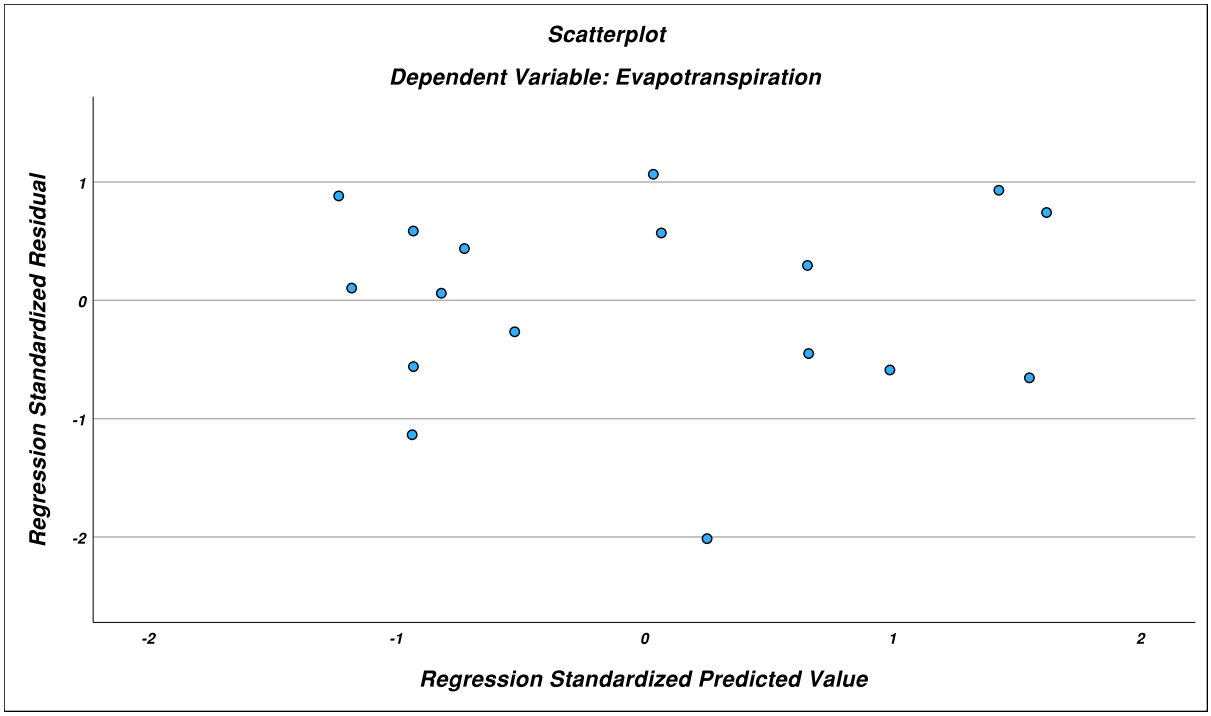
Scatterplot
Dependent Variable: Evapotranspiration
Regression Standardized Residual
Regression Standardized Predicted Value
-2
-1
0
1
2

Multiple Linear Regression of the water limiting phase of evapotranspiration for *H.helix* "Plattensee"

Notes

Output Created		20-JAN-2025 14:14:04
Comments		
Input	Active Dataset	DataSet12
	Filter	<none>
	Weight	<none>
	Split File	<none>
	N of Rows in Working Data File	12
Missing Value Handling	Definition of Missing	User-defined missing values are treated as missing.
	Cases Used	Statistics are based on cases with no missing values for any variable used.
Syntax		REGRESSION /DESCRIPTIVES MEAN STDDEV CORR SIG N /MISSING LISTWISE /STATISTICS COEFF OUTS CI(95) R ANOVA CHANGE /CRITERIA=PIN(.05) POUT(.10) TOLERANCE(.0001) /NOORIGIN /DEPENDENT Evapotranspirationmlm²day_A /METHOD=ENTER pF_A PPFDµmolm²s_A WindKmh_A Temperature°C_A

		VPDkPa_A /SCATTERPLOT=(*ZRESID ,*ZPRED) /RESIDUALS NORMPROB(ZRESID).
Resources	Processor Time	00:00:00.09
	Elapsed Time	00:00:00.26
	Memory Required	7808 bytes
	Additional Memory Required for Residual Plots	488 bytes

Descriptive Statistics

	Mean	Std. Deviation	N
Evapotranspiration (ml/m²/day)	151.00469556708052000	97.304145363588690	12
pF	3.2517	.17918	12
PPFD (µmol/m²/s)	10432.510250000001000	2683.732321366920600	12
Wind (Km/h)	.258163442601479	.275279061604170	12
Temperature °C	15.841171536211284	2.882010564556209	12
VPD (kPa)	.389488727090908	.177632752086677	12

Correlations

		Evapotranspiration (ml/m²/day)	pF	PPFD (µmol/m²/s)
Pearson Correlation	Evapotranspiration (ml/m²/day)	1.000	-.807	.023
	pF	-.807	1.000	.059
	PPFD (µmol/m²/s)	.023	.059	1.000
	Wind (Km/h)	.242	-.059	.262
	Temperature °C	-.439	.494	.207
	VPD (kPa)	-.400	.633	.563
Sig. (1-tailed)	Evapotranspiration (ml/m²/day)	.	<.001	.471
	pF	.001	.	.427

	PPFD (µmol/m²/s)	.471	.427	.
	Wind (Km/h)	.224	.428	.205
	Temperature °C	.077	.051	.259
	VPD (kPa)	.099	.014	.028
N	Evapotranspiration (ml/m²/day)	12	12	12
	pF	12	12	12
	PPFD (µmol/m²/s)	12	12	12
	Wind (Km/h)	12	12	12
	Temperature °C	12	12	12
	VPD (kPa)	12	12	12

Correlations

		Wind (Km/h)	Temperature °C	VPD (kPa)
Pearson Correlation	Evapotranspiration (ml/m²/day)	.242	-.439	-.400
	pF	-.059	.494	.633
	PPFD (µmol/m²/s)	.262	.207	.563
	Wind (Km/h)	1.000	.231	.358
	Temperature °C	.231	1.000	.787
	VPD (kPa)	.358	.787	1.000
Sig. (1-tailed)	Evapotranspiration (ml/m²/day)	.224	.077	.099
	pF	.428	.051	.014
	PPFD (µmol/m²/s)	.205	.259	.028
	Wind (Km/h)	.	.235	.127
	Temperature °C	.235	.	.001
	VPD (kPa)	.127	.001	.
N	Evapotranspiration (ml/m²/day)	12	12	12
	pF	12	12	12
	PPFD (µmol/m²/s)	12	12	12
	Wind (Km/h)	12	12	12
	Temperature °C	12	12	12
	VPD (kPa)	12	12	12

Variables Entered/Removed[a]

Model	Variables Entered	Variables Removed	Method
1	VPD (kPa), Wind (Km/h), PPFD (µmol/m²/s), pF, Temperature °C[b]	.	Enter

a. Dependent Variable: Evapotranspiration (ml/m²/day)

b. All requested variables entered.

Model Summary[b]

Model	R	R Square	Adjusted R Square	Std. Error of the Estimate	Change Statistics	
					R Square Change	F Change
1	.866[a]	.751	.543	65.781071330696560	.751	3.614

Model Summary[b]

Model	Change Statistics		
	df1	df2	Sig. F Change
1	5	6	.075

a. Predictors: (Constant), VPD (kPa), Wind (Km/h), PPFD (µmol/m²/s), pF, Temperature °C

b. Dependent Variable: Evapotranspiration (ml/m²/day)

ANOVA[a]

Model		Sum of Squares	df	Mean Square	F	Sig.
1	Regression	78186.168	5	15637.234	3.614	.075[b]
	Residual	25962.896	6	4327.149		

	Total	104149.064	11			

a. Dependent Variable: Evapotranspiration (ml/m²/day)

b. Predictors: (Constant), VPD (kPa), Wind (Km/h), PPFD (µmol/m²/s), pF, Temperature °C

Coefficients[a]

Model		Unstandardized Coefficients		Standardized Coefficients		
		B	Std. Error	Beta	t	Sig.
1	(Constant)	2097.028	690.193		3.038	.023
	pF	-541.423	187.924	-.997	-2.881	.028
	PPFD (µmol/m²/s)	-.009	.012	-.243	-.722	.498
	Wind (Km/h)	37.238	86.455	.105	.431	.682
	Temperature °C	-15.982	13.420	-.473	-1.191	.279
	VPD (kPa)	384.612	356.704	.702	1.078	.322

Coefficients[a]

Model		95.0% Confidence Interval for B	
		Lower Bound	Upper Bound
1	(Constant)	408.188	3785.869
	pF	-1001.256	-81.590
	PPFD (µmol/m²/s)	-.039	.021
	Wind (Km/h)	-174.310	248.787
	Temperature °C	-48.819	16.854
	VPD (kPa)	-488.212	1257.436

a. Dependent Variable: Evapotranspiration (ml/m²/day)

Residuals Statistics[a]

	Minimum	Maximum	Mean	Std. Deviation	N
Predicted Value	32.747951507568360	283.450653076171900	151.004695567080720	84.307967746954800	12

Residual	-84.174606323242190	73.209091186523440	-.000000000000180	48.582540889879716	12
Std. Predicted Value	-1.403	1.571	.000	1.000	12
Std. Residual	-1.280	1.113	.000	.739	12

a. Dependent Variable: Evapotranspiration (ml/m²/day)

Charts

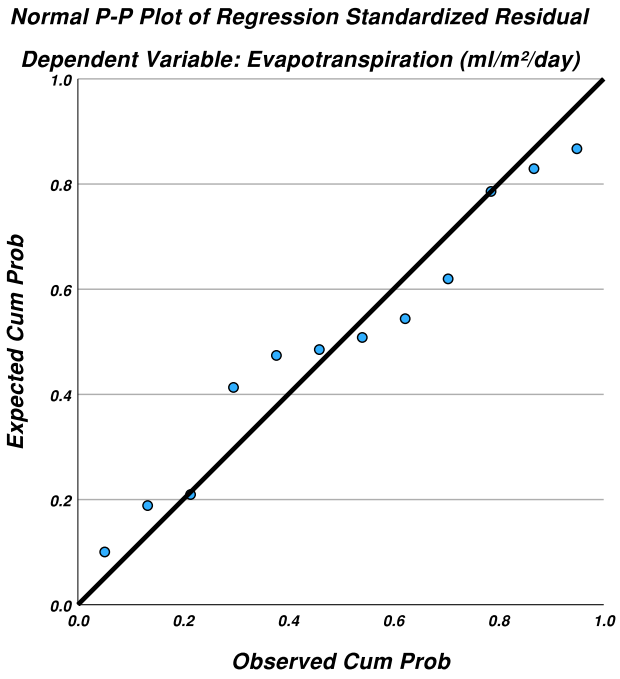

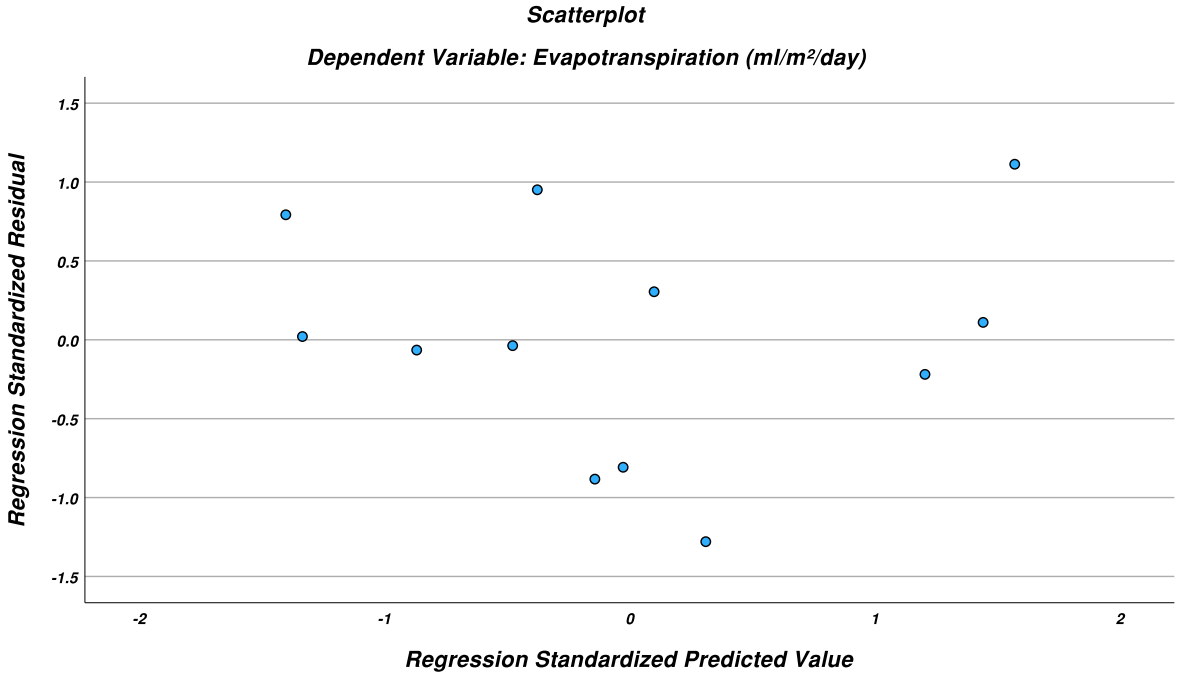

Regression of the water limiting phase of evapotranspiration for *H.hibernica*

Notes

Output Created		20-JAN-2025 14:19:23
Comments		
Input	Active Dataset	DataSet13
	Filter	<none>
	Weight	<none>
	Split File	<none>
	N of Rows in Working Data File	12
Missing Value Handling	Definition of Missing	User-defined missing values are treated as missing.
	Cases Used	Statistics are based on cases with no missing values for any variable used.

Syntax		REGRESSION /DESCRIPTIVES MEAN STDDEV CORR SIG N /MISSING LISTWISE /STATISTICS COEFF OUTS CI(95) R ANOVA CHANGE /CRITERIA=PIN(.05) POUT(.10) TOLERANCE(.0001) /NOORIGIN /DEPENDENT Hederahibernica_A /METHOD=ENTER pF_A PPFDµmolm²s_A WindKmh_A Temperature°C_A VPD_A /SCATTERPLOT=(*ZRESID ,*ZPRED) /RESIDUALS NORMPROB(ZRESID).
Resources	Processor Time	00:00:00.09
	Elapsed Time	00:00:00.17
	Memory Required	7680 bytes
	Additional Memory Required for Residual Plots	488 bytes

Descriptive Statistics

	Mean	Std. Deviation	N
Hedera hibernica	182.858141405191200	85.257231272467640	12
pF	3.1808	.21258	12
PPFD µmol/m²/s	10500.995000000000000	2701.349820194274000	12
Wind (Km/h)	.258163442601479	.275279061604170	12
Temperature °C	15.841171536211284	2.882010564556209	12

VPD	.389488727090908	.177632752086677	12

Correlations

		Hedera hibernica	pF	PPFD µmol/m²/s	Wind (Km/h)
Pearson Correlation	Hedera hibernica	1.000	-.636	-.084	.083
	pF	-.636	1.000	.028	-.099
	PPFD µmol/m²/s	-.084	.028	1.000	.262
	Wind (Km/h)	.083	-.099	.262	1.000
	Temperature °C	-.569	.540	.207	.231
	VPD	-.374	.627	.563	.358
Sig. (1-tailed)	Hedera hibernica	.	.013	.397	.399
	pF	.013	.	.465	.379
	PPFD µmol/m²/s	.397	.465	.	.205
	Wind (Km/h)	.399	.379	.205	.
	Temperature °C	.027	.035	.259	.235
	VPD	.115	.015	.028	.127
N	Hedera hibernica	12	12	12	12
	pF	12	12	12	12
	PPFD µmol/m²/s	12	12	12	12
	Wind (Km/h)	12	12	12	12
	Temperature °C	12	12	12	12
	VPD	12	12	12	12

Correlations

		Temperature °C	VPD
Pearson Correlation	Hedera hibernica	-.569	-.374
	pF	.540	.627
	PPFD µmol/m²/s	.207	.563
	Wind (Km/h)	.231	.358
	Temperature °C	1.000	.787
	VPD	.787	1.000
Sig. (1-tailed)	Hedera hibernica	.027	.115
	pF	.035	.015
	PPFD µmol/m²/s	.259	.028
	Wind (Km/h)	.235	.127
	Temperature °C	.	.001

	VPD	.001	.
N	Hedera hibernica	12	12
	pF	12	12
	PPFD µmol/m²/s	12	12
	Wind (Km/h)	12	12
	Temperature °C	12	12
	VPD	12	12

Variables Entered/Removed[a]

Model	Variables Entered	Variables Removed	Method
1	VPD, Wind (Km/h), PPFD µmol/m²/s, pF, Temperature °C[b]	.	Enter

a. Dependent Variable: Hedera hibernica

b. All requested variables entered.

Model Summary[b]

Model	R	R Square	Adjusted R Square	Std. Error of the Estimate	Change Statistics	
					R Square Change	F Change
1	.839[a]	.703	.456	62.881121819479170	.703	2.844

Model Summary[b]

Model	Change Statistics		
	df1	df2	Sig. F Change
1	5	6	.118

a. Predictors: (Constant), VPD, Wind (Km/h), PPFD µmol/m²/s, pF, Temperature °C

b. Dependent Variable: Hedera hibernica

ANOVA[a]

Model		Sum of Squares	df	Mean Square	F	Sig.
1	Regression	56232.537	5	11246.507	2.844	.118[b]
	Residual	23724.213	6	3954.035		
	Total	79956.750	11			

a. Dependent Variable: Hedera hibernica

b. Predictors: (Constant), VPD, Wind (Km/h), PPFD µmol/m²/s, pF, Temperature °C

Coefficients[a]

Model		Unstandardized Coefficients		Standardized Coefficients		
		B	Std. Error	Beta	t	Sig.
1	(Constant)	1858.282	556.315		3.340	.016
	pF	-395.223	154.643	-.985	-2.556	.043
	PPFD µmol/m²/s	-.020	.012	-.619	-1.686	.143
	Wind (Km/h)	-41.075	85.066	-.133	-.483	.646
	Temperature °C	-29.649	12.406	-1.002	-2.390	.054
	VPD	685.520	330.765	1.428	2.073	.084

Coefficients[a]

Model		95.0% Confidence Interval for B	
		Lower Bound	Upper Bound
1	(Constant)	497.029	3219.535
	pF	-773.622	-16.824
	PPFD µmol/m²/s	-.048	.009
	Wind (Km/h)	-249.223	167.074
	Temperature °C	-60.006	.707
	VPD	-123.833	1494.872

a. Dependent Variable: Hedera hibernica

Residuals Statistics[a]

	Minimum	Maximum	Mean	Std. Deviation	N
Predicted Value	90.700218200683600	300.411346435546900	182.858141405191670	71.498593399425730	12
Residual	-70.450355529785160	63.100105285644530	-.000000000000523	46.440786235276470	12
Std. Predicted Value	-1.289	1.644	.000	1.000	12
Std. Residual	-1.120	1.003	.000	.739	12

a. Dependent Variable: Hedera hibernica

Charts

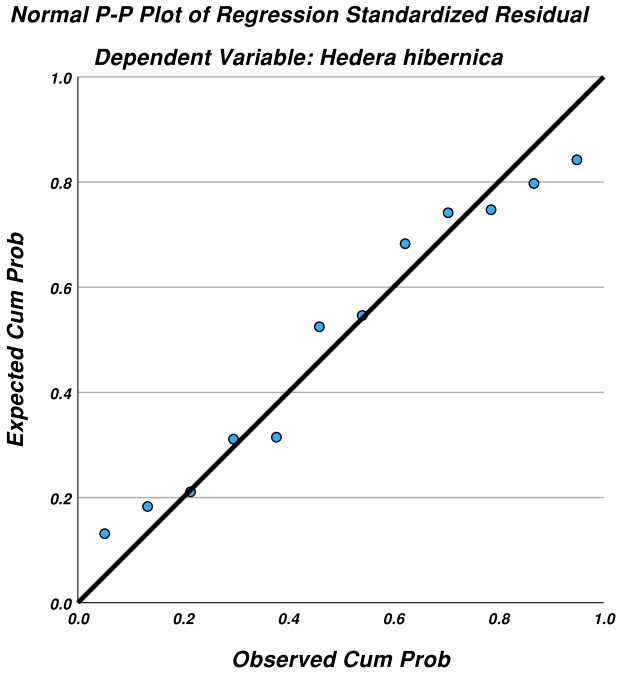
Normal P-P Plot of Regression Standardized Residual
Dependent Variable: Hedera hibernica
Expected Cum Prob
Observed Cum Prob
0.0
0.2
0.4
0.6
0.8
1.0

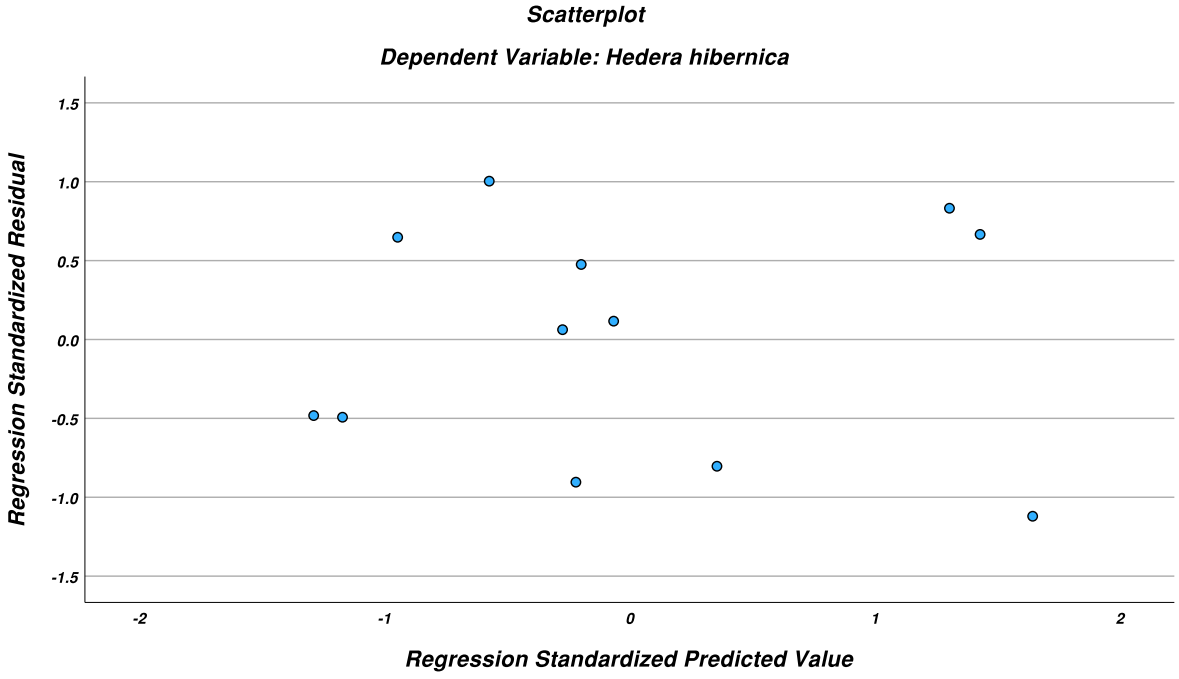
Scatterplot
Dependent Variable: Hedera hibernica
Regression Standardized Residual
Regression Standardized Predicted Value
1.5
1.0
0.5
0.0
-0.5
-1.0
-1.5
-2
-1
0
1
2

Regression of the water limiting phase of evapotranspiration for *H. colchica* "Russland"

Notes

Output Created		20-JAN-2025 14:25:03
Comments		
Input	Active Dataset	DataSet14
	Filter	<none>
	Weight	<none>
	Split File	<none>
	N of Rows in Working Data File	12
Missing Value Handling	Definition of Missing	User-defined missing values are treated as missing.
	Cases Used	Statistics are based on cases with no missing values for any variable used.
Syntax		REGRESSION /DESCRIPTIVES MEAN STDDEV CORR SIG N /MISSING LISTWISE /STATISTICS COEFF OUTS CI(95) R ANOVA CHANGE /CRITERIA=PIN(.05) POUT(.10) TOLERANCE(.0001) /NOORIGIN /DEPENDENT Evapotranspiration_A /METHOD=ENTER pF_A PPFDµmolm²s_A WindKmh_A Temperature°C_A VPD_A

		/SCATTERPLOT=(*ZRESID ,*ZPRED) /RESIDUALS NORMPROB(ZRESID).
Resources	Processor Time	00:00:00.08
	Elapsed Time	00:00:00.19
	Memory Required	7808 bytes
	Additional Memory Required for Residual Plots	488 bytes

Descriptive Statistics

	Mean	Std. Deviation	N
Evapotranspiration	171.95685894607678 0	105.12796512469058 0	12
pF	3.1558	.23091	12
PPFD µmol/m²/s	10500.995000000000 0	2701.349820194274000	12
Wind (Km/h)	.258163442601479	.275279061604170	12
Temperature °C	15.841171536211284	2.882010564556209	12
VPD	.389488727090908	.177632752086677	12

Correlations

		Evapotranspiration	pF	PPFD µmol/m²/s	Wind (Km/h)
Pearson Correlation	Evapotranspiration	1.000	-.842	.004	.076
	pF	-.842	1.000	.085	-.062
	PPFD µmol/m²/s	.004	.085	1.000	.262
	Wind (Km/h)	.076	-.062	.262	1.000
	Temperature °C	-.522	.562	.207	.231
	VPD	-.505	.639	.563	.358
Sig. (1-tailed)	Evapotranspiration	.	<.001	.495	.407
	pF	.000	.	.397	.424
	PPFD µmol/m²/s	.495	.397	.	.205
	Wind (Km/h)	.407	.424	.205	.
	Temperature °C	.041	.029	.259	.235

	VPD	.047	.013	.028	.127
N	Evapotranspiration	12	12	12	12
	pF	12	12	12	12
	PPFD µmol/m²/s	12	12	12	12
	Wind (Km/h)	12	12	12	12
	Temperature °C	12	12	12	12
	VPD	12	12	12	12

Correlations

		Temperature °C	VPD
Pearson Correlation	Evapotranspiration	-.522	-.505
	pF	.562	.639
	PPFD µmol/m²/s	.207	.563
	Wind (Km/h)	.231	.358
	Temperature °C	1.000	.787
	VPD	.787	1.000
Sig. (1-tailed)	Evapotranspiration	.041	.047
	pF	.029	.013
	PPFD µmol/m²/s	.259	.028
	Wind (Km/h)	.235	.127
	Temperature °C	.	.001
	VPD	.001	.
N	Evapotranspiration	12	12
	pF	12	12
	PPFD µmol/m²/s	12	12
	Wind (Km/h)	12	12
	Temperature °C	12	12
	VPD	12	12

Variables Entered/Removed[a]

Model	Variables Entered	Variables Removed	Method
1	VPD, Wind (Km/h), PPFD µmol/m²/s, pF, Temperature °C[b]	.	Enter

a. Dependent Variable: Evapotranspiration

b. All requested variables entered.

Model Summary[b]

Model	R	R Square	Adjusted R Square	Std. Error of the Estimate	Change Statistics	
					R Square Change	F Change
1	.851[a]	.724	.495	74.719200942420160	.724	3.155

Model Summary[b]

Model	Change Statistics		
	df1	df2	Sig. F Change
1	5	6	.097

a. Predictors: (Constant), VPD, Wind (Km/h), PPFD µmol/m²/s, pF, Temperature °C

b. Dependent Variable: Evapotranspiration

ANOVA[a]

Model		Sum of Squares	df	Mean Square	F	Sig.
1	Regression	88073.026	5	17614.605	3.155	.097[b]
	Residual	33497.754	6	5582.959		
	Total	121570.780	11			

a. Dependent Variable: Evapotranspiration

b. Predictors: (Constant), VPD, Wind (Km/h), PPFD µmol/m²/s, pF, Temperature °C

Coefficients[a]

Model	Unstandardized Coefficients		Standardized Coefficients	t	Sig.
	B	Std. Error	Beta		

1	(Constant)	1457.977	548.488		2.658	.038
	pF	-388.364	155.947	-.853	-2.490	.047
	PPFD µmol/m²/s	.001	.013	.014	.044	.966
	Wind (Km/h)	-.697	97.142	-.002	-.007	.995
	Temperature °C	-6.775	14.459	-.186	-.469	.656
	VPD	105.858	359.926	.179	.294	.779

Coefficients[a]

Model		95.0% Confidence Interval for B	
		Lower Bound	Upper Bound
1	(Constant)	115.874	2800.080
	pF	-769.953	-6.775
	PPFD µmol/m²/s	-.031	.032
	Wind (Km/h)	-238.395	237.002
	Temperature °C	-42.156	28.605
	VPD	-774.849	986.565

a. Dependent Variable: Evapotranspiration

Residuals Statistics[a]

	Minimum	Maximum	Mean	Std. Deviation	N
Predicted Value	44.656715393066406	308.020141601562500	171.956858946076860	89.479822828185040	12
Residual	-69.713035583496100	116.387458801269530	-.000000000000099	55.183787092721150	12
Std. Predicted Value	-1.423	1.521	.000	1.000	12
Std. Residual	-.933	1.558	.000	.739	12

a. Dependent Variable: Evapotranspiration

Charts

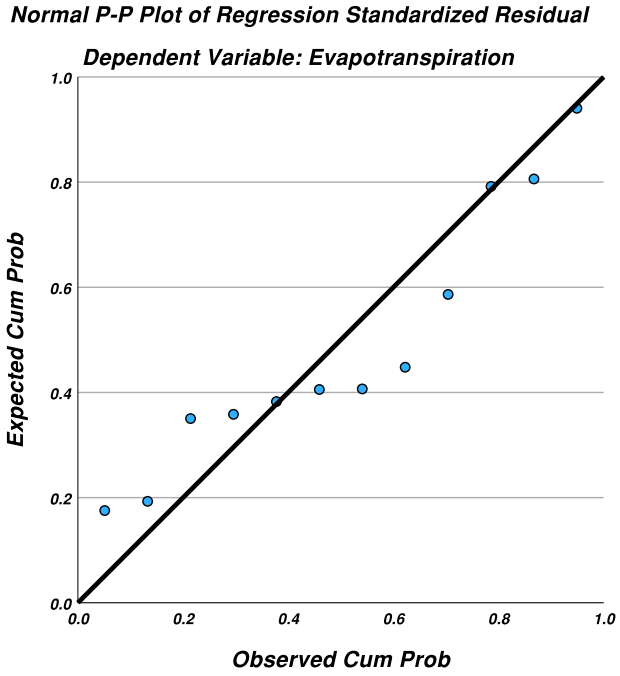
Normal P-P Plot of Regression Standardized Residual
Dependent Variable: Evapotranspiration
Expected Cum Prob
Observed Cum Prob
0.0
0.2
0.4
0.6
0.8
1.0

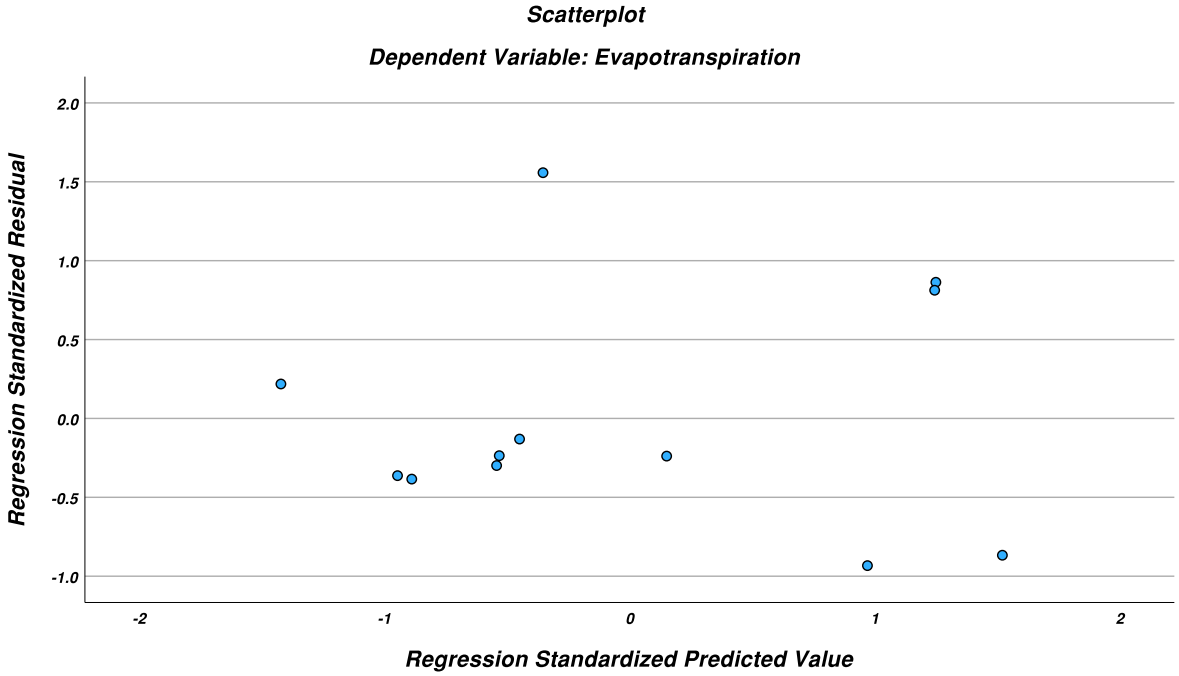
Scatterplot
Dependent Variable: Evapotranspiration
Regression Standardized Residual
Regression Standardized Predicted Value
2.0
1.5
1.0
0.5
0.0
-0.5
-1.0
-2
-1
0
1
2

Generalized Linear Models

Notes

Output Created		02-MAR-2025 08:57:50
Comments		
Input	Active Dataset	DataSet1
	Filter	<none>
	Weight	<none>
	Split File	<none>
	N of Rows in Working Data File	261
Missing Value Handling	Definition of Missing	User-defined missing values for factor, subject and within-subject variables are treated as missing.
	Cases Used	Statistics are based on cases with valid data for all variables in the model.
Weight Handling		not applicable
Syntax		GENLIN E_apparentmmolm²s BY Plantsspecies (ORDER=ASCENDING) WITH Qambµmolm²s /MODEL Plantsspecies Qambµmolm²s Plantsspecies*Qambµmolm²s INTERCEPT=YES DISTRIBUTION=NORMAL LINK=IDENTITY /CRITERIA SCALE=MLE COVB=MODEL PCONVERGE=1E-006(ABSOLUTE) SINGULAR=1E-012 ANALYSISTYPE=3(WAL

		D) CILEVEL=95 CITYPE=WALD LIKELIHOOD=FULL /EMMEANS TABLES=Plantsspecies SCALE=ORIGINAL /MISSING CLASSMISSING=EXCL UDE /PRINT CPS DESCRIPTIVES MODELINFO FIT SUMMARY SOLUTION.
Resources	Processor Time	00:00:00.05
	Elapsed Time	00:00:00.10

Model Information

Dependent Variable	E_apparent (mmol/m²/s)
Probability Distribution	Normal
Link Function	Identity

Case Processing Summary

	N	Percent
Included	261	100.0%
Excluded	0	0.0%
Total	261	100.0%

Categorical Variable Information

			N	Percent
Factor	Plants species	Clematis montana	30	11.5%
		H. hibernica	40	15.3%
		H.colchica"Russland"	38	14.6%
		H.Helix"Plattensee"	40	15.3%
		Lonicera henryi	38	14.6%
		P.tricuspidata	37	14.2%
		Wisteria sinensis	38	14.6%

	Total	261	100.0%

Continuous Variable Information

		N	Minimum	Maximum	Mean
Dependent Variable	E_apparent (mmol/m²/s)	261	.001543	7.832259	1.66128317
Covariate	Qamb (µmol/m²/s)	261	87	1638	897.48

Continuous Variable Information

		Std. Deviation
Dependent Variable	E_apparent (mmol/m²/s)	1.174211705
Covariate	Qamb (µmol/m²/s)	500.514

Goodness of Fit[a]

	Value	df	Value/df
Deviance	200.870	247	.813
Scaled Deviance	261.000	247	
Pearson Chi-Square	200.870	247	.813
Scaled Pearson Chi-Square	261.000	247	
Log Likelihood[b]	-336.170		
Akaike's Information Criterion (AIC)	702.340		
Finite Sample Corrected AIC (AICC)	704.300		
Bayesian Information Criterion (BIC)	755.808		
Consistent AIC (CAIC)	770.808		

Dependent Variable: E_apparent (mmol/m²/s)
Model: (Intercept), Plants species, Qamb (µmol/m²/s), Plants species * Qamb (µmol/m²/s)
[a]

a. Information criteria are in smaller-is-better form.

b. The full log likelihood function is displayed and used in computing information criteria.

Omnibus Test[a]

Likelihood Ratio Chi-Square	df	Sig.
151.175	13	<.001

Dependent Variable: E_apparent (mmol/m²/s)
Model: (Intercept), Plants species, Qamb (µmol/m²/s), Plants species * Qamb (µmol/m²/s)
[a]

a. Compares the fitted model against the intercept-only model.

Tests of Model Effects

Source	Type III Wald Chi-Square	df	Sig.
(Intercept)	66.896	1	<.001
Plants species	29.985	6	<.001
Qamb (µmol/m²/s)	16.870	1	<.001
Plants species * Qamb (µmol/m²/s)	1.957	6	.924

Dependent Variable: E_apparent (mmol/m²/s)
Model: (Intercept), Plants species, Qamb (µmol/m²/s), Plants species * Qamb (µmol/m²/s)

Parameter Estimates

Parameter	B	Std. Error	95% Wald Confidence Interval Lower	95% Wald Confidence Interval Upper	Hypothesis Test Wald Chi-Square
(Intercept)	.385	.2585	-.121	.892	2.222
[Plants species=Clematis montana]	.637	.7503	-.833	2.108	.721
[Plants species=H. hibernica]	1.401	.4307	.557	2.245	10.577

[Plants species=H.colchica"Russland"]	.933	.3948	.160	1.707	5.590
[Plants species=H.Helix"Plattensee"]	1.739	.3871	.981	2.498	20.188
[Plants species=Lonicera henryi]	.639	.3661	-.078	1.357	3.048
[Plants species=P.tricuspidata]	.106	.3734	-.626	.838	.081
[Plants species=Wisteria sinensis]	0[a]	.	.	.	.
Qamb (µmol/m²/s)	.000	.0003	.000	.001	.853
[Plants species=Clematis montana] * Qamb (µmol/m²/s)	.000	.0006	-.001	.001	.027
[Plants species=H. hibernica] * Qamb (µmol/m²/s)	.000	.0005	-.001	.001	.281
[Plants species=H.colchica"Russland"] * Qamb (µmol/m²/s)	.000	.0004	-.001	.001	.077
[Plants species=H.Helix"Plattensee"] * Qamb (µmol/m²/s)	.000	.0004	.000	.001	1.106
[Plants species=Lonicera henryi] * Qamb (µmol/m²/s)	.000	.0004	.000	.001	1.061
[Plants species=P.tricuspidata] * Qamb (µmol/m²/s)	.000	.0004	-.001	.001	.189
[Plants species=Wisteria sinensis] * Qamb (µmol/m²/s)	0[a]	.	.	.	.
(Scale)	.770[b]	.0674	.648	.914	

Parameter Estimates

	Hypothesis Test	
Parameter	df	Sig.

(Intercept)	1	.136
[Plants species=Clematis montana]	1	.396
[Plants species=H. hibernica]	1	.001
[Plants species=H.colchica"Russland"]	1	.018
[Plants species=H.Helix"Plattensee"]	1	<.001
[Plants species=Lonicera henryi]	1	.081
[Plants species=P.tricuspidata]	1	.776
[Plants species=Wisteria sinensis]	.	.
Qamb (µmol/m²/s)	1	.356
[Plants species=Clematis montana] * Qamb (µmol/m²/s)	1	.870
[Plants species=H. hibernica] * Qamb (µmol/m²/s)	1	.596
[Plants species=H.colchica"Russland"] * Qamb (µmol/m²/s)	1	.782
[Plants species=H.Helix"Plattensee"] * Qamb (µmol/m²/s)	1	.293
[Plants species=Lonicera henryi] * Qamb (µmol/m²/s)	1	.303
[Plants species=P.tricuspidata] * Qamb (µmol/m²/s)	1	.663
[Plants species=Wisteria sinensis] * Qamb (µmol/m²/s)	.	.
(Scale)		

Dependent Variable: E_apparent (mmol/m²/s)
Model: (Intercept), Plants species, Qamb (µmol/m²/s), Plants species * Qamb (µmol/m²/s)

a. Set to zero because this parameter is redundant.

b. Maximum likelihood estimate.

Estimated Marginal Means: Plants species

Estimates

Plants species	Mean	Std. Error	95% Wald Confidence Interval	
			Lower	Upper
Clematis montana	1.39	.260	.88	1.899
H. hibernica	2.28	.143	2.00	2.557
H.colchica"Russland"	1.70	.144	1.42	1.981
H.Helix"Plattensee"	2.81	.139	2.53	3.078
Lonicera henryi	1.71	.150	1.41	2.001
P.tricuspidata	.94	.147	.65	1.226
Wisteria sinensis	.66	.164	.34	.981

Covariates appearing in the model are fixed at the following values: Qamb (µmol/m²/s)=897.48

Generalized Linear Models

Notes

Output Created		02-MAR-2025 09:52:12
Comments		
Input	Active Dataset	DataSet1
	Filter	<none>
	Weight	<none>
	Split File	<none>
	N of Rows in Working Data File	261
Missing Value Handling	Definition of Missing	User-defined missing values for factor, subject and within-subject variables are treated as missing.
	Cases Used	Statistics are based on cases with valid data for all variables in the model.
Weight Handling		not applicable
Syntax		GENLIN gswmolm²s BY Plantsspecies (ORDER=ASCENDING) WITH Qambμmolm²s /MODEL Plantsspecies Qambμmolm²s Plantsspecies*Qambμmolm²s INTERCEPT=YES DISTRIBUTION=NORMAL LINK=IDENTITY /CRITERIA SCALE=MLE COVB=MODEL PCONVERGE=1E-006(ABSOLUTE) SINGULAR=1E-012 ANALYSISTYPE=3(WALD) CILEVEL=95 CITYPE=WALD LIKELIHOOD=FULL /EMMEANS SCALE=ORIGINAL /EMMEANS

		TABLES=Plantsspecies SCALE=ORIGINAL /MISSING CLASSMISSING=EXCLUDE /PRINT CPS DESCRIPTIVES MODELINFO FIT SUMMARY SOLUTION.
Resources	Processor Time	00:00:00.05
	Elapsed Time	00:00:00.06

Model Information

Dependent Variable	gsw (mol/m²/s)
Probability Distribution	Normal
Link Function	Identity

Case Processing Summary

	N	Percent
Included	261	100.0%
Excluded	0	0.0%
Total	261	100.0%

Categorical Variable Information

			N	Percent
Factor	Plants species	Clematis montana	30	11.5%
		H. hibernica	40	15.3%
		H.colchica"Russland"	38	14.6%
		H.Helix"Plattensee"	40	15.3%
		Lonicera henryi	38	14.6%
		P.tricuspidata	37	14.2%
		Wisteria sinensis	38	14.6%
		Total	261	100.0%

Continuous Variable Information

	N	Minimum	Maximum	Mean

Dependent Variable	gsw (mol/m²/s)	261	.000	.310	.054
Covariate	Qamb (µmol/m²/s)	261	87	1638	897.48

Continuous Variable Information

		Std. Deviation
Dependent Variable	gsw (mol/m²/s)	.0410
Covariate	Qamb (µmol/m²/s)	500.514

Goodness of Fit[a]

	Value	df	Value/df
Deviance	.236	247	.001
Scaled Deviance	261.000	247	
Pearson Chi-Square	.236	247	.001
Scaled Pearson Chi-Square	261.000	247	
Log Likelihood[b]	544.402		
Akaike's Information Criterion (AIC)	-1058.803		
Finite Sample Corrected AIC (AICC)	-1056.844		
Bayesian Information Criterion (BIC)	-1005.335		
Consistent AIC (CAIC)	-990.335		

Dependent Variable: gsw (mol/m²/s)
Model: (Intercept), Plants species, Qamb (µmol/m²/s), Plants species * Qamb (µmol/m²/s)
[a]

a. Information criteria are in smaller-is-better form.

b. The full log likelihood function is displayed and used in computing information criteria.

Omnibus Test[a]

Likelihood Ratio Chi-Square	df	Sig.
161.757	13	<.001

Dependent Variable: gsw (mol/m²/s)
Model: (Intercept), Plants species, Qamb (µmol/m²/s), Plants species * Qamb (µmol/m²/s)
[a]

a. Compares the fitted model against the intercept-only model.

Tests of Model Effects

Source	Type III Wald Chi-Square	df	Sig.
(Intercept)	81.452	1	<.001
Plants species	43.241	6	<.001
Qamb (µmol/m²/s)	5.209	1	.022
Plants species * Qamb (µmol/m²/s)	.990	6	.986

Dependent Variable: gsw (mol/m²/s)
Model: (Intercept), Plants species, Qamb (µmol/m²/s), Plants species * Qamb (µmol/m²/s)

Parameter Estimates

Parameter	B	Std. Error	95% Wald Confidence Interval Lower	95% Wald Confidence Interval Upper	Hypothesis Test Wald Chi-Square
(Intercept)	.014	.0089	-.004	.031	2.340
[Plants species=Clematis montana]	.023	.0257	-.028	.073	.785
[Plants species=H. hibernica]	.055	.0148	.026	.084	13.877
[Plants species=H.colchica"Russland"]	.031	.0135	.005	.058	5.409
[Plants species=H.Helix"Plattensee"]	.073	.0133	.047	.099	30.642

[Plants species=Lonicera henryi]	.027	.0125	.002	.051	4.526
[Plants species=P.tricuspidata]	.004	.0128	-.021	.029	.103
[Plants species=Wisteria sinensis]	0[a]	.	.	.	.
Qamb (µmol/m²/s)	6.896E-6	1.1343E-5	-1.534E-5	2.913E-5	.370
[Plants species=Clematis montana] * Qamb (µmol/m²/s)	-1.308E-6	2.1577E-5	-4.360E-5	4.098E-5	.004
[Plants species=H. hibernica] * Qamb (µmol/m²/s)	1.767E-6	1.5597E-5	-2.880E-5	3.234E-5	.013
[Plants species=H.colchica"Russland"] * Qamb (µmol/m²/s)	4.301E-7	1.4664E-5	-2.831E-5	2.917E-5	.001
[Plants species=H.Helix"Plattensee"] * Qamb (µmol/m²/s)	9.055E-6	1.4781E-5	-1.991E-5	3.802E-5	.375
[Plants species=Lonicera henryi] * Qamb (µmol/m²/s)	9.449E-6	1.5156E-5	-2.026E-5	3.915E-5	.389
[Plants species=P.tricuspidata] * Qamb (µmol/m²/s)	2.827E-6	1.5008E-5	-2.659E-5	3.224E-5	.035
[Plants species=Wisteria sinensis] * Qamb (µmol/m²/s)	0[a]	.	.	.	.
(Scale)	.001[b]	7.9066E-5	.001	.001	

Parameter Estimates

	Hypothesis Test	
Parameter	df	Sig.
(Intercept)	1	.126
[Plants species=Clematis montana]	1	.376
[Plants species=H. hibernica]	1	<.001

[Plants species=H.colchica"Russland"]	1	.020
[Plants species=H.Helix"Plattensee"]	1	<.001
[Plants species=Lonicera henryi]	1	.033
[Plants species=P.tricuspidata]	1	.748
[Plants species=Wisteria sinensis]	.	.
Qamb (µmol/m²/s)	1	.543
[Plants species=Clematis montana] * Qamb (µmol/m²/s)	1	.952
[Plants species=H. hibernica] * Qamb (µmol/m²/s)	1	.910
[Plants species=H.colchica"Russland"] * Qamb (µmol/m²/s)	1	.977
[Plants species=H.Helix"Plattensee"] * Qamb (µmol/m²/s)	1	.540
[Plants species=Lonicera henryi] * Qamb (µmol/m²/s)	1	.533
[Plants species=P.tricuspidata] * Qamb (µmol/m²/s)	1	.851
[Plants species=Wisteria sinensis] * Qamb (µmol/m²/s)	.	.
(Scale)		

Dependent Variable: gsw (mol/m²/s)
Model: (Intercept), Plants species, Qamb (µmol/m²/s), Plants species * Qamb (µmol/m²/s)

a. Set to zero because this parameter is redundant.

b. Maximum likelihood estimate.

Estimated Marginal Means 1: Grand Mean

Estimates

		95% Wald Confidence Interval	
Mean	Std. Error	Lower	Upper
.05306691	.002183410	.04878751	.05734632

Covariates appearing in the model are fixed at the following values: Qamb (µmol/m²/s)=897.48

Estimated Marginal Means 2: Plants species

Estimates

			95% Wald Confidence Interval	
Plants species	Mean	Std. Error	Lower	Upper
Clematis montana	.041	.0089	.024	.059
H. hibernica	.076	.0049	.067	.086
H.colchica"Russland"	.052	.0049	.042	.061
H.Helix"Plattensee"	.101	.0048	.092	.111
Lonicera henryi	.055	.0051	.045	.065
P.tricuspidata	.026	.0050	.016	.036
Wisteria sinensis	.020	.0056	.009	.031

Covariates appearing in the model are fixed at the following values: Qamb (µmol/m²/s)=897.48

Generalized Linear Models

Notes

Output Created		02-MAR-2025 09:55:18
Comments		
Input	Active Dataset	DataSet1
	Filter	<none>
	Weight	<none>
	Split File	<none>
	N of Rows in Working Data File	261
Missing Value Handling	Definition of Missing	User-defined missing values for factor, subject and within-subject variables are treated as missing.
	Cases Used	Statistics are based on cases with valid data for all variables in the model.
Weight Handling		not applicable
Syntax		GENLIN VPDleafkpa BY Plantsspecies (ORDER=ASCENDING) WITH Qambµmolm²s /MODEL Plantsspecies Qambµmolm²s Plantsspecies*Qambµmolm²s INTERCEPT=YES DISTRIBUTION=NORMAL LINK=IDENTITY /CRITERIA SCALE=MLE COVB=MODEL PCONVERGE=1E-006(ABSOLUTE)

		SINGULAR=1E-012 ANALYSISTYPE=3(WALD) CILEVEL=95 CITYPE=WALD LIKELIHOOD=FULL /EMMEANS SCALE=ORIGINAL /EMMEANS TABLES=Plantsspecies SCALE=ORIGINAL /MISSING CLASSMISSING=EXCLUDE /PRINT CPS DESCRIPTIVES MODELINFO FIT SUMMARY SOLUTION.
Resources	Processor Time	00:00:00.05
	Elapsed Time	00:00:00.06

Model Information

Dependent Variable	VPDleaf (kpa)
Probability Distribution	Normal
Link Function	Identity

Case Processing Summary

	N	Percent
Included	261	100.0%
Excluded	0	0.0%
Total	261	100.0%

Categorical Variable Information

			N	Percent
Factor	Plants species	Clematis montana	30	11.5%
		H. hibernica	40	15.3%
		H.colchica"Russland"	38	14.6%

	H.Helix"Plattensee"	40	15.3%
	Lonicera henryi	38	14.6%
	P.tricuspidata	37	14.2%
	Wisteria sinensis	38	14.6%
	Total	261	100.0%

Continuous Variable Information

		N	Minimum	Maximum	Mean
Dependent Variable	VPDleaf (kpa)	261	2.373867	4.703256	3.19874924
Covariate	Qamb (µmol/m²/s)	261	87	1638	897.48

Continuous Variable Information

		Std. Deviation
Dependent Variable	VPDleaf (kpa)	.475947259
Covariate	Qamb (µmol/m²/s)	500.514

Goodness of Fit[a]

	Value	df	Value/df
Deviance	31.380	247	.127
Scaled Deviance	261.000	247	
Pearson Chi-Square	31.380	247	.127
Scaled Pearson Chi-Square	261.000	247	
Log Likelihood[b]	-93.900		
Akaike's Information Criterion (AIC)	217.801		
Finite Sample Corrected AIC (AICC)	219.760		
Bayesian Information Criterion (BIC)	271.269		
Consistent AIC (CAIC)	286.269		

Dependent Variable: VPDleaf (kpa)
Model: (Intercept), Plants species, Qamb (µmol/m²/s), Plants species * Qamb (µmol/m²/s)
[a]

a. Information criteria are in smaller-is-better form.

b. The full log likelihood function is displayed and used in computing information criteria.

Omnibus Test[a]

Likelihood Ratio Chi-Square	df	Sig.
164.325	13	<.001

Dependent Variable: VPDleaf (kpa)
Model: (Intercept), Plants species, Qamb (µmol/m²/s), Plants species * Qamb (µmol/m²/s)
[a]

a. Compares the fitted model against the intercept-only model.

Tests of Model Effects

Source	Type III Wald Chi-Square	df	Sig.
(Intercept)	2440.079	1	<.001
Plants species	14.294	6	.027
Qamb (µmol/m²/s)	88.304	1	<.001
Plants species * Qamb (µmol/m²/s)	6.248	6	.396

Dependent Variable: VPDleaf (kpa)
Model: (Intercept), Plants species, Qamb (µmol/m²/s), Plants species * Qamb (µmol/m²/s)

Parameter Estimates

Parameter	B	Std. Error	95% Wald Confidence Interval Lower	95% Wald Confidence Interval Upper	Hypothesis Test Wald Chi-Square
(Intercept)	2.958	.1022	2.758	3.159	838.539
[Plants species=Clematis montana]	-.042	.2966	-.623	.539	.020

[Plants species=H. hibernica]	-.263	.1702	-.597	.070	2.392
[Plants species=H.colchica"Russland"]	-.071	.1560	-.376	.235	.205
[Plants species=H.Helix"Plattensee"]	-.484	.1530	-.784	-.184	10.004
[Plants species=Lonicera henryi]	-.312	.1447	-.595	-.028	4.638
[Plants species=P.tricuspidata]	-.075	.1476	-.364	.215	.256
[Plants species=Wisteria sinensis]	0[a]	.	.	.	.
Qamb (µmol/m²/s)	.000	.0001	8.720E-5	.001	6.897
[Plants species=Clematis montana] * Qamb (µmol/m²/s)	.000	.0002	.000	.001	.640
[Plants species=H. hibernica] * Qamb (µmol/m²/s)	2.506E-5	.0002	.000	.000	.019
[Plants species=H.colchica"Russland"] * Qamb (µmol/m²/s)	9.822E-5	.0002	.000	.000	.337
[Plants species=H.Helix"Plattensee"] * Qamb (µmol/m²/s)	6.492E-5	.0002	.000	.000	.145
[Plants species=Lonicera henryi] * Qamb (µmol/m²/s)	.000	.0002	.000	.001	1.503
[Plants species=P.tricuspidata] * Qamb (µmol/m²/s)	.000	.0002	1.737E-6	.001	3.881
[Plants species=Wisteria sinensis] * Qamb (µmol/m²/s)	0[a]	.	.	.	.
(Scale)	.120[b]	.0105	.101	.143	

Parameter Estimates

Hypothesis Test

Parameter	df	Sig.
(Intercept)	1	<.001
[Plants species=Clematis montana]	1	.888
[Plants species=H. hibernica]	1	.122
[Plants species=H.colchica"Russland"]	1	.651
[Plants species=H.Helix"Plattensee"]	1	.002
[Plants species=Lonicera henryi]	1	.031
[Plants species=P.tricuspidata]	1	.613
[Plants species=Wisteria sinensis]	.	.
Qamb (µmol/m²/s)	1	.009
[Plants species=Clematis montana] * Qamb (µmol/m²/s)	1	.424
[Plants species=H. hibernica] * Qamb (µmol/m²/s)	1	.889
[Plants species=H.colchica"Russland"] * Qamb (µmol/m²/s)	1	.562
[Plants species=H.Helix"Plattensee"] * Qamb (µmol/m²/s)	1	.703
[Plants species=Lonicera henryi] * Qamb (µmol/m²/s)	1	.220
[Plants species=P.tricuspidata] * Qamb (µmol/m²/s)	1	.049

[Plants species=Wisteria sinensis] * Qamb (µmol/m²/s) (Scale)	.	.

Dependent Variable: VPDleaf (kpa)
Model: (Intercept), Plants species, Qamb (µmol/m²/s), Plants species * Qamb (µmol/m²/s)

a. Set to zero because this parameter is redundant.

b. Maximum likelihood estimate.

Estimated Marginal Means 1: Grand Mean

Estimates

		95% Wald Confidence Interval	
Mean	Std. Error	Lower	Upper
3.20967322	.025191060	3.16029965	3.25904679

Covariates appearing in the model are fixed at the following values: Qamb (µmol/m²/s)=897.48

Estimated Marginal Means 2: Plants species

Estimates

Plants species	Mean	Std. Error	95% Wald Confidence Interval	
			Lower	Upper
Clematis montana	3.40	.103	3.20	3.61
H. hibernica	3.03	.057	2.92	3.14
H.colchica"Russland"	3.28	.057	3.17	3.40
H.Helix"Plattensee"	2.84	.055	2.73	2.95
Lonicera henryi	3.15	.059	3.03	3.26
P.tricuspidata	3.50	.058	3.38	3.61
Wisteria sinensis	3.27	.065	3.14	3.39

Covariates appearing in the model are fixed at the following values: Qamb (µmol/m²/s)=897.48

Generalized Linear Models

Notes

Output Created		02-MAR-2025 09:56:55
Comments		
Input	Active Dataset	DataSet1
	Filter	<none>
	Weight	<none>
	Split File	<none>
	N of Rows in Working Data File	261
Missing Value Handling	Definition of Missing	User-defined missing values for factor, subject and within-subject variables are treated as missing.
	Cases Used	Statistics are based on cases with valid data for all variables in the model.
Weight Handling		not applicable
Syntax		GENLIN PhiPS2 BY Plantsspecies (ORDER=ASCENDING) WITH Qambµmolm²s

		/MODEL Plantsspecies Qambμmolm²s Plantsspecies*Qambμmol m²s INTERCEPT=YES DISTRIBUTION=NORM AL LINK=IDENTITY /CRITERIA SCALE=MLE COVB=MODEL PCONVERGE=1E-006(ABSOLUTE) SINGULAR=1E-012 ANALYSISTYPE=3(WAL D) CILEVEL=95 CITYPE=WALD LIKELIHOOD=FULL /EMMEANS SCALE=ORIGINAL /EMMEANS TABLES=Plantsspecies SCALE=ORIGINAL /MISSING CLASSMISSING=EXCL UDE /PRINT CPS DESCRIPTIVES MODELINFO FIT SUMMARY SOLUTION.
Resources	Processor Time	00:00:00.06
	Elapsed Time	00:00:00.06

Model Information

Dependent Variable	PhiPS2
Probability Distribution	Normal
Link Function	Identity

Case Processing Summary

	N	Percent

Included	261	100.0%
Excluded	0	0.0%
Total	261	100.0%

Categorical Variable Information

			N	Percent
Factor	Plants species	Clematis montana	30	11.5%
		H. hibernica	40	15.3%
		H.colchica"Russland"	38	14.6%
		H.Helix"Plattensee"	40	15.3%
		Lonicera henryi	38	14.6%
		P.tricuspidata	37	14.2%
		Wisteria sinensis	38	14.6%
		Total	261	100.0%

Continuous Variable Information

		N	Minimum	Maximum	Mean
Dependent Variable	PhiPS2	261	.07	.78	.45
Covariate	Qamb (µmol/m²/s)	261	87	1638	897.48

Continuous Variable Information

		Std. Deviation
Dependent Variable	PhiPS2	.204
Covariate	Qamb (µmol/m²/s)	500.514

Goodness of Fit[a]

	Value	df	Value/df
Deviance	6.587	247	.027
Scaled Deviance	261.000	247	
Pearson Chi-Square	6.587	247	.027
Scaled Pearson Chi-Square	261.000	247	
Log Likelihood[b]	109.815		
Akaike's Information Criterion (AIC)	-189.631		
Finite Sample Corrected AIC (AICC)	-187.671		

Bayesian Information Criterion (BIC)	-136.163		
Consistent AIC (CAIC)	-121.163		

Dependent Variable: PhiPS2
Model: (Intercept), Plants species, Qamb (µmol/m²/s), Plants species * Qamb (µmol/m²/s)
[a]

a. Information criteria are in smaller-is-better form.

b. The full log likelihood function is displayed and used in computing information criteria.

Omnibus Test[a]

Likelihood Ratio Chi-Square	df	Sig.
130.483	13	<.001

Dependent Variable: PhiPS2
Model: (Intercept), Plants species, Qamb (µmol/m²/s), Plants species * Qamb (µmol/m²/s)
[a]

a. Compares the fitted model against the intercept-only model.

Tests of Model Effects

	Type III		
Source	Wald Chi-Square	df	Sig.
(Intercept)	580.777	1	<.001
Plants species	11.650	6	.070
Qamb (µmol/m²/s)	74.481	1	<.001
Plants species * Qamb (µmol/m²/s)	14.322	6	.026

Dependent Variable: PhiPS2
Model: (Intercept), Plants species, Qamb (µmol/m²/s), Plants species * Qamb (µmol/m²/s)

Parameter Estimates

Parameter	B	Std. Error	95% Wald Confidence Interval		Hypothesis Test Wald Chi-Square
			Lower	Upper	
(Intercept)	.591	.0468	.499	.683	159.396
[Plants species=Clematis montana]	-.152	.1359	-.419	.114	1.259
[Plants species=H. hibernica]	-.052	.0780	-.204	.101	.436
[Plants species=H.colchica"Russland"]	.079	.0715	-.061	.219	1.213
[Plants species=H.Helix"Plattensee"]	.147	.0701	.010	.285	4.409
[Plants species=Lonicera henryi]	.093	.0663	-.037	.223	1.964
[Plants species=P.tricuspidata]	.099	.0676	-.034	.231	2.138
[Plants species=Wisteria sinensis]	0[a]	.	.	.	.
Qamb (µmol/m²/s)	.000	5.9960E-5	.000	-3.604E-5	6.559
[Plants species=Clematis montana] * Qamb (µmol/m²/s)	4.696E-5	.0001	.000	.000	.170
[Plants species=H. hibernica] * Qamb (µmol/m²/s)	6.423E-5	8.2449E-5	-9.737E-5	.000	.607
[Plants species=H.colchica"Russland"] * Qamb (µmol/m²/s)	.000	7.7513E-5	.000	4.046E-5	2.068
[Plants species=H.Helix"Plattensee"] * Qamb (µmol/m²/s)	-9.207E-5	7.8133E-5	.000	6.107E-5	1.388
[Plants species=Lonicera henryi] * Qamb (µmol/m²/s)	-5.621E-5	8.0116E-5	.000	.000	.492
[Plants species=P.tricuspidata] * Qamb (µmol/m²/s)	.000	7.9335E-5	.000	-3.010E-5	5.472

[Plants species=Wisteria sinensis] * Qamb (µmol/m²/s)	0[a]	.	.	.	.
(Scale)	.025[b]	.0022	.021	.030	

Parameter Estimates

	Hypothesis Test	
Parameter	df	Sig.
(Intercept)	1	<.001
[Plants species=Clematis montana]	1	.262
[Plants species=H. hibernica]	1	.509
[Plants species=H.colchica"Russland"]	1	.271
[Plants species=H.Helix"Plattensee"]	1	.036
[Plants species=Lonicera henryi]	1	.161
[Plants species=P.tricuspidata]	1	.144
[Plants species=Wisteria sinensis]	.	.
Qamb (µmol/m²/s)	1	.010
[Plants species=Clematis montana] * Qamb (µmol/m²/s)	1	.681
[Plants species=H. hibernica] * Qamb (µmol/m²/s)	1	.436
[Plants species=H.colchica"Russland"] * Qamb (µmol/m²/s)	1	.150
[Plants species=H.Helix"Plattensee"] * Qamb (µmol/m²/s)	1	.239

[Plants species=Lonicera henryi] * Qamb (µmol/m²/s)	1	.483
[Plants species=P.tricuspidata] * Qamb (µmol/m²/s)	1	.019
[Plants species=Wisteria sinensis] * Qamb (µmol/m²/s)	.	.
(Scale)		

Dependent Variable: PhiPS2
Model: (Intercept), Plants species, Qamb (µmol/m²/s), Plants species * Qamb (µmol/m²/s)

a. Set to zero because this parameter is redundant.

b. Maximum likelihood estimate.

Estimated Marginal Means 1: Grand Mean

Estimates

		95% Wald Confidence Interval	
Mean	Std. Error	Lower	Upper
.44082092	.011541733	.41819954	.46344231

Covariates appearing in the model are fixed at the following values: Qamb (µmol/m²/s)=897.48

Estimated Marginal Means 2: Plants species

Estimates

Plants species	Mean	Std. Error	95% Wald Confidence Interval	
			Lower	Upper
Clematis montana	.343	.0471	.250	.435
H. hibernica	.459	.0259	.408	.510
H.colchica"Russland"	.432	.0260	.381	.483
H.Helix"Plattensee"	.518	.0251	.468	.567
Lonicera henryi	.496	.0271	.442	.549
P.tricuspidata	.385	.0267	.333	.438
Wisteria sinensis	.453	.0297	.395	.511

Covariates appearing in the model are fixed at the following values: Qamb (µmol/m²/s)=897.48

Generalized Linear Models

Notes

Output Created		02-MAR-2025 09:58:42
Comments		
Input	Active Dataset	DataSet1
	Filter	<none>
	Weight	<none>
	Split File	<none>
	N of Rows in Working Data File	261
Missing Value Handling	Definition of Missing	User-defined missing values for factor, subject and within-subject variables are treated as missing.

	Cases Used	Statistics are based on cases with valid data for all variables in the model.
Weight Handling		not applicable
Syntax		GENLIN ETRµmolm²s BY Plantsspecies (ORDER=ASCENDING) WITH Qambµmolm²s /MODEL Plantsspecies Qambµmolm²s Plantsspecies*Qambµmolm²s INTERCEPT=YES DISTRIBUTION=NORMAL LINK=IDENTITY /CRITERIA SCALE=MLE COVB=MODEL PCONVERGE=1E-006(ABSOLUTE) SINGULAR=1E-012 ANALYSISTYPE=3(WALD) CILEVEL=95 CITYPE=WALD LIKELIHOOD=FULL /EMMEANS SCALE=ORIGINAL /EMMEANS TABLES=Plantsspecies SCALE=ORIGINAL /MISSING CLASSMISSING=EXCLUDE /PRINT CPS DESCRIPTIVES MODELINFO FIT SUMMARY SOLUTION.
Resources	Processor Time	00:00:00.06
	Elapsed Time	00:00:00.06

Model Information

Dependent Variable	ETR (µmol/m²/s)
Probability Distribution	Normal
Link Function	Identity

Case Processing Summary

	N	Percent
Included	261	100.0%
Excluded	0	0.0%
Total	261	100.0%

Categorical Variable Information

			N	Percent
Factor	Plants species	Clematis montana	30	11.5%
		H. hibernica	40	15.3%
		H.colchica"Russland"	38	14.6%
		H.Helix"Plattensee"	40	15.3%
		Lonicera henryi	38	14.6%
		P.tricuspidata	37	14.2%
		Wisteria sinensis	38	14.6%
		Total	261	100.0%

Continuous Variable Information

		N	Minimum	Maximum	Mean
Dependent Variable	ETR (µmol/m²/s)	261	10.820	436	138.98
Covariate	Qamb (µmol/m²/s)	261	87	1638	897.48

Continuous Variable Information

		Std. Deviation
Dependent Variable	ETR (µmol/m²/s)	93.229
Covariate	Qamb (µmol/m²/s)	500.514

Goodness of Fit[a]

	Value	df	Value/df
Deviance	1214699.303	247	4917.811
Scaled Deviance	261.000	247	

Pearson Chi-Square	1214699.303	247	4917.811
Scaled Pearson Chi-Square	261.000	247	
Log Likelihood[b]	-1472.479		
Akaike's Information Criterion (AIC)	2974.958		
Finite Sample Corrected AIC (AICC)	2976.917		
Bayesian Information Criterion (BIC)	3028.426		
Consistent AIC (CAIC)	3043.426		

Dependent Variable: ETR (µmol/m²/s)
Model: (Intercept), Plants species, Qamb (µmol/m²/s), Plants species * Qamb (µmol/m²/s)
[a]

a. Information criteria are in smaller-is-better form.

b. The full log likelihood function is displayed and used in computing information criteria.

Omnibus Test[a]

Likelihood Ratio Chi-Square	df	Sig.
162.027	13	<.001

Dependent Variable: ETR (µmol/m²/s)
Model: (Intercept), Plants species, Qamb (µmol/m²/s), Plants species * Qamb (µmol/m²/s)
[a]

a. Compares the fitted model against the intercept-only model.

Tests of Model Effects

Source	Type III Wald Chi-Square	df	Sig.
(Intercept)	8.496	1	.004
Plants species	1.341	6	.969

Qamb (µmol/m²/s)	143.202	1	<.001
Plants species * Qamb (µmol/m²/s)	13.133	6	.041

Dependent Variable: ETR (µmol/m²/s)
Model: (Intercept), Plants species, Qamb (µmol/m²/s), Plants species * Qamb (µmol/m²/s)

Parameter Estimates

Parameter	B	Std. Error	95% Wald Confidence Interval		Hypothesis Test Wald Chi-Square
			Lower	Upper	
(Intercept)	19.349	20.0998	-20.046	58.744	.927
[Plants species=Clematis montana]	20.406	58.3488	-93.955	134.768	.122
[Plants species=H. hibernica]	-3.878	33.4950	-69.527	61.771	.013
[Plants species=H.colchica"Russland"]	24.418	30.7021	-35.757	84.593	.633
[Plants species=H.Helix"Plattensee"]	15.291	30.1020	-43.708	74.290	.258
[Plants species=Lonicera henryi]	10.800	28.4678	-44.996	66.596	.144
[Plants species=P.tricuspidata]	23.468	29.0393	-33.448	80.384	.653
[Plants species=Wisteria sinensis]	0[a]	.	.	.	.
Qamb (µmol/m²/s)	.149	.0257	.099	.200	33.586
[Plants species=Clematis montana] * Qamb (µmol/m²/s)	-.062	.0490	-.158	.034	1.626
[Plants species=H. hibernica] * Qamb (µmol/m²/s)	.008	.0354	-.061	.078	.053
[Plants species=H.colchica"Russland"] * Qamb (µmol/m²/s)	-.059	.0333	-.125	.006	3.173

[Plants species=H.Helix"Plattensee"] * Qamb (µmol/m²/s)	-.009	.0336	-.074	.057	.067
[Plants species=Lonicera henryi] * Qamb (µmol/m²/s)	-.005	.0344	-.073	.062	.023
[Plants species=P.tricuspidata] * Qamb (µmol/m²/s)	-.078	.0341	-.145	-.011	5.256
[Plants species=Wisteria sinensis] * Qamb (µmol/m²/s)	0[a]	.	.	.	.
(Scale)	4654.020[b]	407.4019	3920.271	5525.104	

Parameter Estimates

	Hypothesis Test	
Parameter	df	Sig.
(Intercept)	1	.336
[Plants species=Clematis montana]	1	.727
[Plants species=H. hibernica]	1	.908
[Plants species=H.colchica"Russland"]	1	.426
[Plants species=H.Helix"Plattensee"]	1	.611
[Plants species=Lonicera henryi]	1	.704
[Plants species=P.tricuspidata]	1	.419
[Plants species=Wisteria sinensis]	.	.
Qamb (µmol/m²/s)	1	<.001
[Plants species=Clematis montana] * Qamb (µmol/m²/s)	1	.202

[Plants species=H. hibernica] * Qamb (µmol/m²/s)	1	.817
[Plants species=H.colchica"Russland"] * Qamb (µmol/m²/s)	1	.075
[Plants species=H.Helix"Plattensee"] * Qamb (µmol/m²/s)	1	.796
[Plants species=Lonicera henryi] * Qamb (µmol/m²/s)	1	.880
[Plants species=P.tricuspidata] * Qamb (µmol/m²/s)	1	.022
[Plants species=Wisteria sinensis] * Qamb (µmol/m²/s)	.	.
(Scale)		

Dependent Variable: ETR (µmol/m²/s)
Model: (Intercept), Plants species, Qamb (µmol/m²/s), Plants species * Qamb (µmol/m²/s)

a. Set to zero because this parameter is redundant.

b. Maximum likelihood estimate.

Estimated Marginal Means 1: Grand Mean

Estimates

		95% Wald Confidence Interval	
Mean	Std. Error	Lower	Upper
139.85	4.956	130.13	149.56

Covariates appearing in the model are fixed at the following values: Qamb (µmol/m²/s)=897.48

Estimated Marginal Means 2: Plants species

Estimates

			95% Wald Confidence Interval	
Plants species	Mean	Std. Error	Lower	Upper
Clematis montana	117.62	20.236	77.96	157.29
H. hibernica	156.72	11.123	134.92	178.52
H.colchica"Russland"	124.48	11.164	102.60	146.36
H.Helix"Plattensee"	160.77	10.792	139.62	181.93
Lonicera henryi	159.42	11.646	136.59	182.25
P.tricuspidata	106.64	11.452	84.20	129.09
Wisteria sinensis	153.27	12.749	128.28	178.25

Covariates appearing in the model are fixed at the following values: Qamb (µmol/m²/s)=897.48

Generalized Linear Models

Notes

Output Created		02-MAR-2025 09:59:47
Comments		
Input	Active Dataset	DataSet1

	Filter	<none>
	Weight	<none>
	Split File	<none>
	N of Rows in Working Data File	261
Missing Value Handling	Definition of Missing	User-defined missing values for factor, subject and within-subject variables are treated as missing.
	Cases Used	Statistics are based on cases with valid data for all variables in the model.
Weight Handling		not applicable
Syntax		GENLIN Tleaf°C BY Plantsspecies (ORDER=ASCENDING) WITH Qambµmolm²s /MODEL Plantsspecies Qambµmolm²s Plantsspecies*Qambµmolm²s INTERCEPT=YES DISTRIBUTION=NORMAL LINK=IDENTITY /CRITERIA SCALE=MLE COVB=MODEL PCONVERGE=1E-006(ABSOLUTE) SINGULAR=1E-012 ANALYSISTYPE=3(WALD) CILEVEL=95 CITYPE=WALD LIKELIHOOD=FULL /EMMEANS SCALE=ORIGINAL /EMMEANS TABLES=Plantsspecies SCALE=ORIGINAL /MISSING CLASSMISSING=EXCLUDE

		/PRINT CPS DESCRIPTIVES MODELINFO FIT SUMMARY SOLUTION.
Resources	Processor Time	00:00:00.06
	Elapsed Time	00:00:00.07

Model Information

Dependent Variable	Tleaf °C
Probability Distribution	Normal
Link Function	Identity

Case Processing Summary

	N	Percent
Included	261	100.0%
Excluded	0	0.0%
Total	261	100.0%

Categorical Variable Information

			N	Percent
Factor	Plants species	Clematis montana	30	11.5%
		H. hibernica	40	15.3%
		H.colchica"Russland"	38	14.6%
		H.Helix"Plattensee"	40	15.3%
		Lonicera henryi	38	14.6%
		P.tricuspidata	37	14.2%
		Wisteria sinensis	38	14.6%
		Total	261	100.0%

Continuous Variable Information

		N	Minimum	Maximum	Mean
Dependent Variable	Tleaf °C	261	29.15	37.45	32.2853
Covariate	Qamb (µmol/m²/s)	261	87	1638	897.48

Continuous Variable Information

		Std. Deviation
Dependent Variable	Tleaf °C	1.70173
Covariate	Qamb (µmol/m²/s)	500.514

Goodness of Fit[a]

	Value	df	Value/df
Deviance	421.675	247	1.707
Scaled Deviance	261.000	247	
Pearson Chi-Square	421.675	247	1.707
Scaled Pearson Chi-Square	261.000	247	
Log Likelihood[b]	-432.946		
Akaike's Information Criterion (AIC)	895.891		
Finite Sample Corrected AIC (AICC)	897.850		
Bayesian Information Criterion (BIC)	949.359		
Consistent AIC (CAIC)	964.359		

Dependent Variable: Tleaf °C
Model: (Intercept), Plants species, Qamb (µmol/m²/s), Plants species * Qamb (µmol/m²/s)
[a]

a. Information criteria are in smaller-is-better form.

b. The full log likelihood function is displayed and used in computing information criteria.

Omnibus Test[a]

Likelihood Ratio Chi-Square	df	Sig.
151.313	13	<.001

Dependent Variable: Tleaf °C
Model: (Intercept), Plants species, Qamb (µmol/m²/s), Plants species * Qamb (µmol/m²/s)
[a]

a. Compares the fitted model against the intercept-only model.

Tests of Model Effects

Source	Type III Wald Chi-Square	df	Sig.
(Intercept)	22223.808	1	<.001
Plants species	11.560	6	.073
Qamb (µmol/m²/s)	87.834	1	<.001
Plants species * Qamb (µmol/m²/s)	4.144	6	.657

Dependent Variable: Tleaf °C

Model: (Intercept), Plants species, Qamb (µmol/m²/s), Plants species * Qamb (µmol/m²/s)

Parameter Estimates

Parameter	B	Std. Error	95% Wald Confidence Interval Lower	95% Wald Confidence Interval Upper	Hypothesis Test Wald Chi-Square
(Intercept)	31.311	.3745	30.577	32.045	6990.442
[Plants species=Clematis montana]	.034	1.0871	-2.096	2.165	.001
[Plants species=H. hibernica]	-1.044	.6241	-2.267	.180	2.796
[Plants species=H.colchica"Russland"]	-.317	.5720	-1.438	.804	.307
[Plants species=H.Helix"Plattensee"]	-1.387	.5609	-2.486	-.288	6.116
[Plants species=Lonicera henryi]	-1.108	.5304	-2.148	-.069	4.367
[Plants species=P.tricuspidata]	-.047	.5411	-1.108	1.013	.008
[Plants species=Wisteria sinensis]	0[a]	.	.	.	.

Qamb (µmol/m²/s)	.001	.0005	.000	.002	8.014
[Plants species=Clematis montana] * Qamb (µmol/m²/s)	.001	.0009	-.001	.002	.368
[Plants species=H. hibernica] * Qamb (µmol/m²/s)	6.645E-5	.0007	-.001	.001	.010
[Plants species=H.colchica"Russland"] * Qamb (µmol/m²/s)	.000	.0006	-.001	.001	.095
[Plants species=H.Helix"Plattensee"] * Qamb (µmol/m²/s)	.000	.0006	-.001	.001	.144
[Plants species=Lonicera henryi] * Qamb (µmol/m²/s)	.001	.0006	-.001	.002	1.274
[Plants species=P.tricuspidata] * Qamb (µmol/m²/s)	.001	.0006	.000	.002	2.309
[Plants species=Wisteria sinensis] * Qamb (µmol/m²/s)	0[a]	.	.	.	.
(Scale)	1.616[b]	.1414	1.361	1.918	

Parameter Estimates

	Hypothesis Test	
Parameter	df	Sig.
(Intercept)	1	<.001
[Plants species=Clematis montana]	1	.975
[Plants species=H. hibernica]	1	.094
[Plants species=H.colchica"Russland"]	1	.580
[Plants species=H.Helix"Plattensee"]	1	.013

[Plants species=Lonicera henryi]	1	.037
[Plants species=P.tricuspidata]	1	.930
[Plants species=Wisteria sinensis]	.	.
Qamb (µmol/m²/s)	1	.005
[Plants species=Clematis montana] * Qamb (µmol/m²/s)	1	.544
[Plants species=H. hibernica] * Qamb (µmol/m²/s)	1	.920
[Plants species=H.colchica"Russland"] * Qamb (µmol/m²/s)	1	.758
[Plants species=H.Helix"Plattensee"] * Qamb (µmol/m²/s)	1	.705
[Plants species=Lonicera henryi] * Qamb (µmol/m²/s)	1	.259
[Plants species=P.tricuspidata] * Qamb (µmol/m²/s)	1	.129
[Plants species=Wisteria sinensis] * Qamb (µmol/m²/s)	.	.
(Scale)		

Dependent Variable: Tleaf °C
Model: (Intercept), Plants species, Qamb (µmol/m²/s), Plants species * Qamb (µmol/m²/s)

a. Set to zero because this parameter is redundant.

b. Maximum likelihood estimate.

Estimated Marginal Means 1: Grand Mean

Estimates

Mean	Std. Error	95% Wald Confidence Interval	
		Lower	Upper
32.3281	.09234	32.1471	32.5090

Covariates appearing in the model are fixed at the following values: Qamb (µmol/m²/s)=897.48

Estimated Marginal Means 2: Plants species

Estimates

Plants species	Mean	Std. Error	95% Wald Confidence Interval	
			Lower	Upper
Clematis montana	33.06	.377	32.32	33.80
H. hibernica	31.55	.207	31.14	31.95
H.colchica"Russland"	32.38	.208	31.98	32.79
H.Helix"Plattensee"	31.36	.201	30.96	31.75
Lonicera henryi	32.07	.217	31.65	32.50
P.tricuspidata	33.35	.213	32.93	33.77
Wisteria sinensis	32.53	.238	32.06	33.00

Covariates appearing in the model are fixed at the following values: Qamb (µmol/m²/s)=897.48

Generalized Linear Models

Notes

Output Created		02-MAR-2025 10:02:18
Comments		
Input	Active Dataset	DataSet1
	Filter	<none>
	Weight	<none>
	Split File	<none>
	N of Rows in Working Data File	261
Missing Value Handling	Definition of Missing	User-defined missing values for factor, subject and within-subject variables are treated as missing.
	Cases Used	Statistics are based on cases with valid data for all variables in the model.
Weight Handling		not applicable
Syntax		GENLIN WaterUseEfficiency BY Plantsspecies (ORDER=ASCENDING) WITH Qambµmolm²s /MODEL Plantsspecies Qambµmolm²s Plantsspecies*Qambµmolm²s INTERCEPT=YES DISTRIBUTION=NORMAL LINK=IDENTITY /CRITERIA SCALE=MLE COVB=MODEL PCONVERGE=1E-006(ABSOLUTE) SINGULAR=1E-012 ANALYSISTYPE=3(WALD) CILEVEL=95 CITYPE=WALD LIKELIHOOD=FULL /EMMEANS

		SCALE=ORIGINAL /EMMEANS TABLES=Plantsspecies SCALE=ORIGINAL /MISSING CLASSMISSING=EXCL UDE /PRINT CPS DESCRIPTIVES MODELINFO FIT SUMMARY SOLUTION.
Resources	Processor Time	00:00:00.06
	Elapsed Time	00:00:00.06

Model Information

Dependent Variable	WaterUseEfficiency
Probability Distribution	Normal
Link Function	Identity

Case Processing Summary

	N	Percent
Included	261	100.0%
Excluded	0	0.0%
Total	261	100.0%

Categorical Variable Information

			N	Percent
Factor	Plants species	Clematis montana	30	11.5%
		H. hibernica	40	15.3%
		H.colchica"Russland"	38	14.6%
		H.Helix"Plattensee"	40	15.3%
		Lonicera henryi	38	14.6%
		P.tricuspidata	37	14.2%
		Wisteria sinensis	38	14.6%
		Total	261	100.0%

Continuous Variable Information

		N	Minimum	Maximum	Mean
Dependent Variable	WaterUseEfficiency	261	5.11	64557.62	393.22
Covariate	Qamb (µmol/m²/s)	261	87	1638	897.48

Continuous Variable Information

		Std. Deviation
Dependent Variable	WaterUseEfficiency	3999.238
Covariate	Qamb (µmol/m²/s)	500.514

Goodness of Fit[a]

	Value	df	Value/df
Deviance	3889438303.391	247	15746713.779
Scaled Deviance	261.000	247	
Pearson Chi-Square	3889438303.391	247	15746713.779
Scaled Pearson Chi-Square	261.000	247	
Log Likelihood[b]	-2525.813		
Akaike's Information Criterion (AIC)	5081.626		
Finite Sample Corrected AIC (AICC)	5083.585		
Bayesian Information Criterion (BIC)	5135.093		
Consistent AIC (CAIC)	5150.093		

Dependent Variable: WaterUseEfficiency
Model: (Intercept), Plants species, Qamb (µmol/m²/s), Plants species * Qamb (µmol/m²/s)
[a]

a. Information criteria are in smaller-is-better form.

b. The full log likelihood function is displayed and used in computing information criteria.

Omnibus Test[a]

Likelihood Ratio Chi-Square	df	Sig.
17.453	13	.179

Dependent Variable: WaterUseEfficiency
Model: (Intercept), Plants species, Qamb (µmol/m²/s), Plants species * Qamb (µmol/m²/s)
[a]

a. Compares the fitted model against the intercept-only model.

Tests of Model Effects

Source	Type III Wald Chi-Square	df	Sig.
(Intercept)	.038	1	.846
Plants species	.971	6	.987
Qamb (µmol/m²/s)	1.773	1	.183
Plants species * Qamb (µmol/m²/s)	9.134	6	.166

Dependent Variable: WaterUseEfficiency
Model: (Intercept), Plants species, Qamb (µmol/m²/s), Plants species * Qamb (µmol/m²/s)

Parameter Estimates

Parameter	B	Std. Error	95% Wald Confidence Interval Lower	Upper
(Intercept)	-1178.044	1137.3662	-3407.240	1051.153
[Plants species=Clematis montana]	1194.929	3301.7234	-5276.329	7666.188
[Plants species=H. hibernica]	1197.554	1895.3481	-2517.260	4912.368
[Plants species=H.colchica"Russland"]	1225.164	1737.3097	-2179.900	4630.229

[Plants species=H.Helix"Plattensee"]	1201.184	1703.3519	-2137.325	4539.692
[Plants species=Lonicera henryi]	1257.072	1610.8768	-1900.189	4414.332
[Plants species=P.tricuspidata]	1317.111	1643.2155	-1903.532	4537.754
[Plants species=Wisteria sinensis]	0[a]	.	.	.
Qamb (µmol/m²/s)	4.784	1.4570	1.928	7.639
[Plants species=Clematis montana] * Qamb (µmol/m²/s)	-4.690	2.7715	-10.122	.742
[Plants species=H. hibernica] * Qamb (µmol/m²/s)	-4.719	2.0034	-8.646	-.793
[Plants species=H.colchica"Russland"] * Qamb (µmol/m²/s)	-4.741	1.8835	-8.432	-1.049
[Plants species=H.Helix"Plattensee"] * Qamb (µmol/m²/s)	-4.738	1.8985	-8.459	-1.017
[Plants species=Lonicera henryi] * Qamb (µmol/m²/s)	-4.743	1.9467	-8.558	-.927
[Plants species=P.tricuspidata] * Qamb (µmol/m²/s)	-4.573	1.9278	-8.351	-.794
[Plants species=Wisteria sinensis] * Qamb (µmol/m²/s)	0[a]	.	.	.
(Scale)	14902062.465[b]	1304491.1097	12552615.342	17691250.761

Parameter Estimates

	Hypothesis Test		
Parameter	Wald Chi-Square	df	Sig.
(Intercept)	1.073	1	.300
[Plants species=Clematis montana]	.131	1	.717

[Plants species=H. hibernica]	.399	1	.527
[Plants species=H.colchica"Russland"]	.497	1	.481
[Plants species=H.Helix"Plattensee"]	.497	1	.481
[Plants species=Lonicera henryi]	.609	1	.435
[Plants species=P.tricuspidata]	.642	1	.423
[Plants species=Wisteria sinensis]	.	.	.
Qamb (µmol/m²/s)	10.780	1	.001
[Plants species=Clematis montana] * Qamb (µmol/m²/s)	2.864	1	.091
[Plants species=H. hibernica] * Qamb (µmol/m²/s)	5.549	1	.018
[Plants species=H.colchica"Russland"] * Qamb (µmol/m²/s)	6.335	1	.012
[Plants species=H.Helix"Plattensee"] * Qamb (µmol/m²/s)	6.228	1	.013
[Plants species=Lonicera henryi] * Qamb (µmol/m²/s)	5.936	1	.015
[Plants species=P.tricuspidata] * Qamb (µmol/m²/s)	5.627	1	.018
[Plants species=Wisteria sinensis] * Qamb (µmol/m²/s)	.	.	.
(Scale)			

Dependent Variable: WaterUseEfficiency
Model: (Intercept), Plants species, Qamb (µmol/m²/s), Plants species * Qamb (µmol/m²/s)

a. Set to zero because this parameter is redundant.

b. Maximum likelihood estimate.

Estimated Marginal Means 1: Grand Mean

Estimates

		95% Wald Confidence Interval	
Mean	Std. Error	Lower	Upper
555.3345	280.45294	5.6568	1105.0121

Covariates appearing in the model are fixed at the following values: Qamb (µmol/m²/s)=897.48

Estimated Marginal Means 2: Plants species

Estimates

			95% Wald Confidence Interval	
Plants species	Mean	Std. Error	Lower	Upper
Clematis montana	100.81	1145.092	-2143.53	2345.15
H. hibernica	77.35	629.434	-1156.31	1311.02
H.colchica"Russland"	85.63	631.710	-1152.50	1323.75
H.Helix"Plattensee"	64.33	610.664	-1132.55	1261.21
Lonicera henryi	115.62	659.007	-1176.01	1407.25
P.tricuspidata	328.38	648.018	-941.72	1598.47

Wisteria sinensis	3115.22	721.408	1701.29	4529.16

Covariates appearing in the model are fixed at the following values: Qamb (µmol/m²/s)=897.48

Notes

Output Created		04-APR-2025 12:36:47
Comments		
Input	Data	C:\Work\Uni Job^PhD\last data in Gewächshaus\licor spss\SPSS file for all 7 species.sav
	Active Dataset	DataSet2
	Filter	<none>
	Weight	<none>
	Split File	<none>
	N of Rows in Working Data File	261
Missing Value Handling	Definition of Missing	User-defined missing values are treated as missing.
	Cases Used	Statistics for each analysis are based on cases with no missing data for any variable in the analysis.
Syntax		ONEWAY E_apparentmmolm²s BY Plantsspecies /ES=OVERALL /MISSING ANALYSIS /CRITERIA=CILEVEL(0.95) /POSTHOC=BONFERRONI ALPHA(0.05).
Resources	Processor Time	00:00:00.00
	Elapsed Time	00:00:00.02

Notes

Output Created		04-APR-2025 12:40:53
Comments		
Input	Data	C:\Work\Uni Job^PhD\last data in Gewächshaus\licor spss\SPSS file for all 7 species.sav
	Active Dataset	DataSet1
	Filter	<none>
	Weight	<none>
	Split File	<none>
	N of Rows in Working Data File	261
Missing Value Handling	Definition of Missing	User-defined missing values are treated as missing.
	Cases Used	Statistics for each analysis are based on cases with no missing data for any variable in the analysis.
Syntax		ONEWAY E_apparentmmolm²s BY Plantsspecies /ES=OVERALL /MISSING ANALYSIS /CRITERIA=CILEVEL(0.95) /POSTHOC=BONFERRONI ALPHA(0.05).
Resources	Processor Time	00:00:00.00
	Elapsed Time	00:00:00.00

Oneway ANOVA and Post Hoc Tests - Tukey HSD for the GLM significant variables – Chapter 7.

Notes

Output Created		04-APR-2025 13:23:49
Comments		
Input	Active Dataset	DataSet2
	Filter	<none>
	Weight	<none>
	Split File	<none>
	N of Rows in Working Data File	261
Missing Value Handling	Definition of Missing	User-defined missing values are treated as missing.
	Cases Used	Statistics for each analysis are based on cases with no missing data for any variable in the analysis.
Syntax		ONEWAY E_apparentmmolm²s BY PlantID /ES=OVERALL /MISSING ANALYSIS /CRITERIA=CILEVEL(0.95) /POSTHOC=TUKEY ALPHA(0.05).
Resources	Processor Time	00:00:00.00
	Elapsed Time	00:00:00.01

ANOVA

E_apparent (mmol/m²/s)

	Sum of Squares	df	Mean Square	F	Sig.
Between Groups	138.974	6	23.162	26.802	<.001
Within Groups	219.507	254	.864		
Total	358.481	260			

ANOVA Effect Sizes[a]

	Point Estimate	95% Confidence Interval	
		Lower	Upper

E_apparent (mmol/m²/s)	Eta-squared	.388	.285	.454
	Epsilon-squared	.373	.268	.441
	Omega-squared Fixed-effect	.372	.267	.440
	Omega-squared Random-effect	.090	.057	.116

a. Eta-squared and Epsilon-squared are estimated based on the fixed-effect model.

Post Hoc Tests

Multiple Comparisons

Dependent Variable: E_apparent (mmol/m²/s)
Tukey HSD

(I) Plant ID	(J) Plant ID	Mean Difference (I-J)	Std. Error	Sig.	95% Confidence Interval Lower Bound	95% Confidence Interval Upper Bound
C. montana	P. tricuspidata	.660	.228	.06	-.019	1.339
	H.helix ' Plattensee'	-1.273*	.225	<.001	-1.940	-.605
	H.hibernica	-.793*	.225	.01	-1.460	-.125
	W.sinensis	.961*	.227	<.001	.286	1.636
	L.henryi	-.041	.227	1.00	-.716	.634
	H.colchica	-.183	.227	.98	-.858	.491
P. tricuspidata	C. montana	-.660	.228	.06	-1.339	.019
	H.helix ' Plattensee'	-1.933*	.212	<.001	-2.563	-1.302
	H.hibernica	-1.453*	.212	<.001	-2.083	-.823
	W.sinensis	.301	.215	.80	-.337	.939
	L.henryi	-.701*	.215	.02	-1.339	-.063
	H.colchica	-.844*	.215	.00	-1.482	-.205
H.helix ' Plattensee'	C. montana	1.273*	.225	<.001	.605	1.940
	P. tricuspidata	1.933*	.212	<.001	1.302	2.563
	H.hibernica	.480	.208	.24	-.138	1.098
	W.sinensis	2.234*	.211	<.001	1.608	2.859
	L.henryi	1.231*	.211	<.001	.605	1.857

H.hibernica	H.colchica	1.089*	.211	<.001	.463	1.715
	C. montana	.793*	.225	.01	.125	1.460
	P. tricuspidata	1.453*	.212	<.001	.823	2.083
	H.helix ' Plattensee'	-.480	.208	.24	-1.098	.138
	W.sinensis	1.754*	.211	<.001	1.128	2.380
W.sinensis	L.henryi	.751*	.211	.01	.126	1.377
	H.colchica	.609	.211	.06	-.017	1.235
	C. montana	-.961*	.227	<.001	-1.636	-.286
	P. tricuspidata	-.301	.215	.80	-.939	.337
	H.helix ' Plattensee'	-2.234*	.211	<.001	-2.859	-1.608
	H.hibernica	-1.754*	.211	<.001	-2.380	-1.128
	L.henryi	-1.002*	.213	<.001	-1.636	-.368
L.henryi	H.colchica	-1.144*	.213	<.001	-1.778	-.511
	C. montana	.041	.227	1.00	-.634	.716
	P. tricuspidata	.701*	.215	.02	.063	1.339
	H.helix ' Plattensee'	-1.231*	.211	<.001	-1.857	-.605
	H.hibernica	-.751*	.211	.01	-1.377	-.126
	W.sinensis	1.002*	.213	<.001	.368	1.636
H.colchica	H.colchica	-.142	.213	.99	-.776	.492
	C. montana	.183	.227	.98	-.491	.858
	P. tricuspidata	.844*	.215	.00	.205	1.482
	H.helix ' Plattensee'	-1.089*	.211	<.001	-1.715	-.463
	H.hibernica	-.609	.211	.06	-1.235	.017
	W.sinensis	1.144*	.213	<.001	.511	1.778
	L.henryi	.14223855	.21327032	.99	-.492	.776

*. The mean difference is significant at the 0.05 level.

Homogeneous Subsets

E_apparent (mmol/m²/s)

Tukey HSD[a,b]

		Subset for alpha = 0.05			
Plant ID	N	1	2	3	4
W.sinensis	38	.58453524			
P. tricuspidata	37	.88547195			
C. montana	30		1.54555110		
L.henryi	38		1.58677550		
H.colchica	38		1.72901405	1.72901405	
H.hibernica	40			2.33821585	2.33821585
H.helix ' Plattensee'	40				2.81812343
Sig.		.806	.979	.076	.289

Means for groups in homogeneous subsets are displayed.
a. Uses Harmonic Mean Sample Size = 36.977.

b. The group sizes are unequal. The harmonic mean of the group sizes is used. Type I error levels are not guaranteed.

Oneway

Notes

Output Created		04-APR-2025 13:25:39
Comments		
Input	Active Dataset	DataSet2
	Filter	<none>
	Weight	<none>
	Split File	<none>
	N of Rows in Working Data File	261
Missing Value Handling	Definition of Missing	User-defined missing values are treated as missing.
	Cases Used	Statistics for each analysis are based on cases with no

		missing data for any variable in the analysis.
Syntax		ONEWAY gswmolm²s BY PlantID /ES=OVERALL /MISSING ANALYSIS /CRITERIA=CILEVEL(0.95) /POSTHOC=TUKEY ALPHA(0.05).
Resources	Processor Time	00:00:00.00
	Elapsed Time	00:00:00.01

ANOVA

gsw (mol/m²/s)

	Sum of Squares	df	Mean Square	F	Sig.
Between Groups	.195	6	.032	33.947	<.001
Within Groups	.243	254	.001		
Total	.438	260			

ANOVA Effect Sizes[a]

			95% Confidence Interval	
		Point Estimate	Lower	Upper
gsw (mol/m²/s)	Eta-squared	.445	.346	.508
	Epsilon-squared	.432	.330	.497
	Omega-squared Fixed-effect	.431	.329	.496
	Omega-squared Random-effect	.112	.076	.141

a. Eta-squared and Epsilon-squared are estimated based on the fixed-effect model.

Post Hoc Tests

Multiple Comparisons

Dependent Variable: gsw (mol/m²/s)
Tukey HSD

(I) Plant ID	(J) Plant ID	Mean Difference (I-J)	Std. Error	Sig.	95% Confidence Interval Lower Bound	95% Confidence Interval Upper Bound
C. montana	P. tricuspidata	.018	.008	0	-.0045	.0407
	H.helix ' Plattensee'	-.058*	.007	<.001	-.0803	-.0358
	H.hibernica	-.034*	.007	<.001	-.0560	-.0116
	W.sinensis	.025*	.008	0	.0030	.0479
	L.henryi	-.009	.008	1	-.0313	.0136
	H.colchica	-.009	.008	1	-.0311	.0138
P. tricuspidata	C. montana	-.018	.008	0	-.0407	.0045
	H.helix ' Plattensee'	-.076*	.007	<.001	-.0971	-.0552
	H.hibernica	-.052*	.007	<.001	-.0729	-.0309
	W.sinensis	.007	.007	1	-.0139	.0286
	L.henryi	-.027*	.007	0	-.0482	-.0057
	H.colchica	-.027*	.007	0	-.0480	-.0055
H.helix ' Plattensee'	C. montana	.058*	.007	<.001	.0358	.0803
	P. tricuspidata	.076*	.007	<.001	.0552	.0971
	H.hibernica	.024*	.007	0	.0037	.0448
	W.sinensis	.083*	.007	<.001	.0626	.1043
	L.henryi	.049*	.007	<.001	.0284	.0701
	H.colchica	.049*	.007	<.001	.0286	.0703
H.hibernica	C. montana	.034*	.007	<.001	.0116	.0560
	P. tricuspidata	.052*	.007	<.001	.0309	.0729
	H.helix ' Plattensee'	-.024*	.007	0	-.0448	-.0037
	W.sinensis	.059*	.007	<.001	.0384	.0800
	L.henryi	.025*	.007	0	.0041	.0458
	H.colchica	.025*	.007	0	.0043	.0460
W.sinensis	C. montana	-.025*	.008	0	-.0479	-.0030
	P. tricuspidata	-.007	.007	1	-.0286	.0139
	H.helix ' Plattensee'	-.083*	.007	<.001	-.1043	-.0626
	H.hibernica	-.059*	.007	<.001	-.0800	-.0384
	L.henryi	-.034*	.007	<.001	-.0554	-.0132

	H.colchica	-.034*	.007	<.001	-.0551	-.0130
L.henryi	C. montana	.009	.008	1	-.0136	.0313
	P. tricuspidata	.027*	.007	0	.0057	.0482
	H.helix ' Plattensee'	-.049*	.007	<.001	-.0701	-.0284
	H.hibernica	-.025*	.007	0	-.0458	-.0041
	W.sinensis	.034*	.007	<.001	.0132	.0554
	H.colchica	.000	.007	1	-.0209	.0213
H.colchica	C. montana	.009	.008	1	-.0138	.0311
	P. tricuspidata	.027*	.007	0	.0055	.0480
	H.helix ' Plattensee'	-.049*	.007	<.001	-.0703	-.0286
	H.hibernica	-.025*	.007	0	-.0460	-.0043
	W.sinensis	.034*	.007	<.001	.0130	.0551
	L.henryi	.000	.007	1	-.0213	.0209

*. The mean difference is significant at the 0.05 level.

Homogeneous Subsets

gsw (mol/m²/s)

Tukey HSD[a,b]

		Subset for alpha = 0.05				
Plant ID	N	1	2	3	4	5
W.sinensis	38	.01803803				
P. tricuspidata	37	.02537151	.02537151			
C. montana	30		.04346943	.04346943		
H.colchica	38			.05208526		
L.henryi	38			.05229561		
H.hibernica	40				.07725618	
H.helix ' Plattensee'	40					.10151530
Sig.		.949	.158	.883	1.000	1.000

Means for groups in homogeneous subsets are displayed.

a. Uses Harmonic Mean Sample Size = 36.977.

b. The group sizes are unequal. The harmonic mean of the group sizes is used. Type I error levels are not guaranteed.

Oneway

Notes

Output Created		04-APR-2025 13:26:36
Comments		
Input	Active Dataset	DataSet2
	Filter	<none>
	Weight	<none>
	Split File	<none>
	N of Rows in Working Data File	261
Missing Value Handling	Definition of Missing	User-defined missing values are treated as missing.
	Cases Used	Statistics for each analysis are based on cases with no missing data for any variable in the analysis.
Syntax		ONEWAY VPDleafkpa BY PlantID /ES=OVERALL /MISSING ANALYSIS /CRITERIA=CILEVEL(0.95) /POSTHOC=TUKEY ALPHA(0.05).
Resources	Processor Time	00:00:00.03
	Elapsed Time	00:00:00.01

ANOVA

VPDleaf (kpa)

	Sum of Squares	df	Mean Square	F	Sig.
Between Groups	13.934	6	2.322	13.119	<.001
Within Groups	44.963	254	.177		
Total	58.897	260			

ANOVA Effect Sizes[a]

			95% Confidence Interval	
		Point Estimate	Lower	Upper
VPDleaf (kpa)	Eta-squared	.237	.136	.306
	Epsilon-squared	.219	.116	.289
	Omega-squared Fixed-effect	.218	.116	.288
	Omega-squared Random-effect	.044	.021	.063

a. Eta-squared and Epsilon-squared are estimated based on the fixed-effect model.

Post Hoc Tests

Multiple Comparisons

Dependent Variable: VPDleaf (kpa)
Tukey HSD

		Mean Difference (I-J)	Std. Error	Sig.	95% Confidence Interval Lower Bound	95% Confidence Interval Upper Bound
(I) Plant ID	(J) Plant ID					
C. montana	P. tricuspidata	.184	.103	1	-.123	.492
	H.helix 'Plattensee'	.764*	.102	<.001	.462	1.066
	H.hibernica	.544*	.102	<.001	.242	.846
	W.sinensis	.429*	.103	<.001	.124	.735
	L.henryi	.553*	.103	<.001	.247	.858
	H.colchica	.296	.103	0	-.009	.602
P. tricuspidata	C. montana	-.184	.103	1	-.492	.123

	H.helix ' Plattensee'	.580*	.096	<.001	.294	.865
	H.hibernica	.360*	.096	0	.075	.645
	W.sinensis	.245	.097	0	-.044	.534
	L.henryi	.368*	.097	0	.079	.657
	H.colchica	.112	.097	1	-.177	.401
H.helix ' Plattensee'	C. montana	-.764*	.102	<.001	-1.066	-.462
	P. tricuspidata	-.580*	.096	<.001	-.865	-.294
	H.hibernica	-.220	.094	0	-.499	.060
	W.sinensis	-.335*	.095	0	-.618	-.052
	L.henryi	-.211	.095	0	-.495	.072
	H.colchica	-.468*	.095	<.001	-.751	-.184
H.hibernica	C. montana	-.544*	.102	<.001	-.846	-.242
	P. tricuspidata	-.360*	.096	0	-.645	-.075
	H.helix ' Plattensee'	.220	.094	0	-.060	.499
	W.sinensis	-.115	.095	1	-.398	.168
	L.henryi	.008	.095	1	-.275	.292
	H.colchica	-.248	.095	0	-.531	.035
W.sinensis	C. montana	-.429*	.103	<.001	-.735	-.124
	P. tricuspidata	-.245	.097	0	-.534	.044
	H.helix ' Plattensee'	.335*	.095	0	.052	.618
	H.hibernica	.115	.095	1	-.168	.398
	L.henryi	.123	.097	1	-.163	.410
	H.colchica	-.133	.097	1	-.420	.154
L.henryi	C. montana	-.553*	.103	<.001	-.858	-.247
	P. tricuspidata	-.368*	.097	0	-.657	-.079
	H.helix ' Plattensee'	.211	.095	0	-.072	.495
	H.hibernica	-.008	.095	1	-.292	.275
	W.sinensis	-.123	.097	1	-.410	.163
	H.colchica	-.256	.097	0	-.543	.031
H.colchica	C. montana	-.296	.103	0	-.602	.009
	P. tricuspidata	-.112	.097	1	-.401	.177
	H.helix ' Plattensee'	.468*	.095	<.001	.184	.751
	H.hibernica	.248	.095	0	-.035	.531
	W.sinensis	.133	.097	1	-.154	.420

L.henryi	.256	.097	0	-.031	.543

*. The mean difference is significant at the 0.05 level.

Homogeneous Subsets

VPDleaf (kpa)

Tukey HSD[a,b]

		Subset for alpha = 0.05			
Plant ID	N	1	2	3	4
H.helix ' Plattensee'	40	2.84751615			
L.henryi	38	3.05885666	3.05885666		
H.hibernica	40	3.06720910	3.06720910		
W.sinensis	38		3.18231376	3.18231376	
H.colchica	38		3.31507913	3.31507913	
P. tricuspidata	37			3.42712649	3.42712649
C. montana	30				3.61144593
Sig.		.275	.125	.163	.493

Means for groups in homogeneous subsets are displayed.

a. Uses Harmonic Mean Sample Size = 36.977.

b. The group sizes are unequal. The harmonic mean of the group sizes is used. Type I error levels are not guaranteed.

Oneway

Notes

Output Created	04-APR-2025 13:27:51
Comments	

Input	Active Dataset	DataSet2
	Filter	<none>
	Weight	<none>
	Split File	<none>
	N of Rows in Working Data File	261
Missing Value Handling	Definition of Missing	User-defined missing values are treated as missing.
	Cases Used	Statistics for each analysis are based on cases with no missing data for any variable in the analysis.
Syntax		ONEWAY PhiPS2 BY PlantID /ES=OVERALL /MISSING ANALYSIS /CRITERIA=CILEVEL(0.95) /POSTHOC=TUKEY ALPHA(0.05).
Resources	Processor Time	00:00:00.02
	Elapsed Time	00:00:00.01

ANOVA

PhiPS2

	Sum of Squares	df	Mean Square	F	Sig.
Between Groups	1.203	6	.201	5.275	<.001
Within Groups	9.657	254	.038		
Total	10.860	260			

ANOVA Effect Sizes[a]

			95% Confidence Interval	
		Point Estimate	Lower	Upper
PhiPS2	Eta-squared	.111	.033	.168
	Epsilon-squared	.090	.010	.148

	Omega-squared Fixed-effect	.089	.010	.148
	Omega-squared Random-effect	.016	.002	.028

a. Eta-squared and Epsilon-squared are estimated based on the fixed-effect model.

Post Hoc Tests

Multiple Comparisons

Dependent Variable: PhiPS2
Tukey HSD

(I) Plant ID	(J) Plant ID	Mean Difference (I-J)	Std. Error	Sig.	95% Confidence Interval Lower Bound	95% Confidence Interval Upper Bound
C. montana	P. tricuspidata	-.119	.048	0	-.261	.024
	H.helix ' Plattensee'	-.212*	.047	<.001	-.352	-.072
	H.hibernica	-.147*	.047	0	-.287	-.007
	W.sinensis	-.189*	.048	0	-.330	-.047
	L.henryi	-.227*	.048	<.001	-.368	-.085
	H.colchica	-.111	.048	0	-.253	.030
P. tricuspidata	C. montana	.119	.048	0	-.024	.261
	H.helix ' Plattensee'	-.093	.044	0	-.225	.039
	H.hibernica	-.029	.044	1	-.161	.104
	W.sinensis	-.070	.045	1	-.204	.064
	L.henryi	-.108	.045	0	-.242	.026
	H.colchica	.007	.045	1	-.127	.141
H.helix ' Plattensee'	C. montana	.212*	.047	<.001	.072	.352
	P. tricuspidata	.093	.044	0	-.039	.225
	H.hibernica	.065	.044	1	-.065	.194
	W.sinensis	.023	.044	1	-.108	.154
	L.henryi	-.015	.044	1	-.146	.116
	H.colchica	.100	.044	0	-.031	.232

H.hibernica	C. montana	.147*	.047	0	.007	.287
	P. tricuspidata	.029	.044	1	-.104	.161
	H.helix ' Plattensee'	-.065	.044	1	-.194	.065
	W.sinensis	-.042	.044	1	-.173	.090
	L.henryi	-.080	.044	1	-.211	.052
	H.colchica	.036	.044	1	-.095	.167
W.sinensis	C. montana	.189*	.048	0	.047	.330
	P. tricuspidata	.070	.045	1	-.064	.204
	H.helix ' Plattensee'	-.023	.044	1	-.154	.108
	H.hibernica	.042	.044	1	-.090	.173
	L.henryi	-.038	.045	1	-.171	.095
	H.colchica	.077	.045	1	-.055	.210
L.henryi	C. montana	.227*	.048	<.001	.085	.368
	P. tricuspidata	.108	.045	0	-.026	.242
	H.helix ' Plattensee'	.015	.044	1	-.116	.146
	H.hibernica	.080	.044	1	-.052	.211
	W.sinensis	.038	.045	1	-.095	.171
	H.colchica	.116	.045	0	-.017	.249
H.colchica	C. montana	.111	.048	0	-.030	.253
	P. tricuspidata	-.007	.045	1	-.141	.127
	H.helix ' Plattensee'	-.100	.044	0	-.232	.031
	H.hibernica	-.036	.044	1	-.167	.095
	W.sinensis	-.077	.045	1	-.210	.055
	L.henryi	-.116	.045	0	-.249	.017

*. The mean difference is significant at the 0.05 level.

Homogeneous Subsets

PhiPS2

Tukey HSD[a,b]

Plant ID	N	Subset for alpha = 0.05

		1	2
C. montana	30	.30200070	
H.colchica	38	.41338426	.41338426
P. tricuspidata	37	.42065000	.42065000
H.hibernica	40		.44925618
W.sinensis	38		.49088121
H.helix ' Plattensee'	40		.51387400
L.henryi	38		.52894024
Sig.		.125	.147

Means for groups in homogeneous subsets are displayed.
a. Uses Harmonic Mean Sample Size = 36.977.

b. The group sizes are unequal. The harmonic mean of the group sizes is used. Type I error levels are not guaranteed.

Oneway

Notes

Output Created		04-APR-2025 13:29:21
Comments		
Input	Active Dataset	DataSet2
	Filter	<none>
	Weight	<none>
	Split File	<none>
	N of Rows in Working Data File	261
Missing Value Handling	Definition of Missing	User-defined missing values are treated as missing.
	Cases Used	Statistics for each analysis are based on cases with no missing data for any variable in the analysis.

Syntax		ONEWAY ETRµmolm²s BY PlantID /ES=OVERALL /MISSING ANALYSIS /CRITERIA=CILEVEL(0.95) /POSTHOC=TUKEY ALPHA(0.05).
Resources	Processor Time	00:00:00.02
	Elapsed Time	00:00:00.01

ANOVA

ETR (µmol/m²/s)

	Sum of Squares	df	Mean Square	F	Sig.
Between Groups	157423.641	6	26237.274	3.170	.005
Within Groups	2102403.146	254	8277.178		
Total	2259826.787	260			

ANOVA Effect Sizes[a,b]

			95% Confidence Interval	
		Point Estimate	Lower	Upper
ETR (µmol/m²/s)	Eta-squared	.070	.007	.116
	Epsilon-squared	.048	-.016	.095
	Omega-squared Fixed-effect	.048	-.016	.095
	Omega-squared Random-effect	.008	-.003	.017

a. Eta-squared and Epsilon-squared are estimated based on the fixed-effect model.

b. Negative but less biased estimates are retained, not rounded to zero.

Post Hoc Tests

Multiple Comparisons

Dependent Variable: ETR (µmol/m²/s)

Tukey HSD

(I) Plant ID	(J) Plant ID	Mean Difference (I-J)	Std. Error	Sig.	95% Confidence Interval	
					Lower Bound	Upper Bound
C. montana	P. tricuspidata	51.58	22.35	0	-14.85	118.01
	H.helix ' Plattensee'	-12.13	21.97	1	-77.43	53.18
	H.hibernica	-23.48	21.97	1	-88.79	41.83
	W.sinensis	34.25	22.22	1	-31.79	100.29
	L.henryi	14.32	22.22	1	-51.72	80.36
	H.colchica	20.10	22.22	1	-45.94	86.15
P. tricuspidata	C. montana	-51.58	22.35	0	-118.01	14.85
	H.helix ' Plattensee'	-63.70*	20.75	0	-125.38	-2.03
	H.hibernica	-75.06*	20.75	0	-136.74	-13.38
	W.sinensis	-17.33	21.01	1	-79.78	45.12
	L.henryi	-37.26	21.01	1	-99.71	25.19
	H.colchica	-31.47	21.01	1	-93.93	30.98
H.helix ' Plattensee'	C. montana	12.13	21.97	1	-53.18	77.43
	P. tricuspidata	63.70*	20.75	0	2.03	125.38
	H.hibernica	-11.36	20.34	1	-71.82	49.11
	W.sinensis	46.38	20.61	0	-14.88	107.63
	L.henryi	26.44	20.61	1	-34.81	87.70
	H.colchica	32.23	20.61	1	-29.02	93.48
H.hibernica	C. montana	23.48	21.97	1	-41.83	88.79
	P. tricuspidata	75.06*	20.75	0	13.38	136.74
	H.helix ' Plattensee'	11.36	20.34	1	-49.11	71.82
	W.sinensis	57.73	20.61	0	-3.52	118.99
	L.henryi	37.80	20.61	1	-23.46	99.05
	H.colchica	43.58	20.61	0	-17.67	104.84
W.sinensis	C. montana	-34.25	22.22	1	-100.29	31.79
	P. tricuspidata	17.33	21.01	1	-45.12	79.78
	H.helix ' Plattensee'	-46.38	20.61	0	-107.63	14.88
	H.hibernica	-57.73	20.61	0	-118.99	3.52
	L.henryi	-19.93	20.87	1	-81.97	42.10

	H.colchica	-14.15	20.87	1	-76.18	47.89
L.henryi	C. montana	-14.32	22.22	1	-80.36	51.72
	P. tricuspidata	37.26	21.01	1	-25.19	99.71
	H.helix ' Plattensee'	-26.44	20.61	1	-87.70	34.81
	H.hibernica	-37.80	20.61	1	-99.05	23.46
	W.sinensis	19.93	20.87	1	-42.10	81.97
	H.colchica	5.79	20.87	1	-56.25	67.82
H.colchica	C. montana	-20.10	22.22	1	-86.15	45.94
	P. tricuspidata	31.47	21.01	1	-30.98	93.93
	H.helix ' Plattensee'	-32.23	20.61	1	-93.48	29.02
	H.hibernica	-43.58	20.61	0	-104.84	17.67
	W.sinensis	14.15	20.87	1	-47.89	76.18
	L.henryi	-5.79	20.87	1	-67.82	56.25

*. The mean difference is significant at the 0.05 level.

Homogeneous Subsets

ETR (µmol/m²/s)

Tukey HSD[a,b]

		Subset for alpha = 0.05	
Plant ID	N	1	2
P. tricuspidata	37	99.26	
W.sinensis	38	116.59	116.59
H.colchica	38	130.73	130.73
L.henryi	38	136.52	136.52
C. montana	30	150.84	150.84
H.helix ' Plattensee'	40		162.96327
H.hibernica	40		174.31847
Sig.		.187	.095

Means for groups in homogeneous subsets are displayed.
a. Uses Harmonic Mean Sample Size = 36.977.

b. The group sizes are unequal. The harmonic mean of the group sizes is used. Type I error levels are not guaranteed.

Oneway

Notes

Output Created		04-APR-2025 13:30:28
Comments		
Input	Active Dataset	DataSet2
	Filter	<none>
	Weight	<none>
	Split File	<none>
	N of Rows in Working Data File	261
Missing Value Handling	Definition of Missing	User-defined missing values are treated as missing.
	Cases Used	Statistics for each analysis are based on cases with no missing data for any variable in the analysis.
Syntax		ONEWAY Tleaf°C BY PlantID /ES=OVERALL /MISSING ANALYSIS /CRITERIA=CILEVEL(0.95) /POSTHOC=TUKEY ALPHA(0.05).
Resources	Processor Time	00:00:00.00
	Elapsed Time	00:00:00.01

ANOVA

Tleaf °C

	Sum of Squares	df	Mean Square	F	Sig.
Between Groups	152.663	6	25.444	10.766	<.001
Within Groups	600.270	254	2.363		
Total	752.933	260			

ANOVA Effect Sizes[a]

			95% Confidence Interval	
		Point Estimate	Lower	Upper
Tleaf °C	Eta-squared	.203	.106	.270
	Epsilon-squared	.184	.085	.253
	Omega-squared Fixed-effect	.183	.085	.252
	Omega-squared Random-effect	.036	.015	.053

a. Eta-squared and Epsilon-squared are estimated based on the fixed-effect model.

Post Hoc Tests

Multiple Comparisons

Dependent Variable: Tleaf °C
Tukey HSD

		Mean Difference (I-J)	Std. Error	Sig.	95% Confidence Interval	
(I) Plant ID	(J) Plant ID				Lower Bound	Upper Bound
C. montana	P. tricuspidata	.69	.38	.538	-.44	1.81
	H.helix 'Plattensee'	2.41*	.37	<.001	1.31	3.52
	H.hibernica	2.09*	.37	<.001	.98	3.19
	W.sinensis	1.60*	.38	<.001	.48	2.71
	L.henryi	2.05*	.38	<.001	.94	3.17
	H.colchica	1.30*	.38	.011	.19	2.42
P. tricuspidata	C. montana	-.69	.38	.538	-1.81	.44

	H.helix ' Plattensee'	1.73*	.35	<.001	.68	2.77
	H.hibernica	1.40*	.35	.002	.36	2.44
	W.sinensis	.91	.36	.141	-.14	1.97
	L.henryi	1.37*	.36	.003	.31	2.42
	H.colchica	.61	.36	.596	-.44	1.67
H.helix ' Plattensee'	C. montana	-2.41*	.37	<.001	-3.52	-1.31
	P. tricuspidata	-1.73*	.35	<.001	-2.77	-.68
	H.hibernica	-.32	.34	.965	-1.35	.70
	W.sinensis	-.82	.35	.228	-1.85	.22
	L.henryi	-.36	.35	.946	-1.39	.68
	H.colchica	-1.11*	.35	.026	-2.15	-.08
H.hibernica	C. montana	-2.09*	.37	<.001	-3.19	-.98
	P. tricuspidata	-1.40*	.35	.002	-2.44	-.36
	H.helix ' Plattensee'	.32	.34	.965	-.70	1.35
	W.sinensis	-.49	.35	.796	-1.53	.54
	L.henryi	-.03	.35	1.000	-1.07	1.00
	H.colchica	-.79	.35	.268	-1.82	.25
W.sinensis	C. montana	-1.60*	.38	<.001	-2.71	-.48
	P. tricuspidata	-.91	.36	.141	-1.97	.14
	H.helix ' Plattensee'	.82	.35	.228	-.22	1.85
	H.hibernica	.49	.35	.796	-.54	1.53
	L.henryi	.46	.35	.855	-.59	1.50
	H.colchica	-.30	.35	.980	-1.34	.75
L.henryi	C. montana	-2.05*	.38	<.001	-3.17	-.94
	P. tricuspidata	-1.37*	.36	.003	-2.42	-.31
	H.helix ' Plattensee'	.36	.35	.946	-.68	1.39
	H.hibernica	.03	.35	1.000	-1.00	1.07
	W.sinensis	-.46	.35	.855	-1.50	.59
	H.colchica	-.75	.35	.336	-1.80	.30
H.colchica	C. montana	-1.30*	.38	.011	-2.42	-.19
	P. tricuspidata	-.61	.36	.596	-1.67	.44
	H.helix ' Plattensee'	1.11*	.35	.026	.08	2.15
	H.hibernica	.79	.35	.268	-.25	1.82
	W.sinensis	.30	.35	.980	-.75	1.34

	L.henryi	.75	.35	.336	-.30	1.80

*. The mean difference is significant at the 0.05 level.

Homogeneous Subsets

Tleaf °C

Tukey HSD[a,b]

Plant ID	N	Subset for alpha = 0.05			
		1	2	3	4
H.helix ' Plattensee'	40	31.3803			
H.hibernica	40	31.7053	31.7053		
L.henryi	38	31.7400	31.7400		
W.sinensis	38	32.1961	32.1961	32.1961	
H.colchica	38		32.4924	32.4924	
P. tricuspidata	37			33.1070	33.1070
C. montana	30				33.7933
Sig.		.257	.298	.147	.469

Means for groups in homogeneous subsets are displayed.
a. Uses Harmonic Mean Sample Size = 36.977.

b. The group sizes are unequal. The harmonic mean of the group sizes is used. Type I error levels are not guaranteed.

Oneway

Notes

Output Created	04-APR-2025 13:31:45
Comments	

Input	Active Dataset	DataSet2
	Filter	<none>
	Weight	<none>
	Split File	<none>
	N of Rows in Working Data File	261
Missing Value Handling	Definition of Missing	User-defined missing values are treated as missing.
	Cases Used	Statistics for each analysis are based on cases with no missing data for any variable in the analysis.
Syntax		ONEWAY Qambµmolm²s BY PlantID /ES=OVERALL /MISSING ANALYSIS /CRITERIA=CILEVEL(0.95) /POSTHOC=TUKEY ALPHA(0.05).
Resources	Processor Time	00:00:00.02
	Elapsed Time	00:00:00.01

ANOVA

Qamb (µmol/m²/s)

	Sum of Squares	df	Mean Square	F	Sig.
Between Groups	8744731.291	6	1457455.215	6.565	<.001
Within Groups	56388863.797	254	222003.401		
Total	65133595.088	260			

ANOVA Effect Sizes[a]

			95% Confidence Interval	
		Point Estimate	Lower	Upper
Qamb (µmol/m²/s)	Eta-squared	.134	.050	.195
	Epsilon-squared	.114	.028	.176

	Omega-squared Fixed-effect	.113	.028	.176
	Omega-squared Random-effect	.021	.005	.034

a. Eta-squared and Epsilon-squared are estimated based on the fixed-effect model.

Post Hoc Tests

Multiple Comparisons

Dependent Variable: Qamb (µmol/m²/s)
Tukey HSD

(I) Plant ID	(J) Plant ID	Mean Difference (I-J)	Std. Error	Sig.	95% Confidence Interval Lower Bound	95% Confidence Interval Upper Bound
C. montana	P. tricuspidata	486.6*	115.8	<.001	142.54	830.64
	H.helix ' Plattensee'	367.2*	113.8	.024	28.99	705.44
	H.hibernica	271.0	113.8	.211	-67.23	609.22
	W.sinensis	628.6*	115.1	<.001	286.59	970.63
	L.henryi	541.8*	115.1	<.001	199.75	883.79
	H.colchica	313.2	115.1	.097	-28.80	655.23
P. tricuspidata	C. montana	-486.6*	115.8	<.001	-830.64	-142.54
	H.helix ' Plattensee'	-119.4	107.5	.924	-438.79	200.05
	H.hibernica	-215.6	107.5	.413	-535.02	103.82
	W.sinensis	142.0	108.8	.849	-181.42	465.45
	L.henryi	55.2	108.8	.999	-268.26	378.61
	H.colchica	-173.4	108.8	.687	-496.81	150.06
H.helix ' Plattensee'	C. montana	-367.2*	113.8	.024	-705.44	-28.99
	P. tricuspidata	119.4	107.5	.924	-200.05	438.79
	H.hibernica	-96.2	105.4	.970	-409.36	216.91
	W.sinensis	261.4	106.7	.183	-55.84	578.62
	L.henryi	174.5	106.7	.660	-142.68	491.78
	H.colchica	-54.0	106.7	.999	-371.23	263.23
H.hibernica	C. montana	-271.0	113.8	.211	-609.22	67.23

	P. tricuspidata	215.6	107.5	.413	-103.82	535.02
	H.helix ' Plattensee'	96.2	105.4	.970	-216.91	409.36
	W.sinensis	357.6*	106.7	.016	40.39	674.85
	L.henryi	270.8	106.7	.151	-46.45	588.00
	H.colchica	42.2	106.7	1.000	-275.01	359.45
W.sinensis	C. montana	-628.6*	115.1	<.001	-970.63	-286.59
	P. tricuspidata	-142.0	108.8	.849	-465.45	181.42
	H.helix ' Plattensee'	-261.4	106.7	.183	-578.62	55.84
	H.hibernica	-357.6*	106.7	.016	-674.85	-40.39
	L.henryi	-86.8	108.1	.984	-408.11	234.43
	H.colchica	-315.4	108.1	.058	-636.67	5.88
L.henryi	C. montana	-541.8*	115.1	<.001	-883.79	-199.75
	P. tricuspidata	-55.2	108.8	.999	-378.61	268.26
	H.helix ' Plattensee'	-174.5	106.7	.660	-491.78	142.68
	H.hibernica	-270.8	106.7	.151	-588.00	46.45
	W.sinensis	86.8	108.1	.984	-234.43	408.11
	H.colchica	-228.6	108.1	.347	-549.82	92.72
H.colchica	C. montana	-313.2	115.1	.097	-655.23	28.80
	P. tricuspidata	173.4	108.8	.687	-150.06	496.81
	H.helix ' Plattensee'	54.0	106.7	.999	-263.23	371.23
	H.hibernica	-42.2	106.7	1.000	-359.45	275.01
	W.sinensis	315.4	108.1	.058	-5.88	636.67
	L.henryi	228.6	108.1	.347	-92.72	549.82

*. The mean difference is significant at the 0.05 level.

Homogeneous Subsets

Qamb (µmol/m²/s)

Tukey HSD[a,b]

Plant ID	N	Subset for alpha = 0.05		
		1	2	3
W.sinensis	38	651.66		
L.henryi	38	738.50	738.50	
P. tricuspidata	37	793.68	793.68	
H.helix ' Plattensee'	40	913.05	913.05	
H.colchica	38	967.05	967.05	967.05
H.hibernica	40		1009.28	1009.28
C. montana	30			1280.27
Sig.		.065	.174	.068

Means for groups in homogeneous subsets are displayed.

a. Uses Harmonic Mean Sample Size = 36.977.

b. The group sizes are unequal. The harmonic mean of the group sizes is used. Type I error levels are not guaranteed.